2021

Precise extratemporal pattern and intramuscular distribution of the facial nerve

Sukanya Uruwan
Faculty of Medicine

Precise extratemporal pattern and intramuscular distribution of the facial nerve

Miss Sukanya Uruwan

A Dissertation Submitted in Partial Fulfillment of the Requirements
for the Degree of Doctor of Philosophy in Medical Sciences
FACULTY OF MEDICINE
Chulalongkorn University
Academic Year 2021

รูปแบบโดยละเอียดของเส้นประสาทใบหน้าและการแตกแขนงเข้าสู่กล้ามเนื้อ ณ ส่วนที่วางตัวอยู่นอกกระดูกขมับ

น.ส.สุกัญญา อุรุวรรณ

วิทยานิพนธ์นี้เป็นส่วนหนึ่งของการศึกษาตามหลักสูตรปริญญาวิทยาศาสตรดุษฎีบัณฑิต
สาขาวิชาวิทยาศาสตร์การแพทย์ ไม่สังกัดภาควิชา/เทียบเท่า
คณะแพทยศาสตร์ จุฬาลงกรณ์มหาวิทยาลัย
ปีการศึกษา 2564

Thesis Title	Precise extratemporal pattern and intramuscular distribution of the facial nerve
By	Miss Sukanya Uruwan
Field of Study	Medical Sciences
Thesis Advisor	Professor TANVAA TANSATIT

Accepted by the FACULTY OF MEDICINE, Chulalongkorn University in Partial Fulfillment of the Requirement for the Doctor of Philosophy

..... Dean of the FACULTY OF MEDICINE
(Associate Professor CHANCHAI SITTIPUNT)

DISSERTATION COMMITTEE

..... Chairman
(Associate Professor Wisuit Pradidarcheep, Ph.D.)

..... Thesis Advisor
(Professor TANVAA TANSATIT)

..... Examiner
(Professor VILAI CHENTANEZ, Ph.D.)

..... Examiner
(Professor SITHIPORN AGTHONG, Ph.D.)

..... External Examiner
(Kritsada Kowitwibool)

สุกัญญา อุรุวรรณ : รูปแบบโดยละเอียดของเส้นประสาทใบหน้าและการแตกแขนงเข้าสู่กล้ามเนื้อ ณ ส่วนที่วางตัวอยู่นอกกระดูกขมับ. (Precise extratemporal pattern and intramuscular distribution of the facial nerve) อ.ที่ปรึกษาหลัก : ศ. นพ. ธันวา ตันสถิตย์

การแตกแขนงของเส้นประสาทใบหน้ามีความซับซ้อนและความแปรปรวนมากที่สุด ยิ่งไปกว่านั้น ความรู้เกี่ยวกับเส้นประสาทใบหน้ามีความสำคัญอย่างยิ่งต่อการทำหัตถการทั้งทางศัลยกรรมและการรักษาอื่นที่ไม่ใช่ทางศัลยกรรมบริเวณใบหน้า อย่างไรก็ตาม การศึกษาก่อนหน้ามีเพียงเล็กน้อยที่ศึกษาเกี่ยวกับเส้นประสาทใบหน้าตลอดทั้งเส้นของแขนงและรูปแบบของการแตกแขนงของเส้นประสาทใบหน้าในส่วนที่อยู่นอกกระดูกขมับและการแตกแขนงของเส้นประสาทในกล้ามเนื้อของใบหน้า ดังนั้น งานวิจัยนี้จึงมีวัตถุประสงค์เพื่อศึกษารายละเอียดของเส้นประสาทใบหน้าในส่วนอยู่นอกกระดูกขมับและในกล้ามเนื้อของใบหน้า งานวิจัยนี้ได้มีการศึกษา โดยใช้ร่างอาจารย์ใหญ่แบบแข็งจำนวน 42 ตัวอย่าง ด้วยวิธีการชำแหละ, ร่างอาจารย์ใหญ่แบบแข็งจำนวน 14 ตัวอย่าง ด้วยวิธีการศึกษาเนื้อเยื่อ และร่างอาจารย์ใหญ่แบบนุ่มจำนวน 16 ตัวอย่าง ด้วยเทคนิคการย้อมสีของ Sihler เพื่อตรวจสอบลักษณะทางกายวิภาคศาสตร์ต่าง ๆ ของแขนงของเส้นประสาทใบหน้า ผลการศึกษาพบว่า จำนวนเฉลี่ยของแขนง temporal, zygomatic, buccal, marginal mandibular, และ cervical ที่จุดออกจากต่อมน้ำลายหน้าใบหู คือ 2.57 ±0.83, 1.83 ±0.69, 3.10 ±0.82, 1.36 ±0.49 และ 1.07 ±0.26 ตามลำดับ ยิ่งไปกว่านั้น แขนงของเส้นประสาทใบหน้ายังกระจายอยู่ทั่วใต้พังผืด parotido-masseteric, พังผืด temporo-parietal, superficial musculo-aponeurotic system และกล้ามเนื้อ platysma ขึ้นอยู่กับแต่ละแขนงของเส้นประสาทใบหน้า โดยสรุปแล้ว ในการทำหัตถการต่าง ๆ บริเวณควรใช้ความระมัดระวัง โดยขึ้นอยู่กับแต่ละแขนงของเส้นประสาทใบหน้าโดยพิจารณาจากการกระจายของเส้นประสาท เพื่อป้องกันภาวะแทรกซ้อนและผลลัพธ์ที่ไม่คาดคิด

สาขาวิชา วิทยาศาสตร์การแพทย์ ลายมือชื่อนิสิต .....

ปีการศึกษา 2564 ลายมือชื่อ อ.ที่ปรึกษาหลัก .....

6271029730 : MAJOR MEDICAL SCIENCES

KEYWORD: facial nerve, facial paralysis, angular nerve, zygomatico-buccal plexus, facial nerve injury

Sukanya Uruwan : Precise extratemporal pattern and intramuscular distribution of the facial nerve . Advisor: Prof. TANVAA TANSATIT

An arborization of the branches of the facial nerve has the most complexity and variability. Moreover, knowledge of the facial nerve has great importance for surgical and non-surgical interventions in the face region. However, few studies have attempted to determine the entire course and pattern of terminal branching of the facial nerve in the extratemporal and intramuscular parts of the face. Therefore, the purpose of this study was to investigate the precise detail of the facial nerve in extratemporal and intramuscular parts. This study was conducted in forty-two hemifaces of embalmed cadavers by conventional dissection, fourteen hemi-faces of embalmed cadavers by histological study, and sixteen hemi-faces of soft cadavers by Sihler's staining technique to investigate the characteristics of the branches of the facial nerve. The results revealed that the mean number of the temporal, zygomatic, buccal, marginal mandibular, and cervical branches of the facial nerve were 2.57 ±0.83, 1.83 ±0.69, 3.10 ±0.82, 1.36 ±0.49, and 1.07 ±0.26 branches respectively. The branches of the facial nerve were distributed deep to the parotido-masseteric fascia, temporo-parietal fascia, superficial musculo-aponeurotic system, and platysma muscle depending on each branch of the facial nerve. In conclusion, a caution area of each branch of the facial nerve should be carefully performed based on intensive nerve distribution to prevent complications and unexpected outcomes.

Field of Study:	Medical Sciences	Student's Signature .....
Academic Year:	2021	Advisor's Signature .....

ACKNOWLEDGEMENTS

Primarily, I would like to especially thank my thesis advisor, Professor Tanvaa Tansatit, who has continuous support my research with his patience, motivation, and invaluable assistance. If there is a lack of support from my advisor, this thesis will not be successful.

Moreover, I would like to express my sincere gratitude to my thesis committee; Associate Professor Wisuit Pradidarcheep who was the chairman of the thesis, Professor Dr. Vilai Chentanez, Professor Dr. Sithiporn Agthong, and Dr. Kritsada Kowitwibool for their kindness and suggestions.

Additionally, I would like to thank the staff of the Anatomy Department and the Chula soft cadaver surgical training center for their support of facilities and materials during this thesis collection. Furthermore, this research was supported by the 100th Anniversary Chulalongkorn University Fund for Doctoral Scholarship.

Eventually, I would like to express my deepest gratitude to my family and my friends for their fondness, encouragement, assistance, and care that gave me encouragement and try to study my thesis.

Sukanya Uruwan

TABLE OF CONTENTS

Page

..... iii

ABSTRACT (THAI) iii

..... iv

ABSTRACT (ENGLISH) iv

ACKNOWLEDGEMENTS v

TABLE OF CONTENTS vi

LIST OF TABLES xi

LIST OF FIGURES xiii

LIST OF ABBREVIATIONS xxix

CHAPTER I INTRODUCTION 1

1.1 Background and rationale 1

1.2 Research Questions 3

1.3 Research objectives 3

1.4 Conceptual framework 5

1.5 Keywords 5

1.6 Research design 5

1.7 Expect benefits and application 5

CHAPTER II LITERATURE REVIEWS 7

2.1 Face and the soft tissue layers of the face 7

2.2 Facial paralysis 11

2.2.1 Causes of facial paralysis 11

2.2.2 Treatment for facial paralysis caused by facial nerve injury 16
2.3 The facial nerve and its terminal branches 24
2.3.1 The segments of the facial nerve 24
2.3.2 The facial nerve trunk and its branches 27
2.3.3 Temporal branch of the facial nerve 36
2.3.4 Zygomatic branch of the facial nerve 42
2.3.5 Buccal branch of the facial nerve 43
2.3.6 Marginal mandibular branch of the facial nerve 46
2.3.7 Cervical branch of the facial nerve 48
2.3.8 Angular nerve 50
2.4 Innervation the muscle of facial expression of the facial nerve 51
2.4.1 Frontalis muscle 52
2.4.2 Orbicularis oculi muscle 52
2.4.3 Corrugator supercilii muscle 53
2.4.4 Procerus muscle 54
2.4.5 Orbicularis oris muscle 54
2.4.6 Buccinator muscle 54
2.4.7 Zygomaticus major 54
2.4.8 Zygomaticus minor muscle 57
2.4.9 Levator labii superioris muscle 57
2.4.10 Levator labii superioris aleque nasi muscle 57
2.4.11 Levator anguli oris muscle 58
2.4.12 Risorius muscle 58
2.4.13 Nasalis muscle 58

2.4.14 Depressor anguli oris muscle 58
2.4.15 Depressor labii inferioris muscle 58
2.4.16 Mentalis muscle 59
2.4.17 Platysma muscle 59
2.5 Communication of the facial to other nerve 59
2.6 Histological study in the face for identification of the facial nerve 65
2.7 Sihler's technique for study the facial nerve 68
CHAPTER III RESEARCH METHODOLOGY 71
3.1 Target population and sample population 71
3.2 Sample size determination 71
3.2.1 Sample size determination for cadaveric dissection 71
3.2.2 Sample size determination for histological study 72
3.2.3 Sample size determination for Sihler's technique 73
3.3 Material and tool 73
3.4 Methods 76
3.4.1 For cadaveric dissection study 77
3.4.2 For histological study 90
3.4.3 For Sihler's technique 96
3.5 Data collection 100
3.6 Data analysis 112
3.7 Ethical consideration 113
CHAPTER IV RESULTS 114
4.1 The results of cadaveric dissection 114

4.1.1 The number and the emerging point of the branches of the facial nerve 114

4.1.3 The zygomatic branch of the facial nerve 123

4.1.4 The buccal branch of the facial nerve (BB) 125

4.1.5 The marginal mandibular branch of the facial nerve 139

4.1.6 The cervical branch of the facial nerve 143

4.1.7 The facial nerve trunk and division 146

4.1.8 The location and number of the entry site of the facial nerve branch in facial muscles 148

4.2 The results of the histological study 149

4.2.1 Histological section with Masson's trichrome stain at the parotid region 149

4.2.2 Histological section with Masson's trichrome stain at the temporal region 152

4.2.3 Histological section with Masson's trichrome stain at the masseteric region 162

4.2.4 Histological section with Masson's trichrome stain at the nasolabial region 165

4.2.5 Histological section with Masson's trichrome stain at the tear trough region 168

4.2.6 Histological section with Masson's trichrome stain at the mandibular and cervical region 173

4.3 The results of the Sihler’s staining technique 175

CHAPTER V DISCUSSION 184

CHAPTER VI CONCLUSION 206

REFERENCES 208

VITA..... 227

LIST OF TABLES

Page

Table 1 The distance of the facial nerve trunk to the anatomical landmarks. 27

Table 2 The percentage of the number of the marginal mandibular branch 46

Table 3 The communication of the facial nerve and the terminal branches of the trigeminal nerve.[109] 60

Table 4 The number of the branches of the facial nerve 115

Table 5 The emerging points of the branches of the facial nerve. 116

Table 6 The location and diameter of the temporal branch of the facial nerve at emerging point. 119

Table 7 The location and diameter of the temporal branch of the facial nerve at FHL. 120

Table 8 The location and diameter of the temporal branch of the facial nerve at LCHL. 121

Table 9 The location and diameter of the temporal branch of the facial nerve at SOL. 122

Table 10 The communication between the temporal branch of the facial nerve and sensory nerve. 123

Table 11 The location and diameter of the zygomatic branch of the facial nerve at emerging point. 124

Table 12 The location and diameter of the zygomatic branch of the facial nerve correlated to the midFHL. 125

Table 13 The characteristics of the buccal branch of the facial nerve 126

Table 14 The location and diameter of the buccal branch of the facial nerve at emerging point. 128

Table 15 The location and diameter of the buccal branch of the facial nerve correlated to the midFHL. 129

Table 16 The characteristics of the ZBP 133

Table 17 The position of the branches of the facial nerve which form zygomatico-buccal plexus related to the boundary of the zygomaticus major muscle. 134

Table 18 The location and diameter of the angular nerve..... 138

Table 19 The emerging point and crossing point of the marginal mandibular branch correlated to the inferior mandibular line. 140

Table 20 The characteristic of the marginal mandibular branch of the facial nerve. 142

Table 21 The characteristics of the cervical branch of the facial nerve. 144

Table 22 The communication of the cervical branch of the facial nerve with transverse cervical nerve. 146

Table 23 The location of the branching point of the facial nerve trunk and their divisions 147

Table 24 The number of the entry site of the facial nerve branch in facial muscles 148

Table 25 The number of the branches of the facial nerve from histological methods. 152

Table 26 The number and location of the zygomatic and temporal branches of the facial nerve at Frankfort's horizontal line from histological methods. 153

Table 27 The number and location of the zygomatic and temporal branches of the facial nerve at lateral canthal level from histological methods. 155

Table 28 The number and location of the zygomatic and temporal branches of the facial nerve at the supraorbital rim level from histological methods..... 157

Table 29 The number and location of the zygomatic and temporal branches of the facial nerve at the upper eyebrow level in histological methods. 160

LIST OF FIGURES

Page

Figure 1 The sub regions of the face;1, the forehead; 2, eyelids; 3, nose; 4, lips; 5, chin; 6, the temples; 7, cheeks; 7a, infra-orbital region; 7b, buccal region; 7c, zygomatic region; 7d, parotid-masseteric region; and 8, ears.[27] 7

Figure 2 The five basis soft tissue layers of face.[29] 8

Figure 3 Illustration of the layers of the face in the temporal area (a), the parotid area (b), the cheek area (c) and the nasolabial fold area (d).[31] 9

Figure 4 The positions of the facial nerve related to the facial soft tissue layers in each area of the face.[35] 10

Figure 5 The weakness of muscle of the facial expression caused by the facial nerve injury.[36] 11

Figure 6 Illustration of the several procedure can effect facial nerve injury during a facelift dissection.[1] 14

Figure 7 Danger zones of facial nerve injury (green area). The temporal and zygomatic branches might injury at the zygomatic arch and temporal area, and the marginal mandibular and cervical branch might injury at the jawline anterior to the masseter muscle.[12] 15

Figure 8 Danger areas of the buccal branch and marginal mandibular branches.[1] 15

Figure 9 The House-Brackmann facial nerve grading system.[52] 17

Figure 10 Patient with left-sided iatrogenic facial nerve injury after parotidectomy for benign disease, and primary neurorrhaphy is performed lasting 5 months.[51] 18

Figure 11 Masseteric-facial nerve transfer[55] 19

Figure 12 Patient with asymmetrical face at rest (A), in eye closing (B), during smile (C), and the functions of the face were restored by using reanimation procedure (D, E, F)[56] 20

Figure 13 Gracilis muscle transplants[57] 21

Figure 14 Reanimation procedures for generating facial tone and facial expression; one-stage reanimation (A), and two-stage reanimation (B).[38] 21

Figure 15 Lengthening temporalis myoplasty procedure; the temporalis tendon was released from the coronoid process (A), the temporalis tendon was inferomedially transferred to the corner of mouth (B), and the temporalis tendon was passed through the tunnel of the buccal fat pad, then it was connected to the corner of mouth and upper lip (C).[7] 22

Figure 16 Patient with left platysmal and mentalis synkinesis at movement stage (A) and achievement after BoNTA injection on the mentalis, depressor labii inferioris, orbicularis oris and orbicularis oculi muscle.[60] 23

Figure 17 Patient with overactivation of the muscle of the forehead (A) and the eyebrow (D). Injection point of BoNTA at the forehead (B) and the eyebrow (E). Achievement of BoNTA injection (C, F).[62] 24

Figure 18 The pathways of the facial nerve in temporal bone.[66] 26

Figure 19 The measurements of the facial nerve trunk in the intraparotid area. Depth of the stylomastoid foramen from the skin surface (1), Distance between the emerging point of the facial nerve trunk from the stylomastoid foramen to the furcation point (2).[20] 26

Figure 20 Distance of the temporal branch of the facial nerve correlated to the external auditory.[70-72] 27

Figure 21 Right side of the face in the cadaveric dissection presents anatomical landmarks and the facial nerve trunk (FNT). TP, tragal pointer; MT, tip of mastoid process (blue arrow); PBDM, posterior belly of the digastric muscle, mastoid process (black dotted line), the osteocartilagenous junction (OCJ) (green line), the tympanomastoid suture (red line)[77] 31

Figure 22 Six branching pattern of the facial nerve. Type I, Type II; absence of an anastomosis between the temporofacial and cervicofacial division, but presence

anastomosis among the terminal branches of the temporofaciai division only. Type III; single anastomosis among the branches of the temporofacial division and cervicofacial division, Type IV; combination of type II and III, Type V; double anastomosis between the temporofacial and cervicofacial division, Type VI; complex multiple anastomosis between the two divisions, where the buccal branch receives many anastomotic fibers from the cervicofacial and the marginal mandibular branch.[80, 81] 32

Figure 23 Furcation of the facial nerve trunk in cadaveric dissection. Trifurcation (A), Bifurcation and a minor branch (B)[69] 33

Figure 24 Four types of the branching patterns of the facial nerve base on the origin of the buccal branch.[20] 34

Figure 25 Three types of branching pattern of facial nerve at the condylar area. (A) Type I (single trunk), (B) Type II (double trunks), and (C) Type III (nervous loop or plexiform). Tbr, temporal branch; Zbr, zygomatic branch; Bbr, buccal branch; Mbr, marginal mandibular branch; Sb, superior trunk; Ib, inferior trunk.[13] 34

Figure 26 Illustration of the new patterns of the facial nerve was classified by Pascual et al. in 2019.[19] 36

Figure 27 Four types of temporal branch of facial nerve were classified by Bernstein and Nelson in 1984.[25] 37

Figure 28 The temporal branch in the upper part of the orbicularis oculi muscle. Twigs of the temporal branch of the facial nerve ran horizontally follow the muscle fibers of the orbicularis oculi muscle with mutual connections(A). Illustration of the twigs of the temporal branch in the orbicularis oculi muscle. (B)[10] 37

Figure 29 The course of the temporal branch of the facial nerve at temporal area (A). The tissue layers of temporal area (B). [24] 39

Figure 30 The location of the temporal branch correlated to the facial tissue layers in Masson's trichrome stain. The temporal branch was located in the fibrofatty innominate fascia at the level of the zygomatic arch, while it was placed in

innominate fascia where the inferior surface of the superficial temporal fascia at above the area of zygomatic arch (Left). Illustration of the course of temporal branch associated with the fascial planes of the parotid and temporal area (Right). [33]..... 40

Figure 31 The lateral view of the face in the cadaveric dissection with the skin markings of Pitanguy's line, zygomatic arch, and temporal crest (A). The perforation of temporal branch of the facial nerve in the temporoparietal fascia correlated to the zygomatic arch and Pitanguy's line.[87] 41

Figure 32 The zones of injury risk of the temporal branch of the facial nerve at the temporal region that was divided into minor risk (0-5 %), moderate risk (5-15 %), and high risk (more than 85 %).[88] 41

Figure 33 The temporal branches of the facial nerve and other structure at the temporal regions.[89] 42

Figure 34 Illustration of the anatomical surface to identify of the zygomatic branch of the facial nerve. Zuker's Point (x)[91] 43

Figure 35 Illustration of irregular hexagon; A; upper border of the tragus, B; lateral canthus, C; lateral oral commissure, D; angle of the mandible, F; the midpoint of the distance between Point D and the intersection of inferior border of the mandible and the anterior border of facial artery, and G; tip of the mastoid process (A). The Zygomatic-buccal branches (blue dots) pass through B-C line and it located in quadrangle ABCD.[64] 45

Figure 36 Illustration of 4 types of the buccal branch; type I; classic type (A), type II; buccal branches arose from the marginal mandibular branch (B), type III; sweeper type (C), and type IV; the buccal branches arose from the temporozygomaticobuccal branch (D)[64] 45

Figure 37 The main branches of marginal mandibular branch of the facial nerve including superior, middle and inferior branches (a, b and c), respectively. d and e, secondary rami of the marginal mandibular branch; AFv, the anterior facial vein; Fa, the facial artery; BM, inferior border of the mandible; LBB, the lower buccal branch;

PG, parotid gland; PD, parotid duct; PM, platysma muscle; CB, cervical branch of the facial nerve; M, Masseter muscle; MLL, Muscles of the lower lip).[9] 48

Figure 38 The anatomy of the cervical branch of the facial nerve consists of the number of rami of the cervical branches (A-C), communication between cervical and marginal mandibular branches (D), coinnervation the depressor anguli oris of cervical and marginal mandibular branches (E), and submandibular danger zone (F). 1, sternocleidomastoid muscle; 2, parotid gland; 3, submandibular gland; 4, depressor anguli oris muscle; 5, depressor labii inferioris muscle, cervical nerve branches (yellow line), transverse cervical nerve (green line), main cervicofacial trunk (orange line), the marginal mandibular branch (red line); a, distance between the facial nerve trunk and the cervical branch; b, distance between the cervical branch and the angle of the mandible; c, minimum distance between the parotid gland and separation of the cervical branches; d, distance between the inferior border of the mandible and the transverse cervical nerve communication; e, distance between inferior border of the mandible and the most inferior cervical nerve branch.[94] 49

Figure 39 The terminal branch of the buccal branch in cadaveric dissection (right side); E, entering point of the buccal branch into the procerus muscle (PM); M, medial canthus; N, nasion; S, tangential level of the supraorbital rim; C, crossing point.[10, 95] 50

Figure 40 The muscles of the facial expression and masticatory muscles. (1) temporalis, (2) frontalis, (3) corrugator supercilii, (4) orbicularis oculi, (5) procerus, (6) nasalis, (7) levator labii superioris aleque nasi, (8) levator labii superioris, (9) zygomaticus minor, (10) zygomaticus major, (11) orbicularis oris, (12) masseter, (13) buccinator, (14) risorius, (15) modiolus, (16) depressor anguli oris, (17) depressor labii inferioris, (18) mentalis, (19) platysma, (20) sternocleidomastoid, (21) occipitalis.[26] 51

Figure 41 The 3 rami of the temporal branches crossed the superior temporal line, and entered the frontalis muscle. [24] 52

Figure 42 Illustration of the eyebrow area for dissection (A), and the temporal branch the corrugator supercilia and the orbicularis oculi muscle (B); F, temporal branch of the facial nerve.[85] 53

Figure 43 Illustrations of the of arrangement and attachment of the zygomaticus major muscle were classified into the four types. In type I, the superficial fibers of the zygomaticus major (ZMj) are intermingle with the levator anguli oris (LAO), while the deep fibers of the muscle ran inferiorly to blend into the buccinator (Buc) and levator anguli oris. In type II, the superficial fibers of the zygomaticus major (ZMj) are intermingle with the superficial layer of the orbicularis oris (OOr) and the depressor anguli oris (DAO), while the middle fibers of the muscle blended into levator anguli oris. And deep fibers of the muscle ran inferiorly to blend into the buccinator (Buc) and levator anguli oris. In type III, the zygomaticus major (ZMj) ran posterior to the levator anguli oris muscle, then are intermingled with the buccinator (Buc) and levator anguli oris. In type IV, the superficial fibers of the zygomaticus major are intermingled with the orbicularis oris and the depressor anguli oris muscle, and the deep muscle fibers are blended into a buccinator and levator anguli oris muscle. ZMi, zygomaticus minor.[99] 55

Figure 44 Illustration of the five patterns of branching of the facial nerve for innervation the zygomaticus major muscle; Y-type (28%) (a), X-type (28%) (b), H-type (19%) (c), E-type (14%) (d), and F-type (11%) (e); Inconstant branches (dash lines) [102] 57

Figure 45 The sensory nerve for innervation the skin of the face and neck. Green area, the skin surface is supplied by ophthalmic nerve; 1, supraorbital nerve; 1a, medial branch; 1b, lateral branch; 1c, horizontal branch; 1d, palpebral branches; 2, supratrochlear nerve; 2a, forehead branches; 2b, palpebral branch; 3, infratrochlear nerve; 3a, nasal branches; 3b, palpebral branch; 4, palpebral branches of lacrimal nerve; 5, external nasal branch of anterior ethmoidal nerve; blue area, the skin surface is supplied by maxillary nerve; 6, infraorbital nerve; 6a, inferior palpebral branches; 6b, external nasal branch; 6c, internal nasal branch; 6d, medial branch of superior labial branch; 6e, lateral branch of superior labial branch; 7, zygomaticofacial

nerve; 7a, zygomatic branches; 7b, palpebral branch; 8, zygomaticotemporal nerve; 8a, temporal branches; 8b, palpebral branch; yellow area, the skin surface is supplied by mandibular nerve; 9, auriculotemporal nerve; 9a, zygomatic branches; 9b, auricular branches; 9c, temporal branches; 10, long buccal nerve; 11, mental nerve, 11a, angular branch; 11b, lateral labial branch; 11c, medial labial branch; 11d, mental branch; 12, mental branch of mylohyoid nerve; red area, the skin surface is supplied by great auricular nerve and transverse cervical nerve; 13, great auricular nerve; 14, transverse cervical nerve.[27] 61

Figure 46 Illustration of the trigeminal nerve was divided into three branches ophthalmic (1), maxillary (2), and mandibular (3), and percentage of the communication with the branch of the facial nerve in two methods; cadaveric dissections (*) and Sihler stain (**) (A). Illurtration of the communications between the superficial trigeminal branches and the four main branches of the facial nerve; temporal (1), zygomatic (2), buccal (3), and marginal mandibular (4) (B).[109] 62

Figure 47 Infraorbital nerve commingle with the branch of the facial nerve at infraorbital area (A). The critical zone of the nerve injury. The diameter of merging area was 36 mm, and the distances between the center of this area and the infraorbital foremen was 22 mm. (B)[107] 63

Figure 48 The communication of the marginal mandibular branch of the facial nerve (MMB) and the great auricular nerve (GAN) in the right side of the face in cadaveric dissection; ST, sternomastoid muscle; AB, anterior branch of the great auricular nerve; PB, posterior branch the great auricular nerve, a, upper rami of the marginal mandibular branch; b, middle rami of the marginal mandibular branch; c, lower rami of the marginal mandibular branch; M, masseter muscle; L, ear lobule; PG, parotid gland; and PD, Parotid duct.[9] 64

Figure 49 The communications of the auriculotemporal nerve with the temporofacial division of the facial nerve, and the greater auricular nerve with the cervicofacial division of the facial nerve.[111] 65

Figure 50 Hematoxylin and eosin staining at superior parotid area; P, platysma muscle; PG, parotid gland; double-ended arrow, the SMAS layer, and scale bar 1 mm.[30] 66

Figure 51 The nasolabial tissue in the histological section; A, labial area; B, buccal area; arrow, the nasolabial fold.[32] 67

Figure 52 The cross section of the facial soft tissue at the lateral angle of the eye (A), the buccal (B), the inferior masseter (C), the superior parotid (D), the nasolabial fold (E) areas. SK, Skin; *, adipose tissue; CT, connective tissue; Or, Orbicularis oculi muscle; BV, Blood vessels; FN, Facial nerve; red arrowheads: fissure of the lateral angle of the eye; sG, sebaceous gland; ZM, zygomaticus muscle major and minor muscle; Om, oral mucosa; MS, Masseter muscle; BM, Buccinator muscle; PG, Parotid gland; Red arrow, groove of the nasolabial fold; Magnification: x4.[113] 68

Figure 53 Modified Sihler's staining in the face and platysma muscle in fresh cadaver. Anterior view of the facial tissue flap (A) Posterior view of the facial tissue flap (B)[2]. 69

Figure 54 Photograph of the modified Sihler stain in left lower face presenting marginal mandibular branch suppling the depressor anguli oris muscle (A) and the communication of the cervical branch of the facial nerve and the transverse cervical nerve posterior to the platysma muscle (B); MM, marginal mandibular branch of the facial nerve; C, cervical branch of the facial nerve; I, depressor labii inferioris muscle; O, depressor anguli oris muscle; Me, mentalis muscle; CF, cervicofacial division; TCN, transverse cervical nerve; P, platysma muscle.[94] 70

Figure 55 The communication of the superior rami of buccal branch of the facial nerve and inferior palpebral branch of the infraorbital nerve; IP, inferior palpebral branch of the infraorbital nerve; sBbr, superior rami of buccal branch of the facial nerve; arrowhead, target area for supplying by inferior palpebral (the lower eyelid); asterisk (*), communication point[106] 70

Figure 56 Cadaveric dissection; Skin incision line (A), Subcutaneous layer (B)..... 77

Figure 57 Cadaveric dissection to identify anatomy of the facial nerve and its relationship with the facial soft tissue in the SMAS layer (A), Sub-SMAS layer (B)..... 78

Figure 58 Parotid gland removing to identify the divisions of the facial nerve (A), and the facial will be sketched (B). 78

Figure 59 The measurement of the emerging point of the facial nerve correlated to the reference line. AIL; Alar-inferior tragal line, ATL; anterior tragal line, TB; temporal branch, ZB; zygomatic branch, BB; buccal branch, MB; marginal mandibular branch, CB; cervical branch, and TCN; transverse cervical nerve, blue dot; emerging point.... 80

Figure 60 The measurement of the temporal branchof the facial nerve correlated to the reference lines; FHL; the Frankfort's horizontal line, SOL; the supraorbital line, LCHL; the lateral canthal line, ATL; Anterior tragal line. 81

Figure 61 The measurement of the communicating point of the temporal branchof the facial nerve correlated to the reference lines; LCHL; the lateral canthal line, ATL; Anterior tragal line. 82

Figure 62 The measurement of the location of the zygomatic and buccal branch of the facial nerve correlated to the reference lines; FHL; the Frankfort's horizontal line, midFHL; the midpoint of FHL, ZB; zygomatic branch, BB; buccal branch..... 83

Figure 63 The pattern of zygomaticobuccal plexus from branches of the facial nerve correlated to the anatomical landmarks. 84

Figure 64 The location of zygomaticobuccal plexus from branches of the facial nerve correlated to the facial muscle landmarks. 84

Figure 65 The measurement of the location of the zygomaticobuccal plexus correlated to the anatomical landmark; midFHL; the midpoint of FHL. 85

Figure 66 The communication of the zygomaticobuccal plexus with infraorbital nerve (A). The measurement of the communication point of the zygomaticobuccal plexus (B). ZMa; zygomaticus major muscle, LLS; levator labii superioris, ZBP; the zygomaticobuccal plexus..... 86

Figure 67 The measurement of the location of the angular nerve. ICL; intercanthal line..... 87

Figure 68 The measurement of the communicating point of the angular nerve correlated to the medial canthus in x- and y-coordination. 87

Figure 69 The measurement of the marginal mandibular and cervical branch correlated to the reference line; AML, anterior masseteric line; IML, inferior margin of mandibular line 88

Figure 70 The measurement of the communicating point of the marginal mandibular nerve correlated to the corner of mouth in x- and y-coordination. 89

Figure 71 The measurement of the branching point of the facial nerve trunk and division correlated to the reference line; ATL, anterior tragal line; AIL, alar-infratragal line; TFDx, horizontal distance from branching point of temporofacial division to reference line; TFDy, vertical distance from branching point of temporofacial division to reference line; CFDx, horizontal distance from branching point of cervicofacial division to reference line; CFDy, vertical distance from branching point of cervicofacial division to reference line; FNTx, horizontal distance from branching point of facial nerve trunk to reference line; TFDy, vertical distance from branching point of facial nerve trunk to reference line; TB, temporal branch; ZB, zygomatic branch; BB, buccal branch; MB, marginal mandibular branch; CB, cervical branch 90

Figure 72 Six areas of the face in the histological study. 92

Figure 73 Plane for trimming of the harvested tissue. 93

Figure 74 An automatic tissue processor 94

Figure 75 The sectioned tissue after the oven for 15 minutes. 95

Figure 76 The hematoxylin and eosin staining protocol. 95

Figure 77 Histological section of temporal area with H&E staining at the Frankfort's horizontal line. 96

Figure 78 The cadaver dissection for Sihler's stain technique. The SMAS layer of the face and the incision line to harvest facial tissue (A). Harvested facial soft tissue flap (B). 97

Figure 79 The facial tissue flab in Sihler's staining processes; Fixation (A), Maceration and depigmentation (B), Decalcification (C), Staining (D), Destaining (E), Neutralization (F), and Clearing (G). 100

Figure 80 The location of the emerging point of the BB is sporadically distributed throughout the anterior border of the parotid gland. Then, it branched and arranged into the zygomatico-buccal plexus (ZBP) in masseteric and buccal regions, and presented the medial part of the ZBP branched into small twigs to innervate muscles around the mouth and nose. TB, temporal branch; ZB, zygomatic branch; BB1, first buccal branch; BB2, second buccal branch; BB3, third buccal branch; MMB, marginal mandibular branch; CB, cervical branch; AN, angular nerve; PG, the parotid gland; PD, parotid duct; MM, masseter muscle; LLS, levator labii superioris muscle; OO, orbicularis oculi muscle; OOr, orbicularis oris muscle; DAO, depressor anguli oris muscle; red arrowhead, the medial part of the ZBP; yellow arrowhead, small twigs of the BB; blue arrow, ZB gave branch to connect the BB. 131

Figure 81 Three patterns of the zygomatico-buccal plexus; incomplete (A,a), single (B,b), and multi-loop patterns (C,c). SAC, supra-alar crest; CM, the corner of the mouth; PD, parotid duct; FA, facial artery; FV, facial vein; red arrowhead, zygomatico-buccal plexus. 132

Figure 82 The facial nerve correlated with the lateral boundary of the zygomaticus major muscle. 135

Figure 83 The origin and location of the angular nerve that arose from superior part of the ZBP. ZBP, zygomatico-buccal plexus; AN, angular nerve; PD, parotid duct; LLS, levator labii superioris muscle; OO, orbicularis oculi muscle; red arrow head, the origin of the AN; FV, facial vein; FA, facial artery. 136

Figure 84 The AN gave small twigs to innervate facial muscles. OOc, orbicularis oculi muscle; DS, depressor supercilii muscle; CS, corrugator supercilii muscle; LLS, levator labii superioris muscle; LLSAN, levator labii superioris alaeque nasi muscle. 137

Figure 85 The terminal branches of the BB connected with the sensory nerve include ION (A) , ITN (B) and BN (C). AN, angular nerve; LLS, levator labii superioris

muscle; OO, orbicularis oculi muscle; FV, facial vein; ZBP, zygomatico-buccal plexus; red arrow head, the connection point of the motor and sensory nerve; ION, infraorbital nerve; ITN, infratrochlear nerve; OOr, orbicularis oris muscle; PD, parotid duct; BB, buccal branch; BFP, buccal fat pad; BN, buccal nerve. 139

Figure 86 The entry site of the facial nerve branch in facial muscles. OOc, orbicularis oculi muscle; ZMj, zygomaticus major muscle; DAO, depressor anguli oris muscle; DLI, depressor labii inferioris muscle, M, mentalis muscle; pink pin, entry site. 149

Figure 87 Histological section of the parotid region at the AIL, the ear lobule, and the MA levels stained with Masson's trichrome stain. The FN was identified within sub-parotid gland at the AIL level, while it was identified deep to the parotid gland at the MA level. On the contrary, none of the FN at the ear lobule level in this case. arrow-head, facial nerve; PF, parotid fascia; PG, parotid gland, PD, parotid duct..... 151

Figure 88 Histological section of the temporal region at FHL level stained with Masson's trichrome stain. arrow-head, temporal branch of the facial nerve; OOc, orbicularis oculi muscle; TPF, temporoparietal fascia; S-DTF, superficial layer of deep temporal fascia; D-DTF, deep layer of deep temporal fascia; STA, superficial temporal artery. 154

Figure 89 Histological section of the temporal region at lateral canthal level stained with Masson's trichrome stain. arrow-head, temporal branch of the facial nerve; OOc, orbicularis oculi muscle; LV, lacrimal vein; TPF, temporoparietal fascia; S-DTF, superficial layer of deep temporal fascia; D-DTF, deep layer of deep temporal fascia; STA, superficial temporal artery; STV, superficial temporal vein; MTV, middle temporal vein. 156

Figure 90 Histological section of the temporal region at supraorbital rim level stained with Masson's trichrome stain. In medial portion, a temporal branch is identified deep to the orbicularis oculi muscle running horizontal deep to the temporoparietal fascia and muscle. In middle and lateral portion, none present the temporal branch, but present the auriculotemporal nerve is identified above the temporoparietal fascia. red arrow-head, temporal branch of the facial nerve; yellow arrow-head, the

auriculotemporal nerve; TPF, temporoparietal fascia; S-DTF, superficial layer of deep temporal fascia; D-DTF, deep layer of deep temporal fascia; STA, superficial temporal artery; MTV, middle temporal vein. 159

Figure 91 Histological section of the temporal region at upper eyebrow level stained with Masson's trichrome stain. In medial portion, a temporal branch is identified deep to the frontalis muscle running horizontal deep to the temporoparietal fascia. In middle and lateral portion, none present the temporal branch, but present the auriculotemporal nerve is identified above the temporoparietal fascia. arrow-head, temporal branch of the facial nerve; TPF, temporoparietal fascia; S-DTF, superficial layer of deep temporal fascia; D-DTF, deep layer of deep temporal fascia; STA, superficial temporal artery; STV, superficial temporal vein; MTV, middle temporal vein; ATN, auriculotemporal nerve. 161

Figure 92 Histological section of the masseteric region at midFHL stained with Masson's trichrome stain. ZB, zygomatic branch of the facial nerve; BB, buccal branch of the facial nerve; PD, parotid duct; TFA, transverse facial artery. 163

Figure 93 Histological section of the masseteric region after the branches of the pass through the midFHL stained with Masson's trichrome stain. ZB, zygomatic branch of the facial nerve; BB, buccal branch of the facial nerve; PD, parotid duct; TFA, transverse facial artery; ZMj, zygomaticus major muscle. 164

Figure 94 Histological section of the nasolabial region at the corner of the mouth level stained with Masson's trichrome stain. OOr, orbicularis oris muscle; SMAS, superficial musculoaponeurotic system; BFP, buccal fat pad; FV, facial vein. 166

Figure 95 Histological section of the nasolabial region at the upper lip level stained with Masson's trichrome stain. OOr, orbicularis oris muscle; ZMn, zygomaticus minor muscle; ZMj, zygomaticus major muscle; SMAS, superficial musculoaponeurotic system; FV, facial vein. 167

Figure 96 Histological section of the nasolabial region at alar base level stained with Masson's trichrome stain. LLSAN, levator labii superior alaque nasi muscle; LLS, levator labii superioris muscle; OOc, orbicularis oculi muscle; ION, infraorbital nerve;

LAO, levator anguli oris muscle. BB, buccal branch of the facial nerve; ZMn, zygomaticus minor muscle; ZMj, zygomaticus major muscle; FV, facial vein; MT, masseteric tendon. 168

Figure 97 Histological section of the tear trough region at supra-alar crease level stained with Masson's trichrome stain. LLS, levator labii superioris muscle; OOc, orbicularis oculi muscle; ION, infraorbital nerve; IOV, infraorbital vessel, LAO, levator anguli oris muscle; AV, angular vein, ZRL, zygomatic retaining ligament; arrow head, angular nerve. 170

Figure 98 Histological section of the tear trough region at infraorbital rim level stained with Masson's trichrome stain. LLSAN, levator labii superior alaque nasi muscle; LLS, levator labii superioris muscle; OOc, orbicularis oculi muscle; arrow head, angular nerve. 171

Figure 99 Histological section of the tear trough region at medial canthal level stained with Masson's trichrome stain. DS, depressor supercilii muscle; OOc, orbicularis oculi muscle; AV, angular vein. arrow head, angular nerve. 172

Figure 100 Histological section of the tear trough region at supraorbital rim level stained with Masson's trichrome stain. DS, depressor supercilii muscle; OOc, orbicularis oculi muscle; CS, corrugator supercilii muscle; AV, angular vein. arrow head, angular nerve. 172

Figure 101 Histological section of the mandibular and cervical region at the AML stained with Masson's trichrome stain. FA, facial vein; FV, facial vein; SCM, sternocleidomastoid muscle; arrow head, marginal mandibular and cervical branch of the facial nerve. 174

Figure 102 The frontalis muscle in soft cadaveric dissection (A). Intramuscular part of the facial nerve in the frontalis muscle by Sihler’s stain technique (B). STA, superficial temporal artery; OOc, orbicularis oculi; DS, depressor supercilii; SON, supraorbital nerve; STN, supratrochlear nerve; arrow head, temporal branch of the facial nerve. 176

Figure 103 The orbicularis oculi muscle in soft cadaveric dissection (A). Intramuscular part of the facial nerve in the orbicularis oculi muscle (B). OOc, orbicularis oculi; DS, depressor supercilii; ZMj, zygomaticus major; LLS, levator labii superioris; SON, supraorbital nerve; STN, supratrochlear nerve; ITN, infratrochlear nerve; ZTN, zygomaticotemporal nerve; ZFN, zygomaticofacial nerve; TB, temporal branch; ZB, zygomatic branch; BB, buccal branch; arrow head, intramuscular part of the facial nerve in the orbicularis oculi muscle; white asterisk, lateral border of the frontalis muscle; green asterisk, lateral border of the orbicularis oculi muscle; red asterisk, origin of the zygomaticus major muscle..... 178

Figure 104 The zygomaticus major muscle in soft cadaveric dissection (A). Intramuscular part of the facial nerve in the zygomaticus major muscle (B). LLS, levator labii superioris; ZMn, zygomaticus minor; ZMj, zygamicus major; BFP, buccal fat pad; arrow head, intramuscular part of the facial nerve in zygomaticus major muscle; red asterisk, origin and insertion of the zygomaticus major muscle. 179

Figure 105 The depressor anguli oris muscle in soft cadaveric dissection (A). Intramuscular part of the facial nerve in the depressor anguli oris muscle (B). ZMj, zygamicus major; DAO, depressor anguli oris; OOr, orbicularis oris; DLI, depressor labii inferioris; M, mentalis; BFP, buccal fat pad; MB, marginal mandibular branch of the facial nerve; CB, cervical branch of the facial nerve; MN, mental nerve; blue arrow head, nerve innervation of the depressor anguli oris muscle; white arrow head, nerve innervation of the orbicularis oris muscle; green arrow head, nerve innervation of the depressor labii inferioris muscle; yellow arrow head, nerve innervation of the platysma muscle; red asterisk, medial border of the depressor anguli oris muscle; white asterisk, mandibular angle..... 181

Figure 106 The platysma muscle in soft cadaveric dissection (A). Intramuscular part of the facial nerve in the platysma muscle (B). ZMj, zygamicus major; DAO, depressor anguli oris; DLI, depressor labii inferioris; M, mentalis; BB, buccal branch of the facial nerve; MB, marginal mandibular branch of the facial nerve; CB, cervical branch of the facial nerve; TCN, transverse cervical nerve; SG, submandibular gland; blue arrow head, nerve innervation of the platysma muscle; green arrow head, nerve innervation

of the mentalis muscle; green asterisk, insertion of the zygomaticus major muscle; red asterisk, medial border of the depressor anguli oris muscle; white asterisk, mandibular angle. 182

Figure 107 The orbicularis oris muscle in soft cadaveric dissection (A). Intramuscular part of the facial nerve in the orbicularis oris muscle (B). DAO, depressor anguli oris; OOr, orbicularis oris; DLI, depressor labii inferioris; M, mentalis; FA, facial artery; blue arrow head, nerve innervation of the orbicularis oris muscle; green arrow head, nerve innervation of the mentalis muscle; 183

Figure 108 An illustration of the facial nerve 207

LIST OF ABBREVIATIONS

AIL	Alar-inferior tragal line
AML	Anterior margin of masseter muscle line
AN	Angular nerve
ATL	Anterior tragal line
ATN	Auriculotemporal nerve
BB	Buccal branch
BFP	Buccal fat pad
BoNTA	Botulinum toxin type A
Buc	Buccinator
CB	Cervical branch
CFD	Cervicofacial division
CN V	Fifth cranial nerve
CS	Corrugator supercilii muscle
D-DTF	Deep layer of deep temporal fascia
DLI	Depressor labii inferioris muscle
DS	Depressor supercilii muscle
FA	Facial artery
FHL	Frankfort's horizontal line
FNT	Facial nerve trunk
FV	Facial vein

ICL	Inter-canthal line
IFN	Infratrochlear nerve
IML	the inferior margin of the mandible line
ION	Infraorbital nerve
IOV	Infraorbital vessel
LAO	Levator anguli oris
LCHL	Lateral canthal line
LLS	Levator labii superioris muscle
LLSAN	Levator labii superior alaque nasi muscle
LTM	Lengthening temporalis myoplasty
LV	Lacrimal vein
M	Mentalis muscle
MA	Mandibular angle
MB	Marginal mandibular branch
midFHL	midpoint of Frankfort's horizontal line
MN	Mental nerve
MTV	Middle temporal vein
OCJ	Osteocartilagenous junction
OOc	Orbicularis oculi muscle
OOr	Orbicularis oris muscle
ORIF	Open reduction and internal fixation

PD	Parotid duct
PF	Parotid fascia
PG	Parotid gland
SCM	Sternocleidomastoid muscle
S-DTF	Superficial layer of deep temporal fascia
SMAS	The superficial musculoaponeurotic system
SOL	Supraorbital line
SON	Supraorbital nerve
STA	Superficial temporal artery
STN	Supratrochlear nerve
TB	Temporal branch
TCN	Transverse cervical nerve
TFA	Transverse facial artery
TFD	Temporofacial division
TPF	Temporoparietal fascia
ZB	Zygomatic branch
ZBP	Zygomatico-buccal plexus
ZFN	Zygomaticofacial nerve
ZMj	Zygomaticus major
ZMn	Zygomaticus minor muscle
ZRL	Zygomatic retaining ligament
ZTN	Zygomaticotemporal nerve

CHAPTER I

INTRODUCTION

1.1 Background and rationale

Knowledge of the facial nerve has a great importance for surgical and non-surgical interventions in the face region.[1, 2] The facial nerve as the seventh cranial nerve is a peripheral nerve consisting both motor and sensory fibers. The four segments of the facial nerve include cisternal, intracanalicular, petrous and extratemporal segments. The extratemporal terminal branches of the facial nerve are divided into frontal, zygomatic, buccal, marginal mandibular and cervical branches from temporo-facial and cervicofacial division.[3, 4] In facial functions, the facial nerve provides eyes protection, nasal control, lips together and facial animation. Especially, facial animation is a nonverbal signal for emotional expression in human communication.[5] The extratemporal segment of the facial nerve is located outside of the temporal bone and protected by soft tissue; also, it is complexity and travels in several area of the face to supply facial expression muscles. As a result, this segment could be high risk of damage.[6]

In the literature review, the facial paralysis was caused by a wide condition such as trauma, infection, metabolic, neoplastic, toxic, iatrogenic, and idiopathic.[7, 8] The evidences showed that an iatrogenic injury during surgery at the parotid area frequently induced the facial nerve paralysis or paresis.[9-11] These unexpected results might be caused by cutting or excessive stretching in surgical procedure, suturing in the SMAS layer, using large clamps or forceps during hemostasis, undue intensity of treatment protocol[1], or deoxycholic acid injections.[12] Yang and Yoo (2014) [13] described that the facial nerve was damage by the preauricular incision in 3.2% - 42.9% and the submandibular incision in 5.3% - 48.1%. Moreover, rhytidectomy bring about injured in facial nerve was 0.4 to 2.6%, and the most facial nerve branch lesion are the frontal, marginal and cervical branches.[14] Meanwhile, 14.5% of permanent defect in facial

nerve could be occurred after parotidectomy; further, the marginal mandibular branch lesion was the most complication.[15] Although, the zygomatic and buccal branches were separated into many subbranches, temporary facial dysfunction can occur at the oral commissure.[12] In addition, the buccal branch was immolated in the parotidectomy bringing about weakness of zygomaticotemporal division in 9% and cervicomandibular nerve in 43% after operation.[16] Consequently, the facial nerve lesion lead to the facial dysfunction including eye exposure, brow ptosis, difficult to viewing, eating or drinking or communication.[8] It also affected on quality of life, social isolation, and depression.[5, 17, 18]

Despite the fact that the pattern of the facial nerve is asymmetrical in both cervico-facial halves[2], but the information of the facial nerve has been widely explored in location, branching pattern within intraparotid parts[13, 19-21], diameter and its relationship to the sensory nerve[22, 23]. However, few studies have attempted to determine the entire course and pattern of terminal branching the facial nerve in the extratemporal and intramuscular parts of the face.[24, 25] Also, the layers of face are varied in depth and complexity of structure in each region of the face, thus a gross dissection might not be adequate to describe the extratemporal and intramuscular parts of the facial nerve. Therefore, the purpose of this study was to investigate the entire course and pattern of terminal branching the facial nerve in the extratemporal and intramuscular parts; besides, the positions of nerves will be determined by using dissection, histological study and Sihler's technique. The findings of the present study were to provide deep details of the facial nerve for prevention of injuries and prediction of their position during medical intervention.

1.2 Research Questions

Primary research question

1) What is the distance, the diameter, and the number of the temporal, zygomatic, buccal, marginal mandibular and cervical branch of the facial nerve (at the emerging point and the course) correlated to the reference lines in the cadaveric study?

Secondary research questions

2) What is the location of the temporal, zygomatic, buccal, marginal mandibular and cervical branch of the facial nerve correlated to the layer of the face (at anatomical landmark) in the histological study?

3) What is the location, diameter and pattern of the zygomatico-buccal plexus and the angular nerve?

4) What is the communication between the temporal, zygomatic, buccal, marginal mandibular and cervical branch of the facial nerve and sensory nerve of the face?

5) What is the relationship between the buccal and marginal mandibular branches of the facial nerve and facial soft tissue?

6) What is the distance of the facial nerve trunk, temporo-facial and cervicofacial division at the branching point correlated to the reference line?

7) What is the location and number of the entry site of the facial nerve branch in facial muscle in the cadaveric study?

8) What is the pattern of the facial nerve branch in facial muscle in the Sihler' s stain?

1.3 Research objectives

1) To investigate the distance, the diameter and the number of the temporal, zygomatic, buccal, marginal mandibular and cervical branch of the facial nerve (at the emerging point and the course) correlated to the reference lines in the cadaveric study.

2) To investigate the location of the temporal, zygomatic, buccal, marginal mandibular and cervical branch of the facial nerve correlate to the layer of the face (at anatomical landmark) in the histological study.

3) To investigate the location, origin, diameter and pattern of the zygomatico-buccal plexus and the angular nerve.

4) To study the communication between the temporal, zygomatic, buccal, marginal mandibular and cervical branch of the facial nerve and sensory nerve of the face.

5) To explain the relationship between the buccal and marginal mandibular branches of the facial nerve and facial soft tissue.

6) To investigate the distance of the facial nerve trunk, temporo-facial and cervicofacial division at the branching point correlate to the reference line.

7) To investigate the location and number of the entry site of the facial nerve branch in facial muscle in the cadaveric study.

8) To investigate the pattern of the facial nerve branch in facial muscle in the Sihler' s stain.

1.4 Conceptual framework

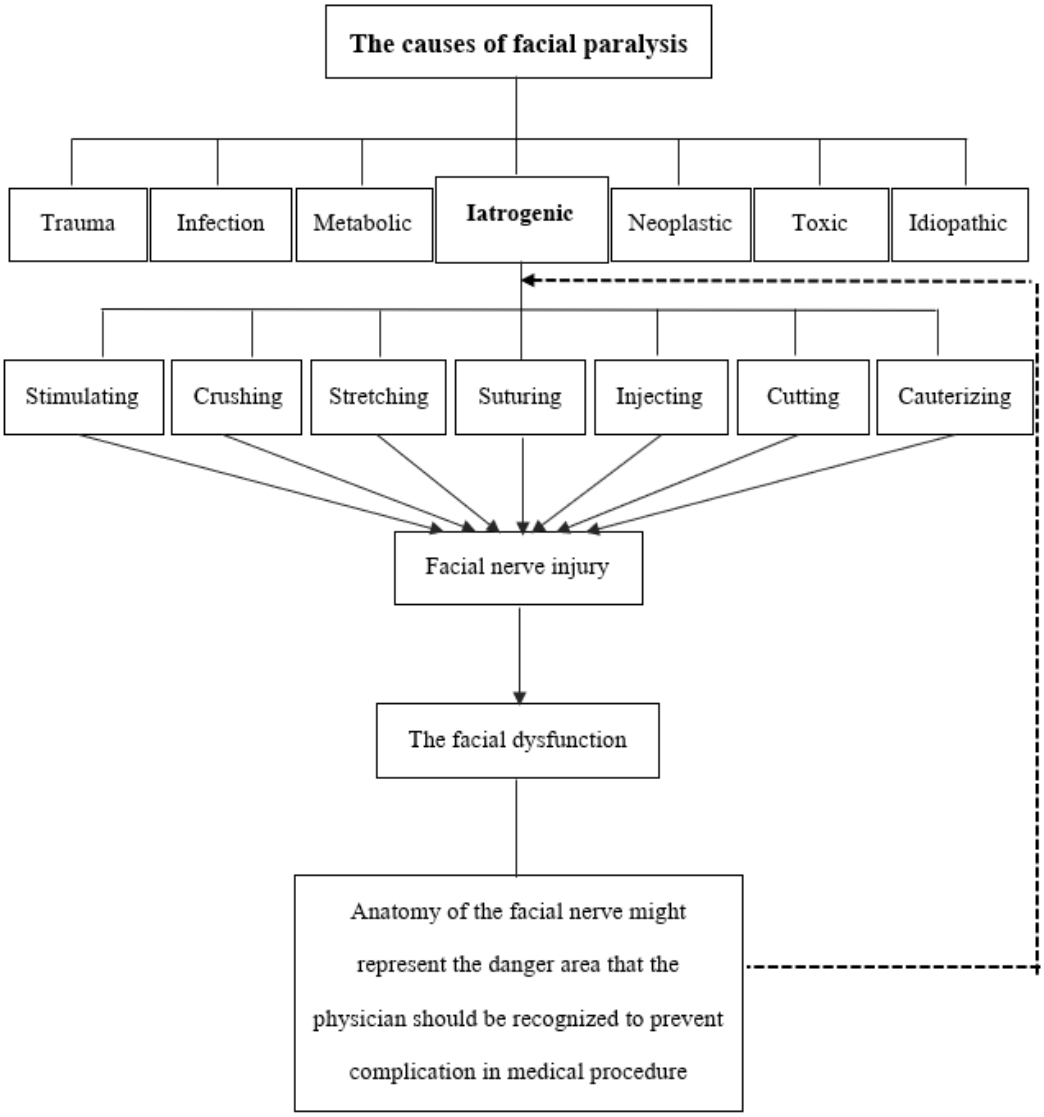

1.5 Keywords

The facial nerve, facial paralysis, angular nerve, zygomatico-buccal plexus, facial nerve injury

1.6 Research design

Descriptive research

1.7 Expect benefits and application

Although information of the facial nerve has been widely investigated, there are still complications from the medical procedure. This study was to investigate the

anatomical knowledge of the facial nerve by using cadaveric dissection correlated to the anatomical landmarks of the face, and H&E stain to identify the location of the facial nerve related to facial soft tissue layer. Moreover, the Sihler's stain was to provide the information of the facial nerve in the terminal part where it can't dissect. Consequently, this study was to explain the deep detail of the facial in extratemporal part from parotid area to intramuscular area. The study was to demonstrate the relationship between the facial nerve and adjacent facial soft tissues to recognize the course and plane of the facial nerve, therefore the physicians can predict and prevent complications that occur during medical procedure.

CHAPTER II

LITERATURE REVIEWS

2.1 Face and the soft tissue layers of the face

In anatomical study, the face can be explained as the anterior region of the head. The boundary of the face extends superiorly to the hairline, inferiorly to the chin and inferior margin of the mandible and laterally to the ear.[26] The face is the region represented special characteristic of the human, and response the human relationship composed of facial expression, esthetic, contact, and social relation. Generally, the face is divided into three parts; upper, middle, and lower face. To understanding the neuroanatomy of the face, the sub regions of the face consist of the forehead, eyelids, nose, lips, chin, the temples, cheeks and ears (Figure 1).[27]

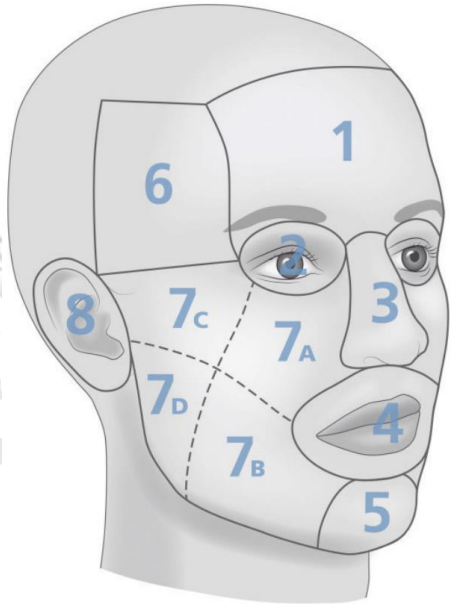

Figure 1 The sub regions of the face;1, the forehead; 2, eyelids; 3, nose; 4, lips; 5, chin; 6, the temples; 7, cheeks; 7a, infra-orbital region; 7b, buccal region; 7c, zygomatic region; 7d, parotid-masseteric region; and 8, ears.[27]

The soft tissue layers of the face

The soft tissue layers of the face are very in depth and complexity of structure in each region of the face. Basically, the layers of the face are arranged into five layers from superficial to deep layers; the skin, the subcutaneous layer, The superficial

musculoaponeurotic system (SMAS), areola tissue, and the periosteum and deep fascia (Figure 2).[28, 29]

1) Skin

Skin is the outer layer of the face which composes of epidermis and dermis. The thickness of both layers is different depending on area. For example, the mean thickness of the is epidermis and dermis in temporal and zygomatic areas were 1.59 ±0.12 and 1.57 ±0.05 mm, respectively.[30] Moreover, the stratified squamous epithelium, keratinocytes, melanocytes and antigen-presenting are positioned in epidermis layer, whereas the components of the dermis are the extracellular matrix, collagen fibers, elastin, proteoglycans, fibronectins, and vascular plexus. The thickness of dermis depending on function and movement, and it is thickest in the skin of the forehead and the nasal tip, while skin of the eyelids is thinnest.[29]

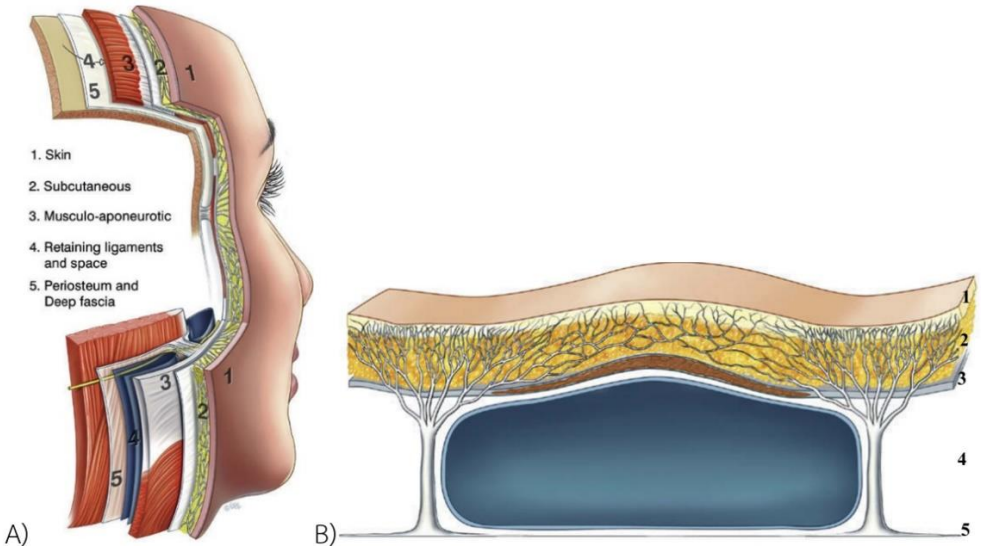

Figure 2 The five basis soft tissue layers of face.[29]

2) The subcutaneous layer

The subcutaneous of the face has two essential structures; the subcutaneous fat and the fibrous retinacular cutis. The subcutaneous fat provides volume of the face, and the fibrous retinacular cutis is the part of the retaining ligament which connects the skin to the underlying the SMAS layer. Moreover, the components of this layers depending on the area of the face. For example, the nasolabial area contents fat more

than the eyelids and lips, and the arrangement of the retinacular cutis is variable follow as the underlying components. According to Macchi et al.[31] (2010), the thickness of the subcutaneous tissue in the temporal area was 6.80 ±0.6 mm.

3) The superficial musculoaponeurotic system (SMAS)

The SMAS was first investigated and explained in parotid and cheek regions of the human face by Mitz and Peyronie in 1976. Later, the anatomy of SMAS was determined continuously in the several term of this layers, for example, the temporoparietal or superficial temporal fascia, the orbicularis fascia, and the SMAS refer to the these layer in temporal, the periorbital, and mid- and lower face, respectively (Figure 3).[30, 32] Agarwal et al. described that the SMAS layer of the midface continue from the superficial temporal fascia superiorly; then, it was performed covering the parotid gland and masseter muscle as the parotidomasseteric fascia.[33] Moreover, the SMAS layer contents the facial muscles in the cheek.[28, 29] Similarly, Ghassemi et al. discovered that the SMAS was separated into three layers including superficial layer, muscular layer, and deep layer of the SMAS.[34]

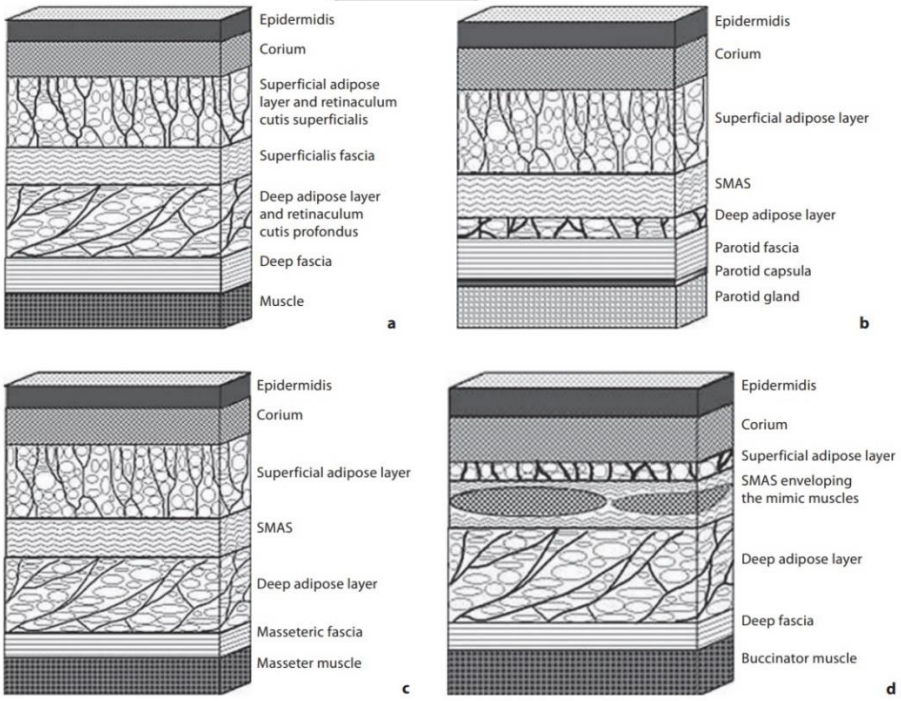

Figure 3 Illustration of the layers of the face in the temporal area (a), the parotid area (b), the cheek area (c) and the nasolabial fold area (d).[31]

4) Areola tissue layer

This layer is the area between the SMAS and the deep fascia layer, and contains essential structure of the face. It composes of the facial nerve branches, deep layers of the intrinsic muscles, retaining ligaments, deep fat, and the facial spaces. The deep intrinsic muscles attach the origin, and pass this area to insert the superficial attachment. Importantly, the facial nerve was located and ran within this layer for innervation muscle of the facial expression (Figure 4).[29]

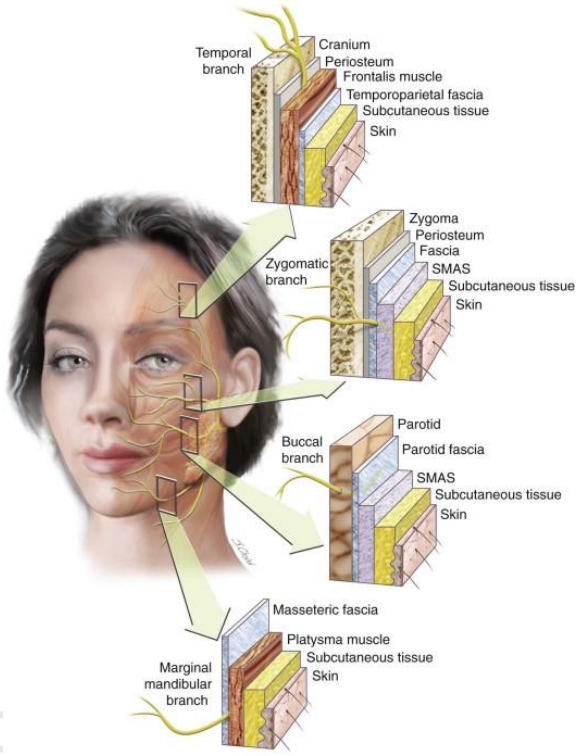

Figure 4 The positions of the facial nerve related to the facial soft tissue layers in each area of the face.[35]

5) Periosteum and deep fascia

The deepest layer of the soft tissue of the face is the deep fascia or the periosteum. It is fascia of the muscle of mastication as masseter and temporalis muscle, and the periosteum where it covers the bone. The deep fascia which covers the parotid area as the parotid fascia, while the investing cervical fascia is deep fascia in the neck area. Moreover, the deep temporal fascia and masseteric fascia is the deep fascia which cover the zygomatic arch and masseter muscle, respectively.[29]

2.2 Facial paralysis

Facial paralysis is a loss of the facial animation resulting from facial nerve injury. In peripheral type of facial paralysis, the facial nerve injury is divided into 2 lesions; extratemporal and intratemporal lesions. Extratemporal lesion might exhibit a loss of function of the muscle of the facial expression, and can assess action of the main muscles that provided forehead wrinkle, eye closure, smile, snarl and lip pucker. On the contrary, hearing loss, tinnitus, imbalance, and facial numbness were assessed in intratemporal lesions also.[15, 36]

In extratemporal part of the facial nerve provides eyes protection, nasal control, lips together and facial animation. Especially, facial animation is a nonverbal signal for emotional expression in human communication.[5] Consequently, the facial nerve lesion lead to the facial dysfunction including eye exposure, brow ptosis, difficult to viewing, eating or drinking or communication.[8, 37] It also affected on quality of life, social isolation, and depression.[5, 17, 18]

Figure 5 The weakness of muscle of the facial expression caused by the facial nerve injury.[36]

2.2.1 Causes of facial paralysis

The facial paralysis was caused by a wide condition such as trauma, infection, metabolic, neoplastic, toxic, iatrogenic, and idiopathic.[7, 8, 38] Each cause results in different severity of the nerve injury.

1) Trauma

The head and neck trauma by blunt and perforating forces may affected temporal bone fracture. As a result, the facial nerve can damage in 7-10%. Normally, this trauma be caused by falls, motor vehicle accidents, violation, gunshot wounds.[7] Longitudinal and transverse types are the main fractures of the temporal bone. Blunt force effected to longitudinal fracture at the temporoparietal region in 70-80%, and influenced facial nerve damage in 15%. In contrast, transverse fracture can occur 10-20% of the blunt force mechanism, it induced facial nerve injury in 92% of this case.[39]

2) Infection

Generally, viral infections may trigger the acute facial nerve disease such as chickenpox, herpes zoster, mumps, influenza, and AIDS, as a result of facial paralysis.[7] Recently, coronavirus disease (COVID-19) can induce the facial paralysis for case report. Evidence indicated that Bell's palsy was supposed in pregnant woman with COVID-19.[40] According to Kerstens at al.[41] (2021), the COVID-19 patient with 27 years presented asymmetrical bilateral peripheral facial palsy; House-Brackmann grade V on the right and grade III on the left side. Moreover, bacterial and fungal infection can cause the facial palsy also. Form case report, patient with syphilis have drooling, facial disability, speech difficulties and progress to severe bilateral facial palsy.[42]

3) Metabolic

Metabolic disorder is one condition associated with abnormal of chemical level in human body such as diabetes mellitus, hyperthyroidism, pregnancy, hypertension, and vitamin A deficiency. These conditions are assumed to be cause of the facial paralysis.[7] Alanazi at al. (2017) explored the factors contributing to the facial palsy in 41 patients. The result revealed that hypertension may cause facial palsy in 4.9%, while diabetes mellitus can induce facial palsy in 12.2%.[43]

4) Neoplastic disease

Neoplastic disease is the abnormality of the tissue that as a result of atypical cell divisions. The facial nerve paralysis is most generally related to parotid undifferentiated carcinoma in 24%, squamous cell carcinoma in 19%, adenoid cystic carcinoma in 17%, adenocarcinoma in 11%, mucoepidermoid carcinoma in 9%, carcinoma ex pleomorphic adenoma in 7%, and acinic cell carcinoma in 1%. Incidentally, parotid malignant presented 7%-20% of facial palsy.[44]

5) Toxic

According to Basnayake et al.[45] (2019), a woman with 26 years old was admitted in the hospital with symptoms as abnormal renal function, short breathing, fever, decreased level of consciousness, stomach, vomiting, and facial palsy in the fight side (lower motor neuron lesion), after eating brake oil. Because it contents ethylene glycols and glycol ethers which effected to neurological and gastrointestinal systems. Similarly, arsenic poisoning has an effect on the facial nerve paresis.[46] Recently, Kim et al. (2020) suggested that air pollution with high concentrations of the nitrogen dioxide (NO_2) associated with Bell's palsy.[47]

6) Iatrogenic

The evidences showed that an iatrogenic injury during surgery at the parotid area frequently induced the facial nerve paralysis or paresis.[9-11, 48] These unexpected results might be caused by cutting or excessive stretching in surgical procedure, suturing in the SMAS layer, using large clamps or forceps during hemostasis, undue intensity of treatment protocol[1], or deoxycholic acid injections.[12]

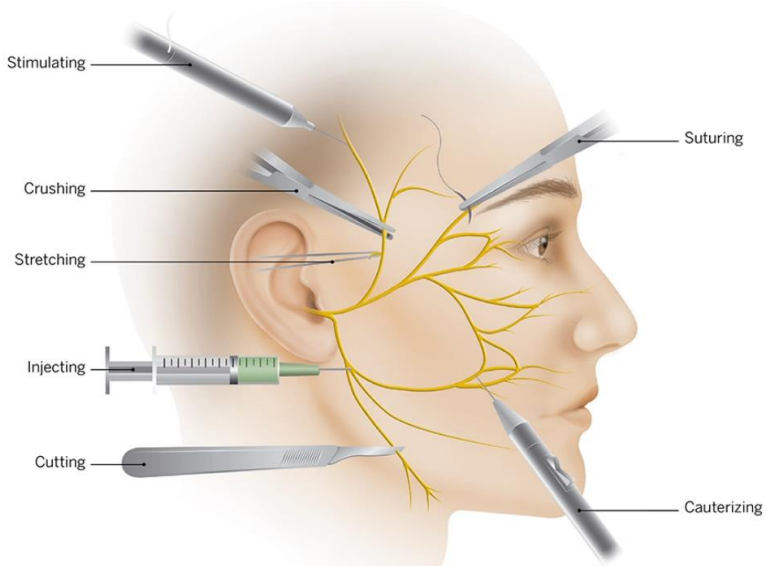

Figure 6 Illustration of the several procedure can effect facial nerve injury during a facelift dissection.[1]

The damage of facial nerve may occur during parotidectomy to treatment parotid diseases such as parotid abscess, parotid fistulas, sialoliths, benign tumors and malignant at parotid area.[49] Yang and Yoo (2014) [13] described that the facial nerve was damage by the preauricular incision in 3.2% - 42.9% and the submandibular incision in 5.3% - 48.1%. Moreover, rhytidectomy bring about injured in facial nerve was 0.4 to 2.6%, and the most facial nerve branch lesion are the frontal, marginal and cervical branches.[14] Meanwhile, 14.5% of permanent defect in facial nerve could be occurred after parotidectomy; further, the marginal mandibular branch lesion was the most complication (Figure 7).[15]

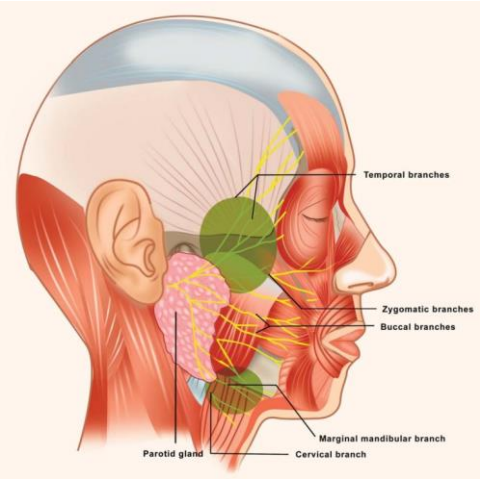

Figure 7 Danger zones of facial nerve injury (green area). The temporal and zygomatic branches might injury at the zygomatic arch and temporal area, and the marginal mandibular and cervical branch might injury at the jawline anterior to the masseter muscle.[12]

Although, the zygomatic and buccal branches were separated into many subbranches, temporary facial dysfunction can occur at the oral commissure (Figure 8).[12] In addition, the buccal branch was immolated in the parotidectomy bringing about weakness of zygomaticotemporal division in 9% and cervicomandibular nerve in 43% after operation.[16]

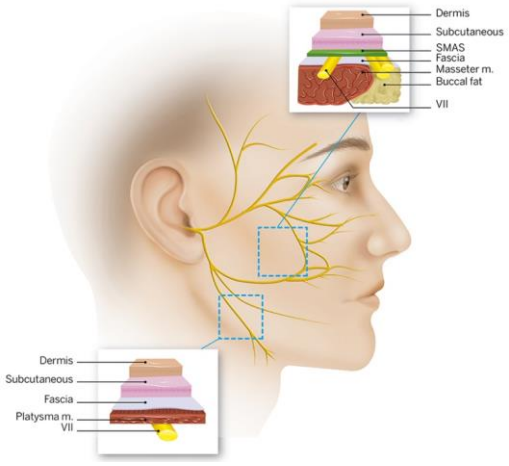

Figure 8 Danger areas of the buccal branch and marginal mandibular branches.[1]

According to Noqueira and Vasconcelos (2007), patients with temporomandibular ankylosis (8 female and 5 male) received treatment composed of gap arthroplasty, interpositional arthroplasty, reconstruction with prosthesis. The

complication was reported in 31% of the temporary facial palsy.[50] Moreover, Hohman et al. summarized that one hundred and two patients who were received medical surgery as oral surgery (20), head and neck surgery (25), orologic surgery (17), cosmetic surgery (11), and other procedure (7). The unexpected result was stated that the patients have the facial nerve injury such as hemiface (45.10%), upper division (23.53%), midfacial division (11.76), lower division (0.98), temporal branch(16.67), and marginal mandibular branch (11.55%).[51] Furthermore, marginal mandibular branch of the facial nerve was damage in 40% after the patients with condylar fractures received open reduction and internal fixation (ORIF) was reported by Singh (2020)[52]

7) Idiopathic

Bell's palsy is most commonly idiopathic peripheral facial paralysis.[47] Zhang et al. (2020) summarized that the main causes of the Bell's palsy composted of anatomical structure, viral infection, ischemia, inflammation, and cold stimulation.[53] The symptoms of this palsy obtain in 72 hours that including unilateral facial paralysis of both upper and lower face together with ear pain, dysgeusia, hyperacusis or facial numbness in 50-60%.[54]

2.2.2 Treatment for facial paralysis caused by facial nerve injury

The severity of the facial nerve injury is described by the House-Brackmann facial nerve grading system which the standardized degree including 6 levels of the facial nerve function; HB I to HB VI (Figure 9).[39] Moreover, the duration of injury and grade of facial function before injure are necessary for treatment. Therefore, duration of injury was classified into three periods; acute as injury within 3 days, subacute as after injury 6-12 months, and longstanding facial paralysis as after injury over 12-18 months. These periods will be analyzed for treatment of the facial paralysis such as direct nerve repair, nerve grafting, or nerve transfer for the best achievement. Furthermore, the intervention was used to regain the facial nerve injury depend on the mechanism and position of facial nerve injury.[38] According to Alomar (2021), the

facial nerve weakness temporarily occurred, and fully discovered in 6-12 months after parotidectomy.[21]

House-Brackmann facial nerve grading system		
Grade	**Description**	
Grade I	Normal	Good function
Grade II	Slight dysfunction	Forehead - moderate to good function Eye - complete closure with minimum effort Mouth - slight asymmetry
Grade III	Moderate dysfunction	Forehead - slight to moderate movement Eye - complete closure with effort Mouth - slightly weak with maximum effort
Grade IV	Moderate severe dysfunction	Forehead - none; Eye - incomplete closure Mouth - asymmetric with maximum effort
Grade V	Severe dysfunction	Forehead - none; Eye - incomplete closure Mouth - slight movement
Grade VI	Total paralysis	No movement

Figure 9 The House-Brackmann facial nerve grading system.[52]

1) Primary neurorrhaphy

Primary neurorrhaphy is the best treatment for acute extracranial facial nerve injuries. The principles of this procedure for good result, the nerve must be remaining of proximal and distal nerve endings, and absent of nerve tension. Because tension will induce scarring and suppress regeneration of axon.[38] End-to-end neurorrhaphy is a directly procedure of the facial nerve repair, and usually manage within 30 days after nerve injury for facial expression recuperation. Both nerve endings are identified and trimmed, they are stained by methylene blue to differentiate them from other tissues. After that, perineurial sutures are performed to connect the both ending. As a result, the function of the facial nerve can recover and symmetry of the face is restored. Although, the result will perform excellent outcome within 30 days, the facial nerve becomes atrophy and has fibrosis after 30 days (after injury).[39]

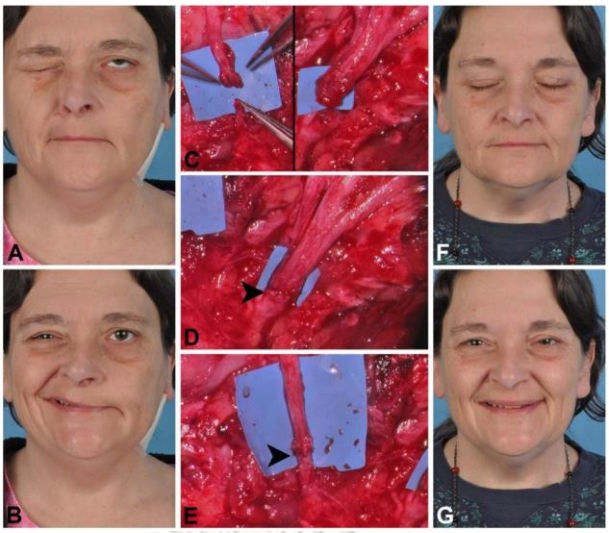

Figure 10 Patient with left-sided iatrogenic facial nerve injury after parotidectomy for benign disease, and primary neurorrhaphy is performed lasting 5 months.[51]

2) Nerve grafting

Nerve grafting is the second selection for repair the facial nerve injury that present gab between proximal and distal nerve endings.[38]

3) Nerve transfer

Nerve transfers are atypical intervention for acute period of the nerve injury, whereas this procedure is common treatment for subacute period.[38] The masseteric nerve is the popular option for replacement facial nerve injury in the same side, since it has suitable size, advisable position and low morbidity. The advantage of the masseteric nerve in facial reanimation composed of better recovery and reducing mass movement, while tone of the facial muscle can restore by using the hypoglossal nerve transposition. Therefore, the masseteric nerve can improve faster symmetrical animation of the face than the hypoglossal nerve.[17]

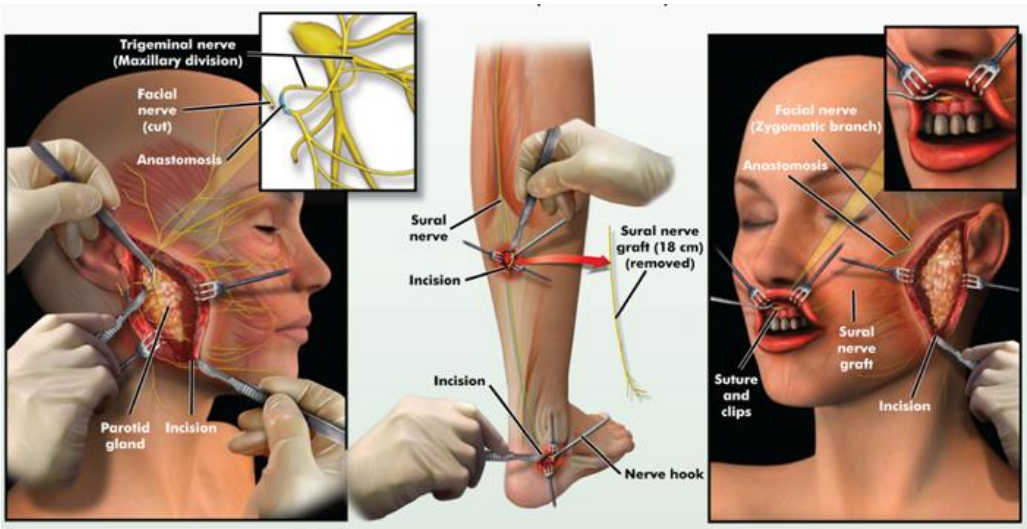

Figure 11 Masseteric-facial nerve transfer[55]

4) Reanimation procedures

Facial reanimation procedure is the surgery for reconstruction of the facial function after nerve paralysis. The destinations of facial reanimation are symmetrical face at rest and excellent facial function without involuntary movement.[36, 56] Facial reanimation is separated into 2 methods; one-stage and two-stage reanimation. The distinction between one-stage and two-stage reanimation that is one-other nerves will be used in stage reanimation, while the facial nerve will be used in two-stage reanimation using for restoration of facial function. Additionally, the movement of face may present in 18 and 4-6 months after received two-stage and one-stage reanimation, respectively.[38]

Figure **12** Patient with asymmetrical face at rest (A), in eye closing (B), during smile (C), and the functions of the face were restored by using reanimation procedure (D, E, F)[56]

Two-stage reanimation

Two-stage reanimation consists of facial nerve donor selection and functional muscle transplant. Firstly, the contralateral facial nerve is stimulated for mapping the location of the branches of the facial nerve for selection to supply the transplanted muscle. Normally, smile or eye closing were activated, then two branches of the facial that perform the same function are mapped. After that, once the facial nerve branch is cut, and the sural nerve was harvested for connection between the normal side to the paralyzed side of the face. Secondly, a functional muscle transplant is performed between 6-12 months after axonal growing in first procedure. Generally, the gracilis muscle was used to transplant in this process (Figure 13).[17, 38]

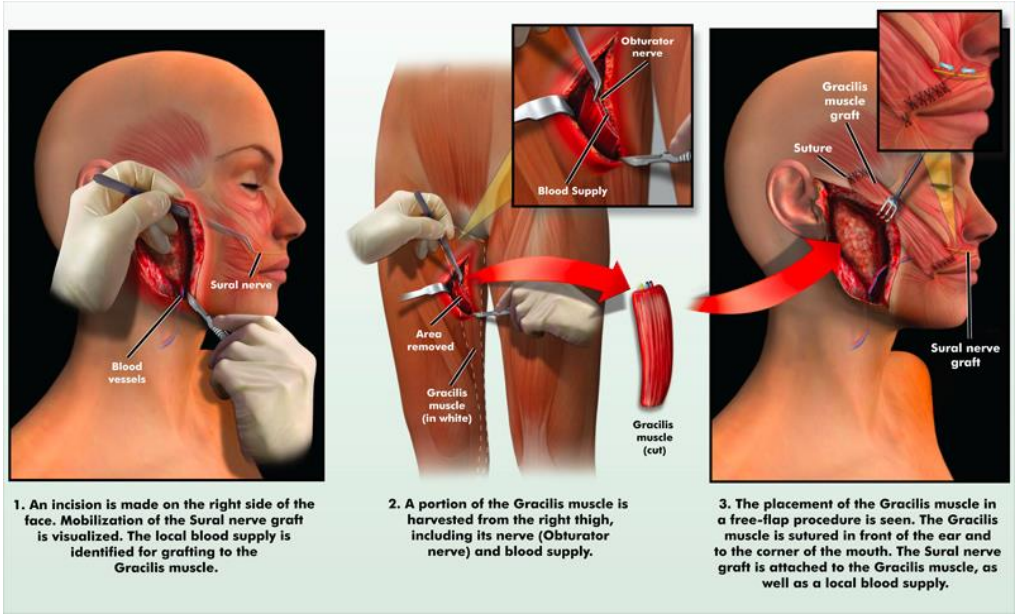

Figure 13 Gracilis muscle transplants[57]

One-stage reanimation

One stage reanimation is reconstructive surgery same as the second procedure of a two-stage reanimation, but the masseteric nerve or other non-facial nerve was used to supply the transplanted muscle instead of using the facial nerve (Figure 14). The masseteric nerve is popular for replacement and was encountered at the subzygomatic triangle.[58]

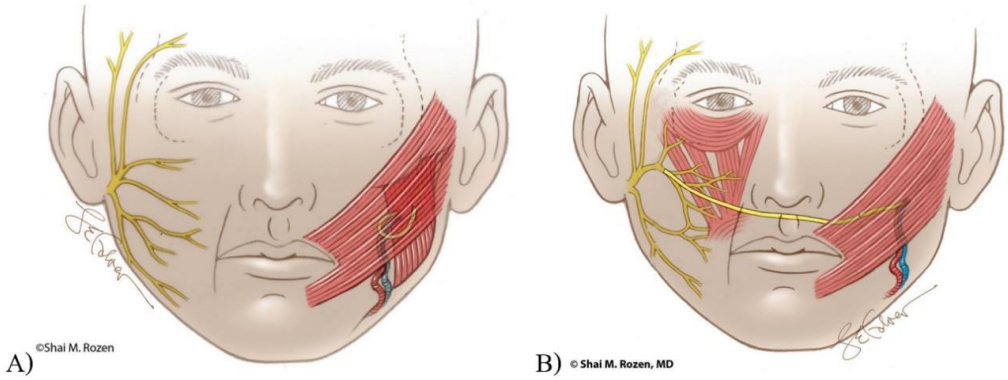

Figure 14 Reanimation procedures for generating facial tone and facial expression; one-stage reanimation (A), and two-stage reanimation (B).[38]

5) Lengthening temporalis myoplasty (LTM)

Formerly, the masseter and temporalis muscles were selected in dynamic muscle transfer for lower facial reanimation. Lately, the masseter muscles have

limitations in their function, because they are a limited range of tissue rotation, and have a less masticatory function.[7] Nowadays, the temporalis muscle can provide good results for improvement the facial function owing to short duration of surgeries, rapid recovery in facial movement, and not requirement for microsurgery proficiency (Figure 15).[38] Panossian[59] (2016) explained that the lengthening temporalis myoplasties were operated in 14 children with facial paralysis which derive from Möbius syndrome, posterior cranial fossa tumors, posttraumatic, hemifacial microsomia, and idiopathic. The result suggested that the lengthening temporalis myoplasties is safe procedure to restore dynamic smile in children.

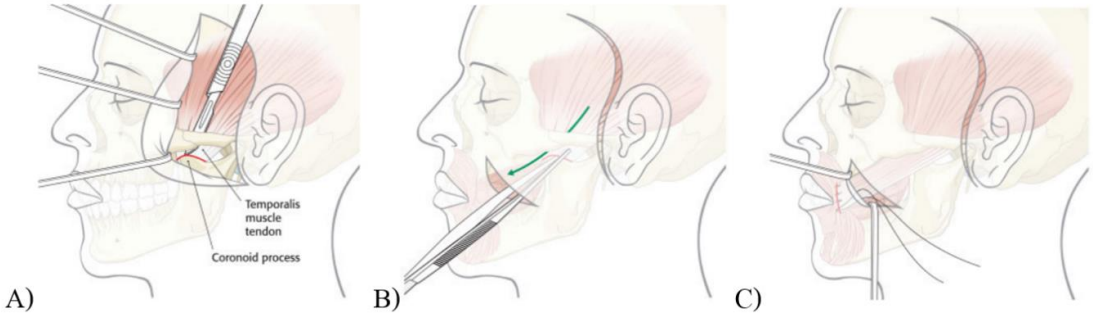

Figure 15 Lengthening temporalis myoplasty procedure; the temporalis tendon was released from the coronoid process (A), the temporalis tendon was inferomedially transferred to the corner of mouth (B), and the temporalis tendon was passed through the tunnel of the buccal fat pad, then it was connected to the corner of mouth and upper lip (C).[7]

6) Other medical treatment

Facial asymmetry is the secondary condition that result from the facial nerve paralysis. A botulinum toxin type A (BoNTA) is minimal invasive procedure to regain symmetrical face at normal and movement stages by using low dose of BoNTA. Additionally, this procedure could be performed in regenerative period approximately 1-6 months after nerve injury. Heydenrych [60, 61] applied BoNTA to inject patients with synkinesis. After BoNTA injections in synkinesis, symmetrical face can restore about 6 months. Synkinesis is the abnormally involuntary coactivation of the facial muscle by reason of atypical facial nerve regeneration about 6 months, and presented in 15-55%

after the facial nerve paralysis. It occurs only ipsilateral side and related to the contraction of both agonists and antagonist muscle. Ordinary synkinetic patterns comprise of oral-ocular, ocular-oral, ocular-glabellar, platysmal, and mentalis synkinesis (Figure 16).[60]

Figure 16 Patient with left platysmal and mentalis synkinesis at movement stage (A) and achievement after BoNTA injection on the mentalis, depressor labii inferioris, orbicularis oris and orbicularis oculi muscle.[60]

Futhermore, hyperkinesis is one involuntary movement, and can occur both at rest and during movement after facial nerve paralysis. Therefore BoNTA was injected on the contralateral of the face in patient with hyperkinesis for improvement overactivity of the muscles (Figure 17).[62] Sadiq et al. suggested that BoNTA can provide symmetrical face in patient with facial paralysis about 4 months, and had complication after injection in 28.57% (4 in 14 cases) approximately 3-7 days.[63]

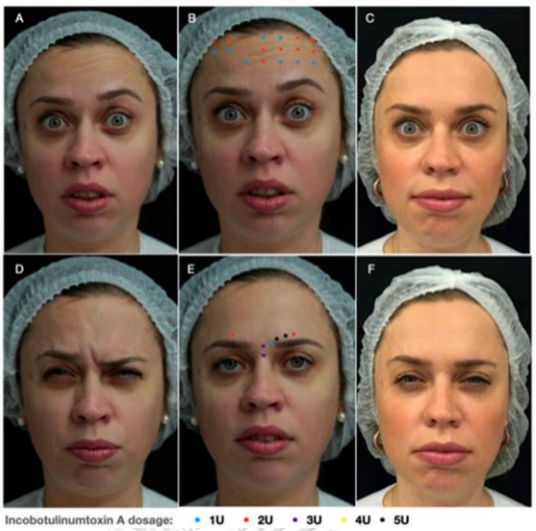

Figure 17 Patient with overactivation of the muscle of the forehead (A) and the eyebrow (D). Injection point of BoNTA at the forehead (B) and the eyebrow (E). Achievement of BoNTA injection (C, F).[62]

2.3 The facial nerve and its terminal branches

The anatomical study of the facial nerve is essential for protection the nerve in a facial treatment procedure. The landmarks for determine the site of the facial nerve are wide such as the zygomatic arch, orbital rim, angle of mandibular bone, mastoid process, eye brow, lateral canthus, lobule and oral commissure.[6] Kwak et al. (2004)[20] mention that the trunk of the facial nerve after exiting from the stylomastoid foramen was identified during parotidectomy together with facial nerve repair. Similarly, length and portion pattern of the trunk of the facial nerve being important in parotidectomy was describe by Alomer (2021).[21] Furthermore, precise landmarks associated with the facial nerve and branches is meaningful to anticipated the specific location and safe area during maxillofacial surgery, neck dissection, face lift or plastic surgery.[6, 64] In addition, the diameter and the number of axons of the facial nerve are clinically significant for nerve graft in facial reanimation.[23]

2.3.1 The segments of the facial nerve

The facial nerve as seventh pair of cranial nerves is a mixed nerve that include motor and sensory nerve fibers, and three nuclei of the facial nerve are situated at the

brain stem. A complex pathway of the facial nerve consists of cisternal, intracanalicular, petrous and extratemporal segments before ramification into terminal branch on the face. In cisternal segment, the motor nerve fiber of the facial nerve ascends from pons to the cerebellopontine angle where the oligodendrocytes transform into Schwan cell. Then, the facial nerve appears from cerebellopontine angle as the motor root and the intermediate nerve. The large motor root of the facial nerve stimulates the muscles of the facial expression, while the small intermediate nerve conducts parasympathetic, special and somatic sensory fibers. In intracanalicular segment, the motor root and the intermediate nerve travel in the subarachnoid space of the posterior cranial fossa, and are assembled at anterosuperior portion of the internal acoustic meatus. In petrous segment, the facial nerve travel laterally, and is divided into three parts; labyrinthine, tympani and mastoidal parts. In labyrinthine part, the facial nerve travel along the fundus of the internal acoustic meatus to the geniculate ganglion. In tympanic part, it runs horizontally between the vestibule and the tympanic membrane from the geniculate ganglion. In mastoidal part, the facial nerve vertically descends between the tympanic membrane and the auditory canal, and originated three branches; acoustic, chorda tympani and sensory branches. In extratemporal segments, the facial nerve appears from the stylomastoid foramen, and provides posterior auricular nerve and digastric nerve. After that, it penetrates the posteromedial surface of the parotid gland, and divides into temporofacial and cervicofacial divisions between superficial and deep lobes of gland which the same as plane of the salivary duct. Next, the terminal branches of the facial nerve emerge the border of the parotid gland for facial muscle innervation.[3, 11, 26, 64, 65]

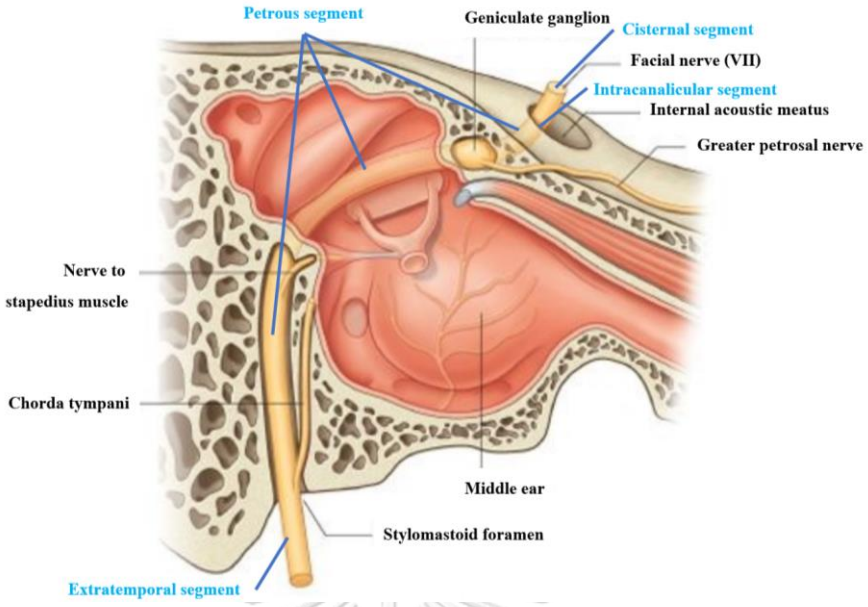

Figure 18 The pathways of the facial nerve in temporal bone.[66]

Furthermore, the length of the facial nerve was 14.0 (8.6 - 22.8) mm.[67], and diameter was 3.27 ±0.75 (2.03-4.88) and 3.44 ±0.68 (2.20-4.81) mm in right and left side respectively.[68] Similarly, Thuku et al.[69](2018) found that the distance of the emerging point of the facial nerve to its furcation was 16.15 (3.28) mm. Previously, the distance between the emerging point of the facial nerve trunk from the stylomastoid foramen to the furcation point was 13.0 ±2.8 mm, and the average depth of the stylomastoid foramen from the skin surface was 21.0 ±3.1 mm (Figure 19).[20]

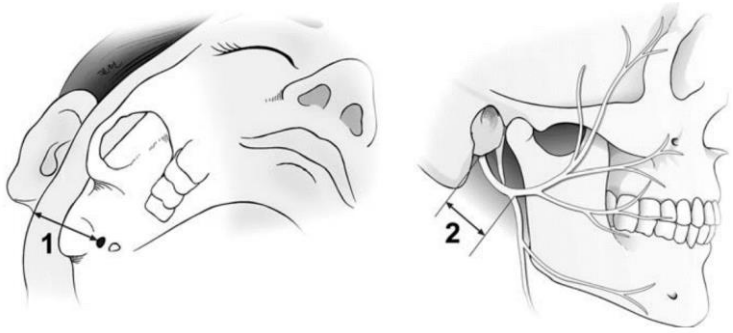

Figure 19 The measurements of the facial nerve trunk in the intraparotid area. Depth of the stylomastoid foramen from the skin surface (1), Distance between the emerging point of the facial nerve trunk from the stylomastoid foramen to the furcation point (2).[20]

2.3.2 The facial nerve trunk and its branches

The anatomy of the face and the extratemporal segment of the facial nerve are essential for dermatologists and surgeons in preservation of the facial nerve, carefully dissection, and completely removing the tumors.[20, 26] Many researches have been widely investigated the distance of the anatomical landmarks to the facial nerve trunk (Table 1)(Figure 20).[4, 67, 70-77]

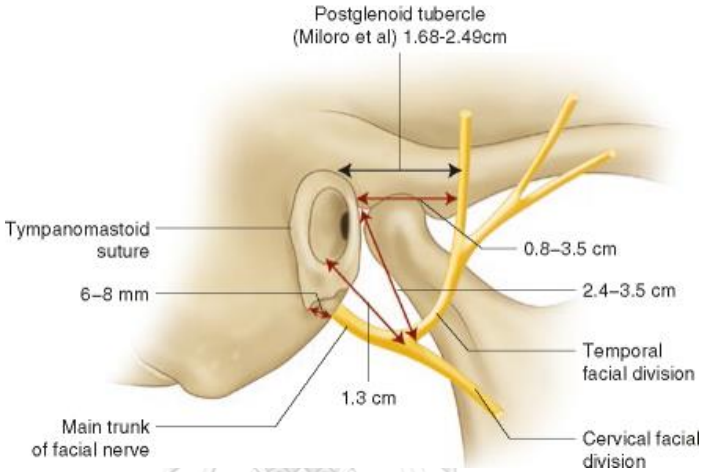

Figure 20 Distance of the temporal branch of the facial nerve correlated to the external auditory.[70-72]

Table 1 The distance of the facial nerve trunk to the anatomical landmarks.

Anatomical landmarks	**Distance to FNT** Mean (mm)	**Specimens**	**Age** (years)	**References**
Tragal pointer	18.6 ± 6.0	Thirty-eight patients with parotidectomy	51.8 (17.3)	Wong[78] (2001)
	8.4 ± 3.6 7.3 ± 2.4	Thirty halves of cadavers.	N/A	de Ru et al.[79] (2001)
	34 (24.3-49.2)	Forty adult South African White cadaveric	72 (51–93 years)	Pather and Osman[67] (2006)

Anatomical landmarks	**Distance to FNT** Mean (mm)	**Specimens**	**Age** (years)	**References**
	6.9 ± 1.8 (3.4-11.3)	Twenty-six embalmed Caucasian cadavers (n =52)	83 (59–98)	Rea et al.[73] (2010)
	16.61 (14-21) 16.36 (13.5-19)	Ten cadaveric Ten patients with parotidectomy	N/A	Saha et al.[74] (2014)
	19.12 (16.5-21.5)	Thirty patients	34 ± 3	Ullah et al.[75] (2017)
	9.30 ± 0.93 (7.67-10.78)	Twenty-two hemifaces of 11 cadavers	N/A	Stankevicius and Suchomlinov[4] (2019)
Posterior belly of digastric	12.4 (7-17)	14 cadavers 22 patients	N/A	Witt et al.[76] (2005)
	13.4 (7.3 - 21.9)	40 adult South African White cadaveric	72 (51–93 years)	Pather and Osman[67] (2006)
	5.5 ± 2.1 (2.5-9.2)	Twenty-six embalmed Caucasian cadavers (n =52)	83 (59–98)	Rea et al.[73] (2010)
	7.41 (6-9.5)	Ten cadaveric Ten patients with parotidectomy	N/A	Saha et al.[74] (2014)

Anatomical landmarks	**Distance to FNT** Mean (mm)	**Specimens**	**Age** (years)	**References**
	8.03 (6-11.5)			
External auditory canal	10.0 (4.9 – 18.6)	40 adult South African White cadavers	72 (51–93 years)	Pather and Osman[67] (2006)
Tympanomastoid suture	1.8 (0-4)	14 cadavers 22 patients	N/A	Witt et al.[76] (2005)
	9.8 (4.3 – 18.6)	40 adult South African White cadavers	72 (51–93 years)	Pather and Osman[67] (2006)
	2.5± 0.4 (2.1-3.6)	Twenty-six embalmed Caucasian cadavers (n =52)	83 (59–98)	Rea et al.[73] (2010)
	3.5 (2.5-4.5) 3.87 (2-6)	Ten cadaveric Ten patients with parotidectomy	N/A	Saha et al.[74] (2014)
Styloid process	16.9 (9.7 - 36.8)	40 adult South African White cadaveric	72 (51–93 years)	Pather and Osman[67] (2006)
Transverse process of the axis	38.1 (25.3 - 48.69)	40 adult South African White cadaveric	72 (51–93 years)	Pather and Osman[67] (2006)
Angle of the mandible	36.45 ± 4.14 (25.84-44.39)	Twenty-two hemifaces of 11 cadavers	N/A	Stankevicius and Suchomlinov (2019)

Anatomical landmarks	**Distance to FNT** Mean (mm)	**Specimens**	**Age** (years)	**References**
Tip of mastoid process	12.52 ± 2.30 (8.99-17.26)	Twenty-two hemifaces of 11 cadavers	N/A	Stankevicius and Suchomlinov (2019)
	10.3 ± 1.79	Thirteen hemiface of 7 Caucasian cadavers	71 (66-77)	Al-Qahtani et al.[77] (2020)
Osteocartilaginous junction	9.2 ± 1.58	Thirteen hemiface of 7 Caucasian cadavers	71 (66-77)	Al-Qahtani et al.[77] (2020)

Pather and Osman[67] [78, 79](2006) indicated that the invariable anatomical landmarks consist of tragal pointer, the posterior belly of digastric and transverse process of the axis, but the tragal pointer is blunt irregular cartilage, unstationary, unsymmetrical edge. In addition, the tympanomastoid suture was the constant landmark to identify the FNT. Moreover, Stankevicius and Suchomlinov[4] (2019) demonstrated that the nerve localization requires anatomical landmarks which are superficial, easy palpation, and noncomplex tissue. Although, the tragal pointer able marked wherever because it is big cartilage, it cannot be considered as a constant landmark to localize the facial nerve trunk.

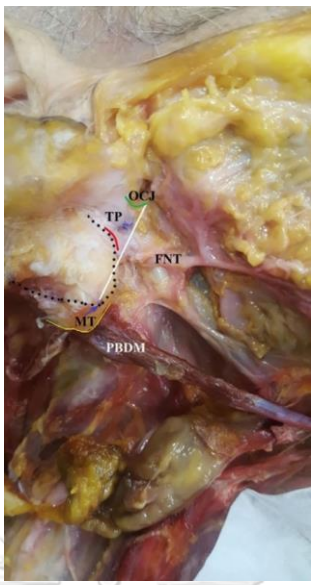

Figure 21 Right side of the face in the cadaveric dissection presents anatomical landmarks and the facial nerve trunk (FNT). TP, tragal pointer; MT, tip of mastoid process (blue arrow); PBDM, posterior belly of the digastric muscle, mastoid process (black dotted line), the osteocartilagenous junction (OCJ) (green line), the tympanomastoid suture (red line)[77]

The patterns of the facial nerve were first explained by Davis et al. in 1956. Six types (I, II, III, IV, V and VI) of this was identified related to anastomosis of the terminal branches (Figure 22). These categories have been widely used in the several literatures.[4, 21] Thuku et al.[69] (2018) explained that the percentages of different patterns of the facial nerve depending on the Davis et al. classification was type I in 25%, type II in 22.5%, type III in 17.5%, type IV in 15%, type V in 5%, and type VI in 15%. Moreover, the facial nerve trunk was divided into bifurcation of the division in 80% and trifurcation in 20% (Figure 22). According to Myint et al.[80] (1992), there are 3.8% of trifurcation of the facial nerve trunk, and the branching pattern of the facial nerve included type I (11.39%), type (II 15.9%), type III (34.18%), type IV (18.98%), type V (7.59%) and type VI (12.67%). Moreover, the distance between the bifurcation and the angle of the mandible was 28.06 mm.

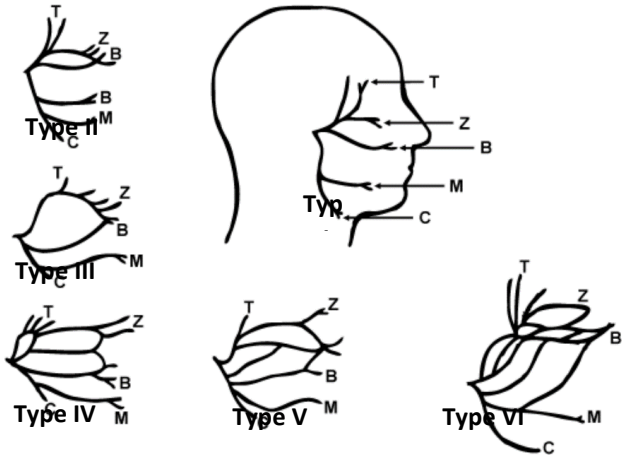

Figure 22 Six branching pattern of the facial nerve. Type I, Type II; absence of an anastomosis between the temporofacial and cervicofacial division, but presence anastomosis among the terminal branches of the temporofaciai division only. Type III; single anastomosis among the branches of the temporofacial division and cervicofacial division, Type IV; combination of type II and III, Type V; double anastomosis between the temporofacial and cervicofacial division, Type VI; complex multiple anastomosis between the two divisions, where the buccal branch receives many anastomotic fibers from the cervicofacial and the marginal mandibular branch.[80, 81]

Next, Katz and Catalono[82] (1987) conducted a new category including I-A, I-B, II, III-A, III-B, III-C, IV-A, V-B and V type by using origin of buccal branch, terminal branches anastomosis, and number of terminal branches for classification that different from Davis et al. categories. After that, Kopuz et al. separated type of branching pattern of the facial nerve in 1994. It was found that 24% of the specimen absented connection (Type I), 12% had connection between the buccal and the zygomatic branches (Type II), 14% had connection between the buccal and another branches (Type III), 38% of the specimen presented complicated connection as multiple loops (Type IV), and 12% of the specimen presented two main trunks of the facial nerve (Type V).[69, 83]

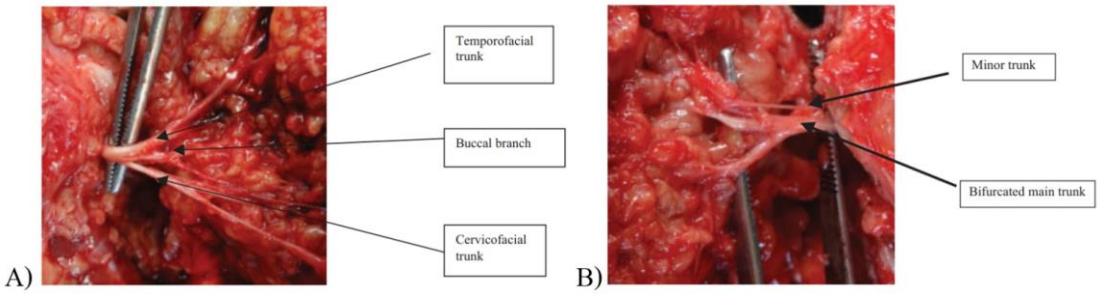

Figure 23 Furcation of the facial nerve trunk in cadaveric dissection. Trifurcation (A), Bifurcation and a minor branch (B)[69]

Furthermore, Kwak et al.[20] (2004) classified the branching pattern of the facial nerve base on the origin of the buccal branch into 4 types (Figure 24). Type I was identified by the buccal branches originated from the temporofacial and cervicofacial divisions. Type II was identified by the buccal branches originated from the temporofacial and cervicofacial divisions that communicated with the zygomatic branch. Type III was identified by the marginal mandibular branch communicated with the buccal branch, which originated from the temporofacial and cervicofacial divisions. Type IV was identified by the buccal branch communicated with both the zygomatic and marginal mandibular branches. The result showed that the branching pattern of the facial nerve consist of type I in 13.8%, type II in 44.8%, type III in 17.3%, and type IV in 17.3%. Likewise, the facial nerve trunk bifurcation was found in 86.7%, while trifurcation was found in 13.3%. Also, the facial nerve communicated with the auriculotemporal nerve were found in 93.3%.

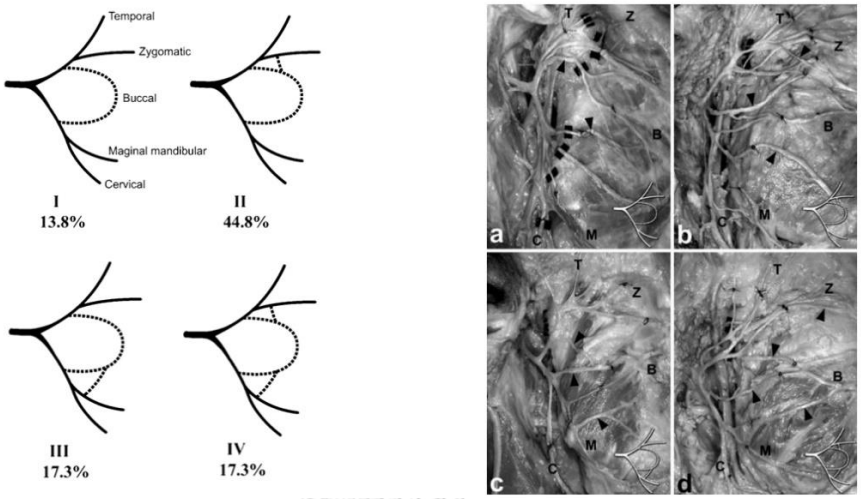

Figure 24 Four types of the branching patterns of the facial nerve base on the origin of the buccal branch.[20]

Later, Yang and Yoo[13] (2014) descripted that the pattern of the facial nerve at the condylar area included type I as single trunk, Type II as double trunks, and Type III as nervous loop or plexiform. Besides, the zygomatic branch of the facial nerve crossed the tragus-alar line 23 mm anterior to the tragus in the most cases, and more than half of the specimen presented the complex branching type at the anterior area of the tragus (Figure 25). [13]

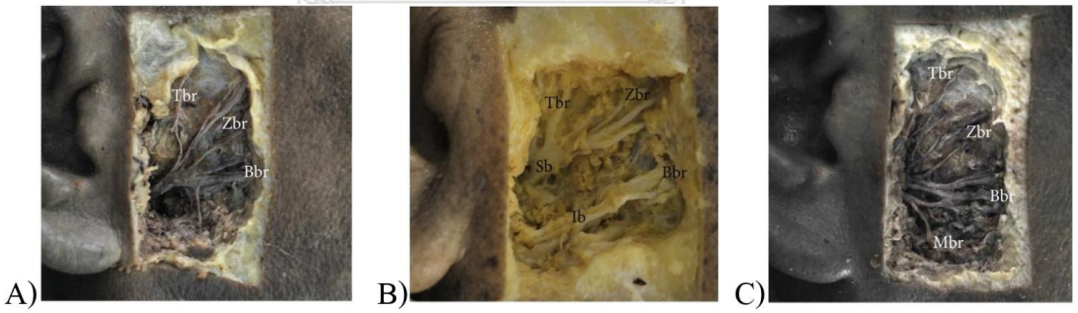

Figure 25 Three types of branching pattern of facial nerve at the condylar area. (A) Type I (single trunk), (B) Type II (double trunks), and (C) Type III (nervous loop or plexiform). Tbr, temporal branch; Zbr, zygomatic branch; Bbr, buccal branch; Mbr, marginal mandibular branch; Sb, superior trunk; Ib, inferior trunk.[13]

Recently, Pascual et al. (2019) investigated the extratemporal part of facial nerve pattern in 23 embalmed Caucasian adult cadavers. The result show that all specimens have temporofacial and cervicofacial division, and terminal branches included temporal, zygomatic, buccal, marginal mandibular and cervical branches. In

addition, there are variation of the number of the terminal branches. Moreover, the branching pattern of the facial nerve can classify into 12 different types consist of type 1; absence communication between terminal branches and the buccal branch originated from either temporofacial or cervicofacial division, type 2; absence communication between terminal branches, presence double mandibular branch and the buccal branch originated from the cervicofacial division, type 3; presence communication between temporal, zygomatic and buccal branches, and the buccal branch originated from either temporofacial or cervicofacial division, type 4; presence a temporofacial–cervicofacial communication, and the buccal branch originated from the cervicofacial division, type 5; presence a buccal–mandibular communication, and the buccal branch originated from temporofacial division, type 6; presence communication between temporofacial branches and the temporofacial and cervicofacial divisions, and the buccal branch originated from the cervicofacial division, type 7; presence communication between temporofacial and cervicofacial divisions, and the buccal branch originated from the cervicofacial division, type 8; presence a complicated connections between temporal, zygomatic, buccal and marginal mandibular branches, and the buccal branch originated from either temporofacial or cervicofacial division, type 9; presence a complicated connections between temporal, zygomatic, buccal and marginal mandibular branches, and the buccal branch originated from both temporofacial and cervicofacial division, type 10; presence a double facial nerve trunk, and the accessory trunk is communicated with the temporofacial division, type 11; presence a double facial nerve, the main trunk as the temporofacial division, and the accesory trunk as the cervicofacial division, and type 12; it is same as type 11 and the accessory trunk communicate with the cervicofacial division (Figure 26).[19]

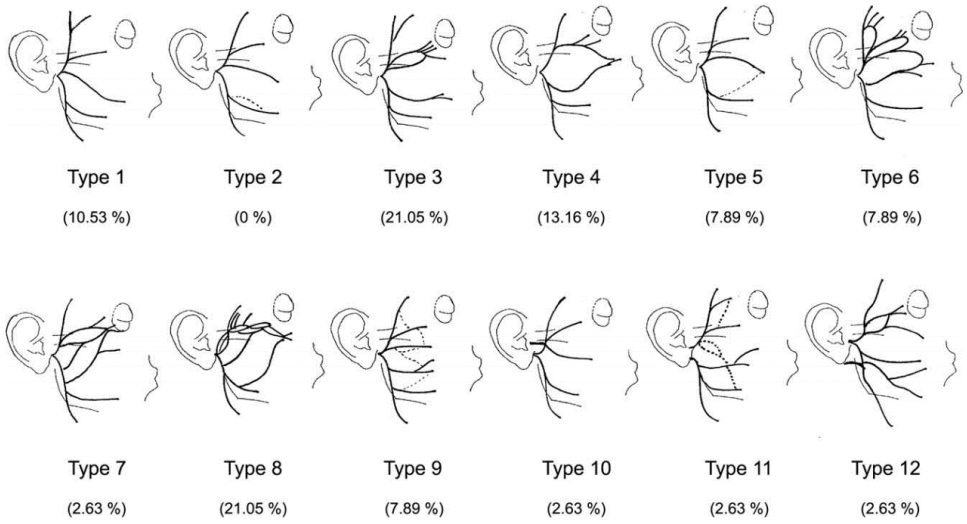

Figure 26 Illustration of the new patterns of the facial nerve was classified by Pascual et al. in 2019.[19]

2.3.3 Temporal branch of the facial nerve

The temporal or temporal branchof the facial nerve appears from superior border of the parotid gland approximately 3-4 rami, which regarding to innervate the orbicularis oculi, the corrugator supercilli and the frontalis muscle. The mean of length and diameter of the temporal branch were 30.10 ±6.89 mm and 0.94 ± 0.33 mm, respectively. [19]

Several researches have been extensively determined the anatomy of the temporal branch for prevention nerve injury. Al-Shaikh et al.[11] (2015) explained that the temporal branchlocated anterior and parallel to the superficial temporal artery, and had single ramus in 80% two branches in 20% of cases. In all cases, the temporal branchwas found to be anterior and parallel to the superficial temporal artery. Formerly, Bernstein and Nelson[25] (1984) reported that the rami of the temporal branch were classified into 4 types; type I (middle ramus support to posterior ramus), type II (posterior ramus mainly support to middle ramus), type III (No support from posterior ramus), and type IV (equal support between posterior and middle rami. Moreover, the percentages of the specimen in each type was 13%, 35%, 13% and 39% respectively (Figure 27).

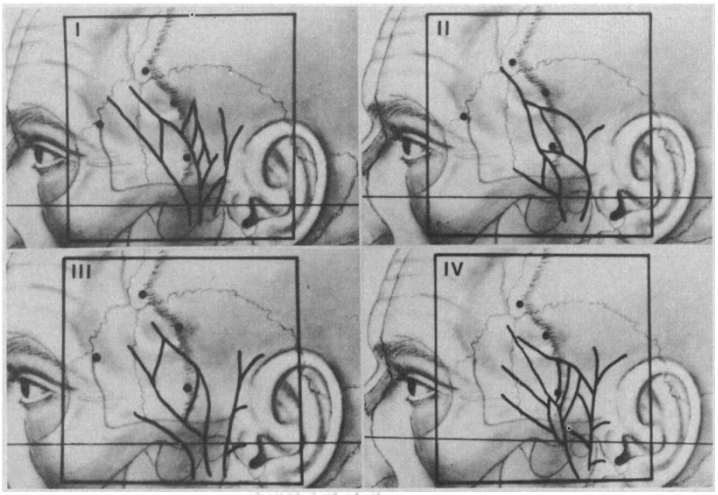

Figure 27 Four types of temporal branch of facial nerve were classified by Bernstein and Nelson in 1984.[25]

According to Hwang, Kim and Chung[84] (2004), the temporal branch of the facial nerve was found 2-4 rami at the zygomatic arch, and there were normally 3 rami. Furthermore, the distance between the temporal branch and supraorbital notch or foramen was 10 mm, and it located superior to the supraorbital rim approximately 2.8-25 mm. It contained 4-7 small twigs (the mean was 5 twigs), and inferior twigs of the middle ramus of the temporal branch supplied the corrugator supercilii muscle at the supraorbital area. Additionally, the anterior and middle rami of the temporal branch run to supply frontalis and the superior portion of the orbicularis oculi muscle.[10, 85]

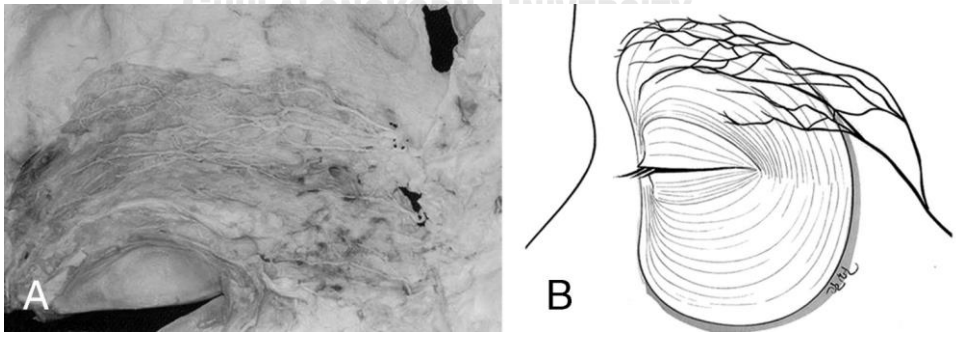

Figure 28 The temporal branch in the upper part of the orbicularis oculi muscle. Twigs of the temporal branch of the facial nerve ran horizontally follow the muscle fibers of the orbicularis oculi muscle with mutual connections(A). Illustration of the twigs of the temporal branch in the orbicularis oculi muscle. (B)[10]

For localization of the temporal branch from the zygomatic arch to the galeal frontalis fusion point was investigated by Lettieri in 2008. The result showed that the main trunk of the temporal branch was located superior to the sentinel vein and it traveled deep and within the fusion point. Therefore, performing procedure in the galeal temporal region should be carefully intervention, and avoid electrocautery or using sharp dissection.[86] For this result, the injury of the temporal branch of the facial nerve in frontotemporal area bring about weakness of the frontalis, orbicularis oculi, and corrugator supercilii muscles.[24] In addition, it is defenseless at the lateral border of the frontalis muscle, because this area has a little of subcutaneous fat between the nerve and the skin. Moreover, the surface anatomy landmarks for identification the temporal branch is still discussion in several surgeons.[39] According to Davies et al.[6] (2013), anatomical landmarks were used to identify temporal branch such as line from lateral canthus to superior border of zygomatic arch, junction of zygomatic arch and root of helix, lateral canthus, anterior aspect of external acoustic meatus, zygomatico-temporal and fronto-zygomatic sutures (Porion).

Later, the course of the temporal branch was examined in 4 of anatomical landmarks (the superior part of the poratid gland, the zygomatic arch, the lateral canthus, and the superior temporal line) by Poblete et al. (2015) in 2015. The result revealed that the temporal branch perforated the parotidmasseteric fascia at the superior part of the parotid gland and inferior to the zygomatic arch. It was found 2-4 rami include anterior, middle and posterior rami. Then, these rami were placed in the loose areolar tissue at the zygomatic arch level. The distance between the anterior border of the tragus and the posterior rami of the temporal branch was 15.3 ±3.5 mm at the level of superior border of the zygomatic arch. At the lateral canthus level, the orbicularis and frontalis muscle were innervated by the temporal branch which usually originated from the anterior and middle rami of the temporal branch. In this level, the temporal nerve was placed in the loose areolar layer between the galea and the temporal fascia that contain the fibrofatty tissue, then it crossed at a mean distance of 40.4 ±3.3 mm superior to the lateral canthus. After that, the anterior and middle

rami of the temporal branch ran obliquely to the superior temporal line for innervation the frontalis and orbicularis muscles, whereas the posterior ramus of the temporal branch approach to the superficial temporal artery and continuous to supply the auricularis muscle. At superior to the superior temporal line, the temporal branch was located above frontal pericranium and divided into 3-5 twigs in frontalis muscles. In addition, the most posterior rami of the temporal branch crossed the superior temporal line at intersection point approximately 35 mm from the lateral canthus.[24]

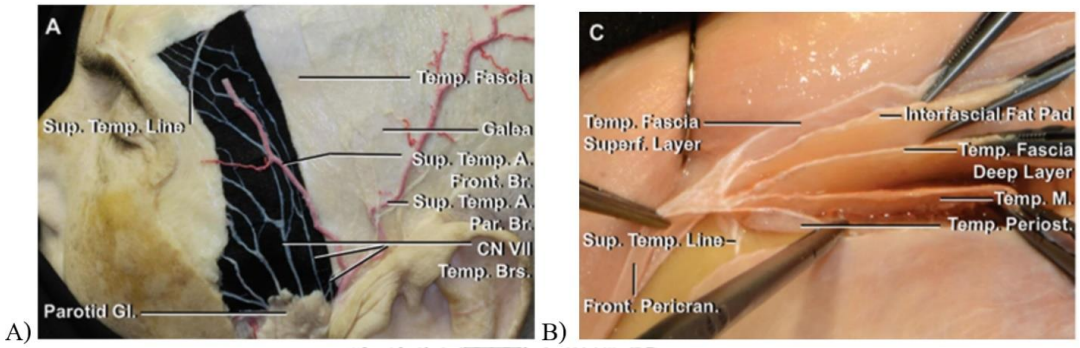

Figure 29 The course of the temporal branch of the facial nerve at temporal area (A). The tissue layers of temporal area (B). [24]

Furthermore, Agarwal et al.[33] (2010) discovered that the temporal branch was located in innominate fascia after perforated the parotid-masseteric fascia, and transitioned to the inferior surface of the superficial temporal fascia before innervation the muscles (Figure 30). The fascial transition point was investigated by using cadaver dissection and Masson's trichrome stain in 18 and 6 hemifaces respectively. It was found that the fascial transition zone covered the area from 15-30 mm superior to the upper border of the zygomatic arch (y axis) and 9-14 mm behind the lateral orbital rim (x axis)

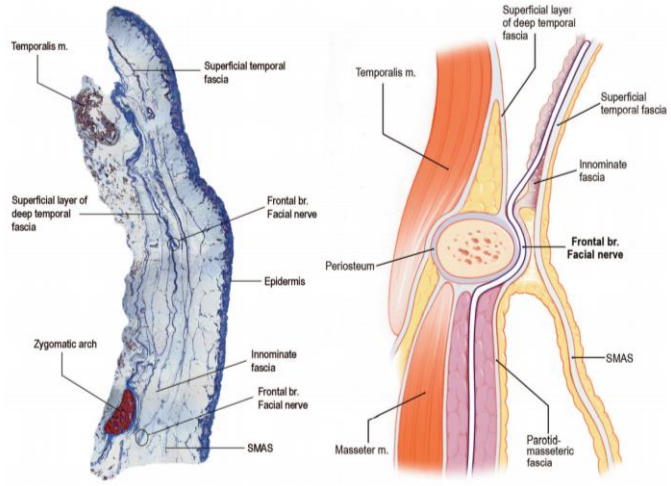

Figure 30 The location of the temporal branch correlated to the facial tissue layers in Masson's trichrome stain. The temporal branch was located in the fibrofatty innominate fascia at the level of the zygomatic arch, while it was placed in innominate fascia where the inferior surface of the superficial temporal fascia at above the area of zygomatic arch (Left). Illustration of the course of temporal branch associated with the fascial planes of the parotid and temporal area (Right). [33]

In the same way, Pankratz et al.[87] (2020) exposed that the course of the temporal branch was embedded in the temporoparietal fascia at level of the superior to the zygomatic arch in 94%, while it placed within the temporoparietal fascia at the zygomatic arch in 6%. Besides, the mean distance between the zygomatic arch and the temporal branch of the facial nerve was 9.61 ±5.08 mm. Furthermore, the temporal branch transitioned from a sub-SMAS to intra-SMAS layers at the distance 12.19 ± 4.77 mm posterior to the Pitanguy's line, and the surgical caution zone was 9.6 mm superior to the zygomatic arch and 12.2 mm posterior to Pitanguy's line.

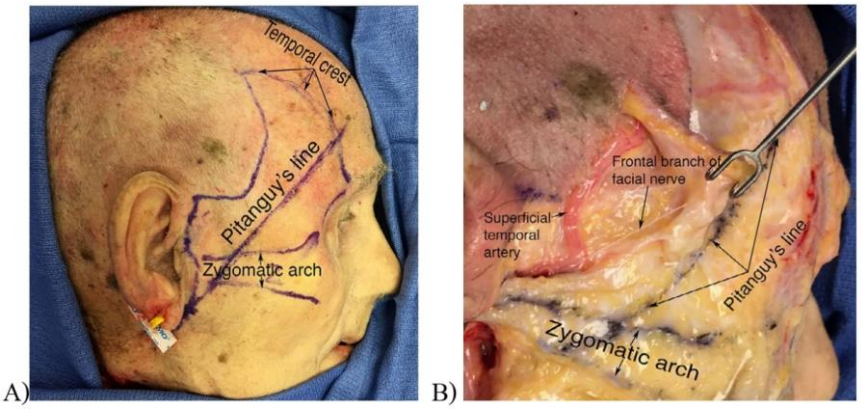

Figure 31 The lateral view of the face in the cadaveric dissection with the skin markings of Pitanguy's line, zygomatic arch, and temporal crest (A). The perforation of temporal branch of the facial nerve in the temporoparietal fascia correlated to the zygomatic arch and Pitanguy's line.[87]

Moreover, Bonnecaze et al.[88] (2015) determined that the zones of the temporal branch to predict the nerve injury risk in twelve fresh cadavers. The result revealed that the high risk of the temporal branch injury was presented in the mean distance 22.60-26.06 mm from the anterior of the tragus at the level of the inferior border of the zygomatic arch, 27.46-30.43 mm from the anterior of the tragus at the level of the superior border of the zygomatic arch, and 16.20-19.17 mm posterior to the lateral border of the orbit.

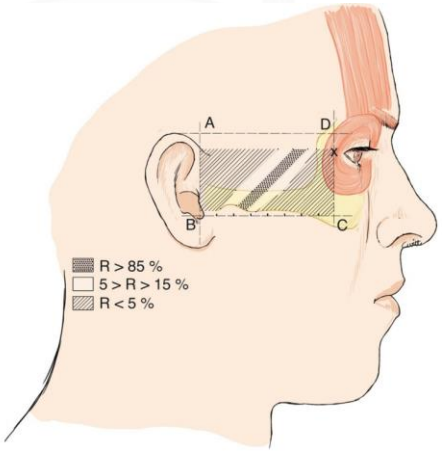

Figure 32 The zones of injury risk of the temporal branch of the facial nerve at the temporal region that was divided into minor risk (0-5 %), moderate risk (5-15 %), and high risk (more than 85 %).[88]

In addition, the temporal branches were divided into the posterior and anterior branches. The posterior branches supply the superior auricular muscle, whereas anterior branches supply the frontalis and upper orbicularis muscles (Figure 33).[89]

Figure 33 The temporal branches of the facial nerve and other structure at the temporal regions.[89]

2.3.4 Zygomatic branch of the facial nerve

The zygomatic branch of the facial nerve commonly has a1-3 rami after emerge from the anterior border of the parotid gland. It penetrated the fascia at about 40 mm anterior to the tragus, then travel to innervate the orbicularis oculi and the zygomaticus major muscle. The mean of the length and diameter of the zygomatic branch was 38.02 ±6.64 mm and 1.00 ±0.46 mm, respectively [19, 39] According to Al-Shaikh et al.[11] (2015), the zygomatic branch has a single ramus in 60% and two rami in 40% of cases after emerging from the parotid gland, then it ran superior and continuous to the lateral canthus.

Moreover, anatomical landmarks were determined to location of the zygomatic branch of the facial nerve consist of anterior border of parotid gland, tragus and lateral canthus, root of helix and oral commissure.[6] Erbil et al.[90] (2007) investigated that the distance from emerging point of the parotid duct to the crisscrossing of the zygomatic branch and duct was 3.53-23.26 mm., and the zygomatic branch communicated with buccal branches at the area where the duct penetrated the buccinator muscle.[81, 90]

In addition, Dorafshar et al. (2013) stated that the zygomatic branch can identify by using Zuker's point which the midpoint between the root of the helix and the oral commissure when the mean distance between the root of the helix and the oral commissure was 107 mm (Figure 34).[91]

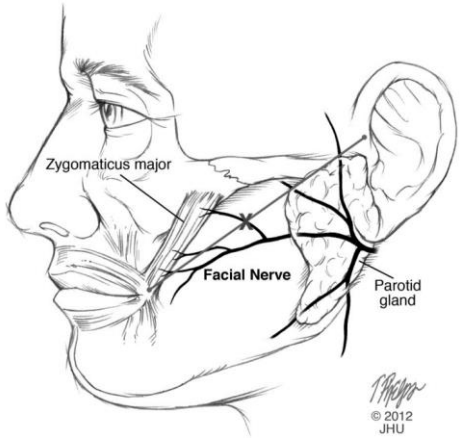

Figure 34 Illustration of the anatomical surface to identify of the zygomatic branch of the facial nerve. Zuker's Point (x)[91]

2.3.5 Buccal branch of the facial nerve

Liu et al.[2] (2010) found that the buccal branches of the facial nerve gave 1-3 rami (8.3%, 33.3% and 58.3% respectively) penetrated the anterior border of the parotid gland. The buccal branch located superior to the parotid duct was 10.3 ±5.1 mm, and inferior to the parotid duct was 10.8 ±5.0 mm. Besides, the diameter of the nearest buccal branch to the parotid duct was 1.6 ±0.4 mm. Additionally, the mean length of the buccal branch was 37.87 ±7.33 mm., and the diameter of the buccal branch was 0.99 ±0.40 mm that was measured by Pascual et al. in 2019. It innervates the zygomaticus, orbicularis oris and levator labii superioris muscle which response for lip movement and blowing.[19] Furthermore, the origin of the buccal branch was classified by in 77 cases. It was found that the buccal branch originated from the temporofacial division in 7.79%, the cervicofacial in 72.73%, main bifurcation in 12.99%, multiple origin in 11.69%.[16] Normally, the parotid duct, and tragus were used to classified the buccal branch of the facial nerve.[6]

Next, Al-Shaikh et al.[11] (2015) explained that the buccal branch were positioned both superior and inferior to the parotid duct and presented multiple rami in highest cases include 2 branches in 50%, 3 branches in 30%, 4 branches in 10%, and 5 branches in 10% of specimens. In addition, the location of the buccal branches was classified into 2 types correlated to the buccal fat pad; type I refers to the course of the nerve crossing superficial to the buccal fat pad, and type II refers to the course of the nerve penetration to the buccal fat pad. It was found that it crossing superficial to the buccal fat pad in 73.7% and penetration to the buccal fat pad in 26.3%. After that, the rami of the buccal branch ran superior-medial to the intercanthal line at approximately one third laterally.

Previously, the buccal branch was divided into 4 types by Saylam et al. in 2006. Firstly, the buccal branch presented single rami emerge from the anterior margin of the parotid gland, and located inferior to the parotid duct was classified to type I. Secondly, types II indicate the buccal branch had single rami and located superior to the parotid duct. Thirdly, the buccal branches shaped a buccal plexus in many forms was identified to type III. Lastly, the buccal branches had rami was located in both superior and inferior to the parotid duct were classified in type IV. The result of this study presented that 35% of the specimens was identified in type I, while 25% of the specimens was identified in type II. Moreover, buccal branches were classified into type III and IV were 26.7% and 13.3% respectively. Besides, the distance between emerging point of the buccal branch and tragus was 35.62 ±7.11 mm.[92]

In addition, the position of the branch of the facial nerve was investigated in 42 hemifaces of cadavers by using irregular hexagon which used the anatomical point follow as A; upper border of the tragus, B; lateral canthus, C; lateral oral commissure, D; angle of the mandible, F; the midpoint of the distance between Point D and the intersection of inferior border of the mandible and the anterior border of facial artery, and G; tip of the mastoid process (Figure 35A). It was revealed that 3 to 7 branches of the zygomatic-buccal branches pass through B-C (Figure 35B). Moreover, the buccal branch was reported into 4 types include type I; classic type, type II; buccal branches

arose from the marginal mandibular branch, type III; sweeper type, and type IV; the buccal branches arose from the temporozygomaticobuccal branch (Figure 36).[64]

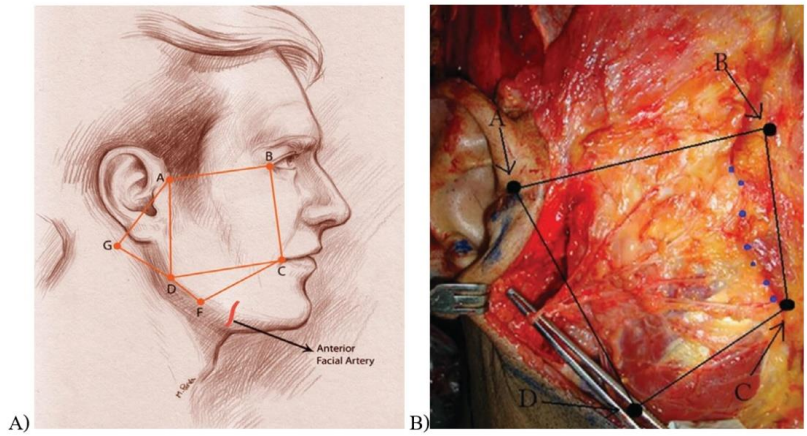

Figure 35 Illustration of irregular hexagon; A; upper border of the tragus, B; lateral canthus, C; lateral oral commissure, D; angle of the mandible, F; the midpoint of the distance between Point D and the intersection of inferior border of the mandible and the anterior border of facial artery, and G; tip of the mastoid process (A). The Zygomatic-buccal branches (blue dots) pass through B-C line and it located in quadrangle ABCD.[64]

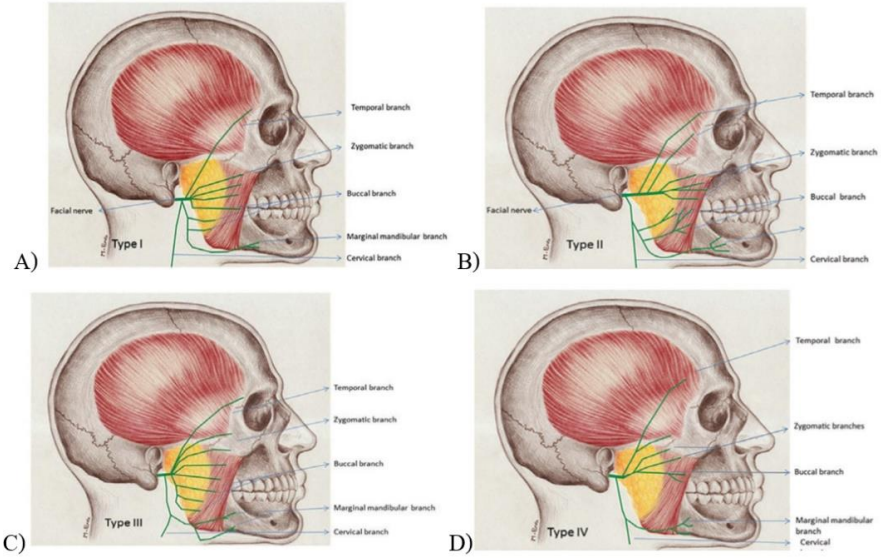

Figure 36 Illustration of 4 types of the buccal branch; type I; classic type (A), type II; buccal branches arose from the marginal mandibular branch (B), type III; sweeper type (C), and type IV; the buccal branches arose from the temporozygomaticobuccal branch (D)[64]

2.3.6 Marginal mandibular branch of the facial nerve

The marginal mandibular branch of the facial nerve was identified by using anatomical landmarks such as angle of mandible, anterior margin of the parotid gland, ear lobule, gonion, facial artery, retromandibular vein, or masseteric tuberosity.[6] After the marginal mandibular branch exiting from the anterior margin of the parotid gland, it gave 1-3 branches which position around the border of mandible, and travel superficial to the facial artery and vein. The percentage of the number of the marginal mandibular branch was summarized in Table 2. Moreover, Pascual et al.[19] (2019) reported that the mean of the diameter of the marginal mandibular branch was 0.8 ±0.34 mm, and the length was 33.13 ±8.98 mm.

Table 2 The percentage of the number of the marginal mandibular branch

Specimens	**Age (years)**	**The number of branches of the marginal mandibular branch**			**Relationship to the vessel**	**References**
		Single branch	2 branches	3 branches		
Six fresh human adult cadavers	36-52	41.7%	50.0%	8.3%	N/A	Liu et al.[2] (2010)
30 hemi face and neck in embalmed cadaver	N/A	36.7%	43.3%	20%	superficial to the facial vessels in 83.3%	Khanfour and Metwally[9] (2014)
20 hemiface in embalmed cadaver	N/A	40%	40%	20%	superficial to the facial artery and vein	Al-Shaikh et al.[11] (2015)

Specimens	Age (years)	The number of branches of the marginal mandibular branch			Relationship to the vessel	References
		Single branch	2 branches	3 branches		
46 hemifaces in embalmed cadavers	N/A	84.2%	15.8%	none	N/A	Pascual et al. [19] (2019)

According to Khanfour and Metwally[9] (2014), the marginal mandibular branch communicate with its branches in 53.6% (Figure 37). For example, the main rami of the marginal mandibular branch connect to its the secondary branches. Furthermore, the marginal mandibular branch communicated with the buccal branch, the anterior branch of the great auricular nerve, and the transverse cervical nerve in 40%, 3.3% and 3.3% respectively. The midpoint between angle of the mandible and symphysis menti was used to observe the relationship of the marginal mandibular branch and inferior border of mandible. It was revealed that the marginal mandibular branch located superior to this point in 80%, inferior to this point in 10%, and at this point in 10% of the specimens. Moreover, the marginal mandibular branch which located superior to the inferior border of the mandible, the branches traveled inferior to the superficial layer of the parotid fascia, whereas the marginal mandibular branch which located inferior to the inferior border of the mandible passed into the investing layer of deep cervical fascia. After that, the distal branch traveled deep to the depressor anguli oris muscle in all cadavers. [9] Likewise, Balagopal, George and Sebastian[93] (2012) conducted in 202 patients (144 males and 58 females) who underwent neck dissection for cancers treatment between June 2005 and October 2006. The result reveled that the lowest branch crossed the facial artery 8 mm inferior to the inferior border of the mandible

and the highest branch crossed the artery 5 mm superior to the inferior border of the mandible. Also, the mean distance between intersection of the marginal mandibular nerve and the facial artery to the inferior border of the mandible was 1.73 ±1.57mm inferior to the mandible.

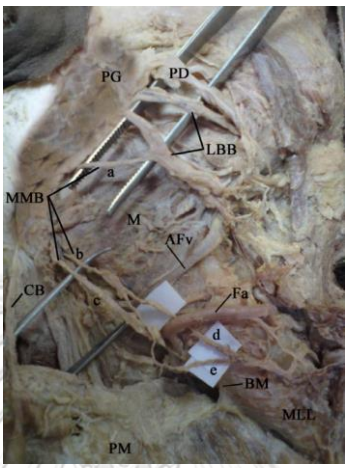

Figure 37 The main branches of marginal mandibular branch of the facial nerve including superior, middle and inferior branches (a, b and c), respectively. d and e, secondary rami of the marginal mandibular branch; AFv, the anterior facial vein; Fa, the facial artery; BM, inferior border of the mandible; LBB, the lower buccal branch; PG, parotid gland; PD, parotid duct; PM, platysma muscle; CB, cervical branch of the facial nerve; M, Masseter muscle; MLL, Muscles of the lower lip).[9]

2.3.7 Cervical branch of the facial nerve

The cervical branch arose from the cervical facial division of the facial nerve, and gave 1-3 rami (Figure 38A, B, C) for supplying the platysma muscle. The mean length and diameter was 40.55 ±12.78 and 0.83 ±0.15 mm, respectively.[19] According to Salinas et al.[94] (2009), the cervical branches was investigated by using the cadaveric dissection and modified Sihler stain for observation the extramuscular and intramuscular rami in 20 and 8 specimens, respectively. The multiple cervical branches were found in 85% of the specimens, and communicate with the transverse cervical nerve. Moreover, it connected to the marginal mandibular branch in 35% (Figure 38D), and co-innervated the depressor anguli oris with the marginal mandibular branch in 5% (Figure 38E).

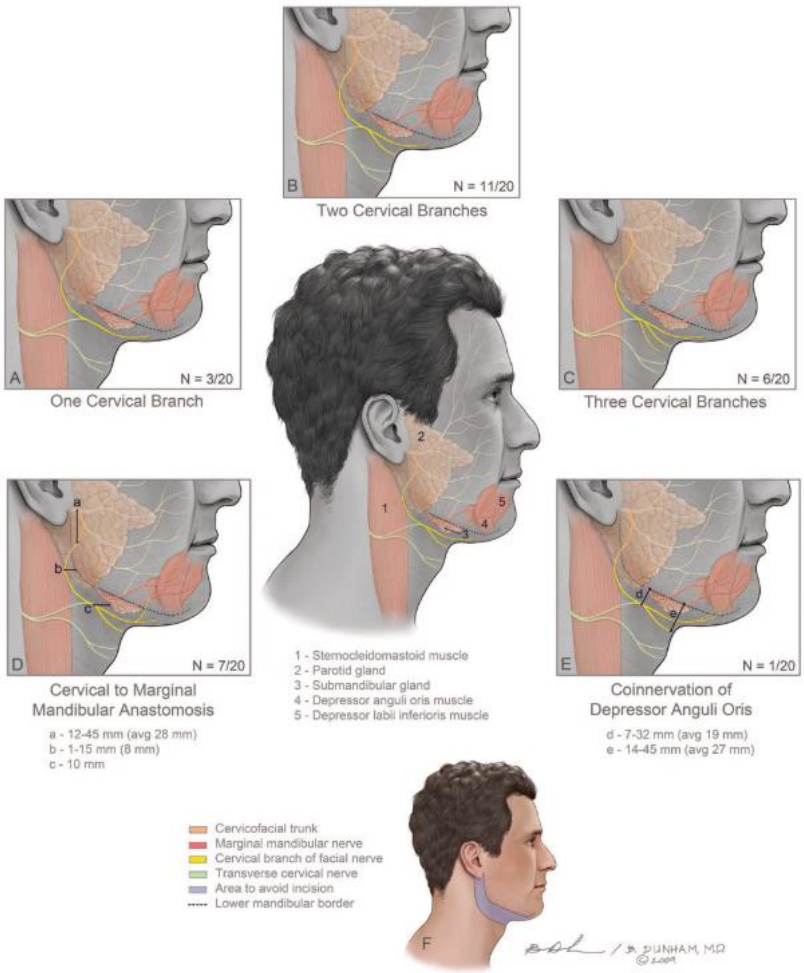

Figure 38 The anatomy of the cervical branch of the facial nerve consists of the number of rami of the cervical branches (A-C), communication between cervical and marginal mandibular branches (D), coinnervation the depressor anguli oris of cervical and marginal mandibular branches (E), and submandibular danger zone (F). 1, sternocleidomastoid muscle; 2, parotid gland; 3, submandibular gland; 4, depressor anguli oris muscle; 5, depressor labii inferioris muscle, cervical nerve branches (yellow line), transverse cervical nerve (green line), main cervicofacial trunk (orange line), the marginal mandibular branch (red line); a, distance between the facial nerve trunk and the cervical branch; b, distance between the cervical branch and the angle of the mandible; c, minimum distance between the parotid gland and separation of the cervical branches; d, distance between the inferior border of the mandible and the transverse cervical nerve communication; e, distance between inferior border of the mandible and the most inferior cervical nerve branch.[94]

2.3.8 Angular nerve

The angular nerve is originated from the buccal branch or zygomatico-buccal plexus which supply the procerus muscle[95] According to Caminar Newman and Boyd[85] (2006), the angular nerve ran superomedially in the levator labii superioris alaeque nasi, and supply this muscle. after that, the angular nerve ran superiorly and crossed medial canthus to innervate the procerus and corrugator supercilia muscles. It was located medially to the angular vein, and laterally to the angular artery. Next, Yang et al.[96] (2010) described that the angular nerve was divided into 3 types in 20 hemiface of fresh cadaver. In type I of the angular nerve, it was identified as single rami from zygomatic-buccal plexus, and it was found in 20%. In type II, the angular nerve from zygomatic-buccal plexus in the "Four Muscle Gap" was found in 20% of the specimens. In type III, the angular nerve gave 2 rami in the "Four Muscle Gap", and it was found in 60% of the specimens. Furthermore, entering point of the rami of the angular nerve in the depressor supercilii or procerus was 2.19-4.28 mm superior to the medial canthus ligament, while entering point of the rami of the angular nerve in the levator labii superioris alaeque nasi was 6.89-9.38 mm inferior to the medial canthus ligament.

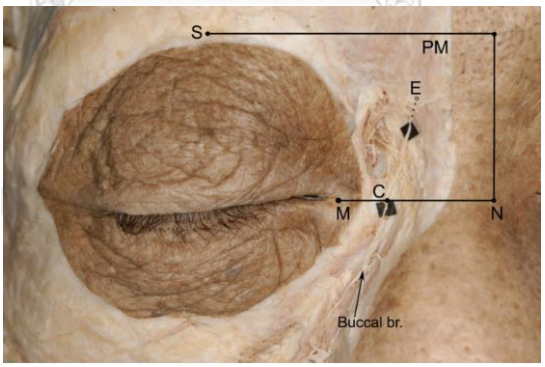

Figure 39 The terminal branch of the buccal branch in cadaveric dissection (right side); E, entering point of the buccal branch into the procerus muscle (PM); M, medial canthus; N, nasion; S, tangential level of the supraorbital rim; C, crossing point.[10, 95]

2.4 Innervation the muscle of facial expression of the facial nerve

The muscles of the facial expression commonly originate from the bone surfaces or periosteum and insert to the skin or combine with other muscles (Figure 40).[97] Moreover, the facial muscles were divided into 4 layers follow as:

First layer muscles; orbicularis oculi, risorius, zygomaticus minor, and depressor anguli oris muscles

Second layer muscles; depressor labii inferior, risorius, zygomaticus major, levator labii superioris aleque nasi, and platysma muscles

Third-layer muscles; orbicularis oris, and levator labii superioris muscles

Fourth-layer muscles; buccinators, mentalis, and levator anguli oris muscles

The first-three layers of the muscles are covered by the superficial fascia and create the SMAS-mimetic muscle complex. As a result, this layers as the SMAS. The branch of the facial are located under to SMAS layers, Consequently, the facial nerve innervate the three superficial layer muscles from their posterior surface, while the deeply muscles are innervated by facial nerve from their anterior surface.[26]

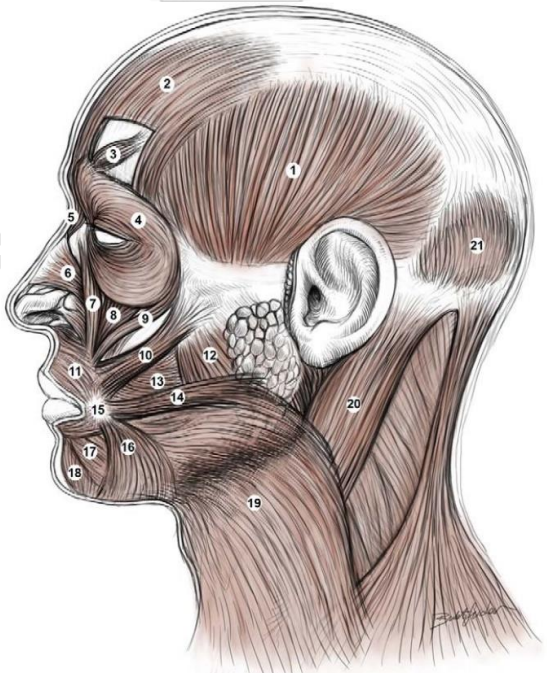

Figure 40 The muscles of the facial expression and masticatory muscles. (1) temporalis, (2) frontalis, (3) corrugator supercilii, (4) orbicularis oculi, (5) procerus, (6) nasalis, (7) levator labii superioris aleque nasi, (8) levator labii superioris, (9) zygomaticus

minor, (10) zygomaticus major, (11) orbicularis oris, (12) masseter, (13) buccinator, (14) risorius, (15) modiolus, (16) depressor anguli oris, (17) depressor labii inferioris, (18) mentalis, (19) platysma, (20) sternocleidomastoid, (21) occipitalis.[26]

2.4.1 Frontalis muscle

The frontalis muscle or the anterior belly of the occipitofrontalis muscle is the largest muscle of the upper face. It originates from the epicranial aponeurosis and inserts the skin of the eyebrow and the orbicularis oculi and corrugator supercilii muscles. Therefore, the tension of the frontalis muscle maintains the normal position of the eyebrow in resting, while its contraction brings to elevate the eyebrows when providing the face act of surprising.[26] Poblete et al.[24] (2015) illustrated the averages length of the frontalis muscle from the supraorbital rim to its superior border was 64.1±5.7 mm. The posterior rami of the temporal branch ran deeply to the lateral border of the frontalis muscle at 19.0 ±2.8 mm superior to the supraorbital rim. Consequently, the temporal branch entered the frontalis muscle at anterior 1/3 of muscle length, and extend upward (Figure 41).

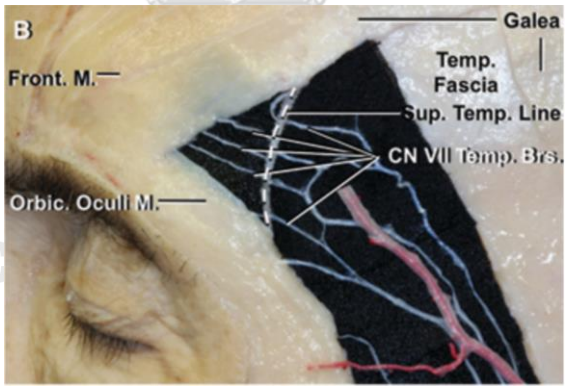

Figure 41 The 3 rami of the temporal branches crossed the superior temporal line, and entered the frontalis muscle. [24]

2.4.2 Orbicularis oculi muscle

The orbicularis oculi muscle is flat muscle surrounding the eyes, and extend to the anterior temporal area, infraorbital cheek, and the superciliary area. Then, it inserts to the skin of the eyelids. The orbicularis oculi muscle is divided into the orbital and palpebral parts. The orbital part originates from the nasal part of the frontal bone, the frontal process of the maxilla, and the medial canthal tendon. Additionally, the

function of the palpebral part play in role blinking to moist the cornea, whereas the orbital part provides closing of the eyes to protect the eye ball. The contraction of the muscle was innervated by the temporal and zygomatic branches of the facial nerve.[26] According to Spiegel and DeRosa[98] (2005), the orbicularis oculi muscle was placed on 5 mm superficial to the zygomaticus major muscle at 20 mm lateral to the lateral canthus, and on 8 mm superficial to the levator labii muscle at the midpupillary line. Furthermore, the zygomatic branch approximately 3-5 rami pierced the orbicularis oculi muscle, then it stimulated the middle and lateral part of the muscle. On the other hand, the medial and lower part of the orbicularis oculi muscle was stimulated by 1-2 rami of the buccal branch.[10]

2.4.3 Corrugator supercilii muscle

The corrugator supercilia muscle is conical muscle was placed posterior to the frontalis and orbicularis oculi muscles. The corrugator supercilia muscle originates from the medial border of the superciliary arch, then it ran superolaterally to the skin of the middle portion of the eyebrow. It acts in the brow depression and frown lines production. The corrugator supercilia muscle was innervated by the middle ramus of the temporal branches of the facial nerve in the supraorbital region.[10, 26, 97] Moreover, the corrugator supercilia muscle was innervated by rami of the temporal, zygomatic and buccal branches of the facial nerve.[85]

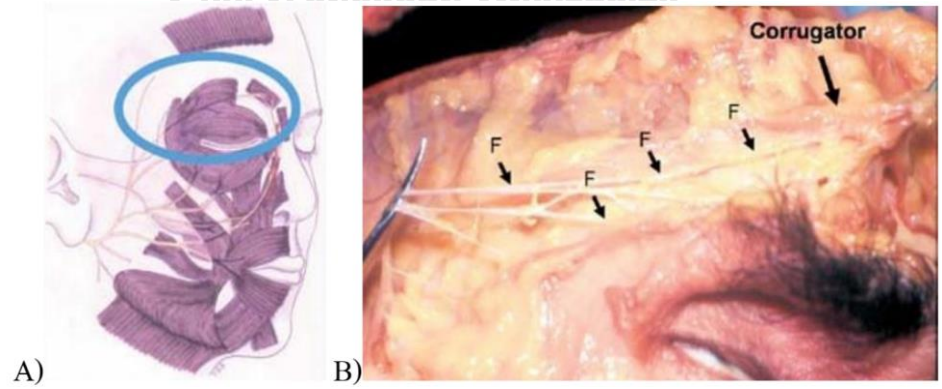

Figure 42 Illustration of the eyebrow area for dissection (A), and the temporal branch the corrugator supercilia and the orbicularis oculi muscle (B); F, temporal branch of the facial nerve.[85]

2.4.4 Procerus muscle

The procerus muscle is the superficial muscle of the bridge of the nasal area, it originates from the lower part of the nasal bone and inserts to the skin of glabella area. The action of procerus muscle creates horizontal wrinkle at the bridge by draw the forehead inferiorly. It was innervated by the temporal branch of the facial nerve.[26] In contrast, Hwang [10] (2014) demonstrated that the superficial buccal branches mainly stimulated the procerus muscle.

2.4.5 Orbicularis oris muscle

The orbicularis oris muscle is the muscle surrounding the mouth, and it separated into deep and superficial part. The deep part of the orbicularis oris muscle extend from one modiolus to the contralateral modiolus to create the lips together. Nevertheless, the superficial part of the orbicularis oris muscle act with other the facial-expression muscles to assist facial expression and retract the lower lip. The orbicularis oris muscle was innervated by the marginal mandibular and buccal branches of the facial nerve.[26]

2.4.6 Buccinator muscle

The buccinator arising from lateral surface the alveolar process of the maxilla and mandible, and pterygomandibular raphe, and ran anteriorly to the modiolus and blend to the orbicularis oris muscle. The contraction of buccinator muscle was generated by the buccal branches of the facial nerve for cheek compression against the molar teeth during chewing and blowing.[26]

2.4.7 Zygomaticus major

The zygomaticus major muscle originated at 1.4-1.5 cm inferiorly to the Frankfort horizontal line and 1 cm laterally to the lateral canthus at the zygomatic bone, then ran inferomedially to intermingle with the orbicularis oris, levator anguli oris, depressor anguli oris, and buccinator at the modiolus (Figure 43). Also, the zygomaticus muscle was placed in female cadavers deeper than the male cadavers as 60 mm versus 41 mm.[26, 98, 99] The zygomaticus major muscle provides elevation of the angle of the mouth during smile by innervation of the zygomatic and buccal branches

of the facial nerve.[26] Kehrer et al.[100] (2018) investigated the nerve supply to the zygomaticus major muscle in 96 hemifaces. It was found that the zygomaticus major muscle was innervated by the zygomatic branches and the buccal branches in 67% and 33%, respectively. Moreover, the Zuker's point was used to locate the buccal branch, which innervation the zygomaticus major muscle. However, the zygomaticus major muscle was innervated by the multiple zygomatic branches; 2 branches in 60%, 3 branches in 36%, and 4 branch in 4%.[22]

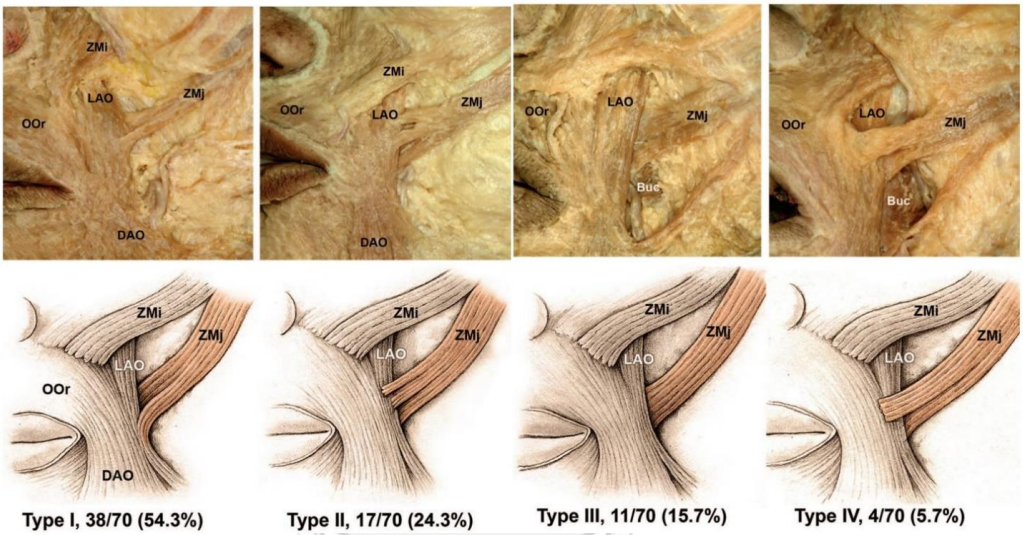

Figure 43 Illustrations of the of arrangement and attachment of the zygomaticus major muscle were classified into the four types. In type I, the superficial fibers of the zygomaticus major (ZMj) are intermingle with the levator anguli oris (LAO), while the deep fibers of the muscle ran inferiorly to blend into the buccinator (Buc) and levator anguli oris. In type II, the superficial fibers of the zygomaticus major (ZMj) are intermingle with the superficial layer of the orbicularis oris (OOr) and the depressor anguli oris (DAO), while the middle fibers of the muscle blended into levator anguli oris. And deep fibers of the muscle ran inferiorly to blend into the buccinator (Buc) and levator anguli oris. In type III, the zygomaticus major (ZMj) ran posterior to the levator anguli oris muscle, then are intermingled with the buccinator (Buc) and levator anguli oris. In type IV, the superficial fibers of the zygomaticus major are intermingled with the orbicularis oris and the depressor anguli oris muscle, and the deep muscle

fibers are blended into a buccinator and levator anguli oris muscle. ZMi, zygomaticus minor.[99]

According to Hu et al.[101] (2008), the arrangement and attachment patterns of the zygomaticus major muscle were recorded in 70 hemifaces of cadavers for the surgical planning in facial reanimation surgery. The result presented that the bifid zygomaticus major was found in 40% of specimens, and 71.4% of bifid zygomaticus major specimens was found in both sides of the face. In addition, the upper bands were larger and wider than the lower bands.

Previously, Caminer et al.[85] (2006) explained that the zygomatic branch ran medially deep to the zygomaticus major and minor muscles (near mid-part), and superficially to the levator anguli oris muscle. Also, it supplies zygomaticus major and minor, inferior part of orbicularis oculi muscle from posterior their surfaces. In addition, the buccal branch ran medially about 20-30 mm inferior to the zygomatic branch, and was placed superficially to levator anguli oris muscle, then supplies it from its anterior surface. On the contrary, the buccal branch doesn't supply zygomaticus major and minor muscle, although it ran deep to them. Moreover, the buccal branch traveled medially deep to the anterior facial vein, thus passed superomedially to the anterior facial vein.

Recently, the branching patterns of the facial nerve to innervate the zygomaticus major muscle were determined in 43 hemifaces of fresh cadavers. The result suggested that the arborization of the facial nerve were classified into 5 types include Y-type (12 specimens, 28%) and X-type (12 specimens, 28%), followed by H-type (8 specimens, 19%), E-type (6 specimens, 14%), and F-type (5 specimens, 11%). Moreover, the number of the axons of the facial nerve was counted in main branches. It was found that all pattern had more than 900 axons (1387.33 ± 406.59 in Y-type, 1021.42 ± 187.79 in X-type, 1222.75 ± 193.82 in H-type, 1496.17 ± 364.567 in E-type, and 1353.40 ± 256.07 in F-type).[102]

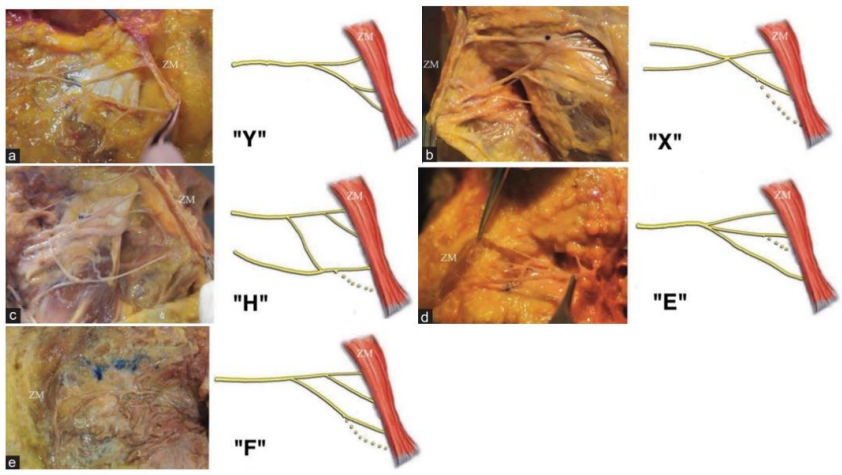

Figure 44 Illustration of the five patterns of branching of the facial nerve for innervation the zygomaticus major muscle; Y-type (28%) (a), X-type (28%) (b), H-type (19%) (c), E-type (14%) (d), and F-type (11%) (e); Inconstant branches (dash lines) [102]

2.4.8 Zygomaticus minor muscle

The zygomaticus minor is originated from the lateral surface of the zygomatic bone, and traveled inferomedially for insertion the upper lip. The contraction of this muscle can provide the upper lip elevation by stimulation from the zygomatic and buccal branches of the facial nerve.[26] furthermore, the zygomaticus minor was absent in 5 of 29 (17%) cases by considering depending on its lateral attachment. [103]

2.4.9 Levator labii superioris muscle

The levator labii superioris muscle is originated superiorly to the infraorbital foramen, and ran directly inferior to the upper lip. It acts in the upper lip elevation to create the nasolabial furrow. the zygomatic and buccal branches of the facial nerve innervate this muscle.[26]

2.4.10 Levator labii superioris aleque nasi muscle

The levator labii superioris aleque nasi muscle originated from the frontal process of maxilla. The two insertions of this muscle are the nasal cartilage and upper lip, so it also dilates the nostrils.[26, 97]

2.4.11 Levator anguli oris muscle

The levator anguli oris originates from the canine fossa of the maxilla inferior to the infraorbital foramen, then extend into the modiolus near the corner of mouth. As a result, its contraction elevates the corner of the mouth and produces the nasolabial furrow. The innervation of the levator anguli oris muscle consist of the zygomatic and buccal branches of the facial nerve.[26]

2.4.12 Risorius muscle

The origin of risorius muscle able to attach in various area such as the zygomatic arch, parotid and masseteric fascia, and the platysma muscle. Next, this muscle ran medially to the modiolus. Its contraction draws the corner of the mouth laterally during laughing. The buccal branch of the facial nerve innervates this muscle.[26, 104]

2.4.13 Nasalis muscle

The nasalis muscle composes of the upper transverse part and the lower alar part. The action of each part as compressor naris and dilator naris, respectively. The transverse part of the nasalis muscle originates from the maxilla superficial to the canine, then it runs superomedially to the dorsum of the nose. Nonetheless, the alar part of the nasalis muscle originates from maxilla medial to the transverse part, then it inserts to the alar cartilage. Moreover, this muscle can generates bunny lines by excessive contraction of the muscle.[26]

2.4.14 Depressor anguli oris muscle

The origin of depressor anguli oris muscle is the oblique line and the mental tubercle of the mandible, then the muscle fibers extend superomedially to orbicularis oris at the modiolus and skin and mucous membrane of the lower lip. The contraction of the depressor anguli oris muscle bring to pull the lateral corner of the mouth inferiorly, and turn outward of the lower lip.[26]

2.4.15 Depressor labii inferioris muscle

The depressor labii inferioris originates from the oblique line of the mandible which medial to the attachment of the depressor anguli oris, then muscle fibers

intermingle with orbicularis oris and insert at the skin and mucosa of the lower lip. The action of this muscle pulls the lower lip inferolaterally.[26, 105]

2.4.16 Mentalis muscle

The mentalis muscle is the muscle that originates from the incisive fossa of the mandible which associated with the labiomental fold, then extend inferiorly to the skin of the chin. It was innervated by the marginal mandibular branch of the facial nerve.[26, 97]

2.4.17 Platysma muscle

The platysma muscle is the thin muscle that arises from the fascia of the upper parts of the pectoralis major and deltoid muscle at the level of the 2nd rib, and extend superior to the inferior margin of the mandible, perioral muscles, modiolus, and the skin and subcutaneous tissue of the lower face. The contraction of the whole muscle bring about skin ridges at the neck, and it was innervated by the cervical branch of the facial nerve.[26]

2.5 Communication of the facial to other nerve

In the previous study, the facial nerve can communicate with itself; moreover, the communication of the facial nerve and the sensory nerve have been widely investigated (Table 3) (Figure 45).[106-108] The sensory of the face is mainly innervated by the trigeminal nerve which the fifth cranial (CN V). The trigeminal nerve for innervation in the face is divided into three branches; ophthalmic, maxillary, mandibular nerve. The terminal branches of trigeminal nerve are responsible for the sensory innervation of the face include the supraorbital, supratrochlear, infratrochlear, external nasal, zygomaticotemporal, zygomaticofacial, infraorbital, auriculotemporal, buccal, and mental nerve (Figure 46).[2, 26, 109]

Table 3 The communication of the facial nerve and the terminal branches of the trigeminal nerve.[109]

The branches of the facial nerve	The branches of the trigeminal nerve
Facial nerve trunk	Auriculotemporal nerve
Temporofacial and cervicofacial divisions	Great auricular nerve
Temporal branch	Zygomaticotemporal nerve Supraorbital nerve Auriculotemporal nerve
Zygomatic branch	Supraorbital nerve Supratrochlear nerve Buccal nerve Zygomaticofacial nerve Auriculotemporal nerve
Buccal branch	Infratrochlear nerve Infraorbital nerve Buccal nerve Mental nerve Zygomaticofacial nerve Auriculotemporal nerve
Marginal mandibular branch	Buccal nerve Mental nerve
Cervical branch	Transverse cervical nerve

According to Yang et al. (2014), the rami of the infraorbital nerve were categorized into five groups that consist of inferior palpebral, external nasal, internal nasal, medial superior labial and lateral superior labial rami. The areas of the face were supplied by these terminal branches including fan-shaped area of the lower eyelid, the ala and philtrum, nasal septum, the superior labial area, respectively. Especially, the infraorbital triangle was entirely supplied by the superior labial ramus. Furthermore,

the infraorbital communicate with the buccal branches of the facial nerve, and creates as an infraorbital nervous plexus. Consequently, the infraorbital triangle was considered a dangerous zone for iatrogenic complications.[106]

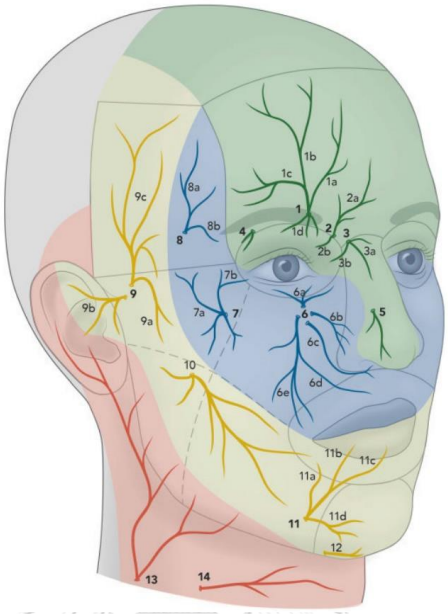

Figure 45 The sensory nerve for innervation the skin of the face and neck. Green area, the skin surface is supplied by ophthalmic nerve; 1, supraorbital nerve; 1a, medial branch; 1b, lateral branch; 1c, horizontal branch; 1d, palpebral branches; 2, supratrochlear nerve; 2a, forehead branches; 2b, palpebral branch; 3, infratrochlear nerve; 3a, nasal branches; 3b, palpebral branch; 4, palpebral branches of lacrimal nerve; 5, external nasal branch of anterior ethmoidal nerve; blue area, the skin surface is supplied by maxillary nerve; 6, infraorbital nerve; 6a, inferior palpebral branches; 6b, external nasal branch; 6c, internal nasal branch; 6d, medial branch of superior labial branch; 6e, lateral branch of superior labial branch; 7, zygomaticofacial nerve; 7a, zygomatic branches; 7b, palpebral branch; 8, zygomaticotemporal nerve; 8a, temporal branches; 8b, palpebral branch; yellow area, the skin surface is supplied by mandibular nerve; 9, auriculotemporal nerve; 9a, zygomatic branches; 9b, auricular branches; 9c, temporal branches; 10, long buccal nerve; 11, mental nerve, 11a, angular branch; 11b, lateral labial branch; 11c, medial labial branch; 11d, mental branch; 12, mental branch of mylohyoid nerve; red area, the skin surface is supplied by great auricular nerve and transverse cervical nerve; 13, great auricular nerve; 14, transverse cervical nerve.[27]

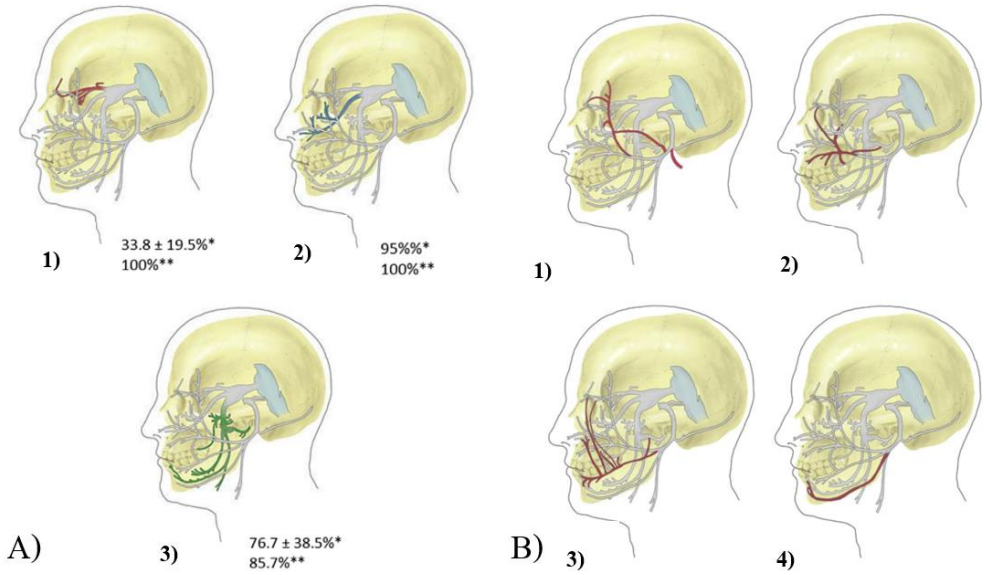

Figure 46 Illustration of the trigeminal nerve was divided into three branches ophthalmic (1), maxillary (2), and mandibular (3), and percentage of the communication with the branch of the facial nerve in two methods; cadaveric dissections (*) and Sihler stain (**) (A). Illurtration of the communications between the superficial trigeminal branches and the four main branches of the facial nerve; temporal (1), zygomatic (2), buccal (3), and marginal mandibular (4) (B).[109]

Formerly, Hwang et al.[107] (2004) determined that the infra orbital nerve is arises from the maxillary nerve, and was classified into three rami; inferior palpebral, external nasal, and superior labial rami that supplied the skin of the face was lower eyelid, the ala, and upper lip, respectively. Importantly, the infraorbital nerve commingles with zygomatic branch of the facial nerve at the infraorbital area, then travel together to the mimetic muscles. The diameter of merging area was 36 mm, and the distances between the center of this area and the infraorbital foremen was 22 mm (Figure 47). Similarly, Tansatit et al.[110] (2016) illustrated that the buccal branch of the facial nerve communicated with the infraorbital nerve in ten patterns; type A, the lower rami of the buccal branch connected with the lateral labial branch of infraorbital nerve in 70%; type B, the lower rami of the buccal branch connected with the medial labial branch of infraorbital nerve in 32.5%; type C, the upper rami of the buccal branch

connected with the lateral labial branch of infraorbital nerve in 27.5%; type D, the middle rami of the buccal branch connected with the lateral labial branch of infraorbital nerve in 20%; type E, the middle rami of the buccal branch connected with the medial labial branch of infraorbital nerve in 17.5%; type F, the upper rami of the buccal branch connected with the medial labial branch of infraorbital nerve in 15%; type G, the upper rami of the buccal branch connected with the nasolabial branch of infraorbital nerve in 10%; type H, the lower rami of the buccal branch connected with the nasolabial branch of infraorbital nerve in 7.5%, type I, the middle rami of the buccal branch connected with the nasolabial branch of infraorbital nerve in 5%; and type J, the middle rami of the buccal branch connected with the alar branch of infraorbital nerve in 5%. Additionally, the communicating area was investigated in 39 specimens. It was found that the mean of the distance between communicating area and the ala of the nose in X and Y axis was 16.3 ±7.8 mm and 8.9 ±4.6 mm, respectively (in the right side), and 16.0 ±6.2 mm and 5.9 ±5.4 mm, respectively (in the left side).

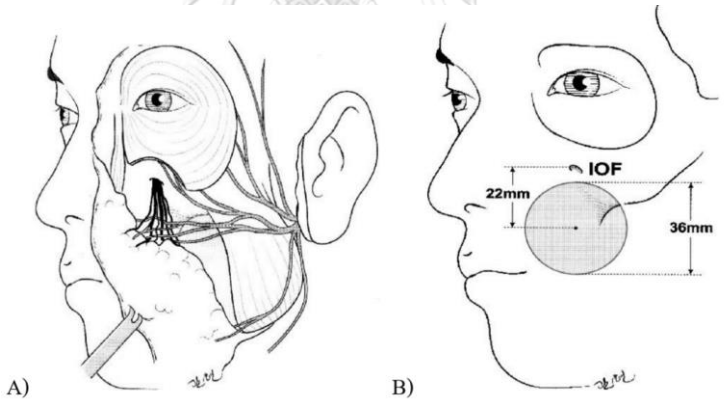

Figure 47 Infraorbital nerve commingle with the branch of the facial nerve at infraorbital area (A). The critical zone of the nerve injury. The diameter of merging area was 36 mm, and the distances between the center of this area and the infraorbital foremen was 22 mm. (B)[107]

In addition, Khanfour and Metwally[9] (2014) demonstrated that the main branch of the marginal mandibular branch connected to the anterior branch of the great auricular nerve in 3.3% of 30 specimens. Moreover, the greater auricular nerve can communicate with the cervicofacial division of the facial nerve at the parotid area.[111]

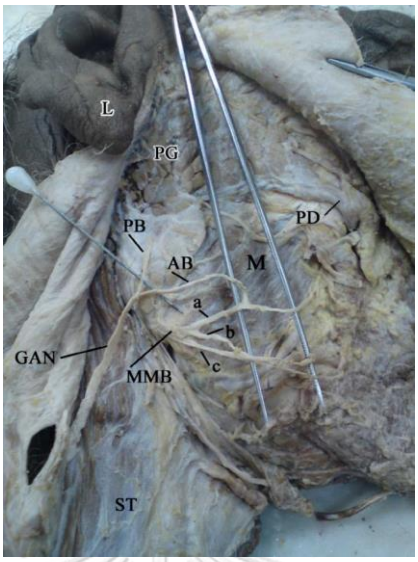

Figure 48 The communication of the marginal mandibular branch of the facial nerve (MMB) and the great auricular nerve (GAN) in the right side of the face in cadaveric dissection; ST, sternomastoid muscle; AB, anterior branch of the great auricular nerve; PB, posterior branch the great auricular nerve, a, upper rami of the marginal mandibular branch; b, middle rami of the marginal mandibular branch; c, lower rami of the marginal mandibular branch; M, masseter muscle; L, ear lobule; PG, parotid gland; and PD, Parotid duct.[9]

Kwak et al. explained that the connection between auriculotemporal nerves and branches of the facial nerve occurred within the parotid gland in 93.3% of 30 specimens.[20] Furthermore, the communicating auriculotemporal nerve connected the temporofacial division of the facial nerve at the posterior margin of the masseter, while the communication of the auriculotemporal nerve and zygomaticotemporal nerve can occurred within the temporal fossa in 13% of specimens.[111] Additionally, Odobescu et al.[112] (2012) stated that the temporal branch of the facial nerve perforated the superficial layer of the deep temporal fascia to connected with the zygomaticotemporal nerve at 36 mm lateral to the lateral and 2 mm superior to the lateral canthus in 82.35% (14 of 17 specimens).

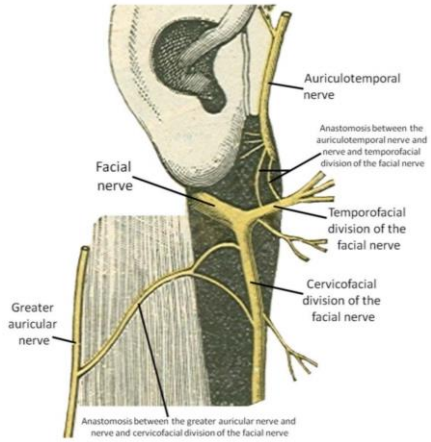

Figure 49 The communications of the auriculotemporal nerve with the temporofacial division of the facial nerve, and the greater auricular nerve with the cervicofacial division of the facial nerve.[111]

2.6 Histological study in the face for identification of the facial nerve

Hematoxylin and eosin (H&E) and Masson's Trichrome were used to stain the tissues which was sectioned at 5 μm for description the characteristics of the structures in the face. Broughton and Fyfe explained that the SMAS was found at the parotid, zygomatic, buccal, temporal, and facial platysma area. The mean thickness of the SMAS was 0.46 ±0.10 mm. On the contrary, the forehead and nasal nasolabial fold areas absent this layer in the specimen. Furthermore, the SMAS enveloped the zygomaticus muscles of the mid-face area. In addition, the property of SMAS was investigated in many areas. In the parotid area, the SMAS was divided into two layers that composed of the deep platysma fascia and the parotid fascia (Figure 50). Moreover, the thickness of the SMAS at the inferolateral parotid area thicker than the superior parotid area, and presented the platysma muscle fiber within the SMAS at the parotid area. In the zygomatic, the SMAS covered the superficial layer of the zygomatic muscle, and expanded to the medial border which superficial to the facial nerve. Additionally, nasolabial fold area absent the SMAS layer, while histological method presented the SMAS layer at the buccal area only.[30]

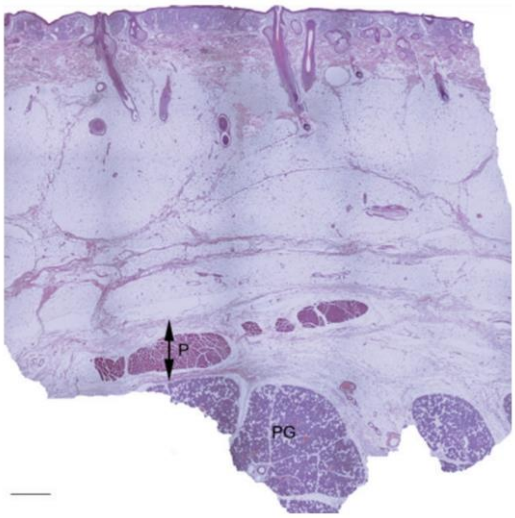

Figure 50 Hematoxylin and eosin staining at superior parotid area; P, platysma muscle; PG, parotid gland; double-ended arrow, the SMAS layer, and scale bar 1 mm.[30]

In the same way, Ghassemi et al. (2003) investigated the position of the facial nerve associated with the facial soft tissue layers in each area of the face. It was found that few branches of nerve were located deeply the subcutaneous tissue at forehead area and the parotid fascia at parotid area. Moreover, the branches of nerve were presented deeply the subcutaneous tissue at zygomatic area, while nerve branches located in the entire tela subcutanea for innervation the muscle at infraorbital area. In nasolabial fold, the most nerve was placed at the buccinator muscle.[34]

Later, the histological study was conducted in the nasolabial fold tissue of embalmed cadavers for identification the nerve branches. The result showed that the main branches of the facial nerve was found in the submuscular plane at the level of upper lip, therefore the area which superficial to the muscular plane was the safety layer for dissection in the nasolabial fold. Moreover, the nasolabial fold was the transition zone between type I and II of the SMAS. Type I SMAS was located laterally to the nasolabial fold, and contained meshwork of the fibro-muscular portions surrounding fat pads. On the contrary, type II SMAS was positioned medially to the nasolabial fold, and indicated dense fibro-muscular septum and a few fat tissues (Figure 51).[32]

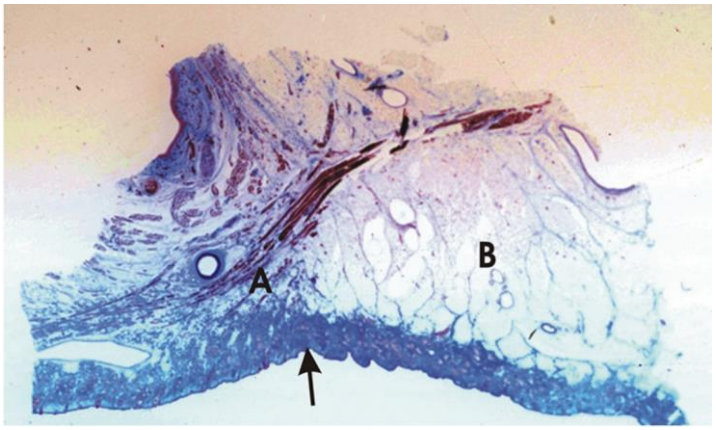

Figure 51 The nasolabial tissue in the histological section; A, labial area; B, buccal area; arrow, the nasolabial fold.[32]

According to Macchi et al. (2010), the facial tissue sections were stained with S100 at parotid, zygomatic, nasolabial fold and buccal, and cheek area for study the SMAS and nerve. The result demonstrated that in cheek area, the mean of the thickness of the subcutaneous tissue and SMAS were 5.45 ±0.1 mm, and 423 ±122 μm, respectively. Moreover, the diameter of the nervous bundles at cheek, nasolabial fold and buccal area, and parotid area 279.7 ±73.6, 169.5 ±23, 171.2 ±22.4 μm, respectively.[31]

Recently, Amano, Naito and Matsuo (2020) examined seven areas of the face by using the H&E staining and scanning electron microscope (SEM) to observe characteristic of the facial soft tissue layers that consisted of forehead, lateral angle of the eye, infra orbital, buccal, inferior masseter, superior parotid, and nasolabial fold areas. The result revealed that the facial nerve was located within orbicularis oculi muscle at the lateral angle of the eye, both superficially and deeply to the zygomatic muscle at the buccal area, below to the inferior masseter muscle, superficially the superior parotid area, and both superficially and deeply to the orbicularis oculi muscle at the nasolabial fold areas.[113]

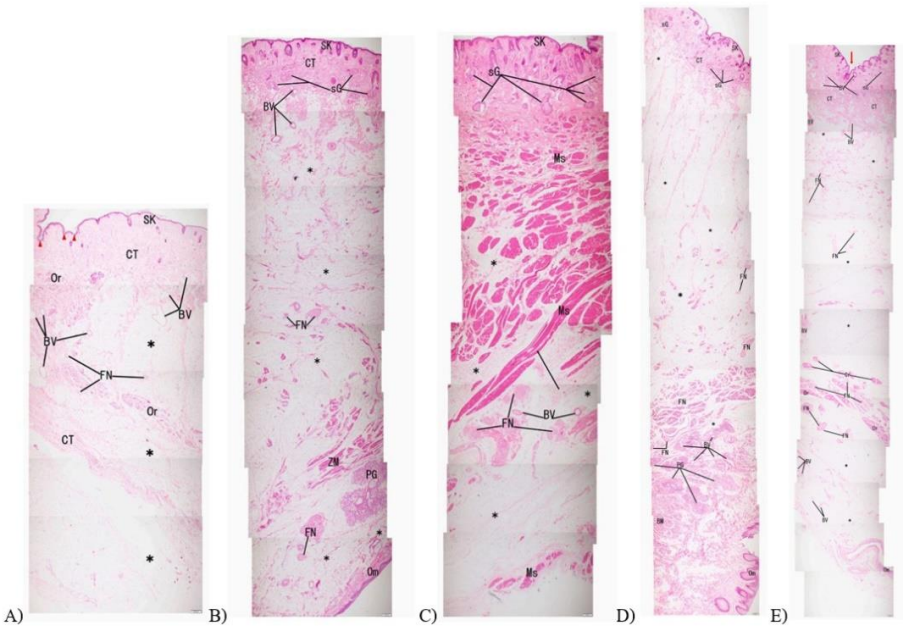

Figure 52 The cross section of the facial soft tissue at the lateral angle of the eye (A), the buccal (B), the inferior masseter (C), the superior parotid (D), the nasolabial fold (E) areas. SK, Skin; *, adipose tissue; CT, connective tissue; Or, Orbicularis oculi muscle; BV, Blood vessels; FN, Facial nerve; red arrowheads: fissure of the lateral angle of the eye; sG, sebaceous gland; ZM, zygomaticus muscle major and minor muscle; Om, oral mucosa; MS, Masseter muscle; BM, Buccinator muscle; PG, Parotid gland; Red arrow, groove of the nasolabial fold; Magnification: x4.[113]

2.7 Sihler's technique for study the facial nerve

Sihler's stain technique was discovered by Sihler in 1895 to distinguish the nerve ending pattern in snake. After that, Sihler's stain has been used widely clarify the mapping of the nerve patterns in organs, skeletal muscles, mucosa, skin, and other structures. The advantage of this procedure, the anatomist can identify the small nerve rami without a dissection, and easier observe communication of nerve with the naked eye.[114, 115] For the facial study, the modified Sihler's stain was applied to observe both motor and sensory nerves of the face. According to Liu et al.[2] (2010), Sihler's stain was used to investigated the extramuscular and intramuscular pattern of the facial nerve in the face for understanding the deep detail of the facial nerve and protecting the nerve during intervention, and the communication between the facial nerve and the

trigeminal nerve can wholly observe by using Sihler stain more than the cadaver dissection (Figure 53). On the other hand, the different of the motor nerve and sensory nerve can't be separated in each other, when nerve was conducted by the Sihler stain, because the terminal branches in muscle or organ were stained by the same color. Moreover, the Sihler stain couldn't explain the detail of the relationship of the nerve and the structure. Accordingly, the nerve must be detected from main trunk to the distal branches.[2, 116]

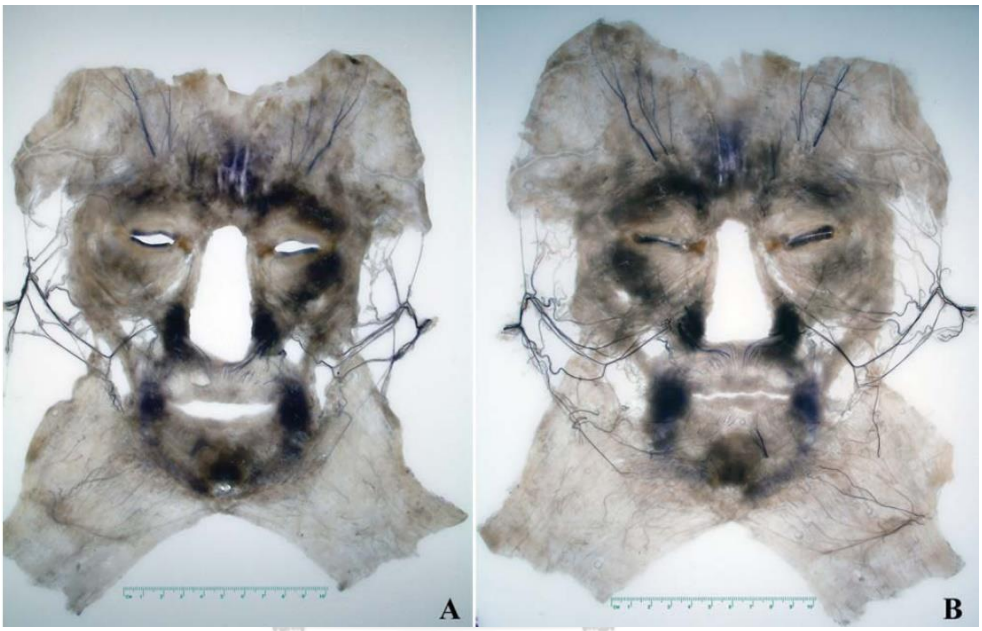

Figure 53 Modified Sihler's staining in the face and platysma muscle in fresh cadaver. Anterior view of the facial tissue flap (A) Posterior view of the facial tissue flap (B)[2]

In addition, Salinas et al.[94] (2009) investigated the extramuscular and intramuscular facial nerve distribution in eight cadavers. The result presented that the whole course of the marginal mandibular and cervical branches can observed by using the modified Sihler stain. It ran to supply the depressor anguli oris and platysma muscle, respectively. Furthermore, the cervical branch of the facial nerve communicated with the transverse cervical nerve posterior to the platysma muscle (Figure 54). Later, the communication between the buccal branches of the facial nerve and inferior palpebral twigs was observed by Yang et al. in 2014 (Figure 55).[106]

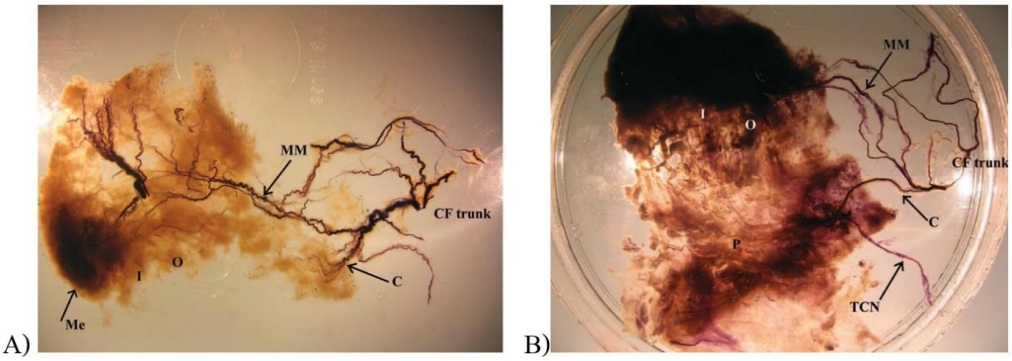

Figure 54 Photograph of the modified Sihler stain in left lower face presenting marginal mandibular branch suppling the depressor anguli oris muscle (A) and the communication of the cervical branch of the facial nerve and the transverse cervical nerve posterior to the platysma muscle (B); MM, marginal mandibular branch of the facial nerve; C, cervical branch of the facial nerve; I, depressor labii inferioris muscle; O, depressor anguli oris muscle; Me, mentalis muscle; CF, cervicofacial division; TCN, transverse cervical nerve; P, platysma muscle.[94]

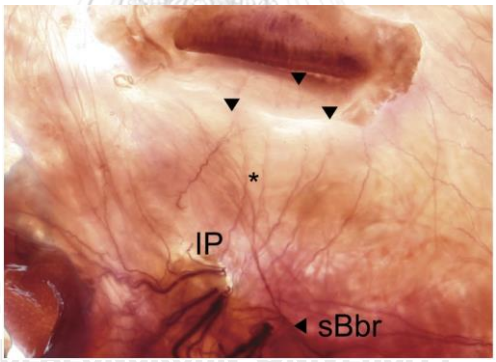

Figure 55 The communication of the superior rami of buccal branch of the facial nerve and inferior palpebral branch of the infraorbital nerve; IP, inferior palpebral branch of the infraorbital nerve; sBbr, superior rami of buccal branch of the facial nerve; arrowhead, target area for supplying by inferior palpebral (the lower eyelid); asterisk (*), communication point[106]

CHAPTER III

RESEARCH METHODOLOGY

3.1 Target population and sample population

This study was conducted on the cervicofacial region of the adult embalmed and soft cadavers who donated and consented the body to education and medical research from the Department of Anatomy and Chula Soft Cadaver Surgical Training center, Faculty of Medicine, Chulalongkorn University and King Chulalongkorn Memorial Hospital, Bangkok, Thailand.

Inclusion criteria

1) The adult embalmed cadavers have been completely preserved and were injected red latex into the common carotid artery.

2) The soft cadavers without injected red latex into the common carotid artery.

Exclusion criteria

1) The adult embalmed and soft cadavers have pathology or damage on the face and neck region.

2) The soft cadavers have decomposed on the face and neck regions.

3.2 Sample size determination

3.2.1 Sample size determination for cadaveric dissection

According to Parcual et al. (2019) [19] they measured the diameter of the temporal branch of the facial nerve in 32 embalmed cadavers. The result showed that the standard deviation of the diameter of the temporal branchwas 0.33 mm. Consequently, the sample size was calculated in this study.

$$n = Z^2_{\alpha/2}\,\sigma^2 / d^2$$

While; The confidence interval (CI) was set at 95%

$Z_{\alpha/2} = Z_{0.05/2} = 1.96$ (two tail)

σ^2 = Variance of data = $(0.33)^2$

d = Acceptable error = 0.1 mm

So; n = $(1.96)^2 (0.33)^2 / (0.1)^2$

n = 41.84

The calculated sample size was at least 42 hemi-cervicofacial regions. Therefore, the 42 hemi- cervicofacial regions were analyzed in the cadaveric study.

3.2.2 Sample size determination for histological study

According to Agarwal et al. (2010)[33], they investigated the transitional zone of the temporal branchthe facial nerve from the innominate fascia to the superficial temporal fascia by using cadaveric dissection in 18 hemi-faces and Masson's trichrome staining in 6 hemi-faces. It was found that the standard deviation of distance between transitional zones to the lateral orbital rim was 3.8 mm. Consequently, the sample size was calculated in this study.

$n = Z^2_{\alpha/2} \sigma^2 / d^2$

While; The confidence interval (CI) was set at 95%

$Z_{\alpha/2} = Z_{0.05/2} = 1.96$ (two tail)

σ^2 = Variance of data = $(3.8)^2$

d = Acceptable error = 2 mm

So; n = $(1.96)^2 (3.8)^2 / (2)^2$

n = 13.87

The calculated sample size was at least 14 hemi-cervicofacial regions. Therefore, the 14 hemi- cervicofacial regions were analyzed in the histological study.

3.2.3 Sample size determination for Sihler's technique

According to Liu et al. (2010)[2], they investigated the intramuscular part of the facial nerve by using cadaveric dissection in 12 hemi-faces and modified Sihler's technique in 10 hemi-faces. It was found that the standard deviation of distance between the angle of mandible to the area of the marginal mandibular branch crossed to the facial artery was 4.9 mm. Consequently, the sample size was calculated in this study.

$$n = Z^2_{\alpha/2}\,\sigma^2 / d^2$$

While; The confidence interval (CI) was set at 95%

$Z_{\alpha/2}$ = $Z_{0.05/2}$ = 1.96 (two tail)

σ^2 = Variance of data = $(4.9)^2$

d = Acceptable error = 2.5 mm

So; $n = (1.96)^2 (4.9)^2 / (2.5)^2$

$n = 14.76$

The calculated sample size was at least 15 hemi-cervicofacial regions. Therefore, the 16 hemi- cervicofacial regions were analyzed in the Sihler's technique.

3.3 Material and tool

3.3.1 For cadaveric dissection

1) Digital vernier caliper
2) Scalpel (No.3)
3) Removable surgical blade (No.10)
4) Forceps
5) Iris micro dissecting curved scissors
6) Pins and small rope

7) Scale (mm.)
8) Tissue paper
9) Gloves and surgical masks
10) Digital camera and memory card

3.3.2 For histological study

1) Histology reagent chemicals
    - 10% neutralized formalin
    - Alcoholic eosin
    - Hematoxylin
    - Working define
    - Blue buffer
    - Ethanol
    - Xylenes
    - Mounting medium
    - Distilled water
    - Paraplast
    - Trichrome stain (Masson) kit
2) Embedding cassette
3) Microtome blade
4) Microscope slide (25.5*76.2*1 mm)
5) Cover glass slide
6) Microscope slide box
7) Tissue embedding molds (20*26*5 and 20*33*5 mm)
8) Paraffin tissue embedding center with cold plate
9) Cold plate for histology
10) Manual rotary microtome
11) Tissue floatation bath
12) Heating and drying ovens

13) Biological microscopes

14) Microscopy slide scanner

15) Pencil and permanent pen

3.3.3 Sihler's technique

1) Sihler's reagent chemicals

- 10% unneutralized formalin
- 3% KOH and 3% H_2O_2
- Glacial acetic acid
- Glycerine
- Aqueous chloral hydrate
- Hematoxylin powder
- Ethanol
- Potassium alum
- Sodium iodate
- Lithium carbonate solution
- Thymo crystals

2) Plastic and glass container

3) Shaking machine

4) Operating microscope

5) Digital camera and memory card

6) Lamp

7) Grid plastic and clear string

8) Black yarn

3.4 Methods

Research framework

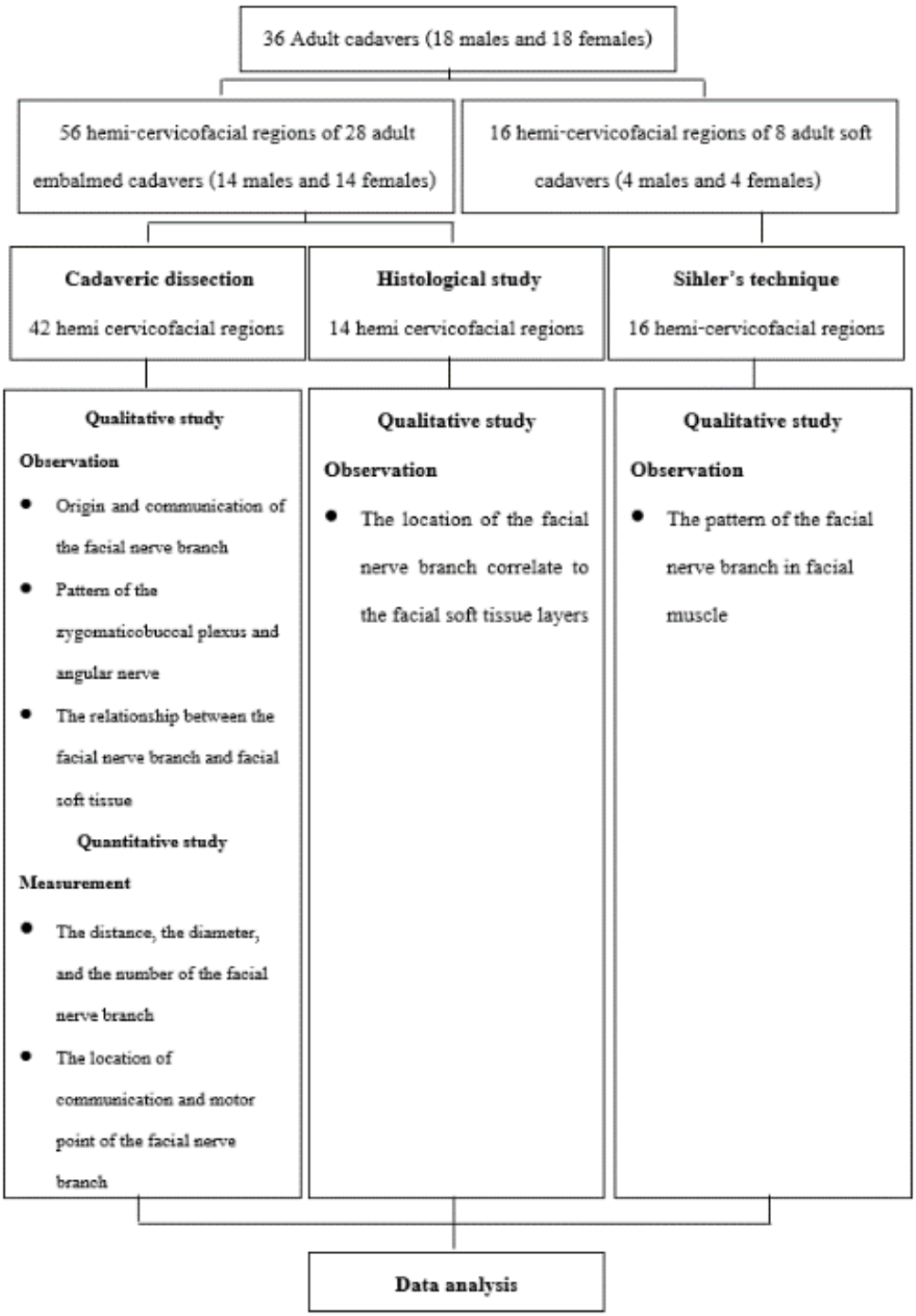

3.4.1 For cadaveric dissection study

1) Cadaveric dissection

1.1) Skin incision and Subcutaneous dissection

All cadavers in this study have been completely preserved and injected red latex in the common carotid artery. The cadaveric dissection was conducted layer by layer according to the facial tissue layers; Skin, subcutaneous, SMAS, and Sub-SMAS layers. Begin with, the cadavers were placed in the supine lying position on the dissecting table, then skin incisions were made following the median line of face and neck, horizontal line at superior border of above the hair line 1 cm and inferior border at the level of the clavicle (Figure 56A). After that, the skin was peeled following skin incision from the median line to the vertical line anterior to the tragus (Figure 56B).

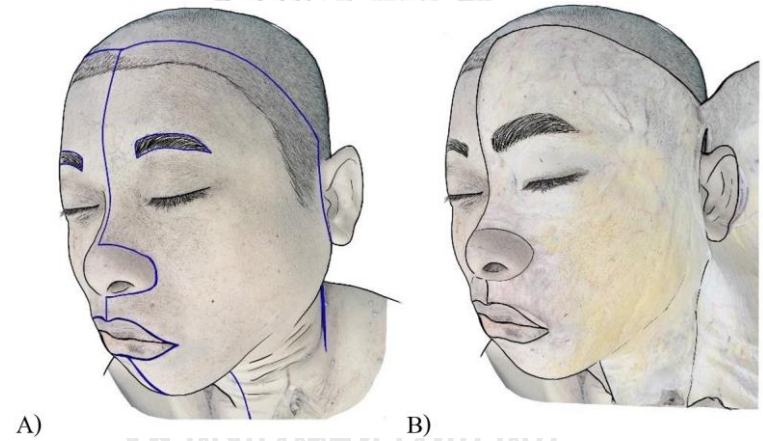

Figure 56 Cadaveric dissection; Skin incision line (A), Subcutaneous layer (B)

1.2) SMAS dissection and identify branch of the facial nerve

Next, the subcutaneous layers were removed to identify the muscle of facial expression or SMAS layer (Figure 57A). Subsequently, the SMAS layer was carefully dissected at the parotid area to find the emerging point of the facial nerve. The dissection was started at the border of the parotid gland, and continually dissected along the all cause to the terminal branch in each branch of the facial nerve; temporal, zygomatic, buccal, marginal mandibular, and cervical branches (Figure 57B). In addition, the entry points of the facial nerve to the muscle were recorded.

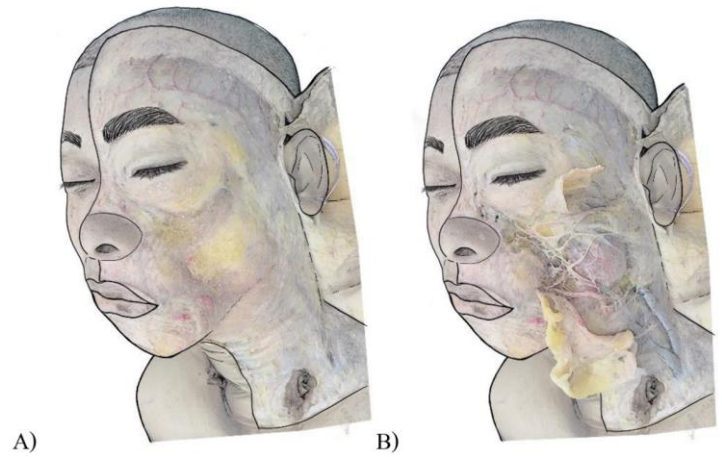

Figure 57 Cadaveric dissection to identify anatomy of the facial nerve and its relationship with the facial soft tissue in the SMAS layer (A), Sub-SMAS layer (B)

1.3) Parotid gland dissection

Finally, the facial nerve in the parotid gland was identified after removing the superficial layer of the parotid gland (Figure 58A, B). The branching point of temporofacial and cervicofacial divisions of the facial nerve trunk was identified. Additionally, the origin of the branch of the facial nerve was observed in this area.

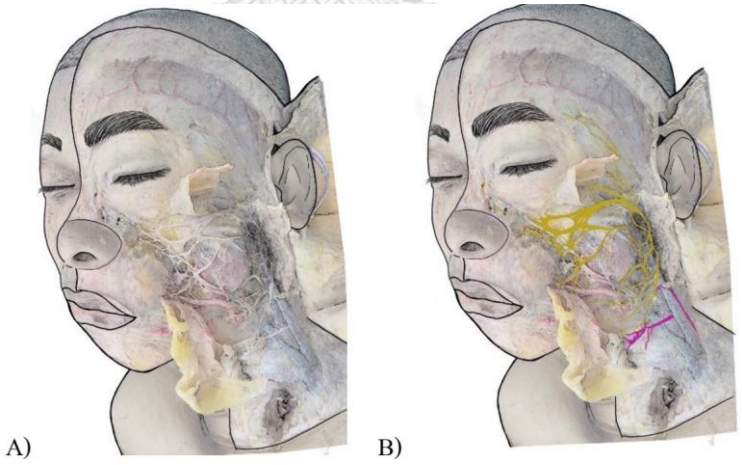

Figure 58 Parotid gland removing to identify the divisions of the facial nerve (A), and the facial will be sketched (B).

1.4) Reference line, anatomical landmarks determination and measurement

To investigate the facial nerve, all cadavers were observed and measured following the facial landmarks. A digital vernier caliper was used to measure the distance and diameter of each facial nerve branch correlated to the reference line and anatomical landmark. The vertical and horizontal line was conducted as X and Y axis respectively. The intersection point of the reference line was determined to the zero number. The distance superior or medial to the intersection point was specified to the positive direction, while the distance inferior or lateral to the intersection point was determined to the negative direction. The protocols were conducted in each area of the facial nerve, because the branch of the facial nerve has complexity. Consequently, the characteristics of the facial nerve were investigated as follow;

- **Emerging point of branch of the facial nerve**

The determination of the reference line and anatomical landmarks

In part of the emerging point of the branch of the facial nerve, the X axis was the horizontal line connecting between the supra-alar crease and the inferior border of the tragus (AIL). The Y axis was the anterior tragal line (ATL) (Figure 59).

Measurement

The number of the branches of the facial nerve was recorded.

The location and diameter of the emerging point of the branch of the facial nerve from the parotid gland was measured correlated to the AIL in x and y coordination (Figure 59).

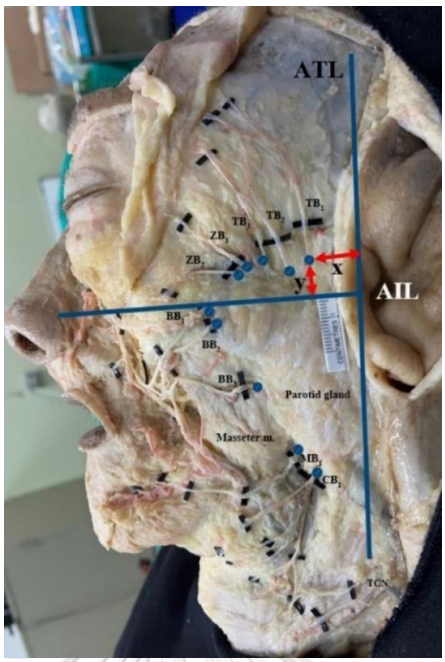

Figure 59 The measurement of the emerging point of the facial nerve correlated to the reference line. AIL; Alar-inferior tragal line, ATL; anterior tragal line, TB; temporal branch, ZB; zygomatic branch, BB; buccal branch, MB; marginal mandibular branch, CB; cervical branch, and TCN; transverse cervical nerve, blue dot; emerging point

- **The temporal branchof the facial nerve**

The determination of the reference line and anatomical landmarks

After the temporal branchemerges from the superior portion of the parotid gland, it continues to the temporal region. The temporal branchwas positioned by using the horizontal reference line in 3 levels. Firstly, the Frankfort's horizontal line (FHL) which is the reference line between the infraorbital rim to the upper margin of the tragus, Secondly, the lateral canthal line (LCHL) which is the line between the lateral orbital rim to the helix. Lastly, the supraorbital line (SOL) which is the horizontal line from supraorbital rim perpendicular to the ATL (Figure 60).

Observation and measurement

The location and diameter of the temporal branch of the facial nerve were mapped as the horizontal distance from the ATL in three levels; FHL, LCHL and SOL (Figure 60).

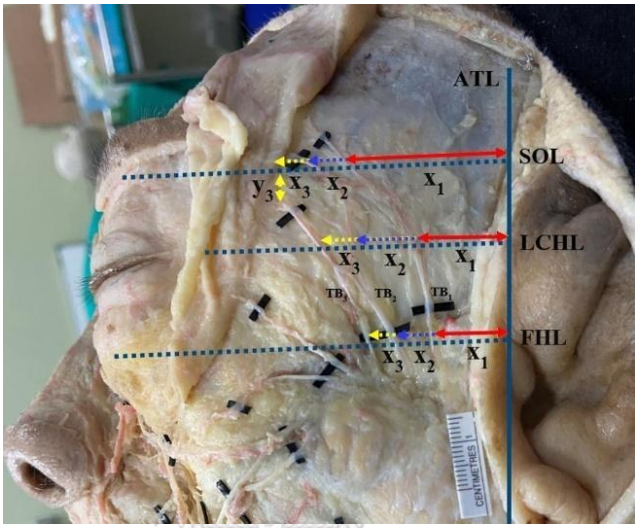

Figure 60 The measurement of the temporal branchof the facial nerve correlated to the reference lines; FHL; the Frankfort's horizontal line, SOL; the supraorbital line, LCHL; the lateral canthal line, ATL; Anterior tragal line.

In addition, the communication of the temporal branch with other nerves was observed, and the location of the communicating point of the temporal branch was measured correlatively to the LCHL in x and y coordination (Figure 61).

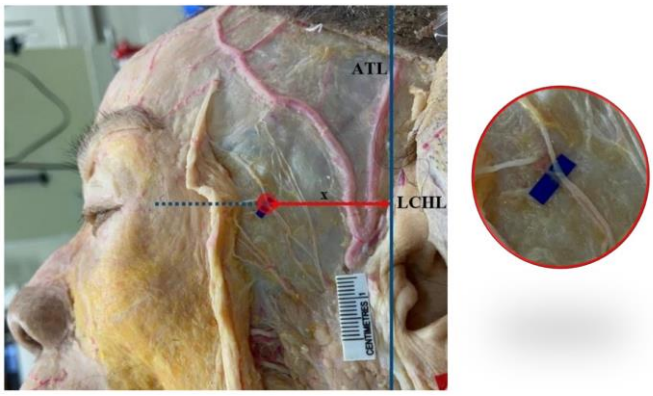

Figure 61 The measurement of the communicating point of the temporal branchof the facial nerve correlated to the reference lines; LCHL; the lateral canthal line, ATL; Anterior tragal line.

- **The zygomatic and buccal branch of the facial nerve**

The determination of the reference line and anatomical landmarks

To study the course of the zygomatic and buccal branch, the Frankfort's horizontal line (FHL) was used as the reference line (Figure 62).

Observation and measurement

The location and diameter of the zygomatic and buccal branch were measured as the vertical distance from the midpoint of FHL (midFHL) to the course of the facial nerve branch (Figure 62). Moreover, the relationship between the buccal branch and parotid duct was recorded.

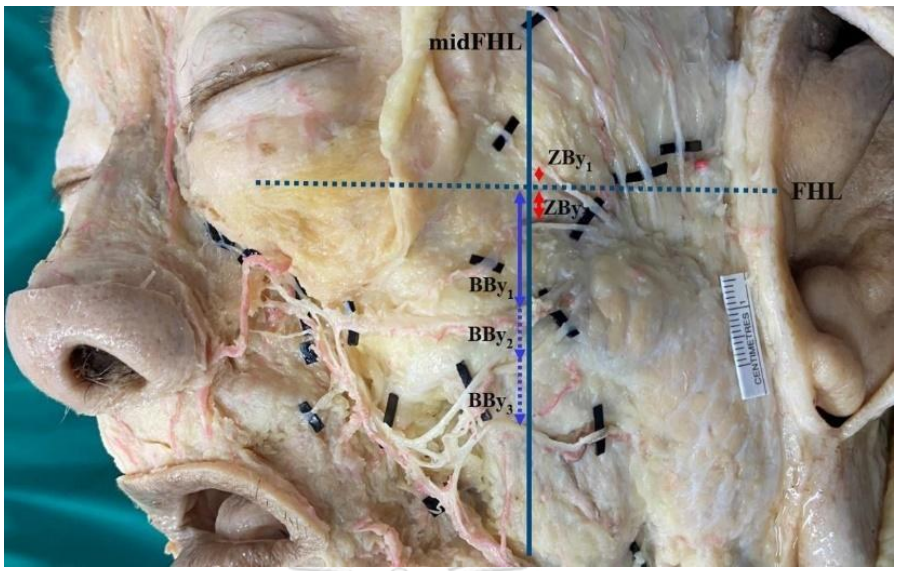

Figure 62 The measurement of the location of the zygomatic and buccal branch of the facial nerve correlated to the reference lines; FHL; the Frankfort's horizontal line, midFHL; the midpoint of FHL, ZB; zygomatic branch, BB; buccal branch

- **The zygomaticobuccal plexus**

The determination of the reference line and anatomical landmarks

- After the zygomatic and buccal passing through the midFHL into the midface region, the origin and pattern of the zygomaticobuccal plexus were collected (Figure 63). The boundary of data collection follows as; superior: supra-alar crease, inferior: horizontal line from the corner of mouth, lateral: midFHL and medial: vertical line from the corner of mouth (Figure 63).

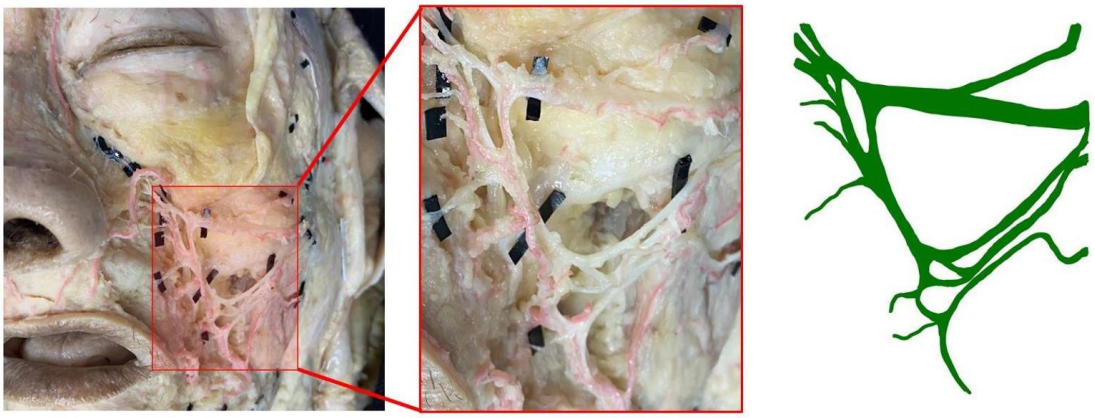

Figure 63 The pattern of zygomaticobuccal plexus from branches of the facial nerve correlated to the anatomical landmarks.

- Moreover, facial muscle was used to be anatomical landmarks for determining the zygomaticobuccal plexus boundary (Figure 64).

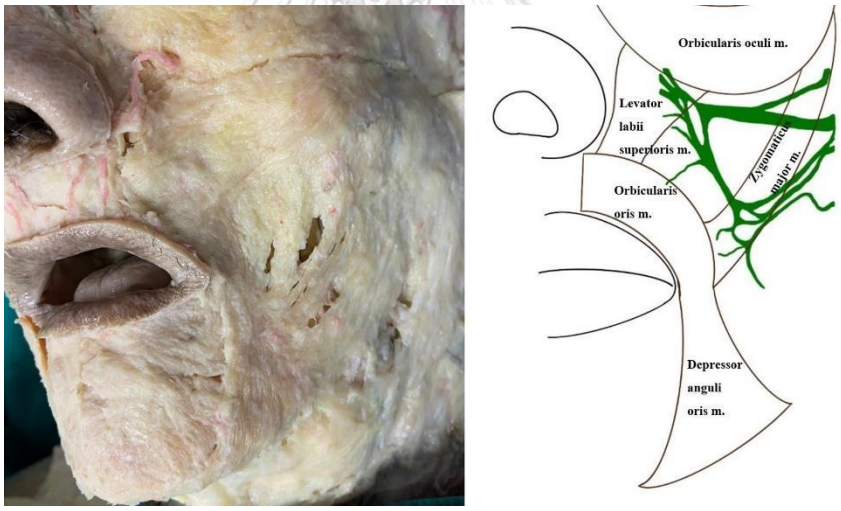

Figure 64 The location of zygomaticobuccal plexus from branches of the facial nerve correlated to the facial muscle landmarks.

- For positioning the zygomaticobuccal plexus, the corner of mouth and alar base were the anatomical landmark (Figure 65).

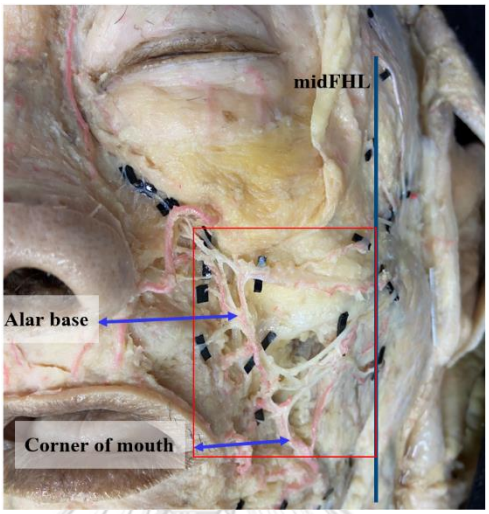

Figure 65 The measurement of the location of the zygomaticobuccal plexus correlated to the anatomical landmark; midFHL; the midpoint of FHL.

Observation and measurement

- Pattern of zygomaticobuccal plexus was collected.
- The horizontal distance (parallel to the Frankfort's horizontal line) from corner of mouth and alar base was measured to the zygomaticobuccal plexus (Figure 65).
- Moreover, the relationship between the zygomaticobuccal plexus and facial vein was recorded.
- The location of the zygomaticobuccal plexus was located by using the boundary of the facial muscle.
- In addition, the communication of the zygomaticobuccal plexus with the infraorbital nerve was observed, and the location of the communicating point was measured correlated to the horizontal line from alar base in x- and y-coordination (Figure 66).

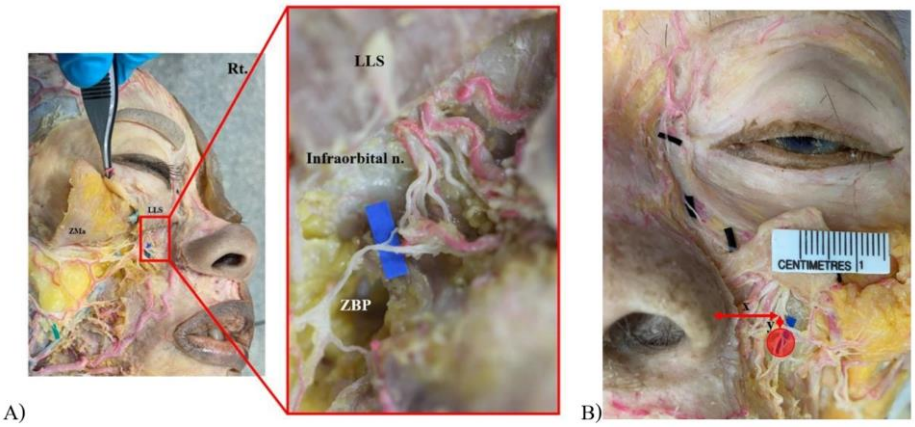

Figure 66 The communication of the zygomaticobuccal plexus with infraorbital nerve (A). The measurement of the communication point of the zygomaticobuccal plexus (B). ZMa; zygomaticus major muscle, LLS; levator labii superioris, ZBP; the zygomaticobuccal plexus

- **The angular nerve**

The determination of the reference line and anatomical landmarks

For positioning the course of the angular nerve, the x axis was the horizontal line passing through the medial canthus or inter-canthal line (ICL).

Observation and measurement

- The transition point and diameter of the angular nerve were recorded and measured correlated to the ala in x- and y- coordination. Then, the location and diameter of the angular nerve were measured correlated to the ICL in vertical distance at anatomical landmarks; mid pupil (y_1), medial limbus (y_2) and medial canthus (y_3). Moreover, the horizontal distance from supra-alar crease (x_1) and medial canthus (x_2) were measured to the angular nerve respectively (Figure 67).
- The origin and relationship between the angular nerve and vessel were recorded.

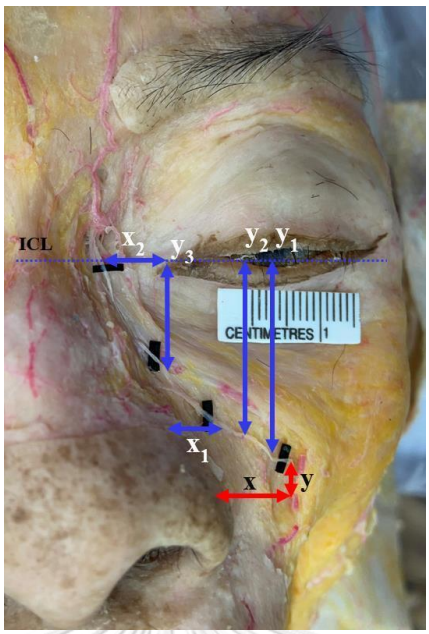

Figure 67 The measurement of the location of the angular nerve. ICL; intercanthal line

In addition, the communication of the angular nerve with sensory nerve was observed. After that, the location of the communicating point was measured correlated to the medial canthus in x- and y-coordination (Figure 68).

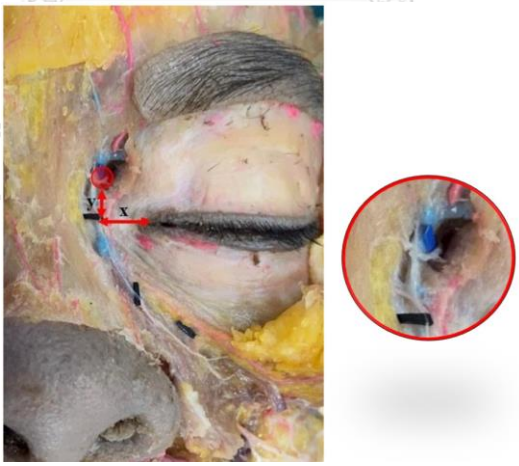

Figure 68 The measurement of the communicating point of the angular nerve correlated to the medial canthus in x- and y-coordination.

- **The marginal mandibular and cervical branch of the facial nerve**

The determination of the reference line and anatomical landmarks

For positioned the marginal mandibular and cervical branch of the facial nerve, the x axis was the inferior margin of the mandible (IML), and y axis was the vertical line perpendicular to the x axis at anterior margin of masseter muscle (AML) (Figure 69).

Observation and measurement

- The location and diameter of the emerging point of the marginal mandibular and cervical branch were measured correlated to the reference line in x- and y-coordination. (MBx, MBy, CBx, CBy)
- The crossing point of the marginal mandibular branch correlated to the reference line. (MBx_1, MBy_1) Additionally, the relationship between the marginal mandibular branch and facial artery was recorded.
- The crossing point of the cervical branch correlated to the reference line. (CBy_1, CBy_2, CBy_3)
- the communication of the cervical branch with sensory nerve was observed, and the location of the communicating point was measured correlated to the reference line in x- and y-coordination. (redline)

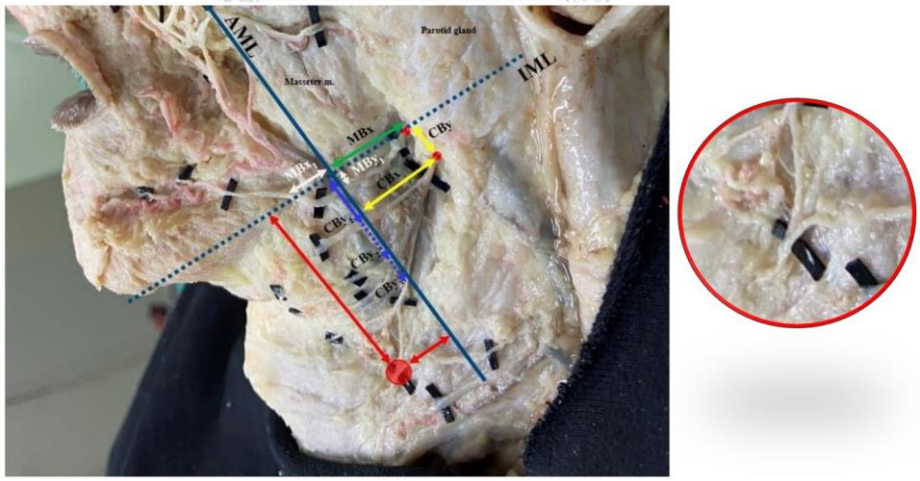

Figure 69 The measurement of the marginal mandibular and cervical branch correlated to the reference line; AML, anterior masseteric line; IML, inferior margin of mandibular line

In addition, the communication of the marginal mandibular nerve with mental nerve was observed. After that, the location of the communicating point was measured correlated to the corner of mouth in x- and y-coordination (Figure 70).

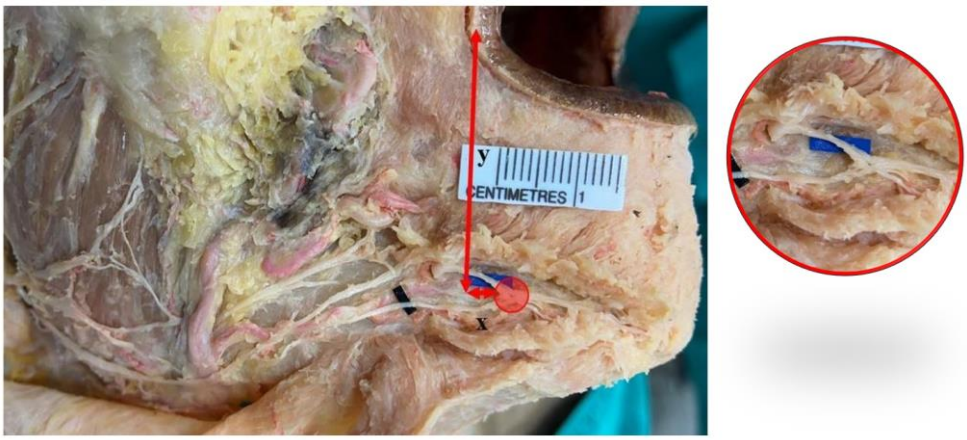

Figure 70 The measurement of the communicating point of the marginal mandibular nerve correlated to the corner of mouth in x- and y-coordination.

- **The facial nerve trunk and division**

The determination of the reference line and anatomical landmarks

For positioning the facial nerve trunk and division of the facial nerve, the X axis was the horizontal line connecting between the supra-alar crease and the inferior border of the tragus (AIL). The Y axis was the anterior tragal line (ATL) (Figure 71).

Observation and measurement

- The location of the branching point of the facial nerve trunk and division was measured correlated to the reference line in x- and y-coordination.
- The origin of the branch of the facial nerve was recorded associated with facial divisions.

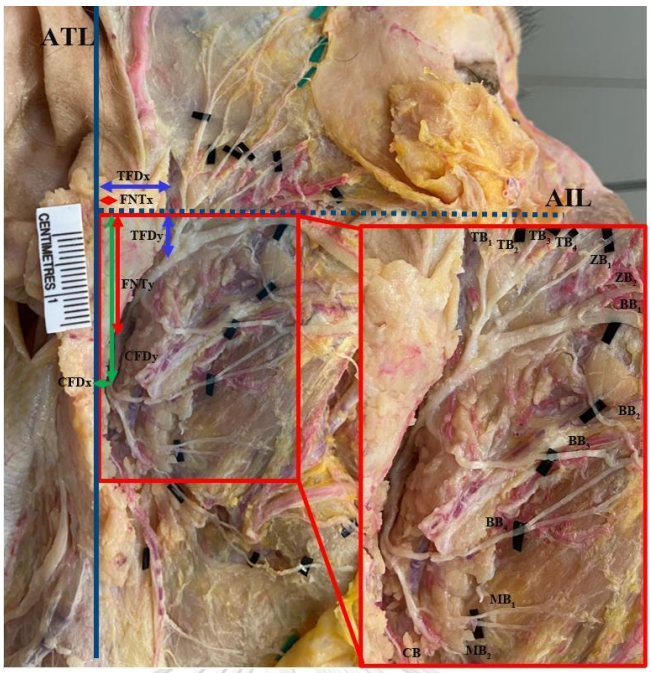

Figure 71 The measurement of the branching point of the facial nerve trunk and division correlated to the reference line; ATL, anterior tragal line; AIL, alar-infratragal line; TFDx, horizontal distance from branching point of temporofacial division to reference line; TFDy, vertical distance from branching point of temporofacial division to reference line; CFDx, horizontal distance from branching point of cervicofacial division to reference line; CFDy, vertical distance from branching point of cervicofacial division to reference line; FNTx, horizontal distance from branching point of facial nerve trunk to reference line; TFDy, vertical distance from branching point of facial nerve trunk to reference line; TB, temporal branch; ZB, zygomatic branch; BB, buccal branch; MB, marginal mandibular branch; CB, cervical branch

3.4.2 For histological study

1) Tissue preparation

To localize the facial nerve relatively to the soft tissue layers of the face, this method was conducted in 7 embalmed cadavers (14 hemi cervicofacial area). The facial soft tissue flap was harvested from the periosteum to the skin in each area following the course of the branch of the facial nerve. Begin with, the face was divided into 6 areas (tear trough, nasolabial, temporal, masseteric, parotid, and mandibular area), and cadaver's skin was marked the boundary (Figure 72). Firstly, a boundary of

temporal area was superior border; 2 cm above the upper eyebrow, inferior border; Frankfort's horizontal line, medial border; vertical line pass through the lateral orbital rim, and lateral border; anterior tragal line. Secondly, the lateral midface will be divided into three columns. Then, 2/3 anterior was the masseteric area, while 1/3 posterior was the parotid area. Thirdly, a boundary of the tear trough area was superior border; superior orbital rim, inferior border; horizontal line from upper ala to the inferior border of the tragus, medial border; midline of the face, and lateral border; vertical line pass through the lateral orbital rim. Fourthly, a boundary of nasolabial area was superior border; horizontal line from of upper alar to the inferior border of the tragus, inferior border; horizontal line from the corner of mouth, medial border; vertical line from the ala, and lateral border; vertical line pass through the lateral orbital rim. Lastly, a boundary of mandibular area was superior border; 2 cm above the inferior margin of the mandibula, inferior border; parallel line of the inferior margin of the mandible at the thyroid cartilage, medial border; midline of neck, and lateral border; parallel line from the anterior masseteric line at the mandibular angle. Next, the tissues were harvested and fixed in 10% formalin approximately 5-7 days.

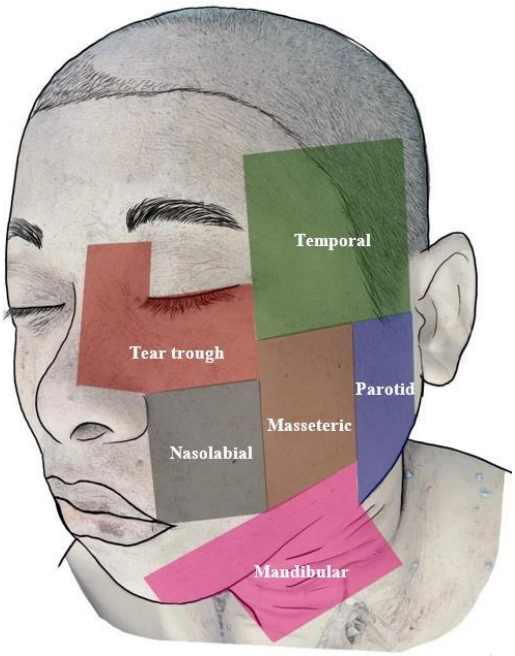

Figure 72 Six areas of the face in the histological study.

2) Tissue trimming

After formalin fixation, the tissue was trimmed in the horizontal plane to the branch of the facial nerve, so it is a different arrangement in each area (Figure 73A). Moreover, the fixed tissue was trimmed with 5 mm width x 20 mm length in all areas except the fixed tissue from the nasolabial area was trimmed with 5 mm width x 15 mm length, because this area is thick tissue. Then, the tissue was put in the cassettes, and labelled follow as column and row in each area; tear trough (TT), nasolabial (N), temporal (T), masseteric (MM), parotid (P), and mandibular (M) area). In addition, the trimmed tissue was recorded if this tissue correlated to the anatomical landmark as upper eyebrow, supraorbital rim, lateral canthus, Frankfort's horizontal line, AIL, ear lobule, mandibular angle, midpoint of the Frankfort's horizontal line, medial canthus, infraorbital rim, supra-alar crease, alar base, upper lip, the corner of mouth and anterior masseteric line (Figure 73B).

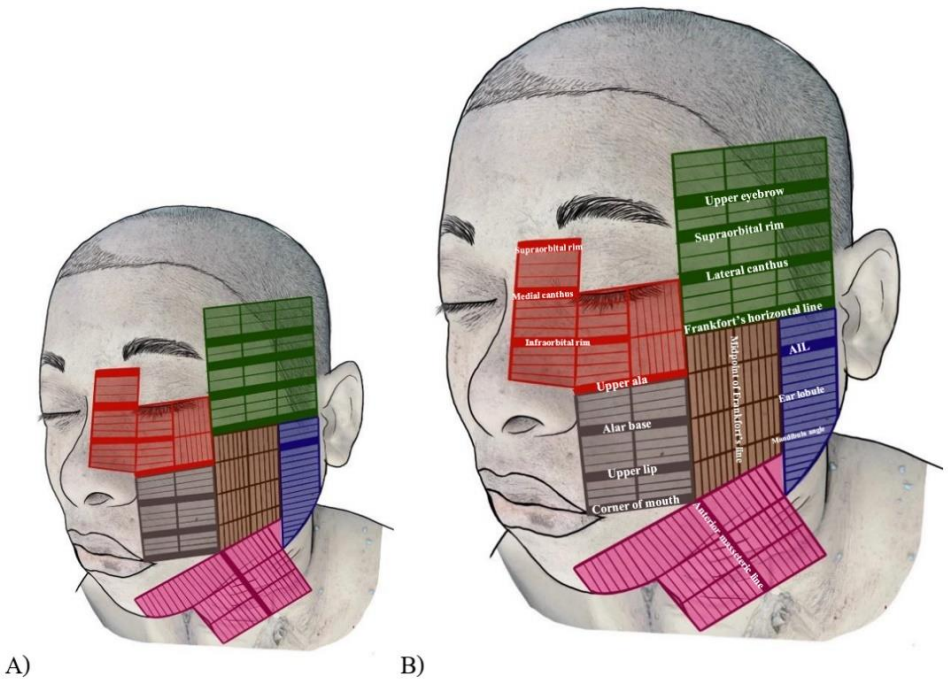

Figure 73 Plane for trimming of the harvested tissue.

3) Tissue processing

There are 3 steps of tissue processing; dehydration, clearing and wax impregnation. Firstly, tissue was removed from the tissue by using increasing concentrations of alcohol (from 70% alcohol to 100% alcohol) for dehydration. Secondly, tissue was utilized by using the xylene (I, II and II) for tissue clearing. Lastly, all areas of the tissue were soaked by paraffin (I, II, III) by 1-2 hour in each step for the impregnation.[117] This procedure was conducted by using an automatic tissue processor (Figure 74).

Figure 74 An automatic tissue processor

4) Tissue embedding

Begin with, 55°C - 60°C liquid paraffin was prepared for tissue embedding. Next, the tissue was put into the mold, and add melting liquid paraffin into the mold. Then, the embedded paraffin mold was placed in the cold area to provide solid paraffin[117].

5) Tissue sectioning

A microtome was used to section the embedded tissue with thickness 4-5 µm. Before section, block paraffin was trimmed, then each tissue was sectioned into 2 sections for hematoxylin and eosin staining and Masson's trichrome staining. Next, each ribbon was put in a hot water bath (35°C- 40°C), and glass slide was used to pick up the ribbon. After that, the glass slide was labeled and was bake in oven at 70 °C for 15 minutes.

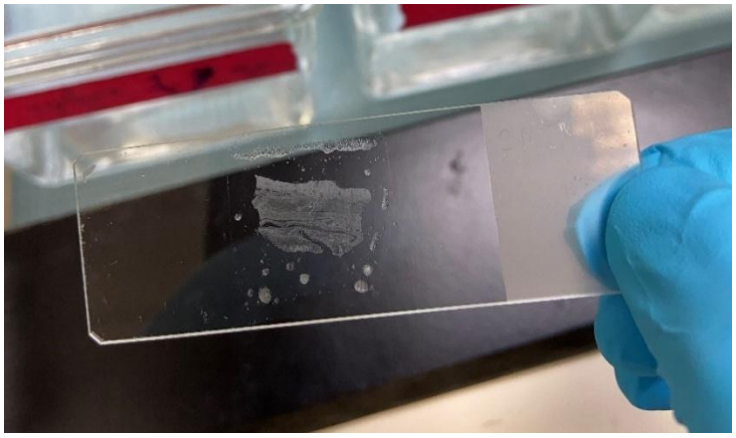

Figure 75 The sectioned tissue after the oven for 15 minutes.

6) Tissue deparaffinization and staining

The tissue was deparaffinized by using xylene, and rehydrated by using alcohol before staining following protocol that present in figure. The hematoxylin and eosin staining and Masson's trichrome staining were used to stain the tissue for observation characteristic of tissue[118].

Firstly, hematoxylin and eosin were used to observe characteristic of tissue for the verification of technical glitch and histopathological transformation. this staining followed protocol in Figure 76.

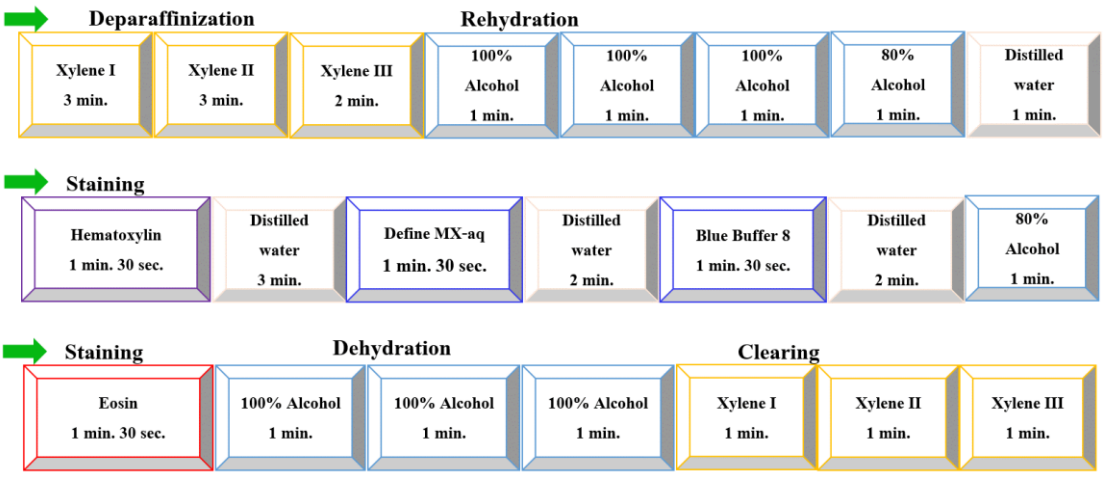

Figure 76 The hematoxylin and eosin staining protocol.

Secondly, Masson's trichrome was detected collagen fibers in tissue. The result showed that collagen was stained with blue, nucleus was stained with black, and muscle, cytoplasm or elastic fiber were stained with red. After that, the glass side was mounted by mounting medium and covered by cover glass.

7) Tissue observation and analysis

Lastly, the microscope with a connected digital camera was used to observe location of the branch of the facial nerve in each area (Figure 77), and Axioscan Z1 scanned the tissue slide. After that, the location of the branch of the facial nerve was recorded relative to the anatomical landmarks following Figure73B.

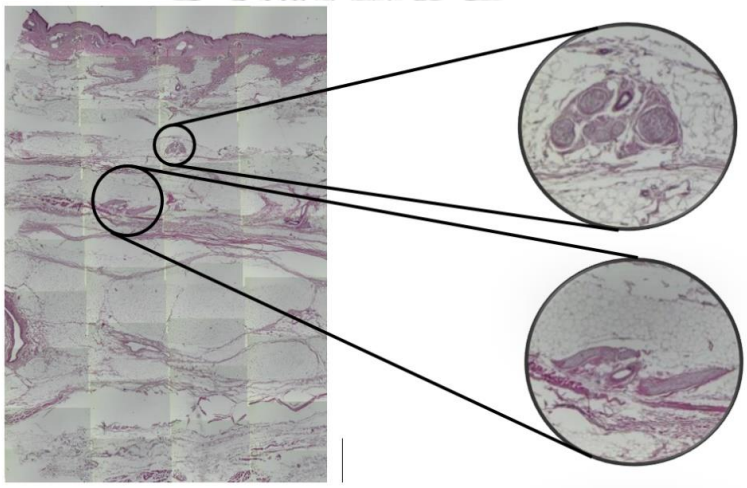

Figure 77 Histological section of temporal area with H&E staining at the Frankfort's horizontal line.

3.4.3 For Sihler's technique

For investigation of the branch of the facial nerve in facial muscle, Sihler's technique was conducted in 8 soft cadavers (16 hemi cervicofacial area). This protocol includes 8 processes and approximately 2-3 months as;

1) Tissue preparing and fixation

The skin and subcutaneous tissue were removed in 8 faces of soft cadaver. After that, the incision line was made from the SMAS to the periosteum following the

midline of face and neck, superior border as horizontal line above the hair line 1 cm and inferior border at level of the clavicle (Figure 78A). After that, the facial soft tissue flap was harvested following the incision line from the periosteum of the both sides of the face (Figure 78B), and the harvested flab was attached on grid plastic by clear string. Additionally, the boundary of all muscles were marked by black yarn. Next, the harvested flab was rinsed by tap water, and fixed in 10% unneutralized formalin for 5-7 days.

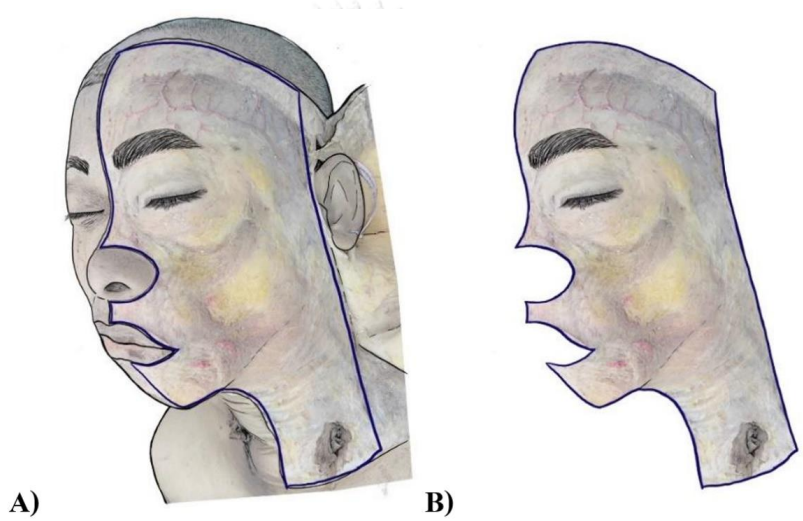

Figure **78** The cadaver dissection for Sihler's stain technique. The SMAS layer of the face and the incision line to harvest facial tissue (A). Harvested facial soft tissue flap (B).

2) Maceration and depigmentation

Solution preparing

The 3% aqueous potassium hydroxide (KOH) solution was prepared. The component of 3% KOH includes 3 grams of KOH per 100 ml of distilled water and 0.2 ml (or 3 drops) of 3% hydrogen peroxide (H_2O_2).

Procedure

The specimens was rinsed by running tap water for 1 hours. Next, the specimen was macerated and depigmented with decreasing 3% KOH solution concentrations (100%, 70%, 50% approximately 1 week in each concentration) for 2-3 weeks. The

solution were changed when it becomes a turbid or browned solution. After 2nd week, the specimen was checked every day for excess maceration prevention. This process was ended when the specimen became whitened and translucent tissue.

3) Decalcification

Solution preparing

Sihler's solution I was prepared. The component of Sihler's solution I includes glacial acetic acid, glycerin, and aqueous chloral hydrate in ratio 1:1:6.

Procedure

The specimens were rinsed by smooth running tap water for 1 hours. Then, the specimens were soaked in Sihler's solution I for 1-2 weeks for decalcification. The solution was changed when it became turbid or twice a week.

4) Staining

Solution preparing

Stock Ehrlich's hematoxylin was prepared. The component of Ehrlich's hematoxylin consists of 2 grams of hematoxylin, 100 ml of 100% alcohol, 100 ml of distilled water, 10 ml of glacial acetic acid, 3 grams of potassium alum, 0.1 gram of the sodium iodate and 100 ml of glycerin. This solution is ready to use approximately 1 month, and it becomes a dark red solution.

After that, Sihler's solution II was prepared before using. The component of Sihler's solution I includes stock Ehrlich's hematoxylin, glycerin, and 1% aqueous chloral hydrate in ratio 1:1:6.

Procedure

The specimens were rinsed by smooth running tap water for 1 hours. Then, the specimens were submerged in Sihler's solution II for 3-4 weeks for staining. The solution was changed once or twice a week. The specimens gradually became dark violet and all nerves of the specimen were stained. This process was ended when the smallest branch of all nerves became violet after the specimen was observed under the surgical microscope.

5) Destaining

The specimens were rinsed by smooth running tap water for 30 minutes. Then, the specimens were bathed in Sihler's solution I with agitation approximately 3-4 hours for destaining. The solution was changed when it became violet or dark brow. The specimen was checked under the surgical microscope during the process, and this process was ended when all nerve branches become violet. On the contrary, the muscle fibers and other soft tissue became glassy purple.

6) Neutralization

The specimens were rinsed by smooth running tap water for 1 hours. Next, the specimens were submersed in freshly 0.05% lithium carbonate solution for 1-2 hours with agitation to neutralize. The solution was changed when it becomes pinkish. The specimen was checked under the surgical microscope during the process every 30 minutes, and this process was stopped when all nerve branches become dark blue from violet.

7) Clearing

The specimens were rinsed by smooth running tap water for 1 hours. Then, the specimens were cleared of excessive staining in dilute aqueous glycerin (40%, 60% and 80% for 1 day each or 50% for 3-5 days). The specimens were checked every day, and stop this process when all nerve branches become noticeable under the surgical microscope.

8) Transparency

The specimens were preserved in 100% glycerin with a little thymol crystal to transparent the tissue.

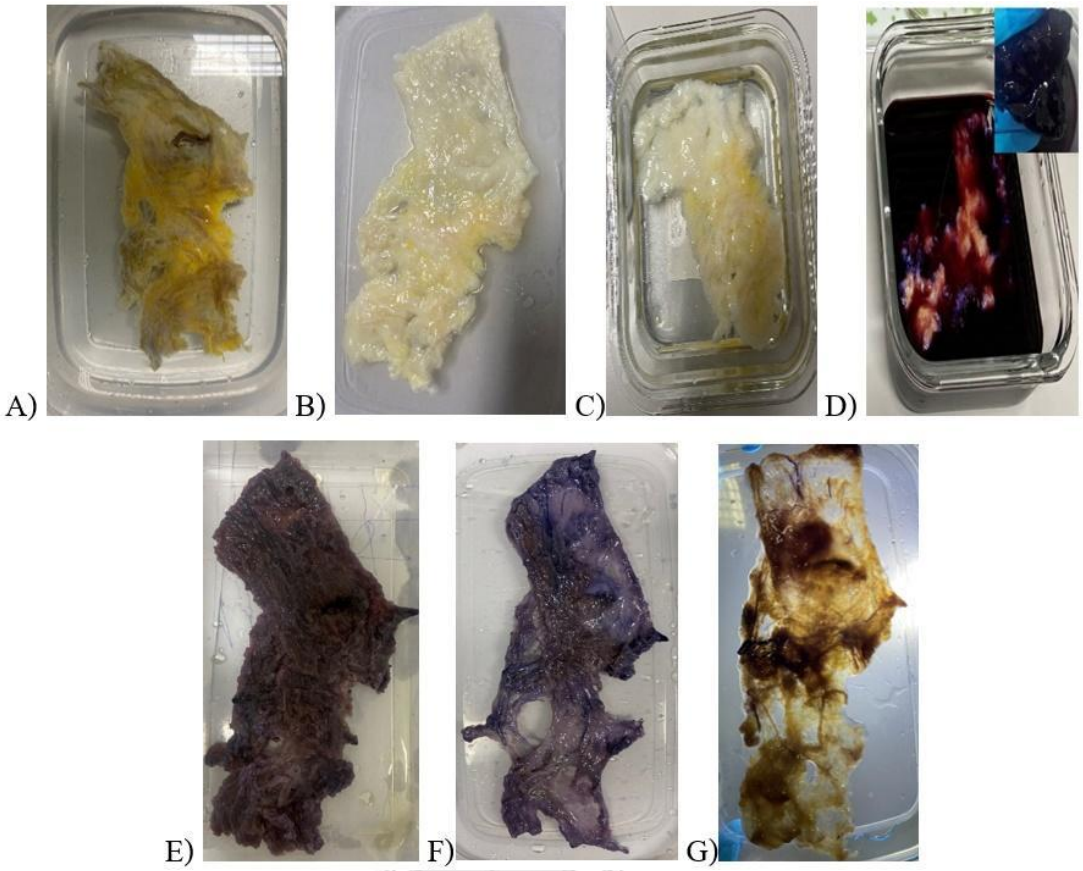

Figure 79 The facial tissue flab in Sihler's staining processes; Fixation (A), Maceration and depigmentation (B), Decalcification (C), Staining (D), Destaining (E), Neutralization (F), and Clearing (G).

In addition, the translucent facial flaps were observed and photographed under low magnification with a surgical microscope.

Observation

- The pattern of the facial nerve branch in the facial muscle

3.5 Data collection

The data was accumulated in the case record form

Case Record Form (Cadaveric dissection)

Date:…….. **Table No**……. **Cadaveric code**…….…… **Gender** ..…Male ..…Female

Side …..Right .....Left **Age**……..……years **Height**……..….cm **Weight** ……..……kg

BFN	**AIL** Emerging point 1)_____ 2)_____ (x, y) mm	**FHL** 1)_____ 2)_____ (x) mm	**LCHL** 1)_____ 2)_____ (x) mm	**SOL** 1)_____ 2)_____ (x) mm	Muscular entry site LOL+ LCHL/ UEL (x, y) mm	Communication point LOL+ LCHL (x, y) mm
Tb1	1)_____, _____ 2)_____, _____ Diameter 1)_____ 2)_____	1)_____ 2)_____ Diameter 1)_____ 2)_____	1)_____ 2)_____ Diameter 1)_____ 2)_____	1)_____ 2)_____ Diameter 1)_____ 2)_____	_____m. _____m. _____m. _____m.	_____n. 1)_____, _____ 2)_____, _____
Tb2	1)_____, _____ 2)_____, _____ Diameter 1)_____ 2)_____	1)_____ 2)_____ Diameter 1)_____ 2)_____	1)_____ 2)_____ Diameter 1)_____ 2)_____	1)_____ 2)_____ Diameter 1)_____ 2)_____	_____m. _____m. _____m. _____m.	_____n. 1)_____, _____ 2)_____, _____
Tb3	1)_____, _____ 2)_____, _____ Diameter 1)_____ 2)_____	1)_____ 2)_____ Diameter 1)_____ 2)_____	1)_____ 2)_____ Diameter 1)_____ 2)_____	1)_____ 2)_____ Diameter 1)_____ 2)_____	_____m. _____m. _____m. _____m.	_____n. 1)_____, _____ 2)_____, _____

Tb4	1)_____, _____ 2)_____, _____ Diameter 1)_____ 2)_____	1)_____ 2)_____ Diameter 1)_____ 2)_____	1)_____ 2)_____ Diameter 1)_____ 2)_____	1)_____ 2)_____ Diameter 1)_____ 2)_____	_____m. _____m. _____m. _____m.	_____n. 1)_____, _____ 2)_____, _____
Tb5	1)_____, _____ 2)_____, _____ Diameter 1)_____ 2)_____	1)_____ 2)_____ Diameter 1)_____ 2)_____	1)_____ 2)_____ Diameter 1)_____ 2)_____	1)_____ 2)_____ Diameter 1)_____ 2)_____	_____m. _____m. _____m. _____m.	_____n. 1)_____, _____ 2)_____, _____

BFN	**AIL** Emerging point 1)_____ 2)_____ (x, y) mm	**FHL** 1)_____ 2)_____ Crossing/Parallel (x, y) mm	**midFHL** (y) mm	Muscular entry site	Communication point FHL+ LOL (x, y) mm
Zb1	1)_____,_____ 2)_____,_____ Diameter 1)_____ 2)_____	1)_____, _____ 2)_____, _____ Diameter 1)_____ 2)_____	1)_____ 2)_____ Diameter 1)_____ 2)_____	_____m. _____m. _____m. _____m.	_____n. 1)_____, _____ 2)_____, _____ _____n. 1)_____, _____ 2)_____, _____
Zb2	1)_____,_____ 2)_____,_____ Diameter 1)_____ 2)_____	1)_____, _____ 2)_____, _____ Diameter 1)_____ 2)_____	1)_____ 2)_____ Diameter 1)_____ 2)_____	_____m. _____m. _____m. _____m.	_____n. 1)_____, _____ 2)_____, _____ _____n. 1)_____, _____ 2)_____, _____
Zb3	1)_____,_____ 2)_____,_____ Diameter 1)_____ 2)_____	1)_____, _____ 2)_____, _____ Diameter 1)_____ 2)_____	1)_____ 2)_____ Diameter 1)_____ 2)_____	_____m. _____m. _____m. _____m.	_____n. 1)_____, _____ 2)_____, _____ _____n. 1)_____, _____ 2)_____, _____
Zb4	1)_____,_____ 2)_____,_____ Diameter 1)_____ 2)_____	1)_____, _____ 2)_____, _____ Diameter 1)_____ 2)_____	1)_____ 2)_____ Diameter 1)_____ 2)_____	_____m. _____m. _____m. _____m.	_____n. 1)_____, _____ 2)_____, _____ _____n. 1)_____, _____ 2)_____, _____

BFN	**AIL** Emerging point 1)_____ 2)_____ (x, y) mm	**midFHL** 1)_____ 2)_____ (y) mm	Relationship to the parotid duct	Muscular entry site CL/ABL (x, y) mm	Communication point LCHL (x, y) mm
Bb1	1)_____,_____ 2)_____,_____ Diameter 1)_____ 2)_____	1)_____ 2)_____ 3)_____ Diameter 1)_____ 2)_____	___Above ___Cross __Below	_____m. _____m. _____m. _____m.	_____n. 1)_____, _____ 2)_____, _____ _____n. 1)_____, _____ 2)_____, _____
Bb2	1)_____,_____ 2)_____,_____ Diameter 1)_____ 2)_____	1)_____ 2)_____ 3)_____ Diameter 1)_____ 2)_____	___Above ___Cross __Below	_____m. _____m. _____m. _____m.	_____n. 1)_____, _____ 2)_____, _____ _____n. 1)_____, _____ 2)_____, _____
Bb3	1)_____,_____ 2)_____,_____ Diameter 1)_____ 2)_____	1)_____ 2)_____ 3)_____ Diameter 1)_____ 2)_____	___Above ___Cross __Below	_____m. _____m. _____m. _____m.	_____n. 1)_____, _____ 2)_____, _____ _____n. 1)_____, _____ 2)_____, _____
Bb4	1)_____,_____ 2)_____,_____ Diameter 1)_____ 2)_____	1)_____ 2)_____ 3)_____ Diameter 1)_____ 2)_____	___Above ___Cross __Below	_____m. _____m. _____m. _____m.	_____n. 1)_____, _____ 2)_____, _____ _____n. 1)_____, _____ 2)_____, _____

BFN	**IML** Emerging point 1)_____ 2)_____ (x, y) mm	**IML** Crossing point (x) mm	**IML at Ant. Masseter** 1)_____ 2)_____ (y) mm	Relationship to the facial artery	Muscular entry site CL (x, y) mm	Commu-nication point IML+ Ant. Tragus (x, y) mm
Mb1	1)_____, _____ 2)_____, _____ Diameter 1)_____ 2)_____	1)_____ 2)_____ Diameter 1)_____ 2)_____	1)_____ 2)_____ Diameter 1)_____ 2)_____	___Superficial ___Deep	_____m. _____m. _____m. _____m.	_____n. 1)_____, _____ 2)_____, _____ _____n. 1)_____, _____ 2)_____, _____
Mb2	1)_____, _____ 2)_____, _____ Diameter 1)_____ 2)_____	1)_____ 2)_____ Diameter 1)_____ 2)_____	1)_____ 2)_____ Diameter 1)_____ 2)_____	___Superficial ___Deep	_____m. _____m. _____m. _____m.	_____n. 1)_____, _____ 2)_____, _____ _____n. 1)_____, _____ 2)_____, _____
Mb3	1)_____, _____ 2)_____, _____ Diameter 1)_____ 2)_____	1)_____ 2)_____ Diameter 1)_____ 2)_____	1)_____ 2)_____ Diameter 1)_____ 2)_____	___Superficial ___Deep	_____m. _____m. _____m. _____m.	_____n. 1)_____, _____ 2)_____, _____ _____n. 1)_____, _____ 2)_____, _____
Mb4	1)_____, _____ 2)_____, _____ Diameter 1)_____ 2)_____	1)_____ 2)_____ Diameter 1)_____ 2)_____	1)_____ 2)_____ Diameter 1)_____ 2)_____	___Superficial ___Deep	_____m. _____m. _____m. _____m.	_____n. 1)_____, _____ 2)_____, _____ _____n. 1)_____, _____ 2)_____, _____

BFN	**IML** Emerging point (x, y) mm	**IML** Branching point (x, y) mm	**IML at Ant. Masseter** (y) mm	Muscular entry site IML+Ant.Masseter (x, y) mm	Communication point IML+ Ant.Tragus (x, y) mm
Cb1	1)_____, _____ 2)_____, _____ Diameter 1)_____ 2)_____	1)_____, _____ 2)_____, _____ Diameter 1)_____ 2)_____	1)_____ 2)_____ Diameter 1)_____ 2)_____	_____m. _____m. _____m. _____m.	_____n. 1)_____, _____ 2)_____, _____ _____n. 1)_____, _____ 2)_____, _____
Cb___		1)_____, _____ 2)_____, _____ Diameter 1)_____ 2)_____	1)_____, _____ 2)_____, _____ Diameter 1)_____ 2)_____	1)_____ 2)_____ Diameter 1)_____ 2)_____	_____m. _____m. _____m. _____m.
Cb___		1)_____, _____ 2)_____, _____ Diameter 1)_____ 2)_____	1)_____, _____ 2)_____, _____ Diameter 1)_____ 2)_____	1)_____ 2)_____ Diameter 1)_____ 2)_____	_____m. _____m. _____m. _____m.
Cb___		1)_____, _____ 2)_____, _____ Diameter 1)_____ 2)_____	1)_____, _____ 2)_____, _____ Diameter 1)_____ 2)_____	1)_____ 2)_____ Diameter 1)_____ 2)_____	_____m. _____m. _____m. _____m.

Zygomaticobuccal plexus							
Branching performs	**Corner of mouth** (x) mm	**Mid ACL** 1)_____ 2)_____ (x) mm	**Alar base point** (x) mm	**Alar** (x) mm	Relation to the facial vein	Muscular entry site CL (x, y) mm	Communication point AIL (x, y) mm
_____n. _____n. _____n. Pattern _____ _____n. _____n. _____n. _____ _____n. _____n. _____n.	1)_____ 2)_____ Diameter 1)_____ 2)_____ 1)_____ 2)_____ Diameter 1)_____ 2)_____ Distance 1)_____ 2)_____	1)_____ 2)_____ Diameter 1)_____ 2)_____ 1)_____ 2)_____ Diameter 1)_____ 2)_____ Distance 1)_____ 2)_____	1)_____ 2)_____ Diameter 1)_____ 2)_____ 1)_____ 2)_____ Diameter 1)_____ 2)_____ Distance 1)_____ 2)_____	1)_____ 2)_____ Diameter 1)_____ 2)_____ 1)_____ 2)_____ Diameter 1)_____ 2)_____ Distance 1)_____ 2)_____	__Medial __Lateral __Above __Below	_____m. _____m. _____m. _____m. _____m. _____m. _____m. _____m.	_____n. 1)_____, _____ 2)_____, _____ _____n. 1)_____, _____ 2)_____, _____

Angular nerve							
AIL Transition point Upper ala (x, y) mm	**Upper Alar** (x) mm	**Mid pupil** (y) mm	**Medial limbus** (y) mm	**Medial canthus** (y) mm	**Medial canthus** Crossing point 1)_____ 2)_____ (x) mm	Muscular entry site medianL+ interCanthal (x, y) mm	Communication point medianL+ interCanthal (x, y) mm
_____n. 1)_____, _____ 2)_____, _____ Diameter 1)_____ 2)_____ _____m. (pernatration)	1)_____ 2)_____ Diameter 1)_____ 2)_____	1)_____ 2)_____ Diameter 1)_____ 2)_____	1)_____ 2)_____ Diameter 1)_____ 2)_____	1)_____ 2)_____ Diameter 1)_____ 2)_____	1)_____ 2)_____ Diameter 1)_____ 2)_____	_____m. _____m. _____m. _____m.	_____n. 1)_____, _____ 2)_____, _____

Intrapa-rotid part	**Main trunk** Branching point AIL+ Ant.Tragus (x, y) mm	**Temporofacial division** Branching point AIL+ Ant.Tragus (x, y) mm	Branching point AIL+ Ant.Tragus (x, y) mm	**Cervicofacial division** Branching point AIL+ Ant.Tragus (x, y) mm	Branching point AIL+ Ant.Tragus (x, y) mm
FNT **Pattern**	1)_____, _____ 2)_____, _____	1)_____, _____ 2)_____, _____ _____n. _____n. _____n. _____n. _____n. _____n.	1)_____, _____ 2)_____, _____ _____n. _____n. _____n. _____n. _____n. _____n.	1)_____, _____ 2)_____, _____ _____n. _____n. _____n. _____n. _____n. _____n.	1)_____, _____ 2)_____, _____ _____n. _____n. _____n. _____n. _____n. _____n.

Case Record Form (Histological study)

Date:…… **Table No**…… **Cadaveric code**…… **Gender** …..Male …..Female

Side …..Right …..Left **Age**……years **Height**……..…..cm **Weight** ……..……kg

Temporal area

Anatomical landmarks	Slide Code __T1	Branch of FN	Location of nerve	Slide Code __T2	Branch of FN	Location of nerve	Slide Code __T3	Branch of FN	Location of nerve
Upper eyebrow									
Superior orbital rim									
Lateral canthus									
Frankfort's horizontal line									

Parotid area

Anatomical landmarks	Slide Code __P1	Branch of FN	Location of nerve	Slide Code __P2	Branch of FN	Location of nerve	Slide Code __P3	Branch of FN	Location of nerve
AIL									
Ear lobule									
Mandibular angle									

Masseteric area

Anatomical landmarks	Slide Code __MM1	Branch of FN	Location of nerve	Slide Code __MM2	Branch of FN	Location of nerve	Slide Code __MM3	Branch of FN	Location of nerve
Midpoint of Frankfort's line									

Tear trough area

Anatomical landmarks	Slide Code __TT1	Branch of FN	Location of nerve	Slide Code __TT2	Branch of FN	Location of nerve	Slide Code __TT3	Branch of FN	Location of nerve
Superior orbital rim									
Medial canthus									
Inferior orbital rim									
Upper ala									

Nasolabial area

Anatomical landmarks	Slide Code __N1	Branch of FN	Location of nerve	Slide Code __N2	Branch of FN	Location of nerve	Slide Code __N3	Branch of FN	Location of nerve
Alar base									
Upper lip									
Corner of mouth									

Mandibular area

Anatomical landmarks	Slide Code __M1	Branch of FN	Location of nerve	Slide Code __M2	Branch of FN	Location of nerve	Slide Code __M3	Branch of FN	Location of nerve
AML									

Case Record Form (Sihler's technique)

Date:…….. **Table No**…….. **Cadaveric code**…….. **Gender** ……Male ……Female

Side …..Right …..Left **Age**……..……years **Height**……..….cm **Weight** ……..……kg

Facial muscle	Number of nerve supply	Nerve	Pattern	Nerve communication
Frontalis				
Orbicularis oculi				
Zygomaticus major				
Levator labii superioris				
Orbicularis oris				
Depressor anguli oris				
Platysma				

3.6 Data analysis

The collected data of this study were analyzed by using IBM SPSS statistics software version 23. The acquired data from cadaveric dissection were analyzed by descriptive statistics including frequency, percentage, mean, standard deviation, min, and max. Furthermore, the collected data were tested by using the Shapiro-Wilk test. Then, independent sample t-test was compared the difference of distance and diameter between sex (male versus female) when the data are normal distribution, while Mann-Whitney U test was compared in nonparametric test. A two-tailed p-value of less than 0.05 was considered statistically significant.

In addition, the acquired data from histological study and Sihler' stain techniques were presented by descriptive statistics including frequency and percentage.

3.7 Ethical consideration

The protocol of this study was conducted in the human cadavers, so this study was approved by the Institutional Review Board of the Faculty of Medicine, Chulalongkorn University and the director of the King Chulalongkorn Memorial Hospital.

CHAPTER IV

RESULTS

The results of present study were described into three parts including the results from cadaveric dissection, histological study, and Sihler's staining technique.

1) Cadaveric dissection; Forty-two hemifaces of embalmed cadavers with an average age of 79.00 ±12.92 (48-98) years, were conducted by conventional dissection.

2) Histological study; the procedure was performed in fourteen hemi-faces of fourteen embalmed cadavers, 7 males and 7 females with an average age of 81.79 ±8.60 (69-96) years.

3) Sihler's staining technique; the procedure was conducted in sixteen hemi-faces of eight soft cadavers, 4 males and 4 females with an average age of 71.50 ±10.03 (55-84) years.

4.1 The results of cadaveric dissection

4.1.1 The number and the emerging point of the branches of the facial nerve

The number and the emerging point of the branches of the facial nerve were investigated by the cadaveric dissection. The number of the temporal and zygomatic branches were counted after they appeared at the superior border of the parotid gland, while the buccal branch was recorded at anterior border of the parotid gland. Moreover, the marginal mandibular and cervical branches were counted at antero-inferior border of the parotid gland. The results revealed that the mean number of the temporal, zygomatic, buccal, marginal mandibular and cervical branches of the facial nerve were 2.57 ±0.83, 1.83 ±0.69, 3.10 ±0.82, 1.36 ±0.49, and 1.07 ±0.26 respectively (Table 4). Moreover, the temporal branch gave a single branch in 4.76%, 2 branches in 45.24%, 3 branches in 42.86%, 4 branches in 2.38%, and 5 branches in 4.76%. The zygomatic branch gave a single branch in 33.33%, 2 branches in 50.00%, and 3 branches in 16.67%. The buccal branch gave 2 branches in 23.81%, 3 branches in 47.62%, 4 branches in 23.81%, and 5 branches in 4.76%. In addition, the marginal mandibular

gave a single branch in 64.29% and 2 branches in 35.71%, while the cervical branch gave a single branch in 92.86% and 2 branches in 7.14%.

Table 4 The number of the branches of the facial nerve

Branch of the facial nerve	Mean of Number of branches	The number of branches				
		Single	2	3	4	5
Temporal (n=42)	2.57 ±0.83	2 (4.76%)	19 (45.24%)	18 (42.86%)	1 (2.38%)	2 (4.76%)
Zygomatic (n=42)	1.83 ±0.69	14 (33.33%)	21 (50.00%)	7 (16.67%)	-	-
Buccal (n=42)	3.10 ±0.82	-	10 (23.81%)	20 (47.62%)	10 (23.81%)	2 (4.76%)
Marginal mandibular (n=42)	1.36 ±0.49	27 (64.29%)	15 (35.71%)	-	-	-
Cervical (n=42)	1.07 ±0.26	39 (92.86%)	3 (7.14%)	-	-	-

The data was presented as frequency (percentage) and mean ±SD.

Moreover, the emerging points were measured correlated to the X-axis and Y-axis. The X-axis was the horizontal line connecting the supra-alar crease and the inferior border of the tragus (AIL), whereas the Y axis was the anterior tragal line (ATL) (Table 5). The results presented that the X and Y distances of the emerging point of temporal branch were 21.95 ±4.87 mm, and 6.75 ±4.51 mm, respectively, while the emerging point of zygomatic branch were 30.63 ±5.73 mm, and 1.36 ±4.09 mm in X and Y axis, respectively. Moreover, the mean distance of the emerging point of the buccal branch in X- axis was 29.71 ±6.58 mm, and in Y axis was -17.94 ±13.18 mm. Additionally, the X and Y distances of the emerging point of the marginal mandibular were 22.48 ±5.19

mm, and -42.37 ±6.53 mm respectively, whereas the X and Y distances of the emerging point of the cervical branches were 19.62 ±6.29 mm, and -49.85 ±6.40 mm respectively.

In addition, the X distance of the emerging point of the temporal branch of male cadavers (22.78 ±4.85 mm) was significantly wider than the female cadaver (21.09 ±4.79 mm) (p = 0.031). In addition, the Y distance of the emerging point of the marginal mandibular and cervical branches were statistically significant difference while comparing between gender (p <0.001). Furthermore, the mean of the diameter of the temporal, zygomatic, buccal, marginal mandibular and cervical branches of the facial nerve were 0.93 ±0.33 mm, 0.95 ±0.36 mm, 1.21 ±0.61 mm, 0.87 ±0.31 mm, and 1.12 ±0.34 mm, respectively. However, the diameter of the branches of the facial nerve of male wider than the female cadavers, and there was statistically significant difference between male and female cadavers in all branch except the cervical branch (p < 0.05).

Table 5 The emerging points of the branches of the facial nerve.

Branches of the facial nerve	Parameters	Grouping variables			t-test/ Z	P-value
		Total	Male	Female		
Temporal (n = 108) Male (n = 55) Female (n = 53)	$AILE_{TB}$-ATL X-axis	21.95 ±4.87 (10.62, 35.75)	22.78 ±4.85 (10.62, 33.75)	21.09 ±4.79 (13.37, 35.75)	-2.160	0.031*
	$AILE_{TB}$-ATL Y-axis	6.75 ±4.51 (-1.48, 17.56)	6.28 ±4.85 (0.00, 17.57)	7.24 ±4.11 (-1.49, 16.80)	-1.451	0.147
	DE_{TB}	0.93 ±0.33 (0.36, 1.86)	1.04 ±0.33 (0.36, 1.86)	0.81 ±0.28 (0.42, 1.85)	-3.903	<0.001*

Branches of the facial nerve	Parameters	Grouping variables			t-test/ Z	P-value
		Total	Male	Female		
Zygomatic (n = 77) Male (n = 41) Female (n = 36)	$AILE_{ZB}$-ATL X-axis	30.63 ±5.73 (19.53, 53.04)	31.81 ±6.04 (19.53, 53.04)	29.28 ±5.10 (19.56, 41.53)	- 1.848	0.065
	$AILE_{ZB}$-ATL Y-axis	1.36 ±4.09 (-9.14, 13.56)	0.99 ±4.34 (-9.14, 13.56)	1.81 ±3.81 (-3.80, 11.97)	- 1.112	0.266
	DE_{ZB}	0.95 ±0.36 (0.41, 1.87)	1.05 ±0.38 (0.47, 1.87)	0.84 ±0.32 (0.41, 1.81)	- 2.522	0.012*
Buccal (n = 130) Male (n = 67) Female (n = 63)	$AILE_{BB}$ - ATL X-axis	29.71 ±6.58 (13.33, 48.27)	30.33 ±7.30 (13.33, 48.27)	29.06 ±5.70 (18.74, 42.99)	- 1.388	0.165
	$AILE_{BB}$-ATL Y-axis	-17.94 ±13.18 (-45.09, 9.76)	-20.03 ±14.08 (-45.09, 9.76)	-15.71 ±11.86 (-40.36, 5.84)	- 1.885	0.062
	DE_{BB}	1.21 ±0.61 (0.35, 5.15)	1.33 ±0.71 (0.43, 5.15)	1.08 ±0.47 (0.35, 2.29)	- 2.264	0.024*
Marginal mandibular (n = 57)	$AILE_{MB}$-ATL X-axis	22.48 ±5.19	22.65 ±5.76 (10.06, 32.52)	22.34 ±4.72 (15.38, 31.12)	0.220	0.827

Branches of the facial nerve	Parameters	Grouping variables			t-test/ Z	P-value
		Total	Male	Female		
Male (n = 27) Female (n = 30)		(10.06, 49.07)				
	$AILE_{MB}$-ATL Y-axis	-42.37 ±6.53 (-56.52, -29.52)	-45.62 ±6.38 (-56.52, -30.72)	-39.44 ±5.20 (-49.66, -29.52)	-4.029	<0.001*
	DE_{MB}	0.87 ±0.31 (0.34, 1.79)	0.99 ±0.34 (0.51, 1.79)	0.77 ±0.23 (0.34, 1.35)	-2.598	0.009*
Cervical (n = 45) Male (n = 22) Female (n = 23)	$AILE_{CB}$-ATL X-axis	19.62 ±6.29 (9.29, 31.67)	20.68 ±6.24 (9.29, 31.67)	18.60 ±6.30 (10.59, 28.85)	-1.033	0.302
	$AILE_{CB}$-ATL Y-axis	-49.85 ±6.40 (-38.26, -65.72)	-53.28 ±6.03 (-44.44, -65.72)	-46.58 ±4.92 (-38.26, -55.68)	4.088	<0.001*
	DE_{CB}	1.12 ±0.34 (0.48, 1.95)	1.11 ±0.32 (0.62, 1.57)	1.12 ±0.36 (0.48, 1.95)	-0.111	0.912

AILE -ATL, Distance between the emerging point of the branches of the facial nerve and ATL in X-axis and Y-axis. DE, Diameter of the branches of the facial nerve at the emerging point. TB, temporal; ZB, zygomatic; BB, buccal; MB, marginal mandibular; CB, cervical. The data was presented as mean ±SD, (min, max) in millimeters.

4.1.2 The temporal branch of the facial nerve

Several temporal branches emerged from the superior portion of the parotid gland, so the emerging point was divided into 10 mm in each part for clearly identify (Table 6). In most cases (62 out of 108 branches (57.41%)), the emerging point of the temporal branch was located at 20.01-30.00 mm correlated to the AIL. The mean distance was 23.78 ±2.42 mm along the X-axis, and 6.87 ±4.15 mm along the Y-axis. The mean diameter was 0.98 ±0.30 mm. On the contrary, a few of the emerging point of the temporal branch was located at distances more than 30 mm (8 of 108 branches (7.41%)). In addition, the min and max distances of the emerging point of the temporal branch in the X-axis were 10.62 and 35.75 mm, respectively.

Table 6 The location and diameter of the temporal branch of the facial nerve at emerging point.

Parameters	Grouping variables (n = 108)		
	At AIL 10.01-20.00 mm n = 38 (35.19%)	At AIL 20.01-30.00 mm n = 62 (57.41%)	At AIL > 30.01 mm n = 8 (7.41%)
$AILE_{TB}$-ATL	16.88 ±2.23	23.78 ±2.42	31.88 ±2.01
X-axis	(10.62, 19.96)	(20.02, 29.22)	(30.04, 35.75)
$AILE_{TB}$-ATL	6.75 ±5.32	6.87 ±4.15	5.74 ±3.06
Y-axis	(-1.48, 17.56)	(0.00, 15.97)	(1.57, 9.82)
DE_{TB}	0.86 ±0.37	0.98 ±0.30	0.88 ±0.27
	(0.36, 1.86)	(0.46, 1.85)	(0.50, 1.19)

AILE– ATL, Distance between the emerging point of the branches of the facial nerve and ATL in X-axis and Y-axis. DE, Diameter of the branches of the facial nerve at the emerging point. TB, temporal branch. The data was presented as mean ±SD, (min, max) in millimeters.

After that, the temporal branch run superomedialy to supply the frontalis and orbicularis oculi muscles. For investigation of the course of the temporal branch, location and diameter of the temporal branch of the facial nerve were mapped as the horizontal distance from the ATL in three levels; FHL, LCHL and SOL**.** The results showed that the most of the temporal branches cross the FHL at mean distance 24.89 ±2.91 mm (Table 7) in 47.37%, and a diameter of the temporal branch was 1.02 ±0.45 mm. Moreover, the temporal branches cross the FHL at 16.89 ±2.29 mm in 24.56%, and 33.44 ±2.74 mm in 23.68%. In addition, the temporal branch distributed along the FHL at 12.40 mm. to 47.31 mm.

Table 7 The location and diameter of the temporal branch of the facial nerve at FHL.

Parameters	Grouping variables				
	All n = 114	At FHL 10.01-20.00 mm n = 28 (24.56%)	At FHL 20.01-30.00 mm n = 54 (47.37%)	At FHL 30.01-40.00 mm n = 27 (23.68%)	At FHL > 40.01 mm n = 5 (4.39%)
FHL_{TB}-ATL X-axis	25.74 ±7.37 (12.40, 47.31)	16.89 ±2.29 (12.40, 19.93)	24.89 ±2.91 (20.39, 29.68)	33.44 ±2.74 (30.29, 39.49)	42.99 ±2.83 (40.03, 47.31)
$DFHL_{TB}$	0.98 ±0.46 (0.32, 2.72)	0.73 ±0.26 (0.32, 1.27)	1.02 ±0.45 (0.51, 2.72)	1.14 ±0.56 (0.50, 2.70)	0.98 ±0.35 (0.68, 1.59)

FHL_{TB}–ATL, Distance between the course of the temporal branches of the facial nerve at FHL. $DFHL_{TB}$, Diameter of the temporal branches of the facial nerve at FHL. The data was presented as mean ±SD, (min, max) in millimeters.

At LCHL, the most of the temporal branches cross the LCHL at mean distance 25.38 ±2.87 mm (Table 8) in 38.74%, and a diameter of the temporal branch was 0.71 ±0.26 mm. Moreover, the temporal branches cross the LCHL at 34.68 ±2.56 mm in 31.53%, and 45.03 ±3.92 mm in 23.42%. In addition, the temporal branch distributed along the LCHL at 15.30 mm. to 52.66 mm.

Table 8 The location and diameter of the temporal branch of the facial nerve at LCHL.

Parameters	Grouping variables				
	All n = 111	At LCHL 10.01-20.00 mm n = 7 (6.31%)	At LCHL 20.01-30.00 mm n = 43 (38.74%)	At LCHL 30.01-40.00 mm n = 35 (31.53%)	At LCHL > 40.01 mm n = 26 (23.42%)
$LCHL_{TB}$-ATL X-axis	32.48 ±8.94 (15.30, 52.66)	18.40 ±1.54 (15.30, 19.86)	25.38 ±2.87 (20.13, 29.78	34.68 ±2.56 (30.35, 39.39)	45.03 ±3.92 (40.39, 52.66)
$DLCHL_{TB}$	0.71 ±0.28 (0.29, 1.74)	0.67 ±0.25 (0.29, 0.93)	0.71 ±0.26 (0.30, 1.38)	0.73 ±0.31 (0.32, 1.74)	0.67 ±0.28 (0.31, 1.50)

$LCHL_{TB}$-ATL, Distance between the course of the temporal branches of the facial nerve at LCHL. $DLCHL_{TB}$, Diameter of the temporal branches of the facial nerve at LCHL. The data was presented as mean ±SD, (min, max) in millimeters.

At SOL, the most of the temporal branches cross the SOL at mean distance 35.48 ±2.93 mm (Table 9) in 40.51%, and a diameter of the temporal branch was 0.66 ±0.26 mm. Moreover, the temporal branches cross the SOL at 25.63 ±2.62 mm in 16.46%, and 44.93 ±2.04 mm in 32.91%. In addition, the temporal branch distributed along the SOL at 19.98 mm. to 58.37 mm.

Table 9 The location and diameter of the temporal branch of the facial nerve at SOL.

Parameters	Grouping variables				
	All n = 79	At SOL 10.01-30.00 mm n = 13 (16.46%)	At SOL 30.01-40.00 mm n = 32 (40.51%)	At SOL 40.01-50.00 mm n = 26 (32.91%)	At SOL > 50.01 mm n = 8 (10.13%)
SOL_{TB}-ATL X-axis	38.82 ±8.68 (19.98, 58.37)	25.63 ±2.62 (19.98, 28.49)	35.48 ±2.93 (30.23, 39.77)	44.93 ±2.04 (40.83, 48.94)	53.71 ±2.80 (51.34, 58.37)
$DSOL_{TB}$	0.70 ±0.27 (0.26, 1.48)	0.65 ±0.18 (0.40, 0.95)	0.66 ±0.26 (0.26, 1.33)	0.70 ±0.28 (0.30, 1.48)	0.92 ±0.39 (0.36, 1.45)

SOL_{TB}-ATL, Distance between the course of the temporal branches of the facial nerve at SOL. $DSOL_{TB}$, Diameter of the temporal branches of the facial nerve at SOL. The data was presented as mean ±SD, (min, max) in millimeters.

Additionally, the temporal branch gives a small twig to connect the zygomaticofacial nerve in 14.29%. The communication point was measured and correlated to LLCHL and ATL. The distance between the communication point and ATL was 31.34 ±9.62 mm at X-axis, and -3.43 ±2.66 mm at Y -axis (Table 10).

Table 10 The communication between the temporal branch of the facial nerve and sensory nerve.

Parameters	Distances
Communication of TB and sensory nerve (n=42)	**Zygomaticofacial nerve** 6 (14.29%)
$ComLCHL_{TB}$-ATL X-axis	31.34 ±9.62 (13.33, 42.30)
$ComLCHL_{TB}$-ATL Y-axis	-3.43 ±2.66 (-6.51, 0.00)

$ComLCHL_{TB}$-ATL, Distance between the location of communication point correlated to LCHL.

4.1.3 The zygomatic branch of the facial nerve

The ZB gave 1-3 branches emerged from the superomedial portion of the parotid gland. The emerging point of the ZB was analyzed in 3 groups (Table 11). Firstly, the emerging point of the ZB was located above the AIL in 44.16%. The mean distance of the emerging point of the ZB was 29.40 ±4.35 mm in the X-axis, and 4.82 ±3.39 mm in the Y-axis. The diameter of the ZB at emerging point (above AIL) was 0.83 ±0.26 mm. Secondly, the emerging point of the ZB was located at the AIL in 32.47%. The mean distance of the emerging point of the ZB was 31.03 ±4.26 mm in the X-axis. The diameter of the ZB at emerging point (at AIL) was 1.00 ±0.41 mm. Lastly, the emerging point of the ZB was located below the AIL in 23.38%. The mean distance of the emerging point of the ZB was 32.39 ±8.81 mm in the X-axis, and -3.26 ±1.81 mm in the Y-axis. The diameter of the ZB at emerging point (below AIL) was 1.09 ±0.40 mm.

Table 11 The location and diameter of the zygomatic branch of the facial nerve at emerging point.

Parameters	Grouping variables (n = 77)		
	Above AIL	At AIL	Below AIL
	n = 34 (44.16%)	n = 25 (32.47%)	n = 18 (23.38%)
$AILE_{ZB}$-ATL	29.40 ±4.35	31.03 ±4.26	32.39 ±8.81
X-axis	(21.67, 40.68)	(24.63, 41.53)	(19.53, 53.04)
$AILE_{ZB}$-ATL	4.82 ±3.39	0.00	-3.26 ±1.81
Y-axis	(0.11, 13.56)		(-9.14, -1.52)
DE_{ZB}	0.83 ±0.26	1.00 ±0.41	1.09 ±0.40
	(0.41, 1.44)	(0.42, 1.81)	(0.54, 1.87)

AILE– ATL, Distance between the emerging point of the branches of the facial nerve and ATL in X-axis and Y-axis. DE, Diameter of the branches of the facial nerve at the emerging point. ZB, Zygomatic branch. The data was presented as mean ±SD, (min, max) in millimeters.

After that, the ZB run superomedially to supply the orbicularis oculi and the zygomaticus major muscles. For investigation of the course of the ZB, location and diameter of the ZB were mapped as the vertical distance from the FHL at the midpoint. The results showed that the course of the ZB located in 3 positions; above FHL, at FHL, and below FHL. The most of the course of the ZB was located below the FHL at vertical distance was -6.06 ±2.91 mm (36.14%). Moreover, 34.94% of the course of the ZB was located below the FHL at vertical distance was -14.60 ±2.53 mm. In addition, the diameter of the all ZB was 0.95 ±0.35 mm.

Table 12 The location and diameter of the zygomatic branch of the facial nerve correlated to the midFHL.

Parameters	Grouping variables					
	All	Above FHL	At FHL	Below FHL	Below FHL	Below FHL
	n = 83	n = 4 (4.82%)	n = 9 (10.84%)	0.01-10.00 mm n = 30 (36.14%)	10.01-20.00 mm n = 29 (34.94%)	>20.01 mm n = 11 (13.25%)
VL_{ZB}-midFHL Y-axis	-10.46 ±8.29 (-31.71, 5.68)	2.92 ±2.00 (1.28, 5.68)	0.00	-6.06 ±2.91 (-9.84, -0.05)	-14.60 ±2.53 (-19.43, -10.29)	-24.98 ±3.30 (-31.71, -20.56)
$DmidFHL_{TB}$	0.95 ±0.35 (0.38, 2.23)	0.79 ±0.25 (0.44, 1.03)	0.82 ±0.22 (0.53, 1.22)	0.83 ±0.24 (0.43, 1.44)	0.98 ±0.30 (0.38, 1.73)	1.36 ±0.55 (0.76, 2.23)

VL_{ZB}-midFHL, distance between the midpoint of FHL (midFHL) to the course of the zygomatic branch of the facial nerve branch. $DmidFHL_{ZB}$, Diameter of the zygomatic branches of the facial nerve at the midFHL. The data was presented as mean ±SD, (min, max) in millimeters.

4.1.4 The buccal branch of the facial nerve (BB)

The characteristics of the BB are summarized in Table 13. The results showed that the BB mostly originated from both temporo-facial and cervico-facial divisions in 88.10%. Moreover, the BB originated from main trunk and temporo-facial division in 2.38% and 9.52%, respectively. The relationship between the BB and the parotid duct

was determined after the BB pass through the vertical line perpendicular to the mid-point of the FHL. The result revealed that the most of the BB located below the parotid duct in 55.41% (82 of 148 branches). Moreover, the BB was located above the parotid duct 22.97%, and travel inferomedially to cross the parotid duct in 21.62%. Furthermore, the terminal branch of the BB communicated with infraorbital nerve, buccal nerve, and infratrochlear nerve (connect with AN) in 78.57%, 2.38%, and 4.76% respectively (Figure 85).

Table 13 The characteristics of the buccal branch of the facial nerve

	Characteristics		Mean ±SD	Min	Max
Origin (n=42)	Main trunk	1 (2.38%)			
	Temporo-facial division	4 (9.52%)			
	Both division	37 (88.10%)			
The relationship between BB and parotid duct (n=148)	Above	34 (22.97%)			
	Crossing	32 (21.62%)			
	Below	82 (55.41%)			
Communication between the BB and sensory nerve (n=42)	Infraorbital nerve 33 (78.57%)	Distance (x, y) From alar base	8.56 ±3.97, 3.16 ±5.18	1.50, -5.71	14.87, 13.28
	Buccal nerve 1 (2.38%)	Distance (x, y) From corner of the mouth	17.21, -11.55		

Characteristics		Mean ±SD	Min	Max
Infratrochlear nerve (connect with AN) 2 (4.76%)	Distance (x, y) From medial canthus	7.45 ±0.89, 9.85 ±4.45	6.82, 6.70	8.08, 12.99

Abbreviation: BB, buccal branch; FHL, Frankfort's horizontal line; MidFHL, midpoint of FHL; ZBP, zygomatico-buccal plexus; AN, angular nerve.

The number of BB was 2-5 branches that emerged at the anterior border of the parotid gland (Figure 80). The emerging point of the BB was divided into 10 mm in each part for clearly identify (Table 14). In most cases (36 of 148 branches (27.69%)), the emerging point of BB was located below AIL, and the mean distance was 27.35 ±7.16 mm in the X-axis, and -24.13 ±2.60 mm in the Y-axis. The mean diameter of the BB (below AIL 20.01-30.00 mm) was 1.07 ±0.44 mm. Moreover, the location of the emerging point of the BB was sporadically distributed throughout the anterior border of the parotid gland. The mean distance of the emerging point was 32.47 ±5.54 mm on the X-axis, whereas the nerves were distributed approximately 20-30% in each 10 mm from 20-50 mm in the vertical distance perpendicular to the FHL. Furthermore, the mean diameter of the BB at the emerging point was 1.21 (0.61) mm, and the maximal diameter was approximately 5 mm.

Table 14 The location and diameter of the buccal branch of the facial nerve at emerging point.

Parameters	Grouping variables						
	Above AIL n = 8 (6.15%)	At AIL n = 8 (6.15%)	Below AIL 0.01-10.00 mm n = 25 (19.23%)	Below AIL 10.01-20.00 mm n = 25 (19.23%)	Below AIL 20.01-30.00 mm n = 36 (27.69 %)	Below AIL 30.01-40.00 mm n = 22 (16.92%)	Below AIL >40.01 mm n = 6 (4.62%)
$AILE_{BB}$-ATL X-axis	32.47 ±5.54 (20.10, 38.74)	35.46 ±5.71 (27.18, 42.39)	33.11 ±4.88 (23.45, 42.99)	31.15 ±4.76 (24.42, 41.47)	27.35 ±7.16 (15.78, 48.27)	24.90 ±4.82 (13.33, 32.57)	30.13 ±8.56 (15.72, 38.85)
$AILE_{BB}$-ATL Y-axis	4.20 ±3.10 (0.20, 9.76)	0.00	-5.38 ±2.54 (-9.49, -1.54)	-14.16 ±2.94 (-19.44, -10.35)	-24.13 ±2.60 (-29.25, -20.30)	-34.45 ±2.67 (-39.27, -30.40)	-41.78 ±0.23 (-45.09, -40.36)
DE_{BB}	1.48 ±0.55 (0.43, 2.04)	1.55 ±0.78 (0.94, 3.35)	1.35 ±0.51 (0.35, 2.36)	1.39 ±0.91 (0.55, 5.15)	1.07 ±0.44 (0.36, 2.19)	0.97 ±0.42 (0.43, 2.06)	0.84 ±0.23 (0.54, 1.22)

AILE -ATL, Distance between the emerging point of the branches of the facial nerve and ATL in X-axis and Y-axis. DE, Diameter of the branches of the facial nerve at the emerging point. BB, buccal. The data was presented as mean ±SD, (min, max) in millimeters.

As the BB passed through the vertical line perpendicular to the midFHL point into the buccal region, some BB gave smaller branches and also distributed throughout the masseter muscle (Figure 80). The mean of vertical distance and diameter of the BB at the midFHL were 33.67 (12.01) and 1.26 (0.63) mm respectively. Moreover, the BB was distributed approximately 20-30% in each 10 mm from 10-50 mm in the vertical distance perpendicular to the midFHL also (Table 15). After that, the BB was arranged to form a plexus superficially to the parotid duct and buccal fat pat at both masseteric and buccal regions, and initiated to branch as small twigs to innervate the facial muscles, especially zygomaticus major muscle. The buccal plexus is known as the ZBP. Moreover, the lowest branch of the BB traveled medially and located above the masseter muscle and deep to the buccal fat pad noticeably to innervate the buccinator muscle, while the ZBP was superficial to the buccal fat pad.

Table 15 The location and diameter of the buccal branch of the facial nerve correlated to the midFHL.

Parameters	Grouping variables					
	All n = 148	Below MidFHL 0.01-20.00 mm n = 24 (16.22%)	Below MidFHL 20.01-30.00 mm n = 31 (20.95%)	Below MidFHL 30.01-40.00 mm n = 49 (33.11%)	Below MidFHL 40.01-50.00 mm n = 29 (19.59%)	Below MidFHL >50.01 mm n = 15 (10.14%)
VL_{BB}-midFHL Y-axis	33.67 (12.01) (11.88, 70.38)	16.43 ±2.19 (11.88, 19.37)	24.94 ±2.90 (20.19, 29.59)	34.69 ±2.65 (30.71, 39.92)	44.29 ±3.23 (40.23, 49.83)	55.41 ±4.54 (50.34, 70.38)

Parameters	Grouping variables					
	All n = 148	Below MidFHL 0.01-20.00 mm n = 24 (16.22%)	Below MidFHL 20.01-30.00 mm n = 31 (20.95%)	Below MidFHL 30.01-40.00 mm n = 49 (33.11%)	Below MidFHL 40.01-50.00 mm n = 29 (19.59%)	Below MidFHL >50.01 mm n = 15 (10.14%)
$DmidFHL_{BB}$	1.26 (0.63) (0.37, 4.59)	1.49 ±0.60 (0.57, 2.70)	1.52 ±0.72 (0.63, 4.45)	1.22 ±0.67 (0.40, 4.59)	1.01 ±0.46 (0.37, 2.58)	0.99 ±0.30 (0.48, 1.67)

VL_{BB}-midFHL, distance between the midpoint of FHL (midFHL) to the course of the buccal branch of the facial nerve branch. $DmidFHL_{BB}$, Diameter of the buccal branches of the facial nerve at the midFHL. The data was presented as mean ±SD, (min, max) in millimeters.

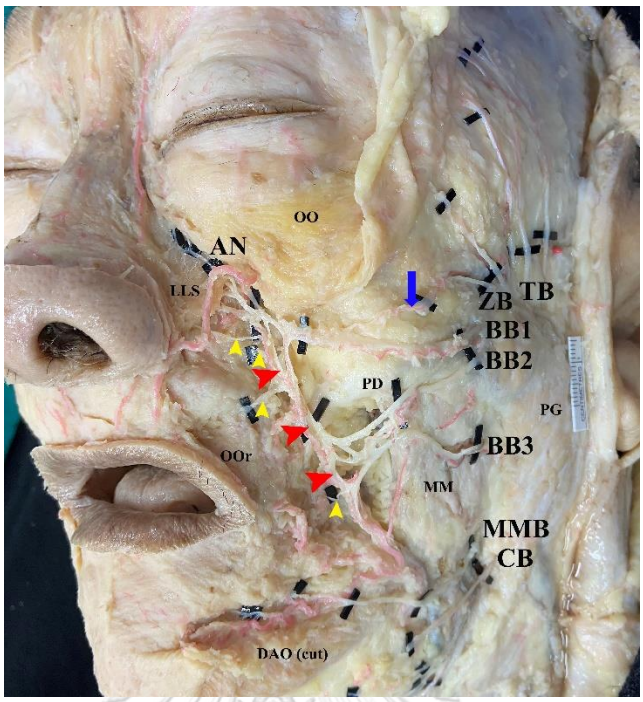

Figure 80 The location of the emerging point of the BB is sporadically distributed throughout the anterior border of the parotid gland. Then, it branched and arranged into the zygomatico-buccal plexus (ZBP) in masseteric and buccal regions, and presented the medial part of the ZBP branched into small twigs to innervate muscles around the mouth and nose. TB, temporal branch; ZB, zygomatic branch; BB1, first buccal branch; BB2, second buccal branch; BB3, third buccal branch; MMB, marginal mandibular branch; CB, cervical branch; AN, angular nerve; PG, the parotid gland; PD, parotid duct; MM, masseter muscle; LLS, levator labii superioris muscle; OO, orbicularis oculi muscle; OOr, orbicularis oris muscle; DAO, depressor anguli oris muscle; red arrowhead, the medial part of the ZBP; yellow arrowhead, small twigs of the BB; blue arrow, ZB gave branch to connect the BB.

The zygomatico-buccal plexus

The characteristics of the ZBP were explained in Table 16. The present study revealed that the BB branched and arranged into the plexus, so the ZBP truly originated from the BB. Surprisingly, the pattern of ZBP could be divided into 3 patterns including incomplete loop, single-loop, and multi-loop patterns. Firstly, an incomplete loop was

arranged from 3-4 branches of the BB and connected together as a medial line after passing through the anterior border of the masseter muscle. Then, the medial part of the ZBP branched into small twigs to innervate muscles around the mouth and nose. Secondly, a single loop was arranged from several branches but apparently observed as a big single loop. Lastly, a multiloop was the BB branched and connected to the plexus which could be observed more than 2 loops (Figure 81). Furthermore, the mean distance and diameter of the medial part of the ZBP at the corner of the mouth level were 31.61 ±6.68 and 1.47 ±0.57 mm, respectively, while at the alar base level were 22.53 ±4.25 and 1.14 ±0.59 mm, respectively.

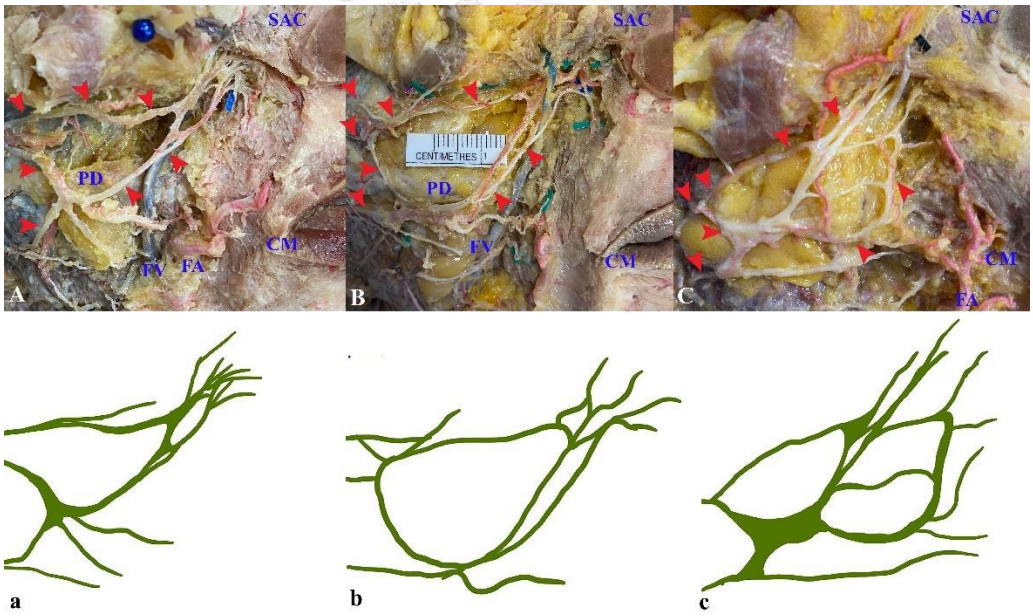

Figure 81 Three patterns of the zygomatico-buccal plexus; incomplete (A,a), single (B,b), and multi-loop patterns (C,c). SAC, supra-alar crest; CM, the corner of the mouth; PD, parotid duct; FA, facial artery; FV, facial vein; red arrowhead, zygomatico-buccal plexus.

Meanwhile, the relationship between the medial part of the ZBP and facial vein (FV) was observed at the corner of the mouth and alar base levels. The results presented that the ZBP positioned superficial to the FV at the corner in 26.19%, and lateral to the FV in 73.81%. Moreover, it mostly located deep to the FV at the alar base level in 66.67%, because the FV changed to locate in a superficial plane at the

alar base level. Interestingly, the angular nerve arose from the superior portion of the ZBP at the alar base level. It located under the levator labii superioris muscle (LLS), then penetrated the LLS to embed in the nasolabial fat locating superiorly to the LLS (Figure 83).

Table 16 The characteristics of the ZBP

Characteristics			Mean ±SD	Min	Max
Pattern of ZBP (n=42)	Incomplete loop	5 (11.90%)			
	Single loop	13 (30.95%)			
	Multiloop	24 (57.14%)			
Location of medial line of ZBP (n=42)	**At corner of the mouth**	Distance (x, y)	31.61 ±6.68, 4.05 ±5.32	17.73, 0	44.32, 15.85
		Diameter	1.47 ±0.57	0.62	3.56
	At alar base	Distance (x)	22.53 ±4.2	13.66	31.30
		Diameter	1.14 ±0.59	0.46	3.17
The relationship between medial part of the ZBP and FV (n=42)	**At corner of the mouth**				
	Superficial to FV	11 (26.19%)			
	Lateral to FV	31 (73.81%)			
	At alar base				
	Superficial to FV	8 (19.05%)			
	Deep to FV	28 (66.67%)			
	Lateral to FV	1 (2.38%)			
	Medial to FV	5 (11.90%)			

Abbreviation: ZBP, zygomatico-buccal plexus; FV, facial vein.

Moreover, the zygomaticus major muscle was used to be the landmark for position of the zygomatic or buccal branches. The result revealed that the numbers

of the zygomatic or buccal branches at lateral border of the zygomaticus major muscle were 3.74 ±0.94 (2, 6) branches (Table 17) (Figure 82). Furthermore, the position of zygomatic or buccal branches was divided into upper and lower part of zygomaticus major muscle. It was found that the numbers of the zygomatic or buccal branches at upper portion were 1.71 ±0.67 (1, 3) branches, while the numbers of the buccal branches at lower portion were 2.02 ±0.87 (1, 5) branches.

Table 17 The position of the branches of the facial nerve which form zygomatico-buccal plexus related to the boundary of the zygomaticus major muscle.

Characteristics		Mean ±SD	Min	Max
The number of the branches of the FN at lateral border of the zygomaticus major muscle (n=42)	**All**	3.74 ±0.94	2	6
	2 points; 2 (4.76%)			
	3 points; 16 (38.10%)			
	4 points; 18 (42.86%)			
	5 points; 3 (7.14%)			
	6 points; 3 (7.14%)			
	Upper portion	1.71 ±0.67	1	3
	1 point; 17 (40.48%)			
	2 points; 20 (47.62%)			
	3 points; (11.90%)			
	Lower portion	2.02 ±0.87	1	5
	1 point; 11 (26.19%)			
	2 points; 22 (52.38%)			
	3 points; 7 (16.67%)			
	4 points; 1 (2.38%)			
	5 points; 1 (2.38%)			

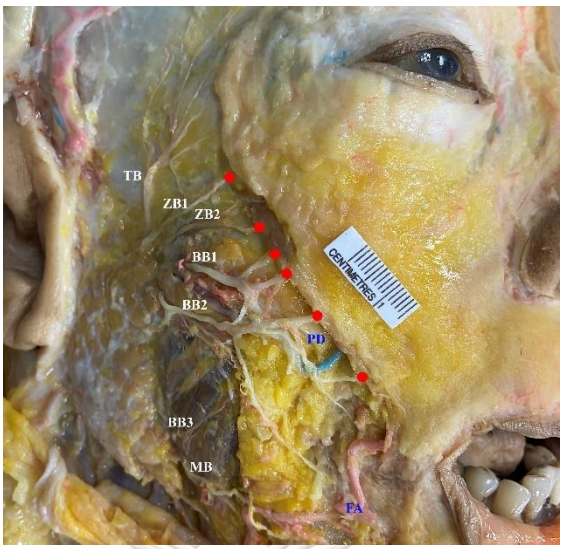

Figure 82 The facial nerve correlated with the lateral boundary of the zygomaticus major muscle.

The angular nerve (AN)

The characteristics of the AN were detailed in Table 18. The AN arose from the superior portion of the ZBP at the alar base level. It located under the levator labii superioris muscle and mostly penetrated the LLS to embed in the nasolabial fat locating superiorly to the LLS (Figure 83).

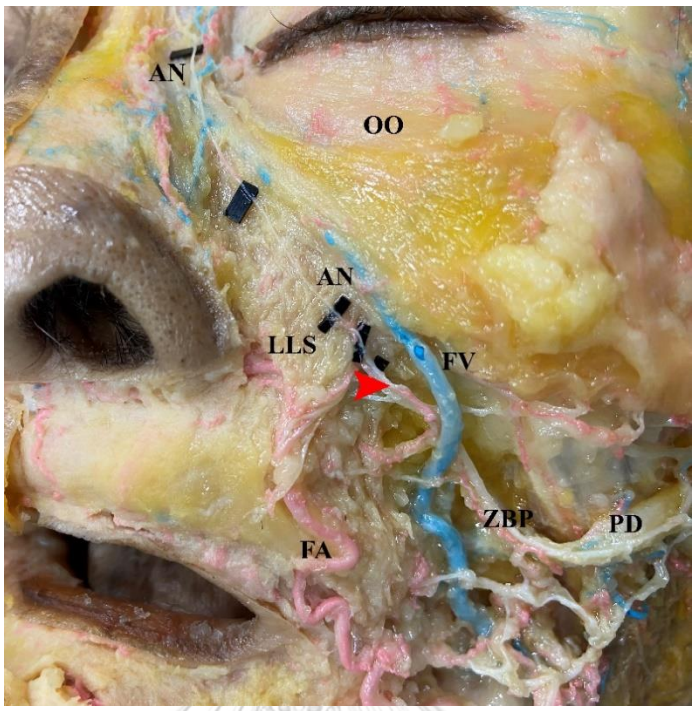

Figure 83 The origin and location of the angular nerve that arose from superior part of the ZBP. ZBP, zygomatico-buccal plexus; AN, angular nerve; PD, parotid duct; LLS, levator labii superioris muscle; OO, orbicularis oculi muscle; red arrow head, the origin of the AN; FV, facial vein; FA, facial artery.

Generally, the AN has a single branch (40 in 42 cases, 95.24%), but it was rarely found as double branches (2 in 42 cases, 4.76%). The mean distances between the alar base and emerging point of the AN were 12.31 ±4.80 mm in x-axis and 2.51 ±6.69 mm in y-axis. Moreover, the mean diameter of the AN was 0.65 ±0.25 mm at this point. After that, the AN traveled mediosuperior to the medial eye brow, and gave small twigs to innervate facial muscles such as levator labii superioris alaeque nasi, nasalis, inferomedial part of the orbicularis oculi, procerus, and depressor supercilii muscles (Figure 84). The location of the AN was measured in vertical distance correlated to the mid-pupil, medial limbus and medial canthus. The result showed that the mean of vertical distances between the course of the AN and the mid-pupil, medial limbus and medial canthus were 26.59 ±3.13, 24.16 ±3.39 mm, and 14.89 ±2.87 mm. Furthermore, horizontal distances between the course of the AN and the supra-alar crest and medial canthus were 12.71 ±3.64 mm and 6.98 ±1.52 mm. Likewise, the distance of the

intercanthal line was 17.24 ±2.77 (10.39, 23.82) mm. The result indicated that the AN was located approximately 1/3 laterally of the intercanthal line.

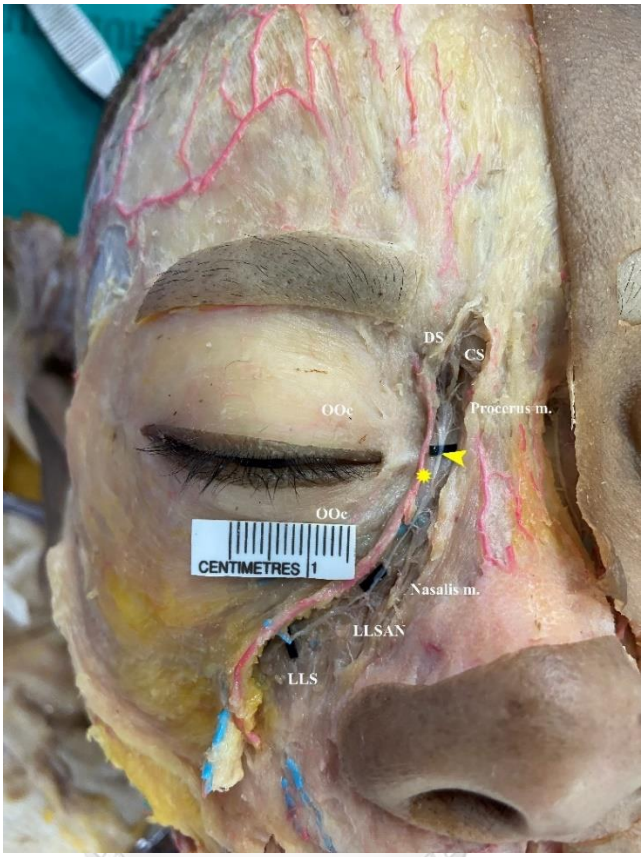

Figure 84 The AN gave small twigs to innervate facial muscles. OOc, orbicularis oculi muscle; DS, depressor supercilii muscle; CS, corrugator supercilii muscle; LLS, levator labii superioris muscle; LLSAN, levator labii superioris alaeque nasi muscle.

Table 18 The location and diameter of the angular nerve

Parameters	Anatomical landmarks					
	Transitional point correlated to the alar base n = 42	Horizontal distance to supra-alar crest n = 44	Vertical distances to mid pupil n = 44	Vertical distances to medial limbus n = 44	Vertical distance to medial canthus n = 44	Horizontal distance to medial canthus n = 42
Distances	12.31 ±4.80, 2.51 ±6.69 (3.54, 24.37) (-13.81, 17.48)	12.71 ±3.64 (5.95, 24.37) 1.07 ±1.92 (0.00, 8.21)	26.59 ±3.13 (21.17, 32.84) -1.65 ±3.12 (-15.75, 3.38)	24.16 (3.39) (14.56, 30.49)	14.89 ±2.87 (5.78, 23.25)	6.98 (1.52) (4.18, 10.95)
Diameter	0.65 ±0.25 (0.24, 1.56)	0.62 ±0.23 (0.27, 1.21)	0.67 (0.35) (0.24, 2.08)	0.69 (0.28) (0.27, 1.46)	0.63 ±0.23 (0.24, 1.07)	0.51 (0.17) (0.28, 0.89)

The data was presented as mean ±SD, (min, max) in millimeters.

The connection of the BB and sensory nerve

The terminal twigs of the BB connected to the sensory nerves including the infraorbital nerve (ION), buccal nerve (BN) and infratrochlear nerve (ITN) in 78.57%, 2.38% and 4.76%, respectively (Figure 85). The superior portion of the medial line of ZBP has a small twig to connect the ION, and the mean distance between connection point and alar base was 8.56(3.97) in x-axis and 3.16(5.18) in y-axis. Moreover, the

connection between the BB and ION had single point in 29 cases and two points in 4 cases, besides it connected with lateral superior labial, medial superior labial and external nasal branches in 75.68%, 10.81% and 13.51% respectively. Unfrequently, the lowest of the BB connected with the BN at buccal region, and the AN connected with the ITN above to the medial canthal level.

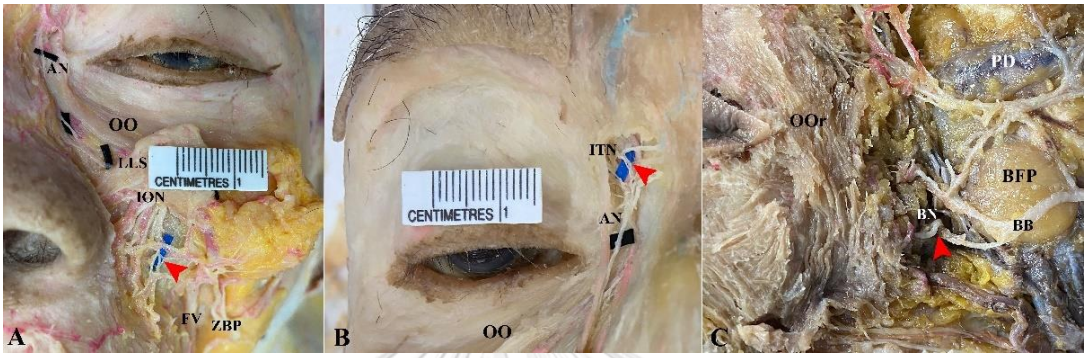

Figure 85 The terminal branches of the BB connected with the sensory nerve include ION (A) , ITN (B) and BN (C). AN, angular nerve; LLS, levator labii superioris muscle; OO, orbicularis oculi muscle; FV, facial vein; ZBP, zygomatico-buccal plexus; red arrow head, the connection point of the motor and sensory nerve; ION, infraorbital nerve; ITN, infratrochlear nerve; OOr, orbicularis oris muscle; PD, parotid duct; BB, buccal branch; BFP, buccal fat pad; BN, buccal nerve.

4.1.5 The marginal mandibular branch of the facial nerve

The MB emerged from the inferior portion of the parotid gland, and traveled medially along the inferior border of the mandible. The emerging point of the MB was measured and correlated to the inferior mandibular line (IML) as X-axis and the anterior masseteric line (AML) as Y-axis (Table 19). The result revealed that the location of the emerging point of the MB were 20.12 ±6.55 mm and -0.75 ±5.55 mm, on X and Y axis, respectively. Moreover, the emerging point of the MB was divided into 2 groups; upper and lower emerging points. Firstly, upper emerging point was the MB emerged from the parotid gland above the IML. The distances between the upper emerging point of MB and ATL was 19.56 ±6.54 mm on X-axis, and 5.20 ±3.27 mm in Y-axis. Secondly, lower emerging point was the MB emerged from the parotid gland at/lower the IML.

The distances between the lower emerging point of MB and ATL was 20.40 ±6.62 mm on X-axis, and -3.73 ±3.77 mm in Y-axis.

Then the MB traveled inferomedially to the muscle of the mouth, so the crossing point of the MB was measured correlated to the IML. The result presented that the MB crossed IML at single point anterior to the AML (A1) in 9 of 42 cases (21.43%), double points anterior to the AML (A2) in 4 of 42 cases (9.52%), single point posterior to the AML (P1) in 11 of 42 cases (26.19%), single point anterior and single point posterior to the AML (P1A1) in 11 of 42 cases (26.19%), %), double point anterior and single point posterior to the AML (P1A2) in 3 of 42 cases (7.14%), and none crossing point (P0A0) in 4 of 42 cases (9.52%). In summary, the number of the crossing point between the MB and IML was single point (50.00%), double points (33.33%), and triple points (7.14%). It was divided into anterior and posterior points. The distance between the posterior crossing point of the MB and AML was 9.95 ±5.17 mm, whereas distance between the anterior crossing point of the MB and AML was 12.54 ±6.85 mm. Moreover, the diameter of the MB at posterior and anterior points were 0.86 ±0.34, and 0.93 ±0.53 respectively.

Table 19 The emerging point and crossing point of the marginal mandibular branch correlated to the inferior mandibular line.

Characteristics	References line	Grouping variables	Distances		
			Mean ±SD	Min	Max
The location of the emerging point of the MB	X; IML Y; AML	Emerging point (n = 57)	20.12 ±6.55 -0.75 ±5.55	11.49 -14.81	37.93 11.72
		Upper Emerging point (n = 19)	19.56 ±6.54 5.20 ±3.27	12.99 1.32	35.29 11.72
		Lower Emerging	20.40 ±6.62 -3.73 ±3.77	11.49 -14.81	37.93 0.00

Characteristics	References line	Grouping variables	Distances		
			Mean ±SD	Min	Max
		point (n = 38)			
The crossing point of the MB at IML (n=42) P0A0; 4 (9.52%) A1; 9 (21.43%) A2; 4 (9.52%) P1; 11 (26.19%) P1A1; 11 (26.19%) P1A2; 3 (7.14%)	X; IML None 4 (9.52%) Single point 21 (50.00%) Double point 14 (33.33%) Triple point 3 (7.14%)	Posterior point (n = 25)	9.95 ±5.17	0	18.01
		Diameter	0.86 ±0.34	0.38	1.83
		Anterior point (n = 34)	12.54 ±6.85	2.08	32.70
		Diameter	0.93 ±0.53	0.52	3.49

Abbreviation: MB, marginal mandibular branch; FA, facial artery.

In addition, the number of twigs of the MB was counted at the masseteric area. The result reveled that the MB had single twig in 30 of 57 branches (52.63%), 2 twigs in 23 of 57 branches (40.35%), and 3 twigs in 4 of 57 branches (7.02%). After that, the crossing point of the twig of the MB was measured at the AML. The result showed that the crossing point of small twig of the MB including superior and inferior points. The distances between the course the MB and crossing points were 6.25 ±5.60 mm, and -6.99 ±4.02 mm at superior and inferior points respectively. Moreover, the diameter of the twig of the MB that crossed the AML at superior and inferior points were 0.79 ±0.21 mm, and 0.86 ±0.33 mm respectively.

Regarding the relationship between the MB and the FA, our found that the MB run superficial to the FA in 48.28%, deep to the FA in 13.79%, both superficial and deep to the FA in 12.07%, inferior to the FA in 15.52%, and other in 10.34%. Then, the MB run medially to innervate depressor anguli oris, depressor labii inferioris, orbicularis oris and mentalis muscles. Furthermore, the communication of the MB with sensory nerve was investigated in each branch. It was found that the MB communicated with the mental nerve in 40.48%. The distances of the anterior communication point and the vertical line to the corner of the mouth were 3.72 ±2.61 mm on X-axis, and 27.43 ±3.40 mm on Y-axis, whereas the distance of the posterior communication point was -8.74 ±3.28 mm on X-axis and 29.06 ±4.87 mm on Y-axis.

Table 20 The characteristic of the marginal mandibular branch of the facial nerve.

Characteristics	References line	Grouping variables	Distances		
			Mean ±SD	Min	Max
Number of twigs of the MB (n=57)	Y; AML Single twig; 30 (52.63%) 2 twigs; 23 (40.35%) 3 twigs; 4 (7.02%)		1.54 ±0.63	1	3
The crossing point of the MB at AML (n=57)	Y; AML	Superior point (n = 28)	6.25 ±5.60	0.00	18.46
		Diameter	0.79 ±0.21	0.30	1.14
		Inferior point (n = 57)	-6.99 ±4.02	-16.33	-1.48
		Diameter	0.86 ±0.33	0.45	1.74
The relationship between the MB and FA	Superficial Deep Both Inferior	28 (48.28%) 8 (13.79%) 7 (12.07%) 9 (15.52%)			

Characteristics	References line	Grouping variables	Distances		
			Mean ±SD	Min	Max
	Other	5 (10.34%)			
The communication of the MB with sensory nerve	Mental nerve 17 (40.48%)	Distance (x, y)	-0.68 ±6.73	-12.68	6.94
			28.01 ±3.90	22.64	35.94
		From the corner of the mouth			
		Anterior point (n = 11)	3.72 ±2.61	0.00	6.94
			27.43 ±3.40	23.77	32.92
		Posterior point (n = 6)	-8.74 ±3.28	-12.68	-4.66
			29.06 ±4.87	22.64	35.94

Abbreviation: MB, marginal mandibular branch.

4.1.6 The cervical branch of the facial nerve

According to the emerging point of the CB, it was measured and correlated to the IML on X-axis and the AML on Y-axis (Table 21). The distance of the emerging point of the CB was 18.26 ±7.17 mm on X-axis, and -10.31 ±5.39 mm on Y-axis. Then, the CB branched into 1-6 twigs, and run inferomedially pass through the AML. The vertical distances of the twigs of the CB were measured and divided into 15 mm in each range. The result revealed that the twig of the CB crossed the AML at a vertical distance 10.93 ±3.06 mm in 21 of 99 twigs, 22.76 ±4.45 mm in 64 in 99 twigs, and 33.47 ±3.24 mm in 14 of 99 twigs. In addition, the diameter of the twigs of the CB was 0.83 ±0.33 mm.

Table 21 The characteristics of the cervical branch of the facial nerve.

Characteristics	References line	Grouping variables	Distances		
			Mean ±SD	Min	Max
The location of the emerging point of the CB	X; IML Y; AML	All (n = 44)	18.26 ±7.17 -10.31 ±5.39	5.70 -19.18	41.51 0.00
Number of twigs of the CB (n=44)	Y; AML Single twig; 14 (31.82%) 2 twigs; 14 (31.82%) 3 swigs; 10 (22.73%) 4 twigs; 4 (9.09%) 5 twigs; 1 (2.27%) 6 twigs; 1 (2.27%)		2.25 ±1.20	1	6
The crossing point of the CB at AML (n=99)	Y; AML	All Diameter (n=99)	21.92 ±7.84 0.83 ±0.33	4.26 0.24	40.42 1.98
		Below IML 0.00 - 15.00 mm Diameter (n=21)	10.93 ±3.06 0.84 ±0.29	4.62 0.24	14.60 1.38
		Below IML 15.00 - 30.00 mm Diameter (n=64)	22.76 ±4.45 0.83 ±0.32	15.27 0.31	29.74 1.98
		Below IML > 30.00 mm	33.47 ±3.24	30.07	40.42

Characteristics	References line	Grouping variables	Distances		
			Mean ±SD	Min	Max
		Diameter (n=14)	0.82 ±0.41	0.34	1.79

Regarding the communication of the CB with sensory nerve, there are 1-3 points of communication of the CB with transverse cervical branch in 80.95% (Table 22). The CB communicated with ascending transverse cervical branch in 13.33%, and descending transverse cervical branch in 86.67%. The distance between the CB and ascending transverse cervical branch was -22.11 ±7.58 mm on the X-axis, and -15.20 ±4.73 mm on the Y-axis. Furthermore, the distance between the CB and descending transverse cervical branch was divided into anterior and posterior points to be clearly locate. It was found that anterior communication point was located at 9.61 ±8.30 mm on X-axis, and 34.74 ±11.67 mm on Y-axis. On the contrary, the posterior communication point was located at -11.83 ±10.67 mm on X-axis, and 26.04 ±14.11 mm on Y-axis.

Table 22 The communication of the cervical branch of the facial nerve with transverse cervical nerve.

Characteristics	References line	Grouping variables	Distances		
			Mean ±SD	Min	Max
The number of the communication point	None Single point 2 points 3 points	8 (19.05%) 24 (57.14%) 9 (21.43%) 1 (2.38%)	1.07 ±0.71	0	3
The location of the communication point (n = 45)	Distance (x, y) X; IML Y; AML	Ascending transverse cervical branch 6 (13.33%)	-22.11 ±7.58 -15.20 ±4.73	-32.03 -11.05	-11.64 -23.80
		Descending transverse cervical branch 39 (86.67%)	1.37 ±13.97 31.39 ±13.20	-41.39 0.00	30.91 72.90
		● Anterior point 24 (61.54%)	9.61 ±8.30 34.74 ±11.67	0.00 16.62	30.91 72.90
		● Posterior point 15 (38.46%)	-11.83 ±10.67 26.04 ±14.11	-41.39 0.00	-1.91 50.21

4.1.7 The facial nerve trunk and division

For positioning the branching point of facial nerve trunk and divisions, the X-axis was the horizontal line connecting between the supra-alar crease and the inferior border of the tragus (AIL). The Y-axis was the anterior tragal line (ATL) (Table 23). The location of the branching point of the facial nerve trunk that divided into temporo-facial and cervico-facial divisions was 10.92 ±4.16 mm on the X-axis, and -20.39 ±4.41

mm on the Y-axis. Moreover, the diameters of the temporo-facial and cervico-facial divisions were 3.65 ±0.94 mm, and 1.76 ±0.44 mm respectively. The branching point of the temporo-facial division was located at 14.41 ±3.91 mm on the X-axis and -9.84 ±4.91 mm on the Y-axis, while the branching point of the cervico-facial division was located at 10.45 ±4.31 mm on the X-axis and -31.43 ±7.20 mm on the Y-axis.

Table 23 The location of the branching point of the facial nerve trunk and their divisions

Characteristics	References line	Parameters	Mean ±SD	Min	Max
The branching point of the facial nerve trunk (n = 42)	X; AIL	Distances	10.92 ±4.16	1.56	18.90
	Y; ATL		-20.39 ±4.41	12.09	31.85
The branching point of the temporo-facial division (n = 42)	X; AIL	Distances	14.41 ±3.91	4.57	21.97
	Y; ATL		-9.84 ±4.91	0.00	24.95
		Diameter	3.65 ±0.94	2.07	5.89
The branching point of the cervico-facial division (n = 42)	X; AIL	Distances	10.45 ±4.31	1.75	24.73
	Y; ATL		-31.43 ±7.20	17.18	48.41
		Diameter	1.76 ±0.44	1.02	2.64

4.1.8 The location and number of the entry site of the facial nerve branch in facial muscles

The location of the entry point of the facial nerve branch was distributed in the target muscle area. The numbers of the entry site of the frontalis muscle, orbicularis oculi, zygomaticus major, depressor anguli oris, risorius, and platysma were 1.05 ±0.73, 3.67 ±1.00, 2.57 ±0.70, 1.35 ±0.48, 1.00 ± 0.00, 2.95 ±0.94 twigs respectively (Table 24) (Figure 86).

Table 24 The number of the entry site of the facial nerve branch in facial muscles

Facial muscles	Mean of number of entry site	Min	Max
Frontalis (n=42)	1.05 ±0.73	0	3
Orbicularis oculi (n=42)	3.67 ±1.00	2	6
Zygomaticus major (n=42)	2.57 ±0.70	2	4
Depressor anguli oris (n=40)	1.35 ±0.48	1	2
Risorius (n=22)	1.00 ± 0.00	1	1
Platysma (n=42)	2.95 ±0.94	2	6

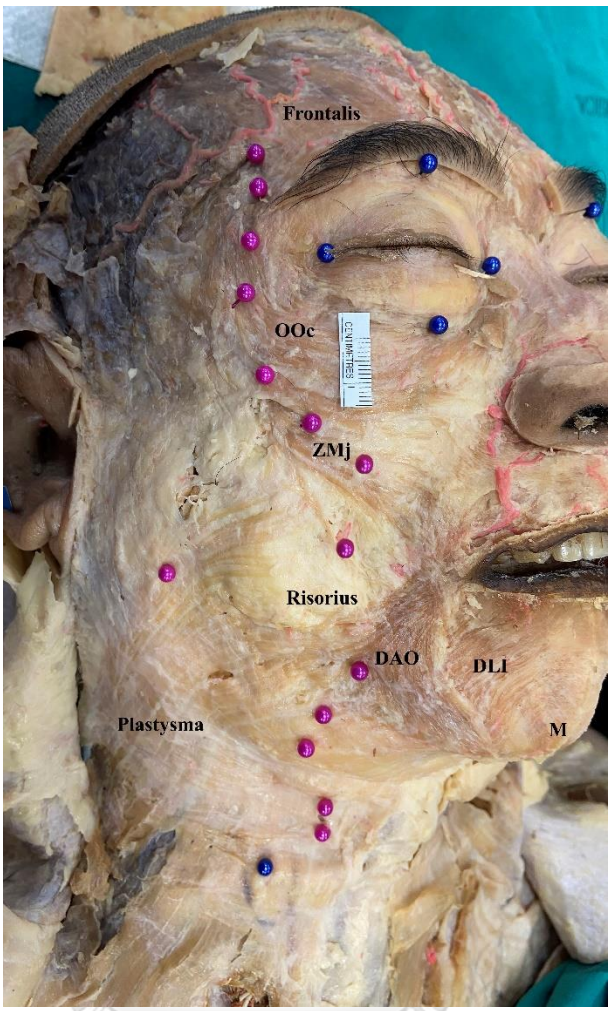

Figure 86 The entry site of the facial nerve branch in facial muscles. OOc, orbicularis oculi muscle; ZMj, zygomaticus major muscle; DAO, depressor anguli oris muscle; DLI, depressor labii inferioris muscle, M, mentalis muscle; pink pin, entry site.

4.2 The results of the histological study

In histological study, the face was divided into 6 regions including tear trough, nasolabial, temporal, masseteric, parotid, and mandibular regions to locate the branches of the facial nerve related to the facial soft tissue layers.

4.2.1 Histological section with Masson's trichrome stain at the parotid region

The histological section with Masson's trichrome stain at the parotid region was investigated in three levels include the AIL, ear lobule and MA levels to observe the location of the facial nerve (Figure 87). The result revealed that the location of the

facial nerve at AIL level was sub-parotidomasseteric fascia (8 of 14 cases, 57.14%), sub-parotid gland (4 of 14 cases, 28.57%), and subS-DTF (2 of 14 cases, 14.29%). Furthermore, the facial nerve was divided into divisions in 4 of 14 cases (28.57%), and main branches in 10 of 14 (72.34%) at AIL level. Moreover, the number of main branches at AIL level was 2.80 ±0.63 (2, 4) branches.

According to ear lobule level (EL), the location of the facial nerve was sub-parotid gland (7 of 14 cases, 50.00%), deep-parotid gland (3 of 14 cases, 21.43%), and sub-parotidomasseteric fascia (2 of 14 cases, 14.29%). Furthermore, the facial nerve was divided into divisions in 1 of 14 cases (7.14%), and main branches in 11 of 14 (78.57%) at EL level. Moreover, the number of main branches at EL level was 1.91 ±0.70 (1, 3).

At MA level, the location of the facial nerve was sub-parotid gland (7 of 14 cases, 50.00%), and deep-parotid gland (7 of 14 cases, 50.00%). Furthermore, the facial nerve was divided into divisions in 6 of 14 cases (42.86%), and main branches in 8 of 14 (57.14%) at MA level. Moreover, the number of main branches at MA level was 2.13 ±0.83 (1, 4).

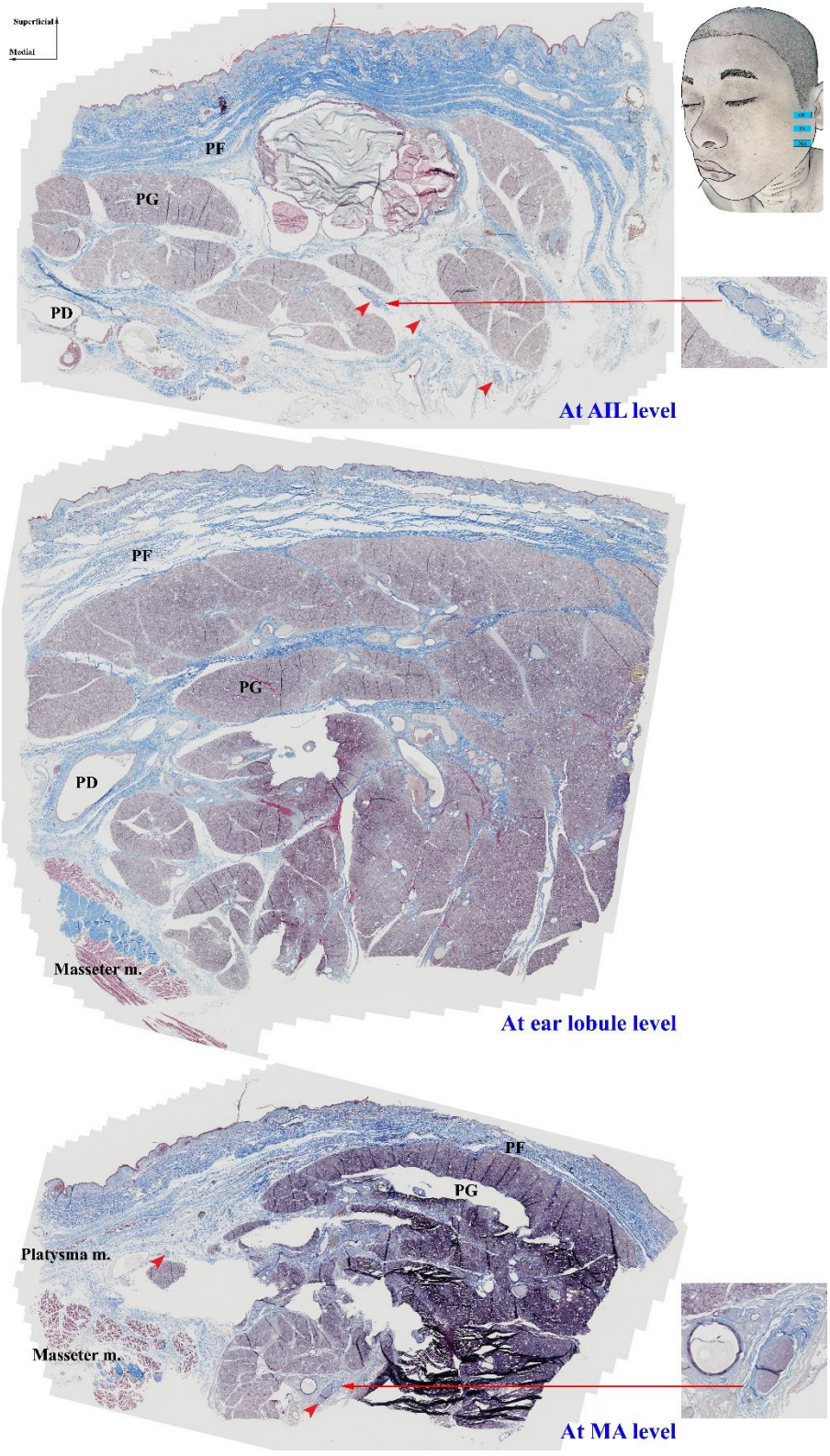

Figure 87 Histological section of the parotid region at the AIL, the ear lobule, and the MA levels stained with Masson's trichrome stain. The FN was identified within

sub-parotid gland at the AIL level, while it was identified deep to the parotid gland at the MA level. On the contrary, none of the FN at the ear lobule level in this case. arrow-head, facial nerve; PF, parotid fascia; PG, parotid gland, PD, parotid duct.

4.2.2 Histological section with Masson's trichrome stain at the temporal region

In histological methods, the branches of the facial nerve were analyzed at the temporal region in Frankfort's horizontal line, lateral canthus, supraorbital rim, and upper eyebrow levels. The result revealed that the number of the branches of the facial nerve was 5.57 ±0.85, 4.57 ±1.09, 3.57 ±1.34, and 2.50 ±0.76, respectively (Table 25).

Table 25 The number of the branches of the facial nerve from histological methods.

Characteristics	References line levels	Mean ±SD	Min	Max
The number of the branches of the facial nerve (n=14)	Frankfort's horizontal line	5.57 ±0.85	4	7
	Lateral canthus	4.57 ±1.09	2	6
	Supraorbital rim	3.57 ±1.34	2	6
	Upper eyebrow	2.50 ±0.76	1	4

According to the Frankfort's horizontal line, the location of the zygomatic or temporal branches of the facial nerve was analyzed in three portions; medial, middle, and lateral (Table 26) (Figure 88). In medial portion, the ZB was found in 13 of 14 cases (92.86%), and TB in 3 of 14 cases (21.43%). It was found single and 2 branches that located at nearest TPF (71.43%), between TPE and S-DTF (7.14%), and nearest S-DTF (14.29%). In middle portion, the TB was found in 2-5 branches that located at between TPE and S-DTF (85.71%), and nearest S-DTF (14.29 %). In lateral portion, the TB was found in single and 2 branches that located at between TPE and S-DTF (35.71%), nearest S-DTF (50.00%), and subS-DTF (14.29%).

Table 26 The number and location of the zygomatic and temporal branches of the facial nerve at Frankfort's horizontal line from histological methods.

References line levels	Portions of the region	Branches of the facial nerve	Number of the branches of the facial nerve		Location of branches	
			Grouping variables	Frequency (%)	Location	Frequency (%)
Frankfort's horizontal line	Medial	Zygomatic 13 (92.86%) Temporal 3 (21.43%) None 1 (7.14%)	Single branch	10 (71.43%)	Nearest TPF	10 (71.43%)
			2 branches	3 (21.43%)	Between TPE and S-DTF	1 (7.14%)
					Nearest S-DTF	2 (14.29%)
	Middle	Temporal 14 (100.00%)	2 branches	4 (28.57%)	Between TPE and S-DTF	12 (85.71%)
			3 branches	8 (57.14%)	Nearest S-DTF	2 (14.29 %)
			4 branches	1 (7.14%)		
			5 branches	1 (7.14%)		
	Lateral	Temporal 14 (100.00%)	Single branch	7 (50.00%)	Between TPE and S-DTF	5 (35.71%)
			2 branches	7 (50.00%)	Nearest S-DTF	7 (50.00%)
					Sub S-DTF	2 (14.29%)

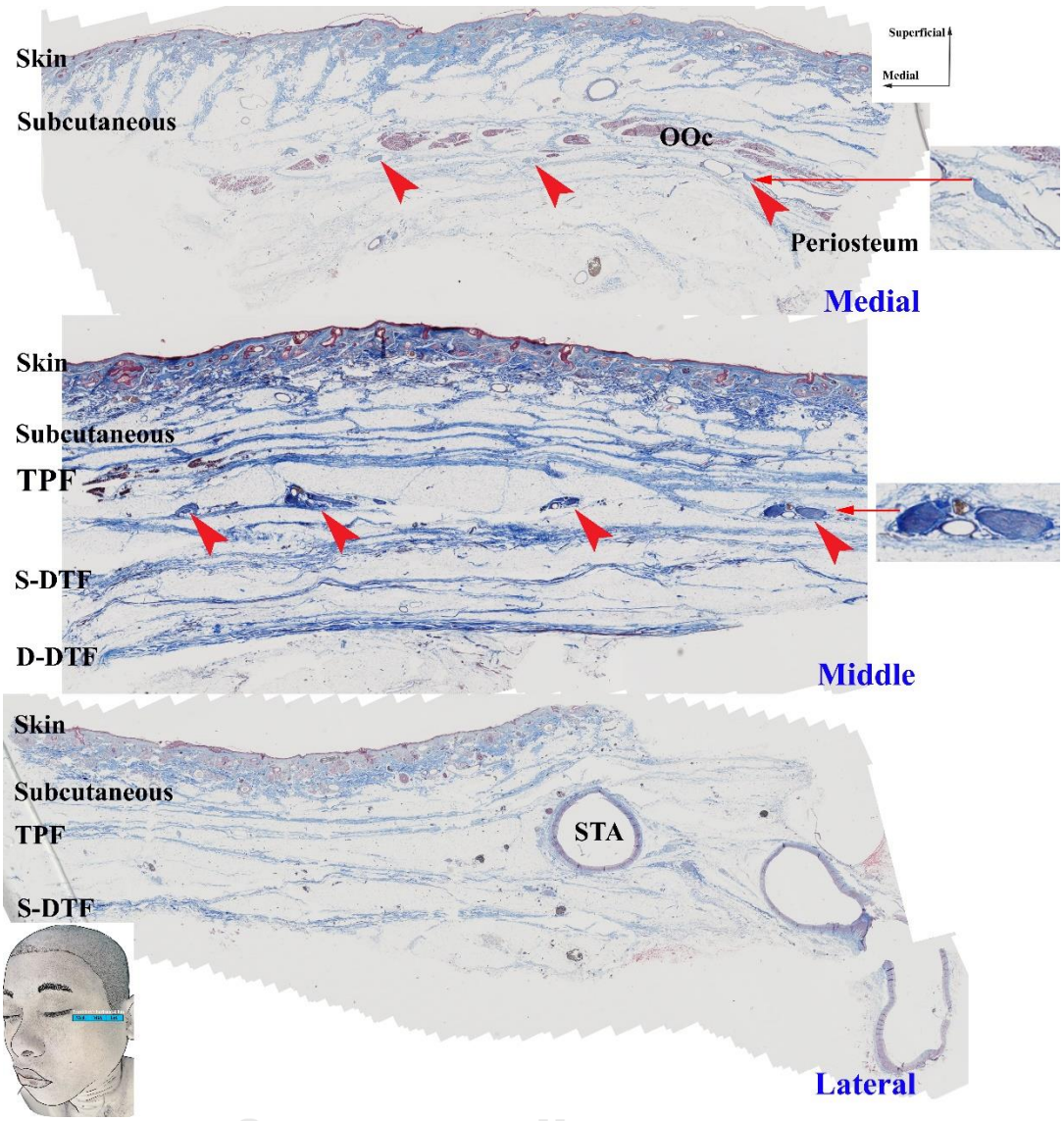

Figure 88 Histological section of the temporal region at FHL level stained with Masson's trichrome stain. arrow-head, temporal branch of the facial nerve; OOc, orbicularis oculi muscle; TPF, temporoparietal fascia; S-DTF, superficial layer of deep temporal fascia; D-DTF, deep layer of deep temporal fascia; STA, superficial temporal artery.

According to the lateral canthal level, the location of the TB was analyzed in three portions; medial, middle, and lateral (Table 27) (Figure 89). In medial portion, the TB was found in single branch that located at nearest TPF (85.71%), and between TPE and S-DTF (14.29 %). In middle portion, the TB was found in 1-5 branches that located at between TPE and S-DTF (57.14%), and nearest S-DTF (42.86%). In lateral

portion, the TB was found in single and 2 branches that located at nearest TPF (14.29%), between TPE and S-DTF (14.29%), nearest S-DTF (7.14%), and within TPF (14.29%).

Table 27 The number and location of the zygomatic and temporal branches of the facial nerve at lateral canthal level from histological methods.

References line levels	Portions of the region	Branches of the facial nerve	Number of the branches of the facial nerve		Location of branches	
			Grouping variables	Frequency (%)	Location	Frequency (%)
Lateral canthus	Medial	Temporal 14 (100.00%)	Single branch	14 (100.00%)	Nearest TPF	12 (85.71%)
					Between TPE and S-DTF	2 (14.29 %)
	Middle	Temporal 14 (100.00%)	Single branch	3 (21.43%)	Between TPE and S-DTF	8 (57.14%)
			2 branches	2 (14.29%)		
			3 branches	5 (35.71%)	Nearest S-DTF	6 (42.86%)
			4 branches	3 (21.43%)		
			5 branches	1 (7.14%)		
	Lateral	Temporal 7 (50.00%) None 7 (50.00%)	Single branch	3 (21.43%)	Nearest TPF	2 (14.29%)
			2 branches	4 (28.57%)	Between TPE and S-DTF	2 (14.29%)
					Nearest S-DTF	1 (7.14%)
					Within TPF	2 (14.29%)

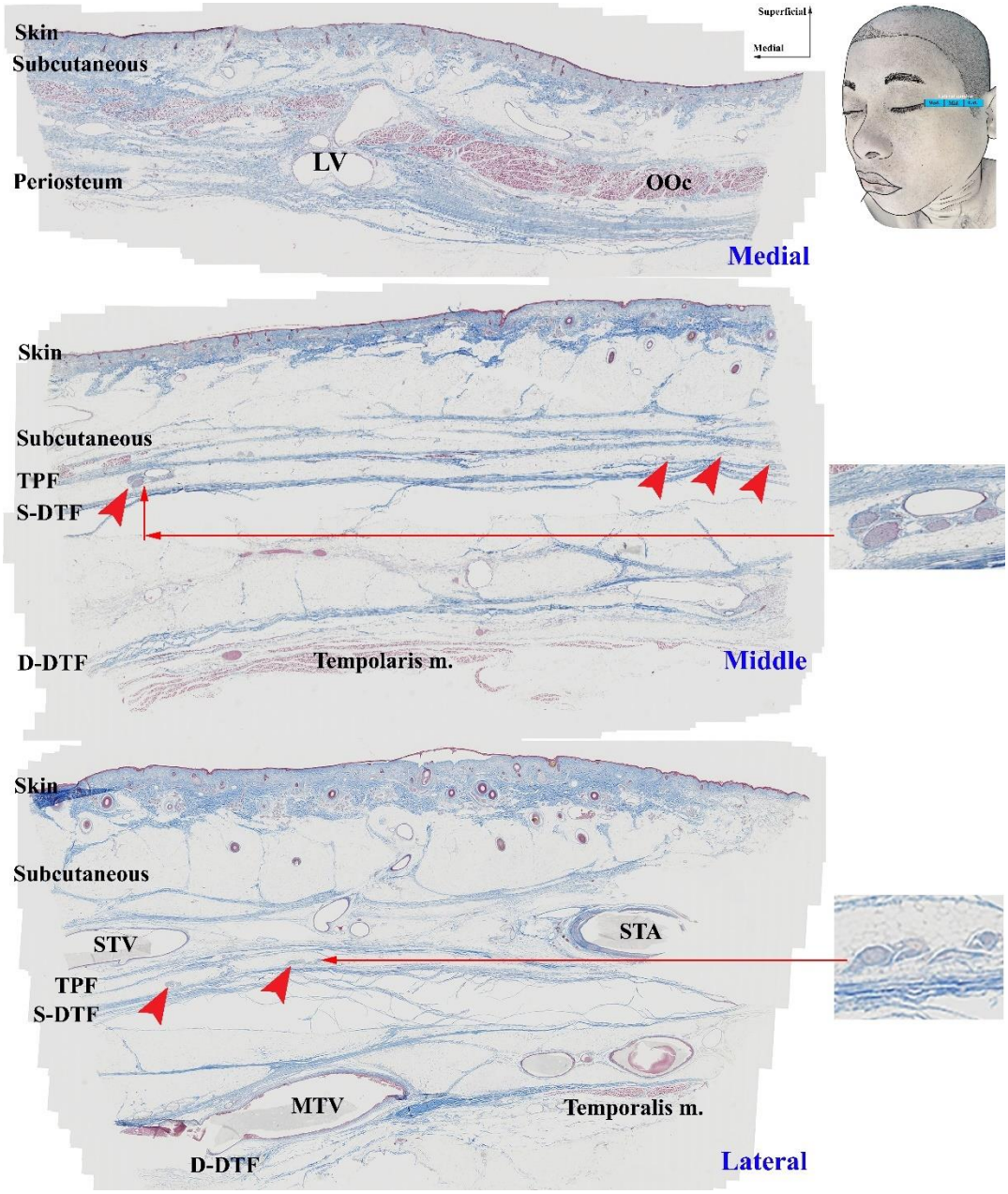

Figure 89 Histological section of the temporal region at lateral canthal level stained with Masson's trichrome stain. arrow-head, temporal branch of the facial nerve; OOc, orbicularis oculi muscle; LV, lacrimal vein; TPF, temporoparietal fascia; S-DTF, superficial layer of deep temporal fascia; D-DTF, deep layer of deep temporal fascia; STA, superficial temporal artery; STV, superficial temporal vein; MTV, middle temporal vein.

According to the supraorbital rim level, the location of the TB was analyzed in three portions; medial, middle, and lateral (Table 28) (Figure 90). In medial portion,

the TB was found in single and 2 branches that located at nearest TPF (85.71%), and between TPE and S-DTF (14.29 %). In middle portion, the TB was found in 1-5 branches that located at nearest TPF (50.00%), between TPE and S-DTF (35.71%), nearest S-DTF (7.14%), and within TPF (7.14%). In lateral portion, the TB was found in single branch that located at nearest TPF (14.29%).

Table 28 The number and location of the zygomatic and temporal branches of the facial nerve at the supraorbital rim level from histological methods.

References line levels	Portions of the region	Branches of the facial nerve	Number of the branches of the facial nerve		Location of branches	
			Grouping variables	Frequency (%)	Location	Frequency (%)
Supraorbital rim	Medial	Temporal 14 (100.00%)	Single branch	11 (78.57%)	Nearest TPF	12 (85.71%)
			2 branches	3 (21.43 %)	Between TPE and S-DTF	2 (14.29 %)
	Middle	Temporal 14 (100.00%)	Single branch	5 (35.71%)	Nearest TPF	7 (50.00%)
			2 branches	4 (28.57%)	Between TPE and S-DTF	5 (35.71%)
			3 branches	3 (21.43%)	Nearest S-DTF	1 (7.14%)
			4 branches	1 (7.14%)	Within TPF	1 (7.14%)
			5 branches	1 (7.14%)		

References line levels	Portions of the region	Branches of the facial nerve	Number of the branches of the facial nerve		Location of branches	
			Grouping variables	Frequency (%)	Location	Frequency (%)
	Lateral	Temporal 2 (14.29%) None 12 (85.71%)	Single branch	2 (14.29%)	Nearest TPF	2 (14.29%)

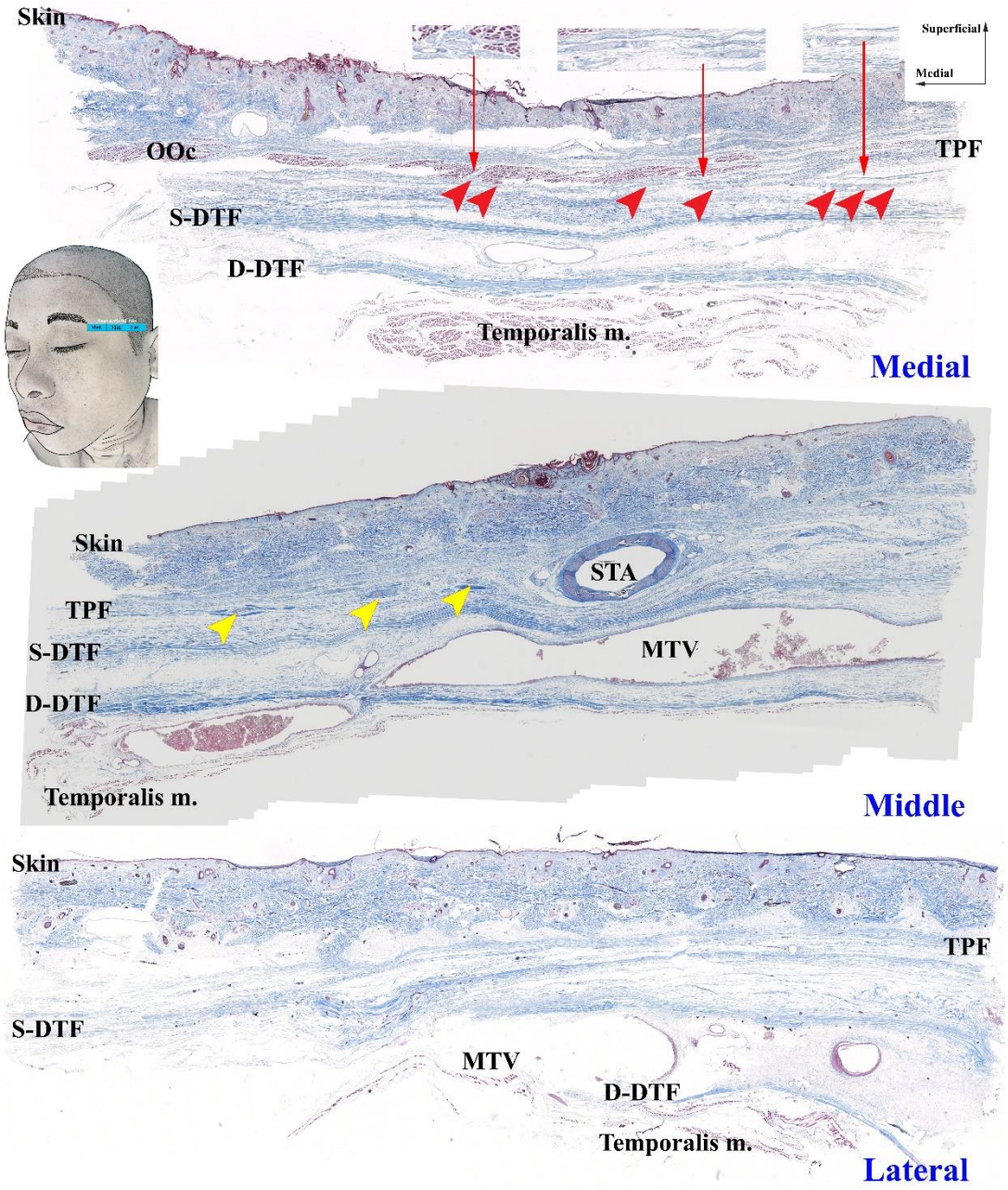

Figure 90 Histological section of the temporal region at supraorbital rim level stained with Masson's trichrome stain. In medial portion, a temporal branch is identified deep to the orbicularis oculi muscle running horizontal deep to the temporoparietal fascia and muscle. In middle and lateral portion, none present the temporal branch, but present the auriculotemporal nerve is identified above the temporoparietal fascia. red arrow-head, temporal branch of the facial nerve; yellow arrow-head, the auriculotemporal nerve; TPF, temporoparietal fascia; S-DTF, superficial layer of deep

temporal fascia; D-DTF, deep layer of deep temporal fascia; STA, superficial temporal artery; MTV, middle temporal vein.

According to the upper eyebrow level, the location of the TB was analyzed in three portions; medial, middle, and lateral (Table 29) (Figure 91). In medial portion, the TB was found in single and 2 branches that located at nearest TPF (78.57%), and between TPE and S-DTF (21.43 %). In middle portion, the TB was found in single and 2 branches that located at nearest TPF (42.86%), and within TPF (42.86%). None found the branch of the facial nerve in lateral portion of the upper eyebrow level.

Table 29 The number and location of the zygomatic and temporal branches of the facial nerve at the upper eyebrow level in histological methods.

References line levels	Portions of the region	Branches of the facial nerve	Number of the branches of the facial nerve		Location of branches	
			Grouping variables	Frequency (%)	Location	Frequency (%)
Upper eyebrow	Medial	Temporal 14 (100.00%)	Single branch	11 (78.57%)	Nearest TPF	11 (78.57%)
			2 branches	3 (21.43 %)	Between TPE and S-DTF	3 (21.43 %)
	Middle	Temporal 12 (85.71%) None 2 (14.29%)	Single branch	6 (42.86%)	Nearest TPF	6 (42.86%)
			2 branches	6 (42.86%)	Within TPF	6 (42.86%)
	Lateral	None 14 (100%)	None	14 (100%)	None	14 (100%)

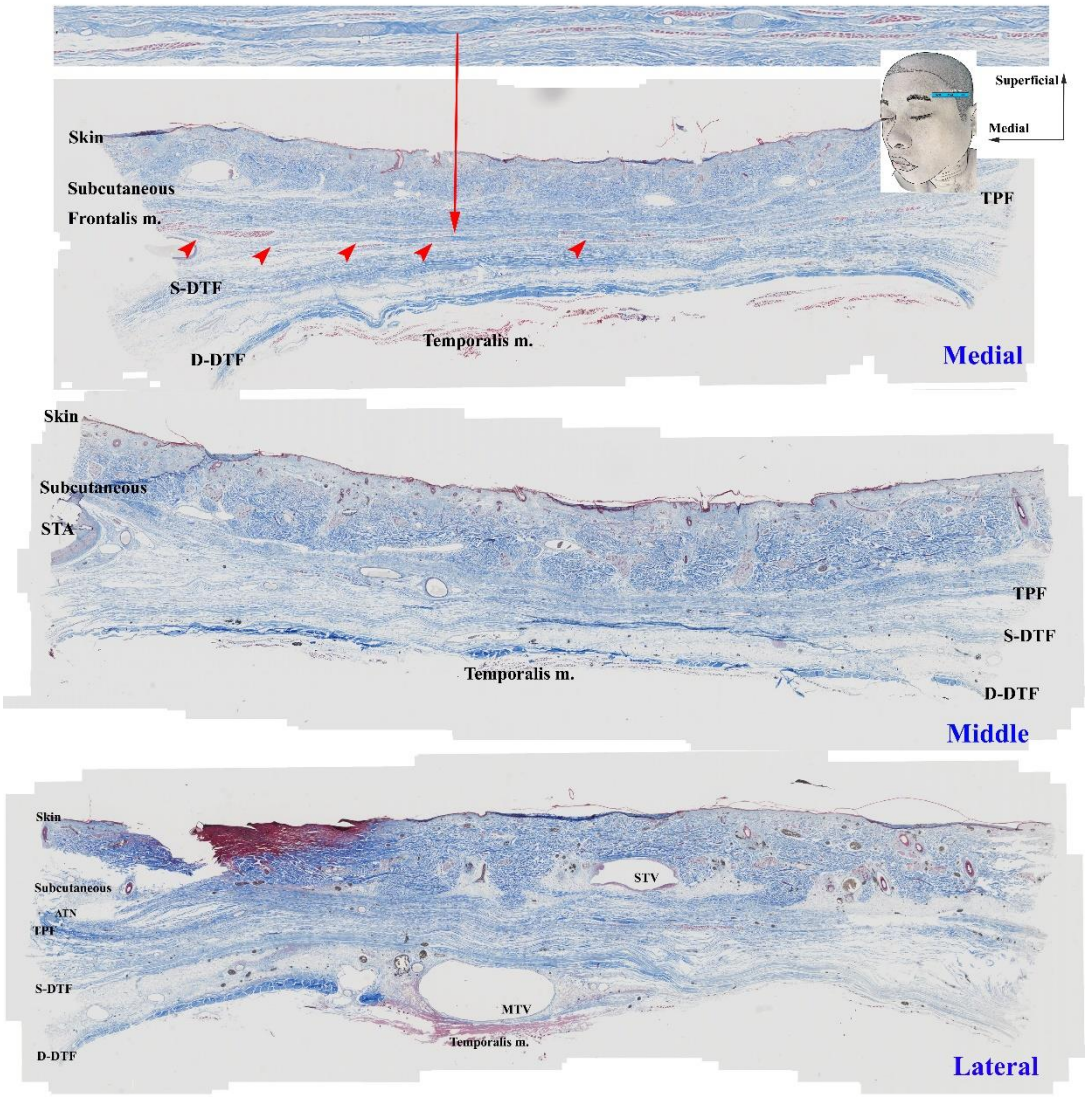

Figure 91 Histological section of the temporal region at upper eyebrow level stained with Masson's trichrome stain. In medial portion, a temporal branch is identified deep to the frontalis muscle running horizontal deep to the temporoparietal fascia. In middle and lateral portion, none present the temporal branch, but present the auriculotemporal nerve is identified above the temporoparietal fascia. arrow-head, temporal branch of the facial nerve; TPF, temporoparietal fascia; S-DTF, superficial layer of deep temporal fascia; D-DTF, deep layer of deep temporal fascia; STA, superficial temporal artery; STV, superficial temporal vein; MTV, middle temporal vein; ATN, auriculotemporal nerve.

4.2.3 Histological section with Masson's trichrome stain at the masseteric region

In histological methods, the zygomatic or buccal branches of the facial nerve were analyzed at the masseteric region in superior, middle and inferior portion. The result revealed that the number of the branches of the facial nerve was 5.64 ±1.22, and the ZB was found in 1.07 ±0.62 branches while the BB was found in 4.57 ±1.16 branches. Moreover, the number of branches of the facial nerve at the masseteric region in superior, middle and inferior portion was 2.36 ±1.08, 1.93 ±0.83, and 1.36 ± 0.63 branches, respectively.

According to superior portion, the ZB was found in 12 of 14 cases (85.71%), while BB was found in 11 of 14 cases (78.57%). It located at nearest SMAS (35.71%), between SMAS and masseter muscle (35.71%), nearest masseter muscle (7.14%), and nearest periosteum (21.43%). In middle portion, the BB was found at nearest SMAS muscle (21.43%), between SMAS and masseter muscle (35.71%), and nearest masseter muscle (42.86%). In the same, the BB was found at nearest platysma muscle (21.43%), between platysma and masseter muscle (21.43%), and nearest masseter muscle (57.14%) in inferior portion (Figure 92). Furthermore, the BB was located same level to the parotid duct at midFHL, while BB was located deep to the parotid duct after it pass troughs the midFHL (Figure 93).

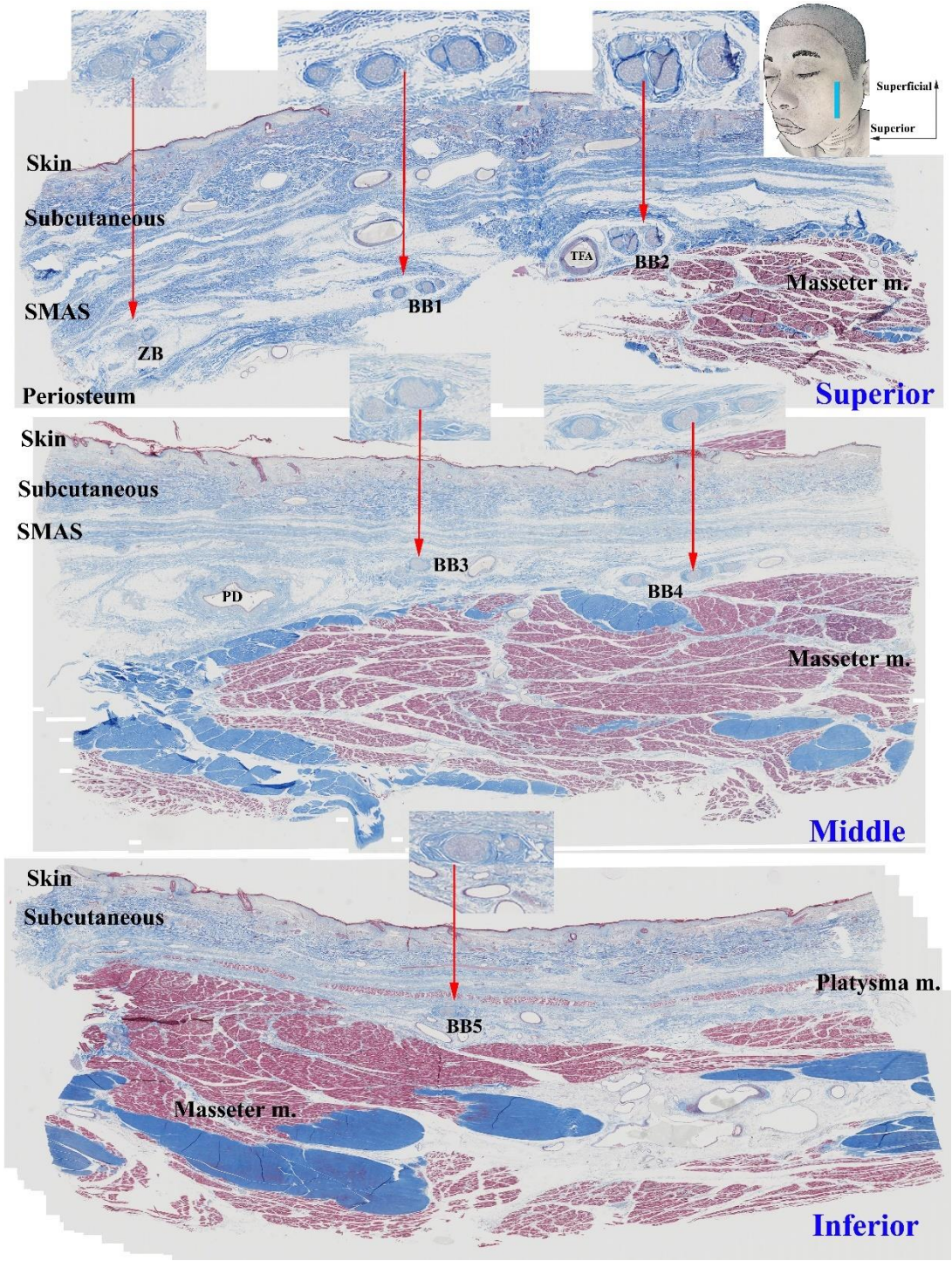

Figure 92 Histological section of the masseteric region at midFHL stained with Masson's trichrome stain. ZB, zygomatic branch of the facial nerve; BB, buccal branch of the facial nerve; PD, parotid duct; TFA, transverse facial artery.

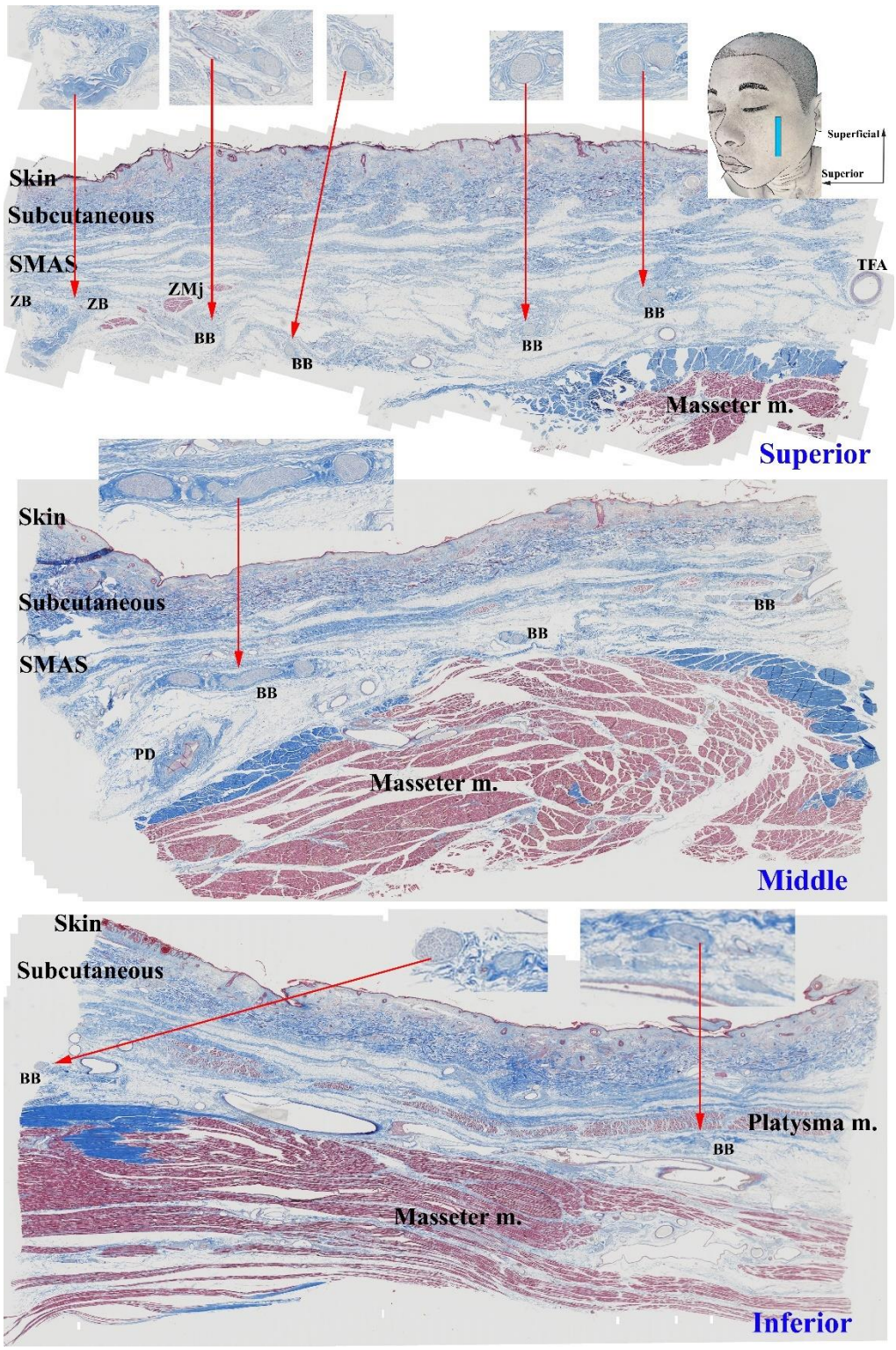

Figure 93 Histological section of the masseteric region after the branches of the pass through the midFHL stained with Masson's trichrome stain. ZB, zygomatic branch of the facial nerve; BB, buccal branch of the facial nerve; PD, parotid duct; TFA, transverse facial artery; ZMj, zygomaticus major muscle.

4.2.4 Histological section with Masson's trichrome stain at the nasolabial region

According to the nasolabial region, the branches of the facial nerve were analyzed at the corner of the mouth, the upper lip, the alar base levels. At the corner of the mouth, the BB was found within buccal fat pad in 6 of 14 cases, and found the long section of the BB above the anterior border of the masseter muscle also. Moreover, the BB was located supero-laterally to the FV (Figure 94). At the upper lip level, all of the BB was found within buccal fat pad and found the cross section of the BB above the anterior border of the masseter muscle (Figure 95). At the alar base level, the ION and the BB were found at medial portion. Moreover, the BB was located superiorly to the FV in 8 of 14 cases and inferiorly to the FV in 6 of 14 cases. In addition, the long section of the BB was found in 2 of 14 cases (Figure 96).

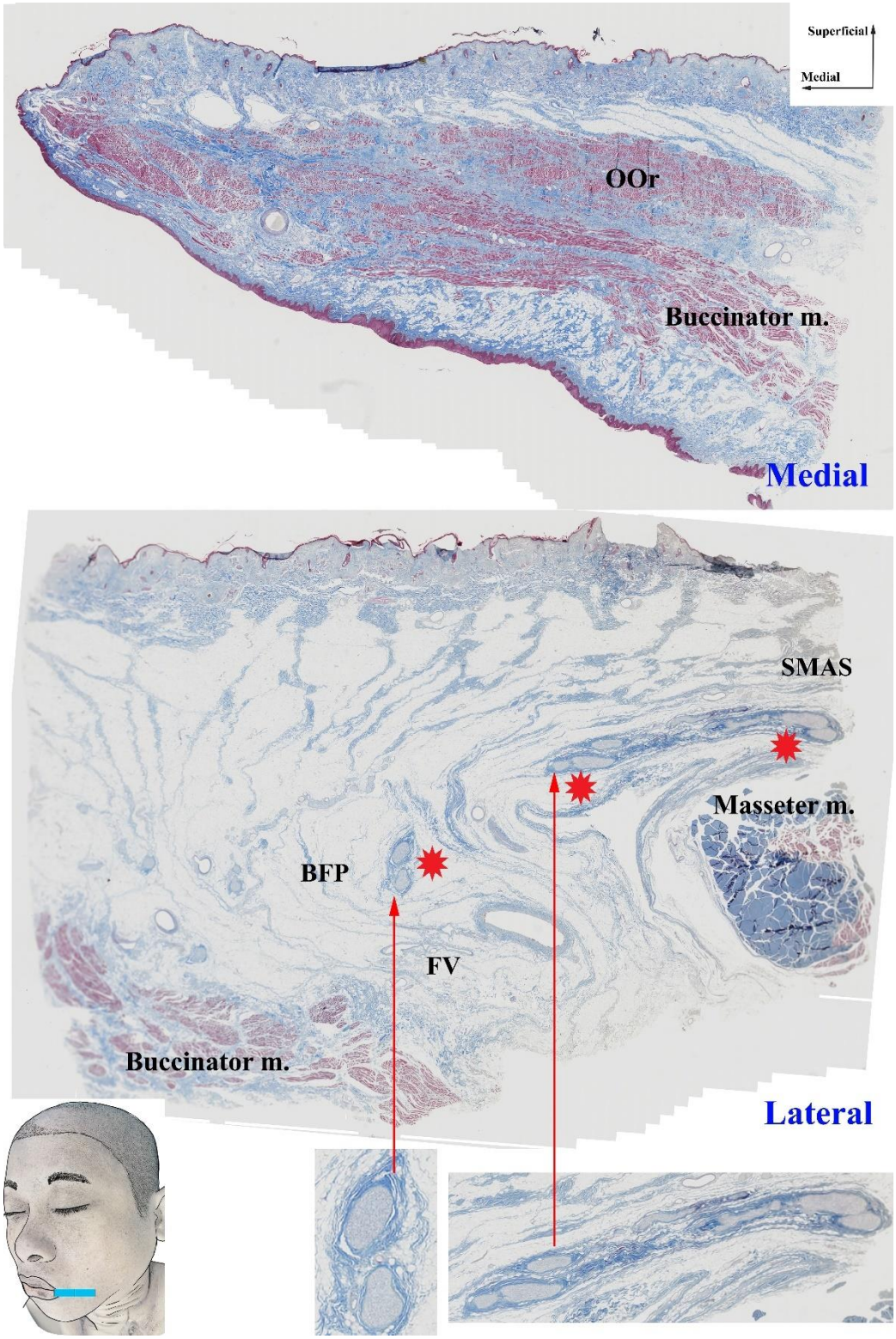

Figure 94 Histological section of the nasolabial region at the corner of the mouth level stained with Masson's trichrome stain. OOr, orbicularis oris muscle; SMAS, superficial musculoaponeurotic system; BFP, buccal fat pad; FV, facial vein.

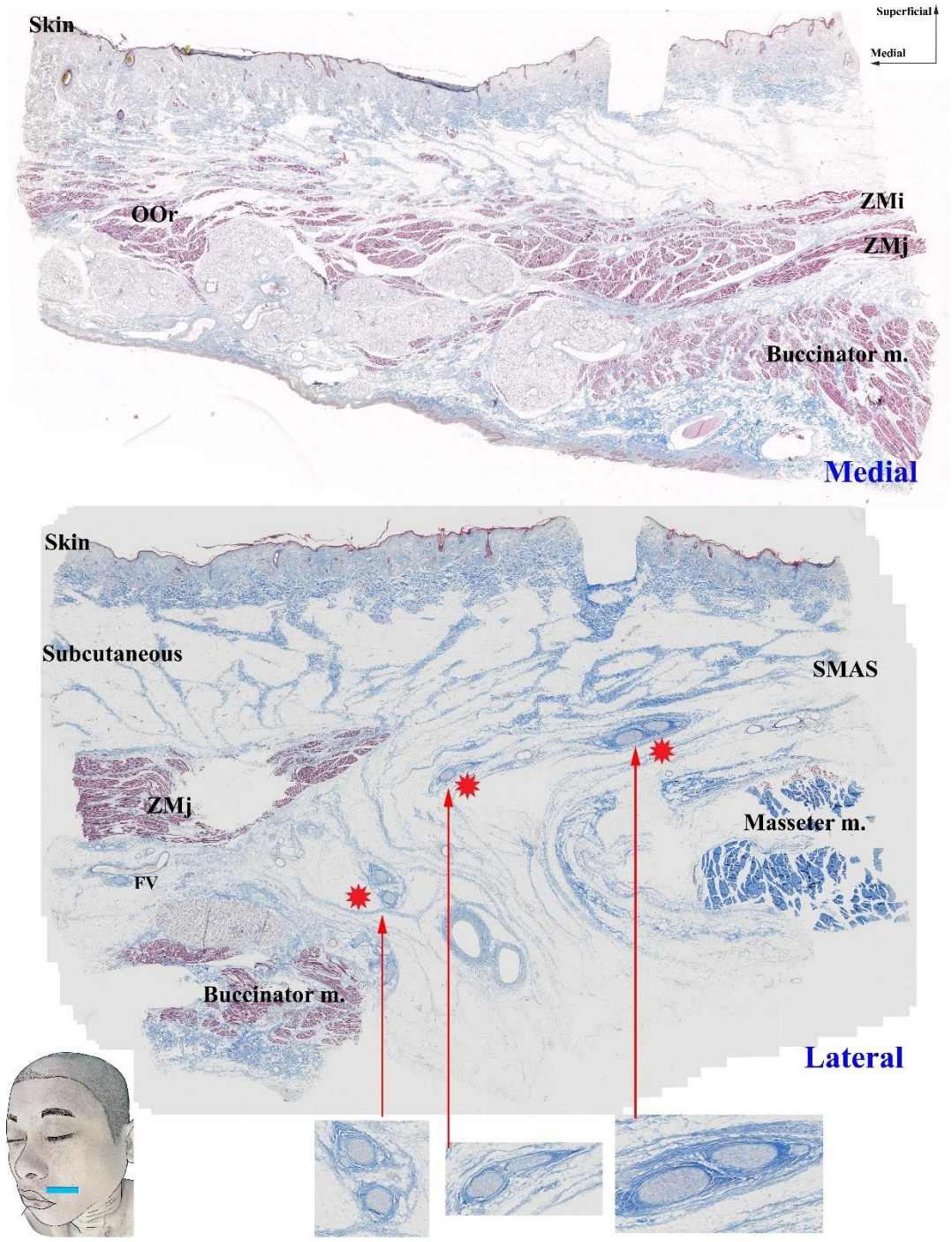

Figure 95 Histological section of the nasolabial region at the upper lip level stained with Masson's trichrome stain. OOr, orbicularis oris muscle; ZMn, zygomaticus minor muscle; ZMj, zygomaticus major muscle; SMAS, superficial musculoaponeurotic system; FV, facial vein.

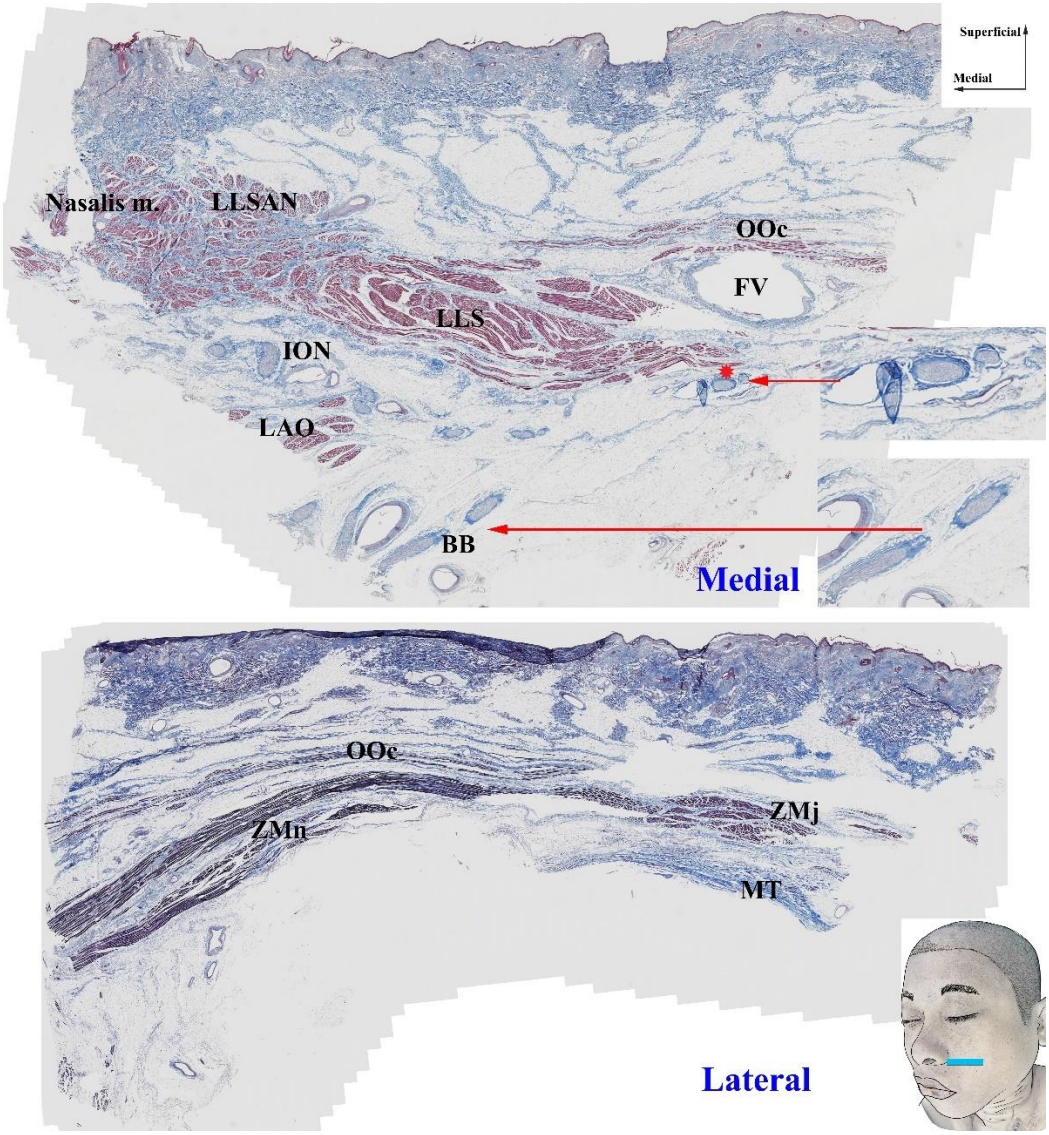

Figure 96 Histological section of the nasolabial region at alar base level stained with Masson's trichrome stain. LLSAN, levator labii superior alaque nasi muscle; LLS, levator labii superioris muscle; OOc, orbicularis oculi muscle; ION, infraorbital nerve; LAO, levator anguli oris muscle. BB, buccal branch of the facial nerve; ZMn, zygomaticus minor muscle; ZMj, zygomaticus major muscle; FV, facial vein; MT, masseteric tendon.

4.2.5 Histological section with Masson's trichrome stain at the tear trough region

According to tear trough area, the angular nerve was identified at supra-alar crease, infra-orbital rim, medial canthal, and supra-orbital rim levels. It was found that the AN embedded in fat that superficial to the LLS and deep to OOc muscles at medial

portion in 8 of 14 cases (57.14%), and 6 of 14 cases (42.56%) at lateral portion. Moreover, the ION was located deep to the LLS at medial portion (Figure 97). At infra-orbital rim level, the AN was identified between OOc and LLS muscles (Figure 98). Then, the AN run superiorly to medial canthus, it was located superficially to the AV in 85.71% (Figure 99), and deep to AV in 14.29%. At supra-orbital rim levels, the AN branched into small twigs to innervate corrugator supercilii, depressor supercilii, and procerus muscles so it's difficult to observe at this level. In the contrast, the sensory nerve can observe at this level (Figure 100).

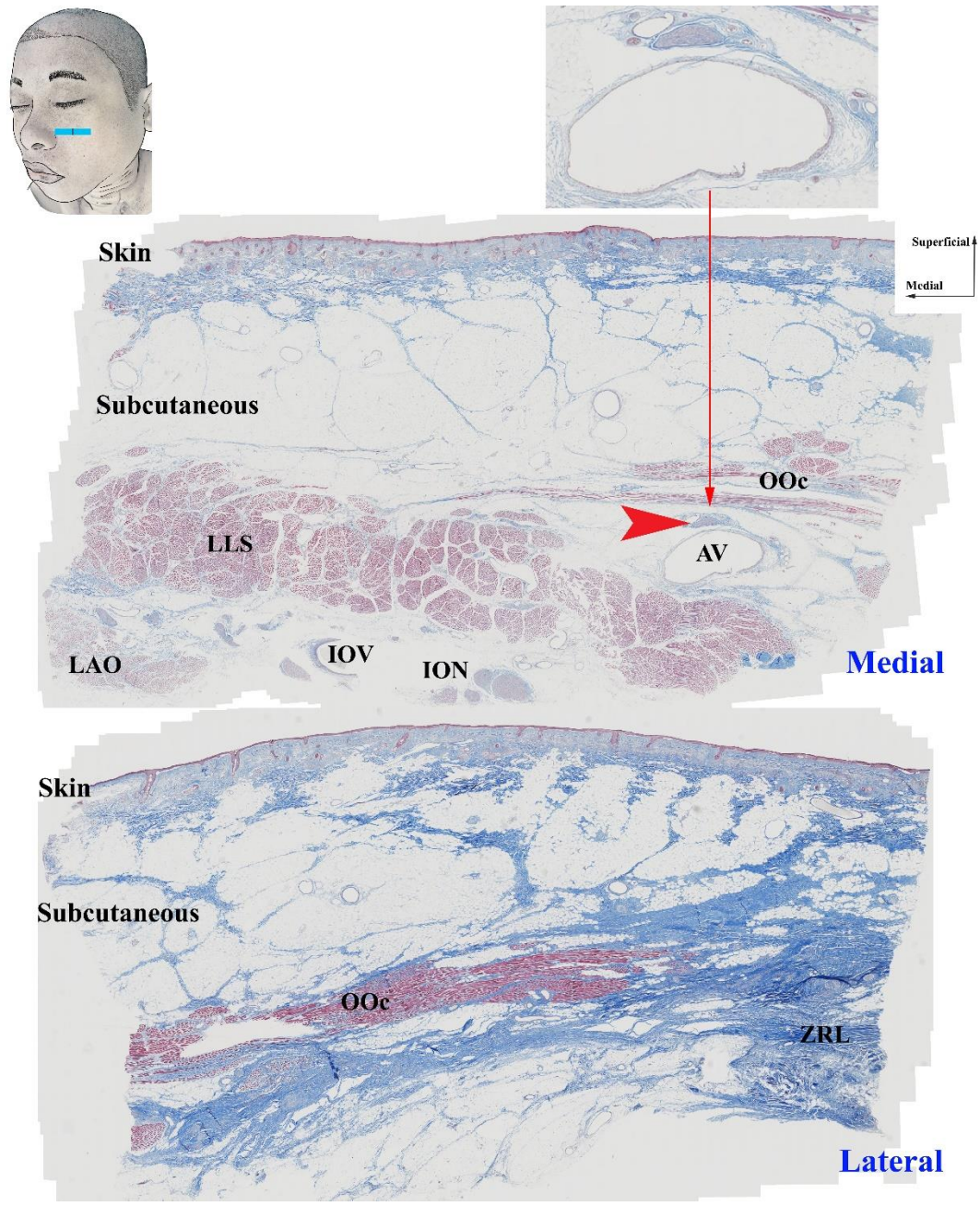

Figure 97 Histological section of the tear trough region at supra-alar crease level stained with Masson's trichrome stain. LLS, levator labii superioris muscle; OOc, orbicularis oculi muscle; ION, infraorbital nerve; IOV, infraorbital vessel, LAO, levator anguli oris muscle; AV, angular vein, ZRL, zygomatic retaining ligament; arrow head, angular nerve.

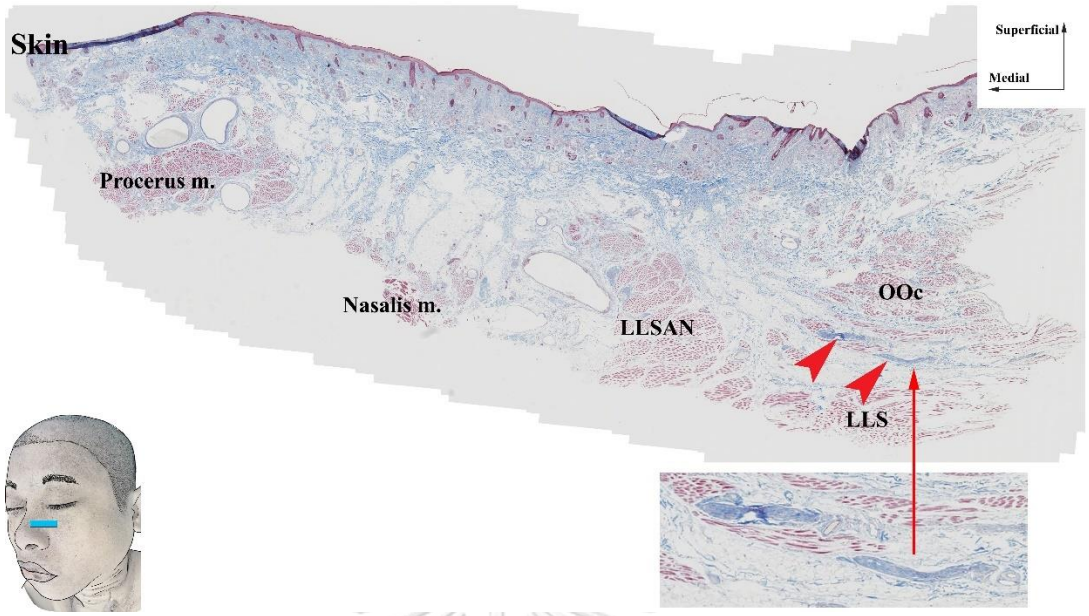

Figure 98 Histological section of the tear trough region at infraorbital rim level stained with Masson's trichrome stain. LLSAN, levator labii superior alaque nasi muscle; LLS, levator labii superioris muscle; OOc, orbicularis oculi muscle; arrow head, angular nerve.

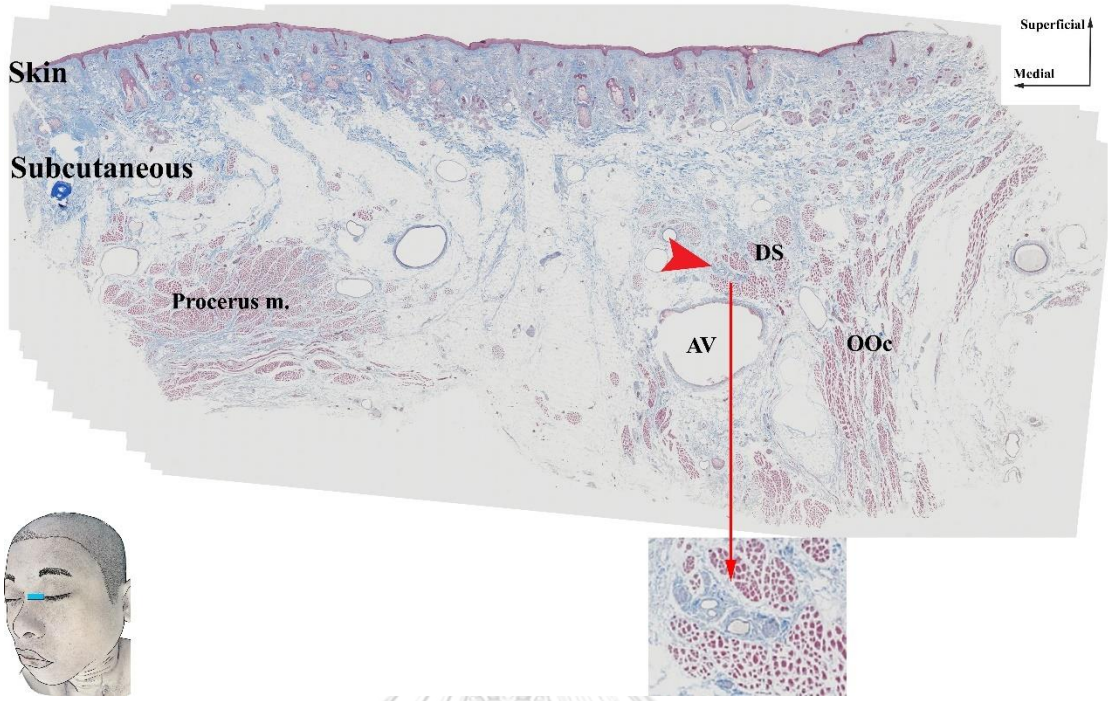

Figure 99 Histological section of the tear trough region at medial canthal level stained with Masson's trichrome stain. DS, depressor supercilii muscle; OOc, orbicularis oculi muscle; AV, angular vein. arrow head, angular nerve.

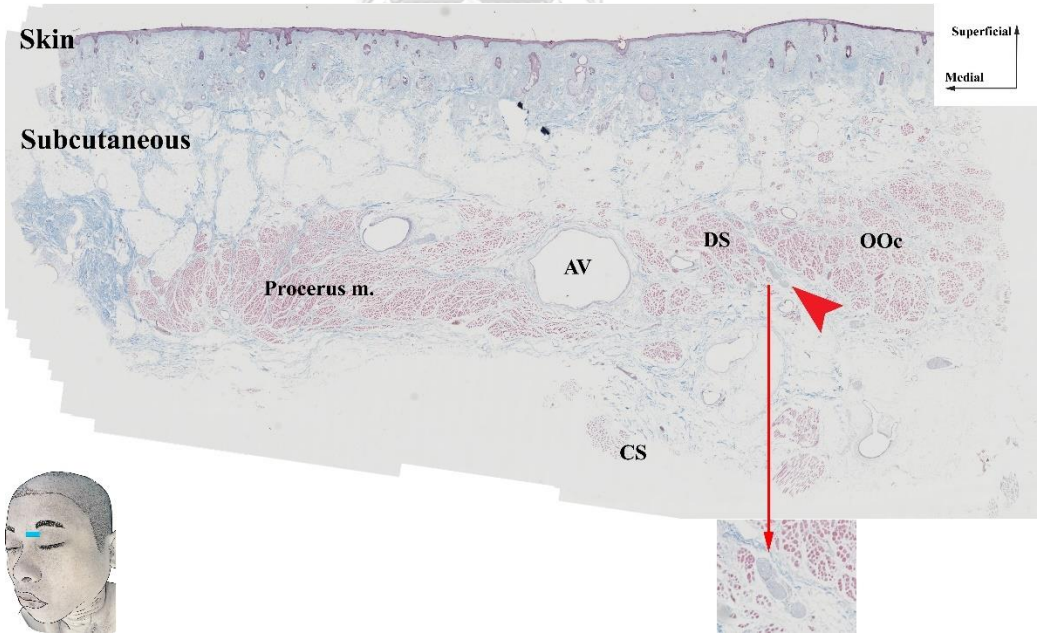

Figure 100 Histological section of the tear trough region at supraorbital rim level stained with Masson's trichrome stain. DS, depressor supercilii muscle; OOc, orbicularis oculi muscle; CS, corrugator supercilii muscle; AV, angular vein. arrow head, angular nerve.

4.2.6 Histological section with Masson's trichrome stain at the mandibular and cervical region

In the mandibular and cervical region, the MB and CB were identified at AML. The results revealed that the MB was found under the platysma muscle in 1.64 ±0.63 (1, 3) branches. Moreover, the MB is identified deep to the FA in 7.14%, superficial to the FA in 57.14%, and both deep and superficial to FA in 35.71%. In addition, the CB was found in 2.79 ±1.25 (1, 6) branches under the platysma muscle (Figure 101).

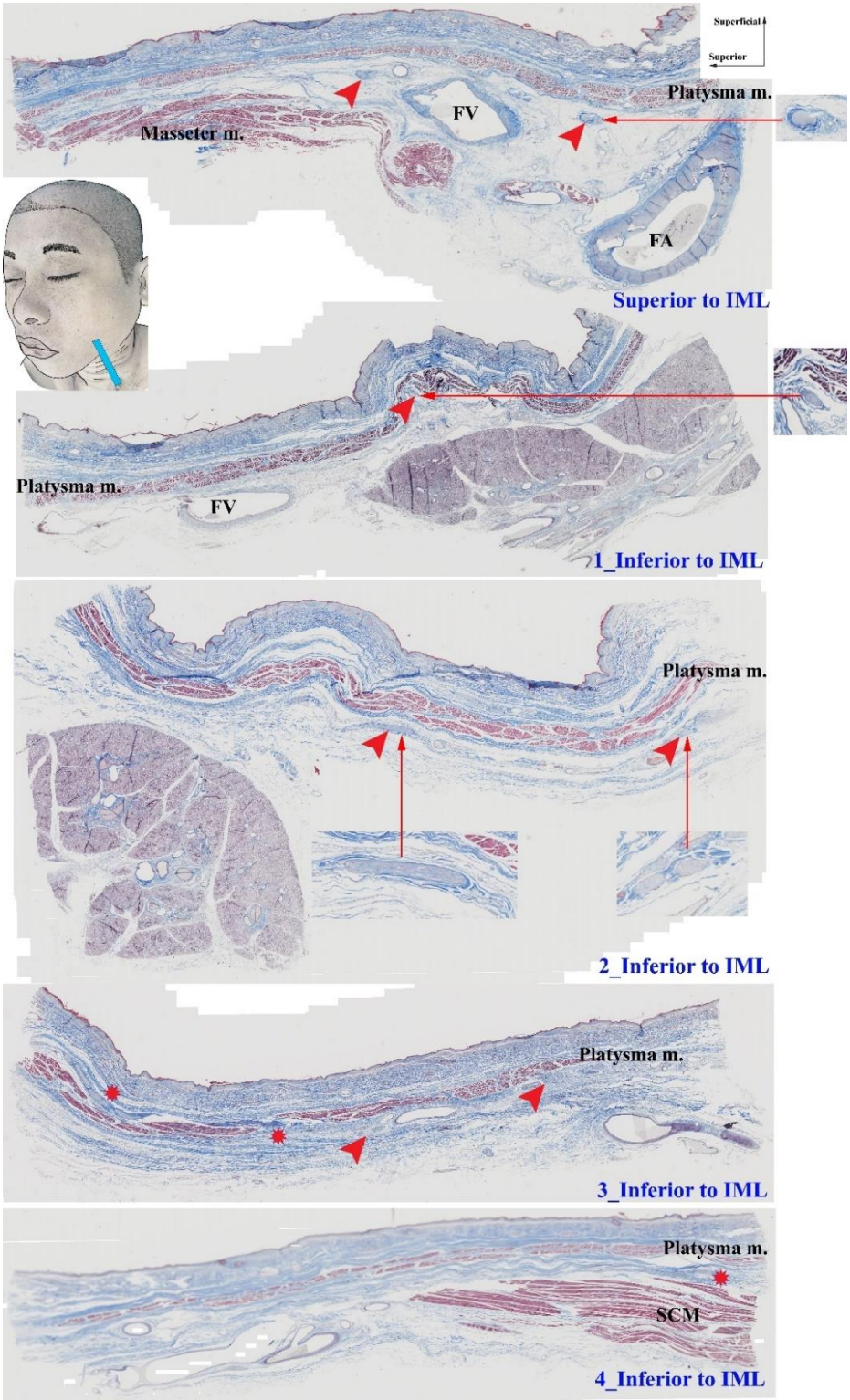

Figure 101 Histological section of the mandibular and cervical region at the AML stained with Masson's trichrome stain. FA, facial vein; FV, facial vein; SCM, sternocleidomastoid muscle; arrow head, marginal mandibular and cervical branch of the facial nerve.

4.3 The results of the Sihler's staining technique

The intramuscular of the branch of the facial nerve were investigated by using Sihler's staining technique. The pattern of the intramuscular of the branches of the facial nerve were collected in frontalis, orbicularis oculi, zygomaticus major, levator labii superioris, orbicularis oris, depressor anguli oris and platysma muscles. The result presented that the intramuscular of the branch of the facial nerve can observe in frontalis, orbicularis oculi, zygomaticus major, orbicularis oris, depressor anguli oris and platysma muscles, excepted levator labii superioris muscle.

According to the frontalis muscle, the several twigs of the TB enter the frontalis muscle at lateral border. Before entering the muscle, the TB connected to each other at medial temporal region. The pattern of the TB was analyzed in 4 portions of the frontalis muscle including superior-medial, superior-lateral, inferior-medial, and inferior-lateral portions. The result revealed that the TB formed into the entangled meshwork at inferior-lateral portion of the frontalis muscle, then this mesh work gave 2-4 long twigs traveled within inferior-medial portion of the frontalis muscle. In the contrast, the TB gave 2-3 long twigs within superior-lateral portion, while the small twig of the TB was found single or 2 twigs within superior-medial portion (Figure 102).

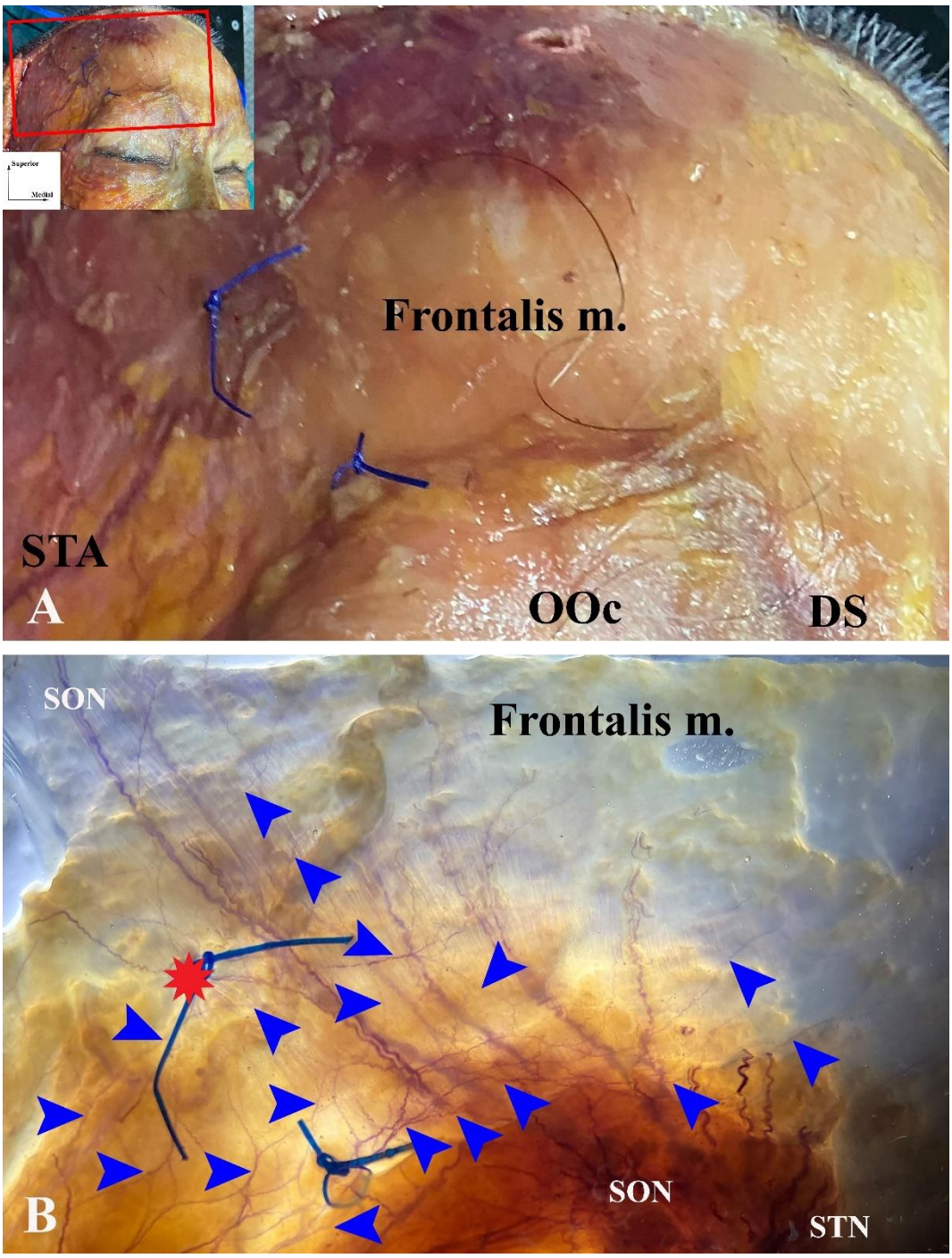

Figure 102 The frontalis muscle in soft cadaveric dissection (A). Intramuscular part of the facial nerve in the frontalis muscle by Sihler's stain technique (B). STA, superficial temporal artery; OOc, orbicularis oculi; DS, depressor supercilii; SON, supraorbital nerve; STN, supratrochlear nerve; arrow head, temporal branch of the facial nerve.

In the orbicularis oculi muscle, the branches of the facial nerve are responsible in four areas including superior-medial, superior-lateral, inferior-medial, and inferior-lateral portions. The TB formed into the entangled meshwork at superior-lateral portion of the orbicularis oculi muscle, while the ZB and BB gave the long twig to innervate orbicularis oculi at inferior-lateral portion. In addition, the BB travel medially to supply OOc muscle at superior-medial and inferior-medial portions (Figure 103).

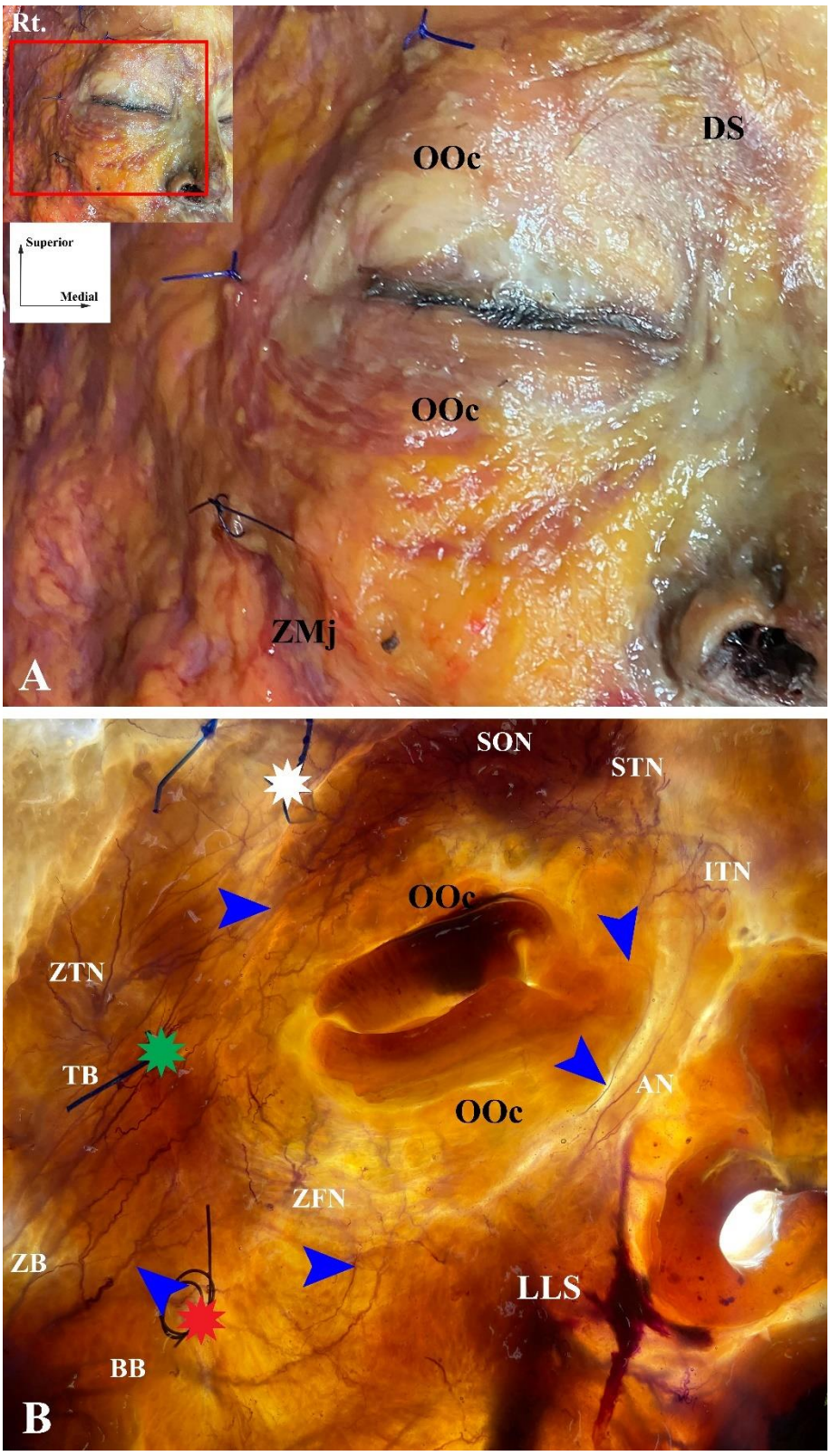

Figure 103 The orbicularis oculi muscle in soft cadaveric dissection (A). Intramuscular part of the facial nerve in the orbicularis oculi muscle (B). OOc, orbicularis oculi; DS,

depressor supercilii; ZMj, zygomaticus major; LLS, levator labii superioris; SON, supraorbital nerve; STN, supratrochlear nerve; ITN, infratrochlear nerve; ZTN, zygomaticotemporal nerve; ZFN, zygomaticofacial nerve; TB, temporal branch; ZB, zygomatic branch; BB, buccal branch; arrow head, intramuscular part of the facial nerve in the orbicularis oculi muscle; white asterisk, lateral border of the frontalis muscle; green asterisk, lateral border of the orbicularis oculi muscle; red asterisk, origin of the zygomaticus major muscle.

According to the zygomaticus major muscle, the superior portion of the muscle was innervated by 2-5 short twigs of the upper and middle branches of the BB, whereas the inferior portion of the muscle was innervated by 1-2 long twigs of the middle and lower branches of the BB (Figure 104).

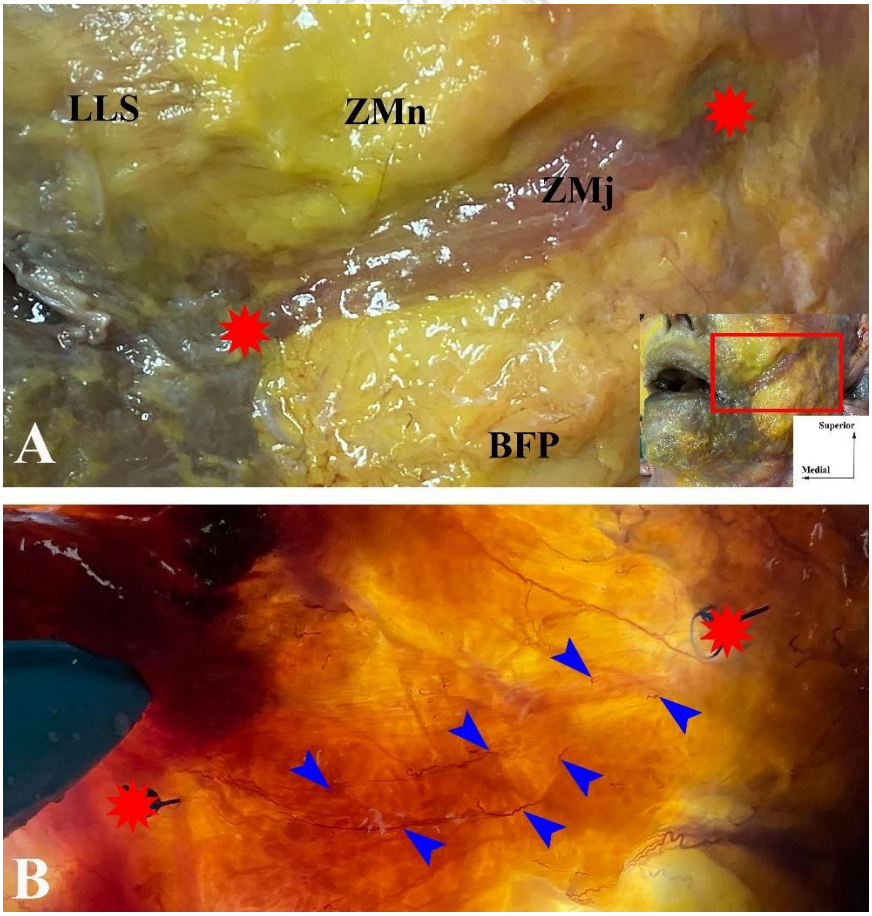

Figure 104 The zygomaticus major muscle in soft cadaveric dissection (A). Intramuscular part of the facial nerve in the zygomaticus major muscle (B). LLS, levator

labii superioris; ZMn, zygomaticus minor; ZMj, zygamicus major; BFP, buccal fat pad; arrow head, intramuscular part of the facial nerve in zygomaticus major muscle; red asterisk, origin and insertion of the zygomaticus major muscle.

According to the depressor anguli oris muscle, the superior portion of the muscle was innervated by 2-3 short twigs of the middle branches of the BB, whereas the inferior portion of the muscle was innervated by 1-2 short twigs of the lower branches of the BB (Figure 105).

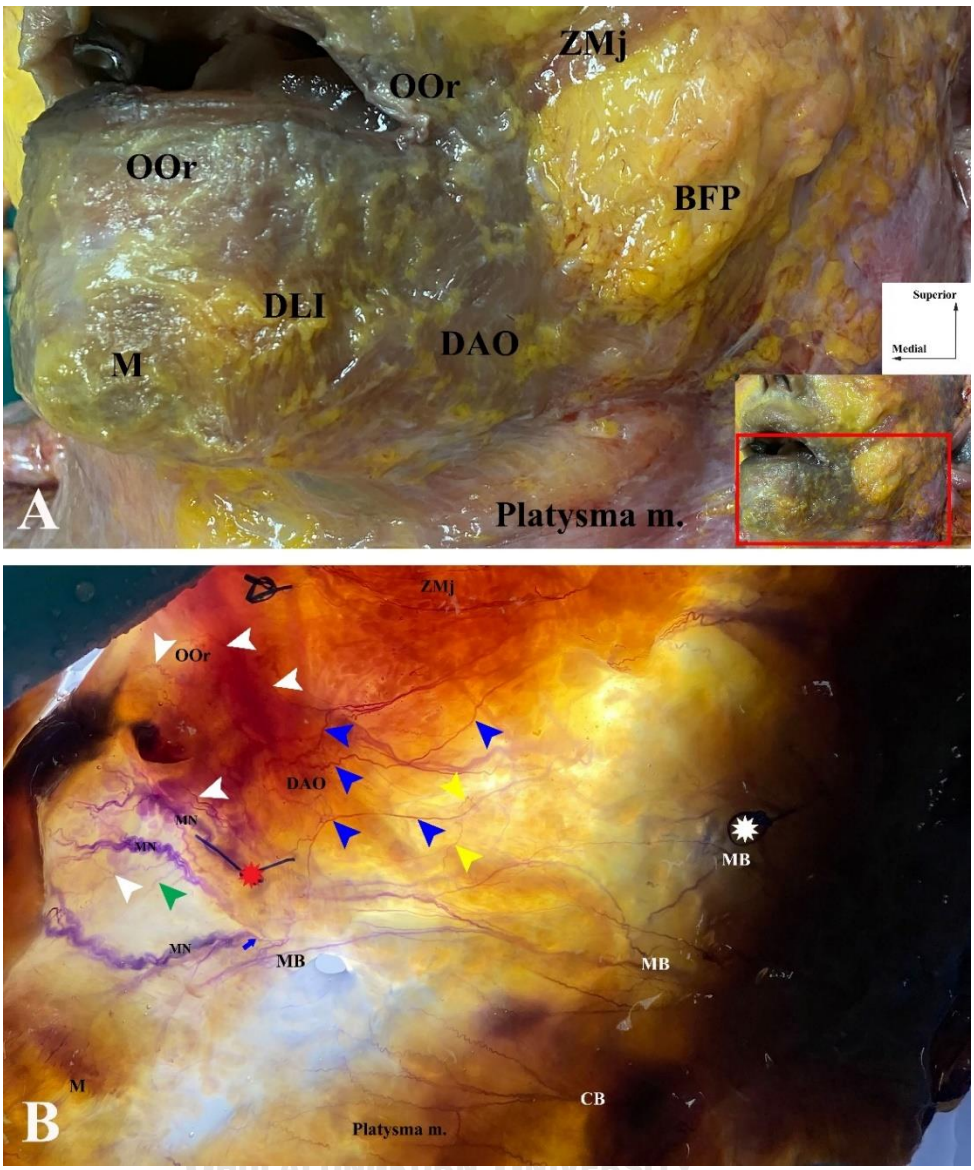

Figure 105 The depressor anguli oris muscle in soft cadaveric dissection (A). Intramuscular part of the facial nerve in the depressor anguli oris muscle (B). ZMj, zygamicus major; DAO, depressor anguli oris; OOr, orbicularis oris; DLI, depressor labii inferioris; M, mentalis; BFP, buccal fat pad; MB, marginal mandibular branch of the facial nerve; CB, cervical branch of the facial nerve; MN, mental nerve; blue arrow head, nerve innervation of the depressor anguli oris muscle; white arrow head, nerve innervation of the orbicularis oris muscle; green arrow head, nerve innervation of the depressor labii inferioris muscle; yellow arrow head, nerve innervation of the platysma muscle; red asterisk, medial border of the depressor anguli oris muscle; white asterisk, mandibular angle.

According to the platysma muscle, the CB is responsible for all portions of the muscle. In a medial portion of the platysma muscle, the CB gave 10-17 long twigs to innervate the muscle until the medial border of the muscle. In addition, the small twigs connected to each other branch within the platysma muscle (Figure 106).

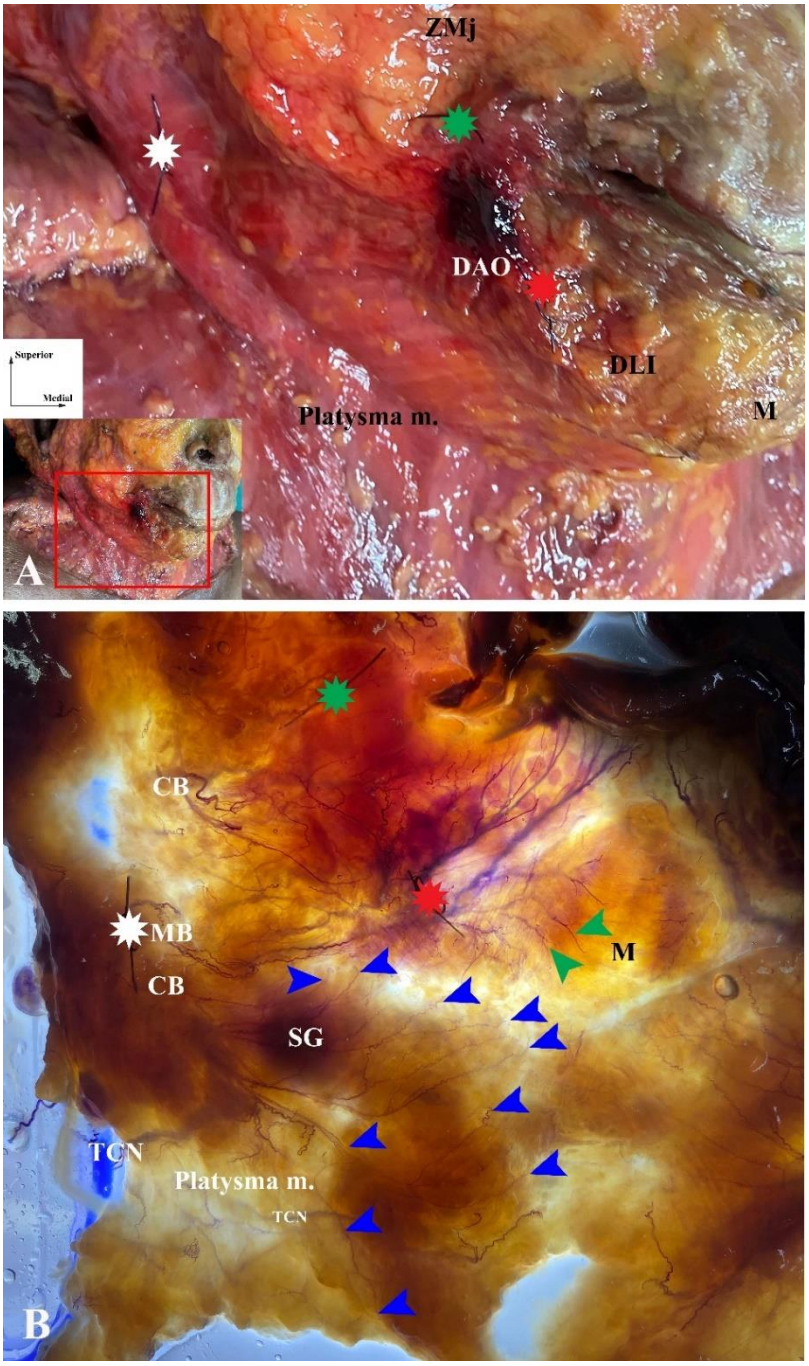

Figure 106 The platysma muscle in soft cadaveric dissection (A). Intramuscular part of the facial nerve in the platysma muscle (B). ZMj, zygamicus major; DAO, depressor

anguli oris; DLI, depressor labii inferioris; M, mentalis; BB, buccal branch of the facial nerve; MB, marginal mandibular branch of the facial nerve; CB, cervical branch of the facial nerve; TCN, transverse cervical nerve; SG, submandibular gland; blue arrow head, nerve innervation of the platysma muscle; green arrow head, nerve innervation of the mentalis muscle; green asterisk, insertion of the zygomaticus major muscle; red asterisk, medial border of the depressor anguli oris muscle; white asterisk, mandibular angle.

In the orbicularis oris muscle, the MB gave long twig to response in inferior portion of the OOr (Figure 107B), while the lower branch of the BB gave small twig to innervate in superior portion of the OOr (Figure 107B).

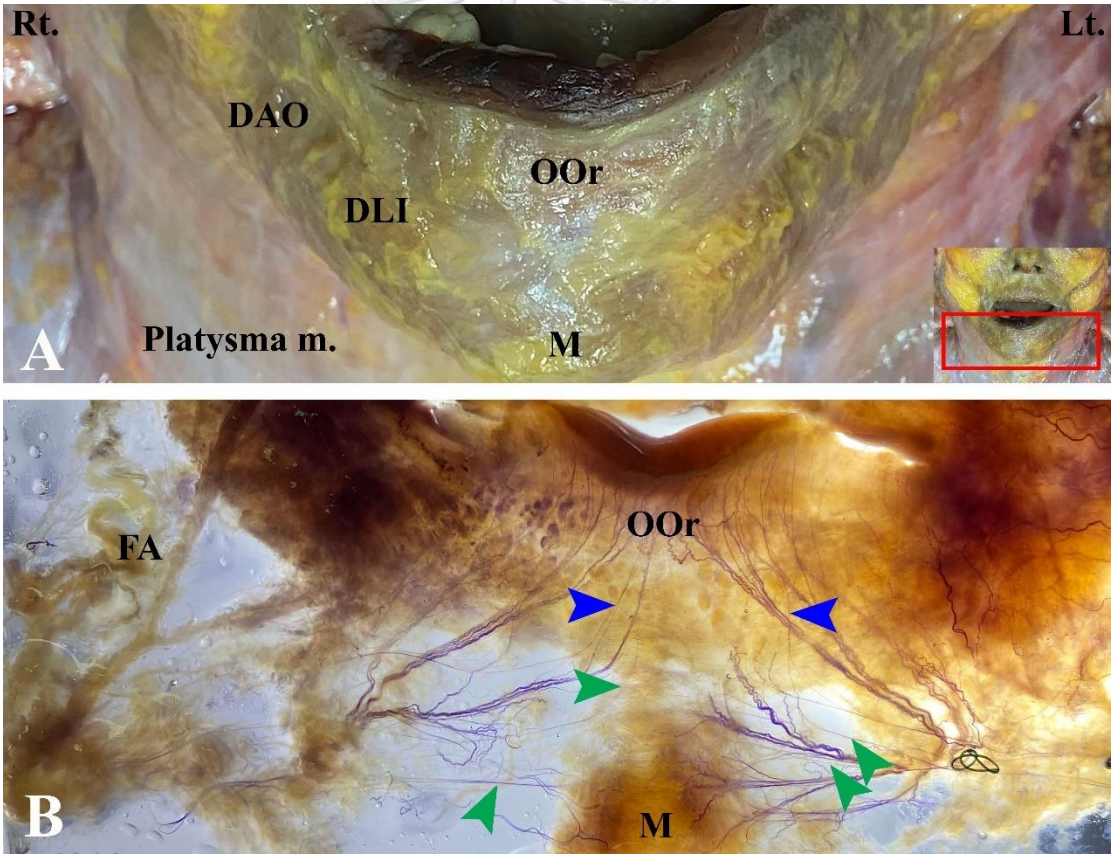

Figure 107 The orbicularis oris muscle in soft cadaveric dissection (A). Intramuscular part of the facial nerve in the orbicularis oris muscle (B). DAO, depressor anguli oris; OOr, orbicularis oris; DLI, depressor labii inferioris; M, mentalis; FA, facial artery; blue arrow head, nerve innervation of the orbicularis oris muscle; green arrow head, nerve innervation of the mentalis muscle;

CHAPTER V

DISCUSSION

In the literature review, the facial nerve has been investigated by using gross dissection, histological study, electromyography surface electrodes[124], and Sihler's stain technique[125]. The facial paralysis resulted from the injury of the facial nerve, especially the injury of the temporal and marginal mandibular branch[126]. Moreover, the temporal, zygomatic and buccal branches injury due to face lift, blepharoplasty, and forehead lift in 7.6%[127]. The ZB and MB were protected during facial reanimation, whereas the BB and CB were cut to reduce facial synkinesis[128]. As the result, the anatomical knowledge of the facial nerve is essential to prevent and predict complication during both surgical and non-surgical intervention[119-123].

The temporal branch of the facial nerve

A detail of the TB is essential to predict complication of the nerve injury during surgery or trauma at the temporal region such as craniofacial surgery to correct congenital deformities or repair maxillofacial trauma, frontal cranioplasty, orbital reconstruction and cosmetic surgery[129, 130]. The zygomatic arch is the commonly damaged area of the TB, because the TB crossed this area to innervate the muscles[131]. The injury of the TB results in eyebrow depression on the ipsilateral, and horizontal forehead wrinkles on the contralateral of the face[132].

In this study, the TB gave 1-5 branches at the emerging points, and the mean number was 2.57 ±0.83 branches. The mean distance of the emerging point of the TB was 21.95 ±4.87, and it is located within 10.62 to 35.75 mm. from the inferior border of the tragus. Moreover, the diameter of the TB at the emerging point was 0.93 ±0.33 (0.36, 1.86) mm. At the FHL, the TB crosses the FHL at a mean distance of 25.74 ±7.37 (12.40, 47.31) mm. In addition, the temporal branch is distributed along the LCHL from 15.30 mm. to 52.66 mm. Furthermore, the temporal branch is distributed at the SOL from 19.98 mm. to 58.37 mm. Additionally, the temporal branch gave a small twig to connect the zygomaticofacial nerve in 14.29%.

According to SIhag et al. (2020) explained that several branches of the TB superficially crossed the zygomatic arch as 2 branches (25%), 3 branches (65%), and 4 branches (10%), and connected with each other at this area. Moreover, the TB was located in the TPF and superficial temporal fat pad, fat between the TPF and superficial layer of deep temporal fascia (S-DTF). The distance of the rami of the TB was measured between the lateral bony canthus and the anterior, middle, and posterior rami on standard line that line connect the lateral bony canthus to the superior margin of the tragus. It was found that the distance of the lateral bony canthus and the TB and anterior, middle, and posterior rami were 32.00 ±5.50 mm, 42.00 ±5.90 mm, and 51 ±4.9 mm, respectively. Furthermore, the mean distance of the lateral bony canthus and the TB was 19 mm, and the distance between each ramus approximately 12 mm[133]**.** Moreover, the frontalis and superior-lateral portion of the OOc were innervated by anterior and middle rami of the TB, while the anterior auricular and the temporoparietal muscles were innervated by the posterior rami[130].

At the superior border of the parotid gland, the TB gave 2-4 (3.2 ±0.6) branches that perforate the parotidomasseteric fascia. Then, the rami of the TB were positioned within the loose areolar fascia at the zygomatic arch level. The distance of the most posterior ramus of the TB and the ATL was 15.30 ±3.50 (11.00-22.90) mm. Subsequently, the rami of the TB passing through the superior temporal line (STL) deep to the frontalis muscle at 19.00 ±2.80 mm from the orbital rim[24]. According to Jose et al. (2021) explained that the TB gave 1-3 rami deep to the SMAS and TPF including single ramus in 2%, 2 rami in 26%, and 3 rami in 70%. After that, the posterior rami of the TB crossed the zygomatic arch at 19.50 ±5.40 mm from the external auditory meatus[134].

Additionally, Lei et al. (2005) demonstrated that the TB penetrated the parotid fascia at 22.00 ±5.00 mm from external auditory meatus, and gave 2-4 branches obliquely crossed the zygomatic arch to supply the frontalis, orbicularis oculi, and corrugator muscles. Furthermore, the TB was located within the TPF at zygomatic arch

same the temporal branchof the superficial temporal artery (STA). At above the eyebrow, the terminal rami of the TB were posited inferior and deep to the STA in 63.33%, while located superior to the STA in 36.67%. Besides, The TB was located deep to the TPF at this level[135].

According to Trussler et al. (2010) summarized that the TB has closely located on the periosteum of the zygomatic arch after emerging from the parotid gland. After that, it became more superficially under the TPF. As the result, the dissection should be preserved the superficial temporal fat pad superficial to protect the TB[136], or using a subperiosteal dissection at the area above the zygomatic arch[130].

In addition, the location of TB is important for lateral face surgery such as rhytidectomy, and brow- elevating. Pankratz et al. (2020) described that the caution zone of the TB was an area within radiation of 9.61 ± 5.08 mm superior to the zygomatic arch, and 12.20 ± 4.77 mm posterior to Pitanguy's line because the TB changed plane into the SMAS plane about 94.4%. However, the TB crossed the anterior branch of STA at a distance 28.09 ± 6.37 mm from the lateral orbital rim superiorly, and at distance 13.06 ± 6.19 mm posterior to the Pitanguy's line [87]. At superior part of the orbicularis oculi entry site, the distances between the TB and the lateral canthus were 25.4 ±4.30 mm in X-axis, and 28.5 ±6.90 mm in Y-axis. The location of the TB changes from a vertical direction to a horizontal direction was 47.00 ±7.90 mm from the lateral canthus[130].

According to Lettieri (2008), the TB was observed within the galeal frontalis fusion point after the loose areolar layer lifting, and it was located within 2 mm in deep surface[86]. Moreover, Barton (2009) explained that the TB runs superior-medially in the area beginning from 5 mm inferior to the tragus until 15 mm superiorly to eyebrow, and Its was located deep to the TPF at zygomatic arch, after that it was located within the TPF[137]. In rhytidectomy, the danger zone of the TB was located 18 mm anterior to the ATL, and 20 mm posterior to the temporal border of the frontal process of the zygomatic bone correlated to the LCHL. Moreover, the TB was identified

at superior to the eyebrow approximately 20 mm. As a result, anchor points are located within the DTF superior to the zygomatic arch for avoiding TB injury[138, 139].

Bonnecaze et al. (2015) determined that the TB crossed the inferior border of the zygomatic arch at 24.25 (11.5, 40) mm from ATL, crossed the superior border of the zygomatic arch at 28.25 (19, 40) mm from ATL, and crossed the line from the lateral canthus at 19.8 (7, 31) mm. Furthermore, the zone of the high risk of TB injury was summarized in three levels of risk. Firstly, the high risk of injury was located in the area elongated from 22.60 to 26.06 mm correlated to the ATL at the inferior border of the zygomatic arch level. Secondly, the area elongated from 27.46 to 30.43 mm correlated to the ATL at the superior border of the zygomatic arch level. Lastly, the area elongated from 16.20 to 19.17 mm posterior to the lateral canthus. Moreover, the area elongated from 26.89 m to 27.46 mm and 30.43 to 30.99 mm were determined into moderated and low risk area, respectively at the superior border of the zygomatic arch level[88]. Similarly, Sanderson et al. (2020) explained that the TB crossed the zygomatic arch at 32.1 ± 0.50 mm from the apex of the tragus[140].

However, Shin, Shin, Lee, Koh, & Song (2018) investigated the location of the TB for preventing the TB injury during the superficial temporal arterial biopsy. It was found that the TB crossed LCHL at 33.2 mm from ATL, and crossed SOL at 49.2 mm from ATL. After that, the terminal twig of the TB innervates the OOc and frontalis muscles[141].

Generally, the locations of the TB were described as correlated to soft tissue layers in the temporal region. At the zygomatic arch and lateral central levels, the TB was located deep to the TPF. And, the TB was located deep to the frontalis muscle at the upper eyebrow level[142, 143]. Similarly, Spiriev et al. (2016) illustrated that the TB was positioned deep to the SMAS at inferior to the zygomatic arch level, then the TB gave many small branches traveled within superficial temporal fat pad superficial to the S-DTF and deep to the TPF for innervation the muscles at superior to the zygomatic arch. On the contrast, none the TB was located within the intermediate temporal fat

pad which the fat is embedded between S-DTF and D-DTF. Moreover, the TB gave three rami including posterior, middle, and anterior rami to innervate the auricularis, frontalis, orbicularis oculi muscles, respectively. The longest rami of the TB perforate the TPF inside the inferior temporal septum and traveled within/superior the TPF before innervation the frontalis muscle[144]. In addition, the TB gave 2-6 twigs to entry the deep surface of the orbicularis oculi muscle, and was located superior to the line connected the lateral canthus and the center of the tragus. The most superior rami of the TB traveled to the frontalis muscle, whereas the most inferior rami of the TB supply the orbicularis oculi and connected to the rami of the ZB. Besides, the middle rami of the TB medially traveled within eyebrow area to innervate the frontalis and corrugator supercilii muscles[145]. Yang, Gil, & Lee (2015) determined that the mean of the rami of the TB was 2.60 ± 1.10 rami traveled over the superior border of the zygomatic arch, and the corrugator supercilia muscle was innervated by small twigs of the TB approximately 1.80 ±0.90 twigs[146]. Similarly, a study by Choi & Kim (2021), the TB gave 2.8 (2-4) rami pass through the zygomatic arch, then obliquely traveled to the intra-orbicularis area. The anterior rami of the TB horizontally traveled to innervate the corrugator supercilia and orbicularis oculi muscles at the eyebrow and upper eyelid levels. The anterior rami of the TB gave small twigs about 5.1 (4-6) twigs to distribute in brow area, and innervate supero-lateral portion of the corrugator supercilii and brow portion of the frontalis muscles. Also, infero-medial portion of the corrugator supercilii and the medial orbital portion of the orbicularis oculi muscles were innervated by 2-4 twigs of the anterior rami of the TB. At upper palpebral area, the anterior rami of the TB gave 4.8 (3-6) twigs. On the contrary, there was no the small twigs at the lower palpebral area[147].

In histological study, Trussler et al. (2010) demonstrated that the TB was located below the parotid-temporal fascia at the zygomatic arch level, whereas the TB perforated the parotid-temporal fascia and was located deep to the TPF at 20 mm superior to the zygomatic arch[136]. Furthermore, Agarwal et al.[33] (2010) discovered that

the temporal branch was located in innominate fascia after perforated the parotid-masseteric fascia, and transitioned to the inferior surface of the superficial temporal fascia before innervation the muscles. The fascial transition point was investigated by using cadaver dissection and Masson's trichrome stain in 18 and 6 hemifaces respectively. It was found that the fascial transition zone covered the area from 15-30 mm superior to the upper border of the zygomatic arch (y axis) and 9-14 mm behind the lateral orbital rim(x axis)[33]. Similarly, Yang et al. (2022) demonstrated that the TB were inspected in the loose areolar layer deep to the TPF at the zygomatic area. As a result, the liposuction was performed in the subcutaneous layer[148].

The zygomatic branch of the facial nerve

The detail of the branches of the FN is important for treatment or cosmetics procedures in the mid-face such as botulinum toxin injection[145], face lifting[149], liposuction[148] Facial Reanimation performing[150-152].

To localization of the ZB and BB, both branches were described together frequently with in area 5 mm from the Zuker's point. The numbers of the ZB and BB were 2.98 ±0.86 (2-5) branches, and 3.45 ±0.96 (2-5) branches, respectively[150]. In our study, the ZB gave 1.83 ±0.69 (1, 3) branches, and the most of number of the ZB was 2 branches in 50.00%. The emerging point of zygomatic branch were 30.63 ±5.73 mm, and 1.36 ±4.09 mm in X and Y axis, respectively. Moreover, the diameter of the ZB at the emerging point was 0.95 ±0.36 (0.41, 1.87) mm. For investigation of the course of the ZB, location and diameter of the ZB were mapped as the vertical distance from the FHL at the midpoint. The result suggested that the most of the course of the ZB was located below the FHL at vertical distance was -6.06 ±2.91 mm (36.14%). Moreover, 34.94% of the course of the ZB was located below the FHL at vertical distance was -14.60 ±2.53 mm. Additionally, the numbers of the zygomatic or buccal branches at lateral border of the zygomaticus major muscle were 3.74 ±0.94 (2, 6) branches.

According to Lee et al. (2014) illustrated that the ZB was observed superficial or same layer to the TFA and PD. The distance between the zygomatic arch and the course of the ZB was 10.9 ±5.9 mm. Moreover, the location of the ZB was 34.0 ±8.8 mm anterior to the tragus, and the angles between FHL and the ZB was +10.4 degrees[149]. Moreover, the superior-lateral and inferior-lateral of the orbicularis oculi muscle was innervated by the upper zygomatic branches that pass through the anterior potion of the zygomatic arch. The entry site for innervation was area at superior to lateral canthal crease 6 mm and inferior to lateral canthal crease 4 mm[147]. In temporomandibular joint surgery, the ZB can injury at the preauricular area. Moreover, the upper zygomatic rami innervated the inferior portion of the orbicularis oculi muscle at deep surface of the muscle that were covered by skin and subcutaneous layers, while lower zygomatic rami innervated the zygomaticus major muscle[130].

Several rami of the ZB (1-3 rami) emerge the parotid gland at 30.71 mm anterior to the tragus. The ZB had the rate of paralysis approximately 60% because it traveled become superficially after exit from the parotid gland[153]. Similarly, Ye et al. (2021) revealed that the ZB gave 2-4 rami to emerge the anterior border of the parotid gland deep to the SMAS, and entry the orbicularis oculi muscle approximately 1-5 twigs. Besides, the ZB gave 1-3 twigs to innervate the zygomaticus major muscle. Additionally, the most superior rami of the ZB connected with the most inferior of the TB, and pierced the orbicularis oculi at 39.23 ±5.38 mm from the center of the tragus with the angle 18.48 ±6.38 degrees[145].

Previously, the ZB gave 3 twigs to innervated the zygomatic major muscle including upper, middle, and lower ZB. The distances between the zygomaticomaxillary (ZM) suture and 3 twigs were 6.20 ± 1.60 mm, 2.30 ± 4.20 mm, and 4.80 ± 3.30 mm, respectively. Moreover, the distances between the tragus and 3 twigs were 6.40 ± 0.40 mm, 6.90 ± 0.30 mm, and 7.20 ± 0.10 mm, respectively. The depth of location of 2 twigs was 1.40 ± 0.40 mm (upper ZB), and 1.30 ± 0.40 mm (middle ZB) from the zygomatic bone[154]. Also, the location of the ZB was area within

10 mm inferior to the most prominent of the zygomatic arch, and it far from the tragus were 26.00 ±5.00 mm, and 25.00 ±1.00 mm in male and female, respectively[151]. Similarly, Lee et al. (2014) presented that the distances between the ZB and zygion was 10.90 ±5.9 mm, and the distances between the ZB and tragus was 34.00 ±8.8 mm[149].

Recently, the communication of the branches of the facial nerve was investigated by Freed rt al. It was found that the branches of the facial nerve connected with each other. The frequencies of the communications were reported that the BB connected to MB in 67.5%, the ZB connected to BB in 67.5%, The TB connected to ZB in 62.5%, and the MB connected to CB in 55% [155].

According to Wong & Mendelson (2013) explained that the rami of the ZB and BB traveled become superficially related to the AV, then it entered the orbicularis oculi muscle at the superior border of the premaxillary space. Also, the ZB and upper BB are connected with ION, and from the plexus both sensory and motor nerve to supply muscle or skin at the cheek and upper lip[156]. Moreover, the several twigs of the upper ZB innervated the zygomaticus minor and orbicularis oculi muscles at the malar area[147].

The buccal branch of the facial nerve

The present study concentrated on the detail of the BB in the mid-face region to pointedly explain the complicated anatomical information. Most of the BB originated from both temporo-facial and cervico-facial divisions and had 2-5 branches at the anterior border of the parotid gland. The findings suggested that the BB was rather constantly distributed in the area between anterior border of the parotid gland and midFHL. On the contrary, it became very complex and unstable after passing through midFHL for the reason that the BB branched and arranged into the ZBP. Although the ZBP was formed by several BB branches. In some cases, the ZB gave branches to connect with the BB also. As a result, term of ZBP was still used in this

study. Furthermore, many literatures defined the upper BB as the lower zygomatic branch in medical surgery.[90, 157, 158]

Lam et al. (2022) explained that the BB crossed the parotid duct in area 30 mm for intersection, as a result paralysis of the BB can occur approximately 88%[153]. Then, the BB superficially surmounted the capsule of the BFP[159]. From the complexity of the BB, the distances of the course of the BB were measured and correlated to the zygion. It was revealed that the distances between the course of the upper, middle, and lower of the BB and zygion were 26.70 ±9.20, 40.70 ±9.10, and 45.00 ±8.10 mm, respectively. Besides, the distances of the location of the upper, middle, and lower of the BB were 39.50 ±7.50, 45.30 ± 8.60, and 45.80 ±8.20 mm, respectively[149].

Liu et al. (2010) found that the BB gave 1-3 rami in 8.3%, 33.3%, and 58.3% respectively, and located superiorly to the parotid duct was 10.3 ±5.1 mm., and inferiorly to the parotid duct was 10.8 ±5.0 mm.[2] Besides, the diameter of the nearest buccal branch to the parotid duct was 1.6 ±0.4 mm. Additionally, the mean length of the BB was 37.87 ±7.33 mm., and the diameter of the BB was 0.99 ±0.40 mm.[160] It innervated the zygomaticus, orbicularis oris and levator labii superioris muscles which responed to lip movement and blowing. Furthermore, the BB originated from the temporo-facial division in 7.79%, the cervico-facial division in 72.73%, main bifurcation in 12.99%, and multiple origins in 11.69%.[16] Nonetheless, Eltohami, Huang, and Suleiman (2019) reported that the BB originated from the cervico-facial division and both divisions in 78.8% and 21.1% respectively, but none of the BB originated from the temporo-facial division.[161] Besides, Dhiwakar and khan suggested that the BB normally arose from the cervico-facial division.[16]

Additionally, Ahmed et al. (2015) explained that the BB were positioned both superior and inferior to the parotid duct. The BB mostly presented with multiple rami including 2 branches in 50%, 3 branches in 30%, 4 branches in 10%, and 5 branches in 10% of specimens. In addition, the location of the BB was classified into 2 types

correlated to the buccal fat pad; type I refered to the course of the nerve crossing superficially to the buccal fat pad, and type II refered to the course of the nerve penetration to the buccal fat pad. These nerve crossed superficially to the buccal fat pad in 73.7% and penetrated to the buccal fat pad in 26.3%.[162]

In a previous study, the pattern of the facial nerve branches was classified into several patterns.[20, 64, 81, 157, 160, 163] This study exclusively focused on the ZBP pattern. The results illustrated that the ZBP was positioned under the SMAS, but superficial to the parotid duct and buccal fat pat at both masseteric and buccal regions. Moreover, it formed a multi-loop pattern in 57.14%. It was possible that the BB injury could be occurred in these regions during facial surgery or parotidectomy. In the same way, the complex arrangement of the BB related to the parotid duct was firstly classified at the anterior of the parotid gland by Tsai et al. in 2019.[164] The results presented that the BB is located superiorly or/and inferiorly to the parotid duct. These nerves crossed the duct in several points. Additionally, the number of intersections between the BB and the parotid duct was 1 point (20%), 2 points (37%), 3 points (23%), 4 points (16%), and 5 points (6%). Similarly, Bendella et al. (2017) summarized the attribute of the facial nerve to prevent the complications that might be occurred in head and neck surgery. They explained that the BB related to the parotid duct and formed plexus around the parotid duct, but it was referred in terms of the facial parotid plexus.[157] Moreover, the BB traveled superficially at the lateral side of the corner of the mouth at approximately 20 mm; as a result, the BB could be damaged. However, this plexus was different from the infraorbital plexus, because it was merely arranged from several branches of the BB, while an infraorbital plexus was arranged by the BB with the superior labial branches of the infraorbital nerve.[157]

Surprisingly, the finding demonstrated that the medial part of the ZBP at the buccal region forms a constant line along the nasolabial fold. After that, it branched small twigs to innervate facial muscles. It is assumed that the cadavers were injected

with red latex into the artery, therefore, the nerves could be clearly observed. Then, the medial line was carefully dissected by using the small artery for following the course of these nerves. The present study inspected the medial part of the ZBP correlated to the anatomical landmarks such as the corner of the mouth and the alar base, and the relationship between the nerves and the facial vein. This finding suggests that the possibility that several branches of the BB do not separate individual branches, but each the BB was located harmoniously as nerve plexus, and formed a medial line at approximately 30 and 20 mm far from the corner of the mouth, and alar base respectively. After that the plexus gave small twigs to innervate muscles. These could conceivably describe why the BB has a low rate of transient weakness after nerve injury.

Furthermore, this study was conducted to determine the feature of the AN. It was found that the superior part of ZBP branched a small branch that pierces through the LLS, then it innervates levator labii superioris alaeque nasi, nasalis, inferomedial part of the orbicularis oculi, procerus, depressor supercilii muscles. The mean of vertical distance between the course of the AN and the medial limbus was 24.16 ±3.39 mm., then it traveled superomedially and passed the medial canthus at approximately 1/3 laterally of the half intercanthal line. The AN was first explored by Hwang, Jin, Park and Chung in 2006[95]. It was presented that the AN originated from the BB or ZBP, and innervated the procerus muscle. On the contrary, Talmor et al. (2020) reported that the AN is arose from both the ZB and BB to innervates the target muscles[165]. According to Caminar Newman and Boyd (2006), the angular nerve ran superomedially in the levator labii superioris alaeque nasi, and innervated this muscle. After that, the AN ran superiorly and crossed medial canthus to innervate the procerus and corrugator supercilii muscles. It was located medially to the angular vein, and laterally to the angular artery[85]. Next, Yang et al. (2010) described that the angular nerve was divided into 3 types include single rami (20%) from ZBP in the orbicularis oculi muscle, single rami (20%) from ZBP in four muscle gap, and double rami (60%) in four muscle gaps[96].

In contrast, our study showed that the AN generally had a single branch (95.24%), and found double branches in 4.76%. Recently, the BB was investigated correlated to the intercanthal line which is the line between the nasion and the medial canthus. It was presented that the BB pass laterally at 1/3 of the intercanthal line[10].

Moreover, the BB connected with the sensory nerve include ION, ITN and BN. The distance between connection point and alar base was approximately 10 mm deep to LLS muscle. According to Yang, Hu and Kim summarized that ION communicated with the BB at infra orbital area[166]. In addition, the BN connected with the BB at the external layer of the deep fascia of the anterior part of the buccinator and orbicularis oris muscles. The connection of the BB mostly appeared under LLS, its connection between the BB (lower trunk) and the lateral labial branch of the ION (70%). The information of the connection between the motor and sensory nerves is important about proprioception of facial muscle. Consequently, these connections should be protected during medical surgery or intervention[108].

The marginal mandibular branch of the facial nerve

The MB can injury during or after the iatrogenic treatment such as neck surgery in 16%, submandibular gland surgery in 20%, and parotidectomy in 15%[167]. As the result, the action of the lip function become loss including the weakness of the DAO and LLI muscles[122, 167]. For this result, the anatomical study of the MB is important to avoid the complication that occur after medical intervention[168, 169]. The MB penetrated the parotid fascia at anterior margin of the parotid gland, then it medially traveled to supply the chin and lower lip muscles. The MB was protected by the platysma muscle because it was located deep to this muscle. At the oral commissure, the MB was positioned at 20 mm lateral to this point, consequently, the medical procedure in this area should be conducted in the subcutaneous layer[139, 170]. Furthermore, the MB was located superior to the posterior branch of the FV, so the surgery at the parotid gland should be carefully performed[171].

In this study, the result revealed that the location of the emerging point of the MB correlated to the IML were 20.12 ±6.55 mm and -0.75 ±5.55 mm, on X and Y axis, respectively. Moreover, the mean number of the MB was 1.36 ±0.49 (1, 2) branches. Furthermore, the number of the crossing point between the MB and IML was single point (50.00%), double points (33.33%), and triple points (7.14%). It was divided into anterior and posterior points. The distance between the posterior crossing point of the MB and AML was 9.95 ±5.17 mm, whereas distance between the anterior crossing point of the MB and AML was 12.54 ±6.85 mm. Moreover, the diameter of the MB at posterior and anterior points were 0.86 ±0.34, and 0.93 ±0.53 respectively. Additionally, the number of twigs of the MB at the masseteric area was 1-3 twigs, and the crossing point of small twig of the MB were 6.25 ±5.60 mm, and -6.99 ±4.02 mm at superior and inferior to the IML. Moreover, the diameter of the twig of the MB that crossed the AML at superior and inferior points were 0.79 ±0.21 mm, and 0.86 ±0.33 mm respectively.

Regarding the relationship between the MB and the FA, it found that the MB run superficial to the FA in 48.28%, deep to the FA in 13.79%, both superficial and deep to the FA in 12.07%, inferior to the FA in 15.52%, and other in 10.34%. Besides, the MB communicated with the mental nerve in 40.48%.

According to Sindel et al. (2021) revealed that the MB were located 6.90 mm, and 6.50 mm superior to the MIL in right and left sides, respectively. Also, it was located 3.00 mm, and 4.00 mm inferior to the MIL on right and left sides, respectively. Moreover, courses of the MB begin the parotid gland to the terminal twig under DAO were measured to prevent the complication during neck surgery. It was found that the MB traveled superficial to the deep cervical investing fascia, and the mean lengths of the MB were 33.57 ±3.41 mm and 33.51 ±4.88 mm on the right and the left sides, respectively[167]. Formerly, the number of the MB was determined by Touré, Vacher, & Bertrand in 2004. The results showed that the MB gave single branch (43%), double branch (44%), and triple branch (13%). The lowest MB was located inferior to IML at 17.5 mm and travel superficial to the FA at 24 mm from the MA. Furthermore, the MB

was located lateral to FA in 85%, while it was located medial to FA in 15% in inferior to the mandibular area[172]. Recently, the mean distance of the MB was found inferior to the gonion at 0.75 (-15.00 to 17.00) mm.[153].

Similarly, Jose et al. (2021) presented that the mean number of the MB was 1.7 rami, and it was single branch in 15%, and double branches in 85%. The MB was located superficial to the FA in all cases. Moreover, the MB was positioned superior to the IML in 85%, whereas it was positioned inferior to the IML in 15%[134].

Charafeddine et al. (2019) summarized that the MB gave 2.1 rami from the parotid gland in areas 10 to 20 mm. to the mandibular angle. Then, it run superficial to the FA at 23.1 mm in the X-axis and 3.1 mm in the Y-axis that corelated to the inferior border of the mandible. Moreover, the MB was found under the parotidomasseteric fascia, and positioned superior to the IML approximately 80% before crossing the FA[170]. Furthermore, the MB was described that it traveled to follow the IML and was located superficial to the FV and retromandibular vein under the deep cervical fascia[122]. The distance between the IML and the crossing point of the MB and FA was 1.73 ±1.57 mm inferior to the mandibular margin. Moreover, the MB gave several rami at this point[93].

Furthermore, Yang et al. (2016) revealed that the number of MB was 1.5 ±0.6 rami. The locations of the rami of the MB were measured in vertical distance from the MA and the intersection of the IML and the FA (FM). The result suggested that the mean distance between the lowermost MB and the MA was -5.00 ±2.20 mm inferior to the IML, while the mean distance between the uppermost MB and the MA was 1.00 ±3.20 mm superior to the IML. Moreover, the mean distance between the lowermost MB and FM was -9.80 ±1.90 mm inferior to the IML, while the mean distance between the uppermost MB and the FM was 5.0 ±7.1 mm superior to the IML. And the distance between the MA and the crossing point of the MB at IML was 33.10 mm anterior to the MA. In summary, the lowest distance of the MB was 6.00 mm inferior to the IML, and the MB was located less than 10 mm from the FM in 89.70%. The danger zone of

the MB was the posterior region of the mandibular bone approximately 40 mm anterior to the MA. As the result, the medical procedure should be performed 45 mm anterior to the MA, and 20 mm inferior to the IML to protect the MB[173].

The number of MB was investigated at the emerging point, during the course, and terminal rami. It was found that the MB gave single ramus in 88%, and double rami in 12% at the emerging point anterior to the parotid gland. During the course, the MB had single ramus in 92%, and double rami in 8%. After that, it gave a single twig in 4%, two twigs in 12%, and more than two twigs in 84%. Moreover, the location of the MB was investigated that correlated to the inferior border of the mandible. The result revealed that the MB was located superior to the IML in 100% after crossing the FA, while it was located superior to the IML in 16%, inferior to the IML in 32%, and along to the IML in 52% before it crossed the FA. And, it crossed superficially to both the FA and FV in 100%. Interestingly, the communication of the MB and the mental nerve was found in 28%. [174] Rarely, the MB gave four rami to innervate the lip depressor[175]. In addition, Touré et al. demonstrated that the number of the rami of the MB included single rami in 43%, 2 rami in 44%, and 3 rami in 13%. It passed through the FA at 24 mm from the MA. The lowest ramus was located 17.5 mm inferior to the IML [176]. Regarding the study of Touré et al. (2019), the MB had single rami in 22.6%, 2 rami in 29%, 3 rami in 12.9%, and 4 to more than10 rami in 35.48%. Noticeably, the rami of the MB were arranged into the plexus in the area around the FA anterior to the masseter muscle. Also, the rami of the MB formed a loop around the FA in 14.29%[177].

In 2014, Baur et al. measured the distances between the MB to the anatomical landmarks including mandibular angle, posterior border of the antegonial notch, anterior border of the antegonial notch, intersection of the FA and IML, and corner of the mouth. The result suggested that locations of the MB were 0.75 (-15.00, 17.00) mm inferior to the mandibular angle, 0.08 (-11.00, 20.00) mm superior to the posterior border of the antegonial notch, 1.29 (-13.00, 20.00) mm superior to the anterior border of the antegonial notch, 3.6 (-6.00, 25.00) mm superior to the intersection of the FA

and IML, and 10.9 (-2.00, 28.00) mm inferior to the MIL at corner of the mouth. Moreover, the directions of the MB were classified into three patterns. Firstly, the MB was located inferior to the MIL at the emerging point, then superior-medially traveled to cross the FA in 59%. Secondly, the MB was located superior to the IML from the emerging point until the entry point of the terminate muscles in 26%. Lastly, the MB was located superior to the IML at emerging point, then it inferio-medially traveled to cross IML, and traveled along the IML. After that, it was located superior to the IML at anterior area of the FA in 15%[178].

Recently, Marolt et al. (2021) explained that the location of the MB was 4.22 ±0.51 mm inferior to the IML in 90.30%, while it was located superior to the IML in 9.60%. Moreover, the safe zone of the MB was 30 mm inferior to the IML[179]. The diameter of the MB was 1.13 ±0.33 mm, with no significant differences between gender and sides of the samples. Moreover, the correlation between the diameter and the number of the axons was 900 axons ratio of 0.97 mm with 90% of specificity and 72% of sensitivity[180].

The MB triangle was determined by Rossell-Perry in 2016 to locate the MB in aesthetic surgery. The boundaries of this triangle were the corner of the mouth, the mastoid process, and the anterior border of the extracellular matrix muscle. The MB was found in this area, it gave single ramus in 90.62%, and double rami in 9.38%. However, this triangle is easy to identify the MB and CB, but the terminal twig cannot be observed in this area[182].

In systematic reviews of Kudva et al. study[183], the MB gave 1 to 4 rami at the intersection between of the FA and the IML. Besides, the MB communicated with BB, MN, CB, other MMB, anterior branch of great auricular nerve, and transverse cervical nerve. In the same way, Brennan et al. (2017) reported that the MB connected with the TCN inferior to the IML[184]. Moreover, the great auricular nerve communicated with the MB in 2%. The location of the great auricular nerve is identified at McKinney's point that the point is located at 65 mm inferior to the external acoustic meatus and 5 mm

posterior to the external jugular vein[185]. The communication of the MB and TCN was investigated by Brennan, Mak, Massetti, and Parry in 2019. The result presented that the MB connected with the TCN in 2.3%[181] also.

The cervical branch of the facial nerve

In aesthetic surgery, the knowledge of the CB is used in neck lift and platysmaplasty frequently[186]. The cervical branch arose from the cervico-facial division of the facial nerve, and gave 1-3 rami for supplying the platysma muscle[187]. The mean length and diameter was 40.55 ±12.78 and 0.83 ±0.15 mm, respectively[19]. In this study, the emerging point of the CB, it was measured and correlated to the IML on X-axis and the AML on Y-axis. The distance of the emerging point of the CB was 18.26 ±7.17 mm on X-axis, and -10.31 ±5.39 mm on Y-axis. Then, the CB branched into 1-6 twigs, and run inferomedially pass through the AML. In addition, the diameter of the twigs of the CB was 0.83 ±0.33 mm. Regarding the communication of the CB with sensory nerve, there are 1-3 points of communication of the CB with transverse cervical branch in 80.95%.

According to Salinas et al.[94] (2009), the cervical branches was investigated by using the cadaveric dissection and modified Sihler stain for observation the extramuscular and intramuscular rami in 20 and 8 specimens, respectively. The multiple cervical branches were found in 85% of the specimens, and communicate with the transverse cervical nerve. Moreover, it connected to the marginal mandibular branch in 35%, and co-innervated the depressor anguli oris with the marginal mandibular branch in 5%. Recently, Sinno and Thorne (2019) summarized that the CB gave only single rami to innervate the platysma mucle. Moreover, the CB medially traveled to the medial margin of the platysma muscle inferior to the thyroid cartilage[188].

According to Malins et al. (2022), the distances between the CB and anterior border of the SCM were measured at three levels. The result showed that the distance between the SCM and the CB at MA was 12.10 ±1.7 (10.10-15.40) mm, the narrowest

distance between the middle part of the SCM and the CB was 8.80 ±3.00 (5.60-12.20) mm, and most distances between the inferior part of the SCM and the CB at the entry point of the platysma muscle was 10.90 ±2.10 (7.90-16.70) mm[189]. The danger zone of the CB was described together with the MB. This zone is the area within 10 mm superior to the IML and 30 mm inferior to the IML. Moreover, the CB communicated with TCN and MB[190]. Moreover, the depth of the CB is essential for dissection at the mandible and anterior area to the SCM[191]. In the same way, Righini et al. presented that the CB was located posterior to the MB, and far from the MA was 8.3 (2.00-14.00) mm. Furthermore, the danger area of the MB and CB was the area between vertical lines from the MA approximately 30 mm, and the first premolar approximately 40 mm[192]. Additionally, the CB frequently communicated with the anterior rami of the superficial branch of the TCN [193].

The facial nerve trunk

In this study, the location of the branching point of the facial nerve trunk that divided into temporo-facial and cervico-facial divisions was 10.92 ±4.16 mm on the X-axis, and -20.39 ±4.41 mm correlated to the AIL. Moreover, the diameters of the temporo-facial and cervico-facial divisions were 3.65 ±0.94 mm, and 1.76 ±0.44 mm respectively. The branching point of the temporo-facial division was located at 14.41 ±3.91 mm on the X-axis and -9.84 ±4.91 mm on the Y-axis, while the branching point of the cervico-facial division was located at 10.45 ±4.31 mm on the X-axis and -31.43 ±7.20 mm on the Y-axis. According to Jose et al. (2021) reported that the mean distance between the bifurcation point of the facial nerve and the external auditory meatus was 17.90 ±2.70 (1.20, 2.30) mm, and the postglenoid tubercle off zygomatic arch and bifurcation point was 23.70 ±3.50 (2.10, 3.30) mm[134]. Moreover, Khoa et al. revealed that the FNT gave 2 divisions in 93.3% and 3 divisions in 6.7%. The mean number of the divisions was 2.1 divisions. Besides, the diameter of the FNT was 25 mm. The distance between the MA and the bifurcation point was 40.8 mm[194].

In histological study

In this study, the location of the TB was analyzed at the Frankfort's horizontal line. It was found that the most of the TB was located nearest TPF (71.43%) in medial portion, located at between TPE and S-DTF (85.71%) in middle portion, and nearest S-DTF (50.00%) in lateral portion. In the same, the TB was observed at lateral canthal level, and the result showed that the most of the TB was located nearest TPF (85.71%) in medial portion, located at between TPE and S-DTF (57.14%) in middle portion, and nearest TPF, between TPE and S-DTF, within TPF (14.29%) in lateral portion. According to the supraorbital rim and the upper eyebrow levels, the most location of the TB was located at nearest TPF.

Moreover, the number of the branches of the facial nerve was 5.64 ±1.22, and the ZB was found in 1.07 ±0.62 branches while the BB was found in 4.57 ±1.16 branches under the SMAS layer. In the mandibular and cervical region, the MB and CB were identified under the platysma muscle in 1.64 ±0.63 (1, 3) branches. Moreover, the MB is identified deep to the FA in 7.14%, superficial to the FA in 57.14%, and both deep and superficial to FA in 35.71%. In addition, the CB was found in 2.79 ±1.25 (1, 6) branches under the platysma muscle in cervical region.

According to Ghassemi et al. (2003), few branches of facial nerve were located deeply the subcutaneous tissue at forehead region and the parotid fascia at parotid region. Moreover, the branches of nerve were presented deeply the subcutaneous tissue at zygomatic area, while nerve branches located in the entire tela subcutanea for innervation the muscle at infraorbital area. In nasolabial fold, the most nerve was placed at the buccinator muscle.[34]

Later, the histological study was conducted in the nasolabial fold tissue of embalmed cadavers for identification the nerve branches. The result showed that the main branches of the facial nerve was found in the submuscular plane at the level of upper lip, therefore the area which superficial to the muscular plane was the safety layer for dissection in the nasolabial fold. Moreover, the nasolabial fold was the transition zone between type I and II of the SMAS. Type I SMAS was located laterally

to the nasolabial fold, and contained meshwork of the fibro-muscular portions surrounding fat pads. On the contrary, type II SMAS was positioned medially to the nasolabial fold, and indicated dense fibro-muscular septum and a few fat tissues[32].

According to Macchi et al. (2010), the facial tissue sections were stained with S100 at parotid, zygomatic, nasolabial fold and buccal, and cheek area for study the SMAS and nerve. The result demonstrated that in cheek area, the mean of the thickness of the subcutaneous tissue and SMAS were 5.45 ±0.1 mm, and 423 ±122 μm, respectively. Moreover, the diameter of the nervous bundles at cheek, nasolabial fold and buccal area, and parotid area 279.7 ±73.6, 169.5 ±23, 171.2 ±22.4 μm, respectively[31]. Recently, Amano, Naito and Matsuo (2020) examined seven areas of the face by using the H&E staining and scanning electron microscope (SEM) to observe characteristic of the facial soft tissue layers that consisted of forehead, lateral angle of the eye, infra orbital, buccal, inferior masseter, superior parotid, and nasolabial fold areas. The result revealed that the facial nerve was located within orbicularis oculi muscle at the lateral angle of the eye, both superficially and deeply to the zygomatic muscle at the buccal area, below to the inferior masseter muscle, superficially the superior parotid area, and both superficially and deeply to the orbicularis oculi muscle at the nasolabial fold areas[113].

The Sihler's staining technique

The intramuscular branches of the FN were investigated by using Sihler's staining technique. In this study, the intramuscular of the branch of the facial nerve can observe in frontalis, orbicularis oculi, zygomaticus major, orbicularis oris, depressor anguli oris and platysma muscles, excepted levator labii superioris muscle.

According to frontalis muscle, the most oft TB formed into the entangled meshwork at an inferior-lateral portion of the muscle, then this mesh work gave 2-4 long twigs traveled within inferior-medial portion of the frontalis muscle. In the contrast, the TB gave 2-3 long twigs within superior-lateral portion, while the small twig of the TB was found single or 2 twigs within superior-medial portion.

According to orbicularis oculi muscle, the TB formed into the entangled meshwork at superior-lateral portion of this muscle, while the ZB and BB gave the long twig to innervate orbicularis oculi at inferior-lateral portion. In addition, the BB travel medially to supply OOc muscle at superior-medial and inferior-medial portions.

According to the zygomaticus major muscle, the superior portion of the muscle was innervated by 2-5 short twigs of the upper and middle branches of the BB, whereas the inferior portion of the muscle was innervated by 1-2 long twigs of the middle and lower branches of the BB.

According to the depressor anguli oris muscle, the superior portion of the muscle was innervated by 2-3 short twigs of the middle branches of the BB, whereas the inferior portion of the muscle was innervated by 1-2 short twigs of the lower branches of the BB.

According to the platysma muscle, the CB is responsible for all portions of the muscle. In a medial portion of the platysma muscle, the CB gave 10-17 long twigs to innervate the muscle until the medial border of the muscle. In addition, the small twigs connected to each other branch within the platysma muscle.

In the orbicularis oris muscle, the MB gave long twig to response in inferior portion of the OOr. while the lower branch of the BB gave small twig to innervate in superior portion of the OOr.

For the facial study, the modified Sihler's stain was applied to observe both motor and sensory nerves of the face. According to Liu et al.[2] (2010), Sihler's stain was used to investigated the extramuscular and intramuscular pattern of the facial nerve in the face for understanding the deep detail of the facial nerve and protecting the nerve during intervention, and the communication between the facial nerve and the trigeminal nerve can wholly observe by using Sihler stain more than the cadaver dissection. On the other hand, the different of the motor nerve and sensory nerve can’t be separated in each other, when nerve was conducted by the Sihler stain, because the terminal branches in muscle or organ were stained by the same color. Moreover, the Sihler stain couldn’t explain the detail of the relationship of the nerve

and the structure. Accordingly, the nerve must be detected from main trunk to the distal branches.[2, 116]

In addition, Salinas et al.[94] (2009) investigated the extramuscular and intramuscular facial nerve distribution in eight cadavers. The result presented that the whole course of the marginal mandibular and cervical branches can observed by using the modified Sihler stain. It ran to supply the depressor anguli oris and platysma muscle, respectively. Furthermore, the CB communicated with the transverse cervical nerve posterior to the platysma muscle. Later, the communication between the BB and inferior palpebral twigs was observed by Yang et al. in 2014.[106]

A limitation of this study was the observation of the posterior auricular nerve. According to Smith and Ross (2012), the posterior auricular nerve is the first extratemporal branch of the FN. It gave a single ramus in 45.4%, two rami in 36.4%, and three rami in 18.2% after originating from the FNT approximately 5 mm from the stylomastoid foramen, and superficially located posterior to the external acoustic meatus. The posterior auricular nerve innervated the occipitalis and the auricular muscles, and receive sensory from skin of pinna and mastoid process. [195]. Moreover, Liu at al. (2018) explain that the posterior auricular nerve run parallel to the posterior auricular artery in 70% that can observe between the mastoid tip and the pinna[196]. Additionally, the mean length and diameter of the posterior auricular nerve were 27.11 ±5.02 mm and 0.85 ±0.20 mm, respectively[197]. Importantly, the anatomical landmark of the posterior auricular nerve was used to identify the FN for decreasing iatrogenic injury[198].

CHAPTER VI

CONCLUSION

The knowledges of the facial nerve had been investigated in several research. However, the facial nerve injury can occur during medical intervention or several cases. These complications bring about facial paresis and paralysis. In this study, the precise detail of the FN was investigated by the cadaveric dissection, histological study and Sihler's stain technique. These results provide the anatomical information that can both prevent and predict unexpected outcomes in the medical intervention in the face. In the clinical procedure, the physicians or technicians should be very careful when performing maxillofacial surgery depending on the regions of the face, since the branches of the facial nerve were distributed deep to the parotido-masseteric fascia, temporo-parietal fascia, superficial musculo-aponeurotic system, and platysma muscle depending on each branch of the facial nerve.

An illustration of the facial nerve was summarized in Figure 108. The TB gave 2-5 branches to emerge from the parotid gland, and the distance between the posterior rami and ATL was 10.62 mm. with a mean diameter of 0.93 mm at emerging point. Then, the TB gradually became superficially from FHL to the upper eyebrow under the TPF. After that, it formed into the entangled meshwork at a superior-lateral portion of the orbicularis oculi muscle and an inferior-lateral portion of the frontalis muscle. In addition, the ZB gave 1-3 branches to emerge from the parotid gland, and it was mostly located below the FHL within 20 mm approximately 70%.

The BB gave 2-5 branches to emerge from the parotid gland, then it passed through the vertical line perpendicular to the midpoint of the FHL. After that, the BB formed the ZBP superficial to the parotid duct at both the masseteric and buccal areas. Moreover, the medial part of the ZBP was observed at the nasolabial, far from the corner of the mouth and alar base approximately 30 and 20 mm, respectively. Furthermore, the superior part of the ZBP gave angular nerve at the area under the

LLS, then it perforated the LLS and run superior-medial crossed 1/3 laterally to the intercanthal line.

The MB and CB gave 1-2 branches to emerge from the parotid gland. After that, the MB crossed IML at the posterior crossing point within a distance of approximately 10 mm far from AML, whereas the distance between the anterior crossing point of the MB and AML was approximately 13 mm. Moreover, the crossing points of the MB correlated to AML were 6.25 ±5.60 mm, and -6.99 ±4.02 mm at superior and inferior to the IML. Then, the MB runs superficial to the FA in 48.28%, deep to the FA in 13.79%, both superficial and deep to the FA in 12.07%. Additionally, The CB gave 10-17 long twigs to innervate the platysma muscle until the medial border of the muscle, and the small twigs connected to each other branch within the platysma muscle also.

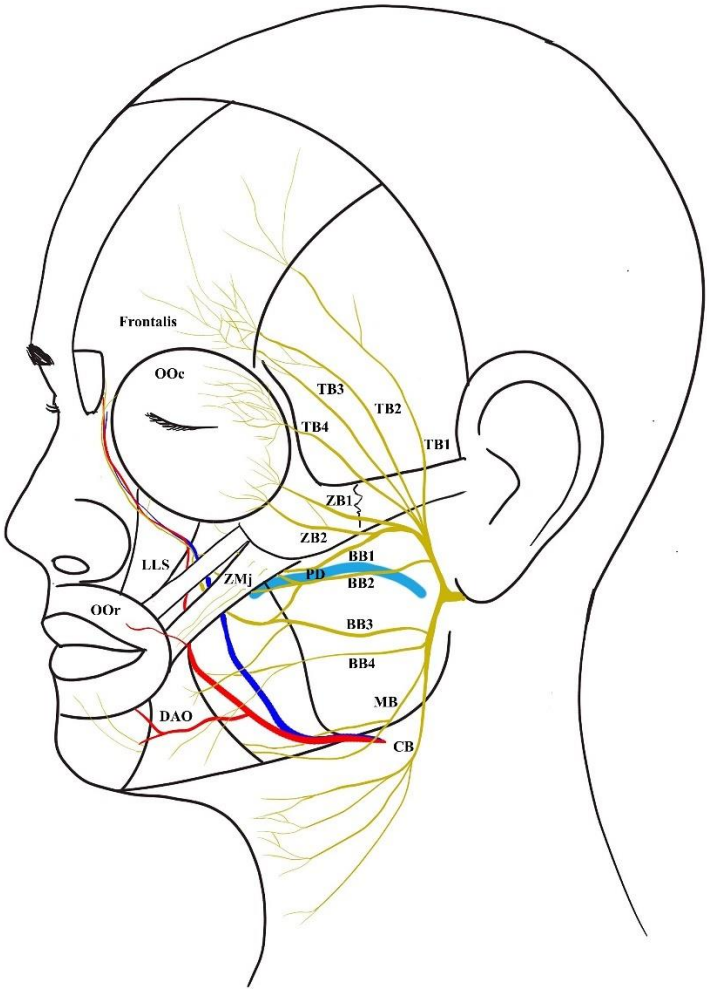

Figure 108 An illustration of the facial nerve

REFERENCES

1. Rocha FDS, Rocha CM, Viterbo F, Labbe D. Facelift and facial nerve injury: how to deal with? Rev Bras Cir Plást 2019;34(2):299-305.

2. Liu AT, Yu DZ, Chen G, Dang RS, Zhang YF, Zhang WJ, et al. Profiling of innervations of mimetic muscles in fresh human cadavers using a modified Sihler's technique. Muscle Nerve. 2010;42(1):88-94.

3. Toulgoat F, Sarrazinb JL, Benoudibac F, Pereond Y, Auffray-Calvier E, Daumas-Duport B, et al. Facial nerve: from anatomy to pathology. Diagnostic and Interventional Imaging 2013;94:1033-42.

4. Stankevicius D, Suchomlinov A. Variations in facial nerve branches and anatomical landmarks for Its trunk Identification: A pilot cadaveric study in the Lithuanian population. Cureus. 2019;11(11):e6100.

5. Owusu JA, Stewart CM, Boahene K. Facial nerve paralysis. Med Clin North Am. 2018;102(6):1135-43.

6. Davies J, Agur A, Fattah A. Anatomic landmarks for localisation of the branches of the facial nerve. OA Anatomy. 2013;1(4):33-41.

7. Gordin E, Lee TS, Ducic Y, Arnaoutakis D. Facial nerve trauma: evaluation and considerations in management. Craniomaxillofac Trauma Reconstr. 2015;8(1):1-13.

8. Sun Y, Liu L, Han Y, Xu L, Zhang D, Wang H. The role of great auricular-facial nerve neurorrhaphy in facial nerve damage. Int J Clin Exp Med. 2015;8(8):12970-6.

9. Khanfour AA, Metwally ESAM. Marginal mandibular branch of the facial nerve: An anatomical study. Alexandria Journal of Medicine. 2014;50:131-8.

10. Hwang K. Surgical Anatomy of the facial nerve relating to facial rejuvenation surgery. The Journal of craniofacial surgery. 2014;25:1476-81.

11. Al-Shaikh KMS, Mutwakil M, Ahmed M, Zaghloul S. Anatomical study of the facial Nerve. World Journal of Zoology. 2015;10(4):267-73.

12. Condie D, Tolkachjov SN. Facial Nerve Injury and Repair: A practical review for cutaneous surgery. Dermatologic surgery : official publication for American Society for Dermatologic Surgery [et al]. 2019;45(3):340-57.

13. Yang H-M, Yoo Y-B. Anatomy of the facial nerve at the condylar area: measurement study and clinical implications. ScientificWorldJournal. 2014;2014:473568.

14. Bloom JD, Immerman SB, Rosenberg DB. Face-lift complications. Facial plastic surgery : FPS. 2012;28(3):260-72.

15. Costa M, Maranhao-Filho PA, Santos IC, Luiz RR, Vincent MB. Parotidectomy-related facial nerve lesions: proposal for a modified Sunnybrook Facial Grading System. Arq Neuropsiquiatr. 2019;77(7):460-9.

16. Dhiwakar M, Khan ZA. Sacrificing the buccal branch of the facial nerve during parotidectomy. Head & neck. 2016;38(12):1821-5.

17. Langhals NB, Urbanchek MG, Ray A, Brenner MJ. Update in facial nerve paralysis: tissue engineering and new technologies. Curr Opin Otolaryngol Head Neck Surg. 2014;22(4):291-9.

18. Joseph ST, Sharankumar S, Sandya CJ, Sivakumar V, Sherry P, Krishnakumar T, et al. Easy and safe method for facial nerve identification in parotid surgery. J Neurol Surg B Skull Base. 2015;76(6):426-31.

19. Pascual PM, Maranillo E, Vazquez T, Simon de Blas C, Lasso JM, Sanudo JR. Extracranial course of the facial nerve revisited. Anat Rec (Hoboken). 2019;302(4):599-608.

20. Kwak HH, Park HD, Youn KH, Hu KS, Koh KS, Han SH, et al. Branching patterns of the facial nerve and its communication with the auriculotemporal nerve. Surg Radiol Anat. 2004;26(6):494-500.

21. Alomar OSK. New classification of branching pattern of facial nerve during parotidectomy: A cross sectional study. Ann Med Surg (Lond). 2021;62:190-6.

22. Hembd A, Nagarkar PA, Saba S, Wan D, Kutz JW, Isaacson B, et al. Facial nerve axonal analysis and anatomical localization in donor nerve: Optimizing Axonal Load for Cross-Facial Nerve Grafting in Facial Reanimation. Plastic and reconstructive surgery. 2017;139(1):177-83.

23. Hembd A, Nagarkar P, Perez J, Gassman A, Tolley P, Reisch J, et al. Correlation between facial nerve axonal load and age and its relevance to facial reanimation. Plastic and reconstructive surgery. 2017;139(6):1459-64.

24. Poblete T, Jiang X, Komune N, Matsushima K, Rhoton AL, Jr. Preservation of the nerves to the frontalis muscle during pterional craniotomy. J Neurosurg. 2015;122(6):1274-82.

25. Bernstein L, Nelson RH. Surgical anatomy of the extraparotid distribution of the facial nerve. Arch Otolaryngol. 1984;110(3):177-83.

26. Marur T, Tuna Y, Demirci S. Facial anatomy. Clin Dermatol. 2014;32(1):14-23.

27. von Arx T, Abdelkarim A, Lozanoff S. The face-a neurosensory perspective a literature review introduction. Swiss dent. 2017;127.

28. Mendelson BC, Jacobson SR. Surgical anatomy of the midcheek: facial layers, spaces, and the midcheek segments. Clinics in plastic surgery. 2008;35(3):395-404; discussion 393.

29. Mendelson B, Wong C, editors. I Aesthetic Surgery of the Face 6 Anatomy of the aging face2012.

30. Broughton M, Fyfe GM. The superficial musculoaponeurotic system of the face: a model explored. Anat Res Int. 2013;2013:794682.

31. Macchi V, Tiengo C, Porzionato A, Stecco C, Vigato E, Parenti A, et al. Histotopographic study of the fibroadipose connective cheek system. Cells Tissues Organs. 2010;191(1):47-56.

32. Sandulescu T, Spilker L, Rauscher D, Naumova EA, Arnold WH. Morphological analysis and three-dimensional reconstruction of the SMAS surrounding the nasolabial fold. Ann Anat. 2018;217:111-7.

33. Agarwal CA, Mendenhall SD, 3rd, Foreman KB, Owsley JQ. The course of the frontal branch of the facial nerve in relation to fascial planes: an anatomic study. Plastic and reconstructive surgery. 2010;125(2):532-7.

34. Ghassemi A, Prescher A, Riediger D, Axer H. Anatomy of the SMAS revisited. Aesthetic plastic surgery. 2003;27(4):258-64.

35. Drzezo. The anatomy of the face, mouth, and jaws 2016 [Available from: https://pocketdentistry.com/the-anatomy-of-the-face-mouth-and-jaws/.

36. Divi V, Deschler DG. Re-animation and rehabilitation of the paralyzed face in head and neck cancer patients. Clinical anatomy (New York, NY). 2012;25(1):99-107.

37. Ton G, Lee L-W, Chen Y-H, Tu C-H, Lee Y-CJCtim. Effects of laser acupuncture in a patient with a 12-year history of facial paralysis: A case report. 2019;43:306-10.

38. Rozen SM. 1.5 - Traumatic Facial Nerve Injury. In: Dorafshar AH, Rodriguez ED, Manson PN, editors. Facial Trauma Surgery. London: Elsevier; 2020. p. 58-78.

39. Davies J, Al-Hassani F, Kannan R. Facial nerve disorder: a review of the literature. nternational Journal of Surgery Oncology. 2018;3:e65.

40. Figueiredo R, Falcão V, Pinto MJ, Ramalho C. Peripheral facial paralysis as presenting symptom of COVID-19 in a pregnant woman. BMJ Case Rep. 2020;13(8).

41. Kerstens J, Deschuytere L, Schotsmans K, Maréchal E. Bilateral peripheral facial palsy following asymptomatic COVID-19 infection: a case report. Acta Neurologica Belgica. 2021;121(3):815-6.

42. Burakgazi AZ, Schmidley JW. A rare cause of bilateral facial palsy. 2016;4(2):62-4.

43. Alanazi WL, El-Fetoh NMA, Alanazi SL, Alkhidhr MA, Alanazi MA, Alonazi DS, et al. Profile of facial palsy in Arar, northern Saudi Arabia. Electron Physician. 2017;9(10):5596-602.

44. Gandolfi MM, Slattery W, 3rd. Parotid gland tumors and the facial nerve. Otolaryngologic clinics of North America. 2016;49(2):425-34.

45. Basnayake B, Wazil AWM, Nanayakkara N, Mahanama R, Premathilake PNS, Galkaduwa K. Ethylene glycol intoxication following brake fluid ingestion complicated with unilateral facial nerve palsy: a case report. J Med Case Rep. 2019;13(1):203.

46. Zaloga GP, Deal J, Spurling T, Richter J, Chernow B. Unusual manifestations of arsenic intoxication. The American Journal of the Medical Sciences. 1985;289(5):210-4.

47. Kim SY, Min C, Choi J, Park B, Choi HG. Air pollution by NO(2) is associated with the risk of Bell's palsy: A nested case-controlled study. Sci Rep. 2020;10(1):4221.

48. Zourntou S-E, Makridis KG, Tsougos C-I, Skoulakis C, Vlychou M, Vassiou A. Facial nerve: A review of the anatomical, surgical landmarks and its iatrogenic injuries. Injury. 2021;52(8):2038-48.

49. Devi KVNG, Toleti S. A study of variations in the branching pattern of facial nerve in the face. International Journal of Research in Medical Sciences. 2015;3(2):466-9.

50. Nogueira RV, Vasconcelos BC. Facial nerve injury following surgery for the treatment of ankylosis of the temporomandibular joint. Med Oral Patol Oral Cir Bucal. 2007;12(2):E160-5.

51. Hohman MH, Bhama PK, Hadlock TA. Epidemiology of iatrogenic facial nerve injury: a decade of experience. Laryngoscope. 2014;124(1):260-5.

52. Singh M. The retromandibular transparotid approach for reduction and internal fixation of mandibular condylar fractures2020.

53. Zhang W, Xu L, Luo T, Wu F, Zhao B, Li X. The etiology of Bell's palsy: a review. Journal of Neurology. 2020;267(7):1896-905.

54. Eviston TJ, Croxson GR, Kennedy PGE, Hadlock T, Krishnan AV. Bell's palsy: aetiology, clinical features and multidisciplinary care. 2015;86(12):1356-61.

55. Azizzadeh B. Masseter to facial nerve transfer 2021 [Available from: https://www.facialparalysisinstitute.com/treatments/masseter-facial-nerve-transfer/.

56. Yoshioka N. Hypoglossal-facial side-to-end neurorrhaphy with concomitant masseteric-zygomatic nerve branch coaptation and muscle transfer for facial reanimation: technique and case Report. Operative Neurosurgery. 2020;19(3):E230-E5.

57. Azizzadeh B. Gracilis free flap - Gracilis muscle transplant 2021 [Available from: https://www.facialparalysisinstitute.com/treatments/gracilis-muscle-transplant/.

58. Oh TS, Kim HB, Choi JW, Jeong WS. Facial reanimation with masseter nerve-innervated free gracilis muscle transfer in established facial palsy patients. Arch Plast Surg. 2019;46(2):122-8.

59. Panossian A. Lengthening temporalis myoplasty for single-stage smile reconstruction in children with facial paralysis. Plastic and reconstructive surgery. 2016;137.

60. Heydenrych I. The treatment of facial asymmetry with botulinum toxin: current concepts, guidelines, and future trends. Indian Journal of Plastic Surgery. 2020;53.

61. Nduka C, Cooper L, Lui M. Botulinum toxin treatment for facial palsy: A systematic review. Journal of Plastic Reconstructive & Aesthetic Surgery. 2017;70.

62. de Sanctis Pecora C, Shitara D. Botulinum toxin type A to improve facial symmetry in facial palsy: a practical guideline and clinical experience. 2021;13(2):159.

63. Sadiq SA, Khwaja S, Saeed SR. Botulinum toxin to improve lower facial symmetry in facial nerve palsy. Eye. 2012;26(11):1431-6.

64. Farahvash MR, Yaghoobi A, Farahvash B, Farahvash Y, Hadadi Abiyaneh S. The extratemporal facial nerve and its branches: analysis of 42 hemifacial dissections in fresh Persian (Iranian) cadavers. Aesthetic surgery journal. 2013;33(2):201-8.

65. Takezawa K, Townsend G, Ghabriel M. The facial nerve: anatomy and associated disorders for oral health professionals. Odontology. 2018;106(2):103-16.

66. Drake RL, Vogl W, Mitchell AWM, Gray H, Gray H. Gray's anatomy for students. Philadelphia, PA: Churchill Livingstone/Elsevier; 2010.

67. Pather N, Osman M. Landmarks of the facial nerve: implications for parotidectomy. Surg Radiol Anat. 2006;28(2):170-5.

68. Kriengkraikasem K, Kowitwibool K, Chanpoo M. Variation of the great auricular nerve and prediction of the facial nerve trunk size. Plast Reconstr Surg Glob Open. 2018;6(12):e2000.

69. Thuku FM, Butt F, Guthua SW, Chindia M. An anatomic study of the facial nerve trunk and branching pattern in an African population. Craniomaxillofac Trauma Reconstruction Open. 2018;2:e31–e7.

70. Emam H, Jatana C, Ness GM. Facial nerve injury. In: Bouloux GF, editor. Complications of Temporomandibular Joint Surgery. Cham: Springer International Publishing; 2017. p. 57-74.

71. Miloro M, Redlinger S, Pennington DM, Kolodge T. In situ location of the temporal branch of the facial nerve. Journal of oral and maxillofacial surgery : official journal of the American Association of Oral and Maxillofacial Surgeons. 2007;65(12):2466-9.

72. Ness GM. Arthroplasty and discectomy of the temporomandibular joint. Atlas Oral Maxillofac Surg Clin North Am. 2011;19(2):177-87.

73. Rea PM, McGarry G, Shaw-Dunn J. The precision of four commonly used surgical landmarks for locating the facial nerve in anterograde parotidectomy in humans. Ann Anat. 2010;192(1):27-32.

74. Saha S, Pal S, Sengupta M, Chowdhury K, Saha VP, Mondal L. Identification of facial nerve during parotidectomy: a combined anatomical & surgical study. Indian J Otolaryngol Head Neck Surg. 2014;66(1):63-8.

75. Ullah I, Khan SA, Iqbal M, Hussain G. Tragal pointer as a surgical landmark for the identification of facial nerve trunk in parotidectomy: our experience. Journal of Saidu Medical College 2017;7(1).

76. Witt RL, Weinstein GS, Rejto LK. Tympanomastoid suture and digastric muscle in cadaver and live parotidectomy. Laryngoscope. 2005;115(4):574-7.

77. Al-Qahtani KH, AlQahtani FM, Muqat MM, AlQahtani MS, Al-Qannass AM, Islam T, et al. A new landmark for the identification of the facial nerve during parotid surgery: A cadaver study. Laryngoscope Investig Otolaryngol. 2020;5(4):689-93.

78. Wong DS. Surface landmarks of the facial nerve trunk: a prospective measurement study. ANZ J Surg. 2001;71(12):753-6.

79. de Ru JA, van Benthem PP, Bleys RL, Lubsen H, Hordijk GJ. Landmarks for parotid gland surgery. J Laryngol Otol. 2001;115(2):122-5.

80. Myint K, Azian AL, Khairul FA. The clinical significance of the branching pattern of the facial nerve in Malaysian subjects. Med J Malaysia. 1992;47(2):114-21.

81. Hendi A. Transient buccal nerve paresis. Dermatologic surgery : official publication for American Society for Dermatologic Surgery [et al]. 2008;34(2):258-60.

82. Katz AD, Catalano P. The clinical significance of the various anastomotic branches of the facial nerve. Report of 100 patients. Arch Otolaryngol Head Neck Surg. 1987;113(9):959-62.

83. Kopuz C, Turgut S, Yavuz S, Ilgi S. Distribution of facial nerve in parotid gland: analysis of 50 cases. Okajimas Folia Anat Jpn. 1994;70(6):295-9.

84. Hwang K, Kim YJ, Chung IH. Innervation of the corrugator supercilii muscle. Annals of plastic surgery. 2004;52(2):140-3.

85. Caminer DM, Newman MI, Boyd JB. Angular nerve: new insights on innervation of the corrugator supercilii and procerus muscles. Journal of plastic, reconstructive & aesthetic surgery : JPRAS. 2006;59(4):366-72.

86. Lettieri S. Frontal branch of the facial nerve: galeal temporal relationship. Aesthetic surgery journal. 2008;28(2):143-6.

87. Pankratz J, Baer J, Mayer C, Rana V, Stephens R, Segars L, et al. Depth transitions of the frontal branch of the facial nerve: Implications in SMAS rhytidectomy. JPRAS Open. 2020;26:101-8.

88. Bonnecaze Gd, Chaput B, Filleron T, Al Hawat A, Vergez S, Chaynes P. The frontal branch of the facial nerve: can we define a safety zone? Surg Radiol Anat. 2015;37(5):499-506.

89. Yoshioka N, Rhoton Jr MDAL. Atlas of the facial nerve and related structures2015.

90. Erbil KM, Uz A, Hayran M, Mas N, Senan S, Tuncel M. The relationship of the parotid duct to the buccal and zygomatic branches of the facial nerve; an anatomical study with parameters of clinical interest. Folia Morphol (Warsz). 2007;66(2):109-14.

91. Dorafshar AH, Borsuk DE, Bojovic B, Brown EN, Manktelow RT, Zuker RM, et al. Surface anatomy of the middle division of the facial nerve: Zuker's point. Plastic and reconstructive surgery. 2013;131(2):253-7.

92. Saylam C, Ucerler H, Orhan M, Ozek C. Anatomic landmarks of the buccal branches of the facial nerve. Surg Radiol Anat. 2006;28(5):462-7.

93. Balagopal PG, George NA, Sebastian P. Anatomic variations of the marginal mandibular nerve. Indian journal of surgical oncology. 2012;3(1):8-11.

94. Salinas NL, Jackson O, Dunham B, Bartlett SP. Anatomical dissection and modified Sihler stain of the lower branches of the facial nerve. Plastic and reconstructive surgery. 2009;124(6):1905-15.

95. Hwang K, Jin S, Park JH, Chung IH. Innervation of the procerus muscle. 2006;17(3):484-6.

96. Yang NZ, Wang B, Wang ZJ, Zhang C, Ma XK, Ma Y, et al. [Angular nerve of facial nerve: anatomic research]. Zhonghua Zheng Xing Wai Ke Za Zhi. 2010;26(3):221-5.

97. Thomas Von Arx T, Nakashima MJ, Lozanoff S. The face - a musculoskeletal perspective. A literature review. Swiss Dent J. 2018;128(9):678-88.

98. Spiegel JH, DeRosa J. The anatomical relationship between the orbicularis oculi muscle and the levator labii superioris and zygomaticus muscle complexes. Plastic and reconstructive surgery. 2005;116(7):1937-42; discussion 43-4.

99. Shim KS, Hu KS, Kwak HH, Youn KH, Koh KS, Fontaine C, et al. An anatomical study of the insertion of the zygomaticus major muscle in humans focused on the muscle arrangement at the corner of the mouth. Plastic and reconstructive surgery. 2008;121(2):466-73.

100. Kehrer A, Engelmann S, Bauer R, Taeger C, Grechenig S, Kehrer M, et al. The nerve supply of zygomaticus major: Variability and distinguishing zygomatic from buccal facial nerve branches. Clinical anatomy (New York, NY). 2018;31(4):560-5.

101. Hu KS, Jin GC, Youn KH, Kwak HH, Koh KS, Fontaine C, et al. An anatomic study of the bifid zygomaticus major muscle. The Journal of craniofacial surgery. 2008;19(2):534-6.

102. Jirawatnotai S, Kaewpichai K, Tirakotai W, Mothong W, Kaewsema A, Sriswadpong P. Nerve to the zygomaticus major muscle for facial reanimation surgery: a cadaveric study for branching patterns and axonal count. Asian J Neurosurg. 2020;15(3):516-20.

103. Elvan O, Bobus Ors A, Tezer MS. Anatomical Evaluation of Zygomaticus Major Muscle With Relation to Orbicularis Oculi Muscle and Parotid Duct. The Journal of craniofacial surgery. 2020;31(6):1844-7.

104. Kim HS, Pae C, Bae JH, Hu KS, Chang BM, Tansatit T, et al. An anatomical study of the risorius in Asians and its insertion at the modiolus. Surg Radiol Anat. 2015;37(2):147-51.

105. Amar RE, Fox DM, Balin A. Cannulation and injection of the muscles of facial expression: a cadaver study. Dermatologic surgery : official publication for American Society for Dermatologic Surgery [et al]. 2010;36(3):331-8.

106. Yang HM, Won SY, Lee YI, Kim HJ, Hu KS. The Sihler staining study of the infraorbital nerve and its clinical complication. The Journal of craniofacial surgery. 2014;25(6):2209-13.

107. Hwang K, Han JY, Battuvshin D, Kim DJ, Chung IH. Communication of infraorbital nerve and facial nerve: anatomic and histologic study. The Journal of craniofacial surgery. 2004;15(1):88-91.

108. Cobo JL, Sole-Magdalena A, Menendez I, Vicente JCd, Vega JA. Connections between the facial and trigeminal nerves: Anatomical basis for facial muscle proprioception. JPRAS Open. 2017;12:9-18.

109. Cobo JL, Sole-Magdalena A, Menendez I, Vicente JCd, Vega JA. Connections between the facial and trigeminal nerves: Anatomical basis for facial muscle proprioception. JPRAS Open 2017;12:9-18.

110. Tansatit T, Phanchart P, Chinnawong D, Apinuntrum P, Phetudom T, Sahraoui YM. A cadaveric study of the communication patterns between the buccal trunks of

the facial nerve and the infraorbital nerve in the midface. The Journal of craniofacial surgery. 2016;27(1):214-8.

111. Shoja MM, Oyesiku NM, Griessenauer CJ, Radcliff V, Loukas M, Chern JJ, et al. Anastomoses between lower cranial and upper cervical nerves: a comprehensive review with potential significance during skull base and neck operations, part I: trigeminal, facial, and vestibulocochlear nerves. Clinical anatomy (New York, NY). 2014;27(1):118-30.

112. Odobescu A, Williams HB, Gilardino MS. Description of a communication between the facial and zygomaticotemporal nerves. Journal of plastic, reconstructive & aesthetic surgery : JPRAS. 2012;65(9):1188-92.

113. Amano K, Naito M, Matsuo M. Morphological study of human facial fascia and subcutaneous tissue structure by region through SEM observation. Tissue and Cell. 2020;67:101437.

114. Mu L, Sanders I. Sihler's whole mount nerve staining technique: a review. Biotech Histochem. 2010;85(1):19-42.

115. Won SY, Kim DH, Yang HM, Park JT, Kwak HH, Hu KS, et al. Clinical and anatomical approach using Sihler's staining technique (whole mount nerve stain). Anatomy & cell biology. 2011;44(1):1-7.

116. Hwang K, Yang SC, Song JS. Communications between the trigeminal nerve and the facial nerve in the face: a systematic review. The Journal of craniofacial surgery. 2015;26(5):1643-6.

117. Rodriguez H, Espinoza-Navarro O, Silva I, Quiroz P, Arriaza C, Sanchez C, et al. Histological description of the interaction between muscle fibers and connective tissue of the fascia of the human trapezius muscle. Int J Morphol. 2011;29(1):299-303.

118. Calvi ENdC, Nahas FX, Barbosa MV, Calil JA, Ihara SSM, Silva MdS, et al. An experimental model for the study of collagen fibers in skeletal muscle. Acta Cirúrgica Brasileira. 2012;27(10):681-6.

119. Eren SB, Dogan R, Ozturan O, Veyseller B, Hafiz AM. How deleterious is facial nerve dissection for the facial nerve in parotid surgery: An Electrophysiological Evaluation. The Journal of craniofacial surgery. 2017;28(1):56-60.

120. Lam AQ, Chung TTP, Viet LT, Quang HD, Van DT, Fox AJ. The anatomic landmark approach to extratemporal facial nerve repair in facial trauma. Cureus. 2022;14(3):e22787.

121. Beutner D, Grosheva M. Reconstruction of complex defects of the extracranial facial nerve: technique of "the trifurcation approach". European archives of oto-rhino-laryngology : official journal of the European Federation of Oto-Rhino-Laryngological Societies (EUFOS) : affiliated with the German Society for Oto-Rhino-Laryngology - Head and Neck Surgery. 2019;276(6):1793-8.

122. Kochhar A, Larian B, Azizzadeh B. Facial nerve and parotid gland anatomy. Otolaryngologic clinics of North America. 2016;49(2):273-84.

123. Suzuki K, Iwai H, Yagi M, Fujisawa T, Kanda A, Konishi M, et al. Indications for partial parotidectomy using retrograde dissection of the marginal mandibular branch of the facial nerve for benign tumours of the parotid gland. The British journal of oral & maxillofacial surgery. 2018;56(8):727-31.

124. Lin B, Lu X, Shan X, Zhang L, Cai Z. Preoperative percutaneous nerve mapping of the mandibular marginal branch of the facial nerve. The Journal of craniofacial surgery. 2015;26(2):411-4.

125. Ruewe M, Engelmann S, Huang CW, Klein SM, Anker AM, Lamby P, et al. Microanatomy of the frontal branch of the facial nerve: the role of nerve caliber and axonal capacity. Plastic and reconstructive surgery. 2021;148(6):1357-65.

126. Manosalva RE, Dyckman D, Melzer JM. Delayed facial nerve palsy after open reduction of an isolated zygomaticomaxillary complex fracture. The Journal of craniofacial surgery. 2016;27(4):e392-4.

127. Swanson E. Clinical evaluation of 225 sub-SMAS facelifts with no temporal incision. Plastic and reconstructive surgery Global open. 2020;8(2):e2640.

128. Azizzadeh B, Frisenda JL. Surgical management of postparalysis facial palsy and synkinesis. Otolaryngologic clinics of North America. 2018;51(6):1169-78.

129. Kleinberger AJ, Jumaily J, Spiegel JH. Safety of modified coronal approach with dissection deep to temporalis fascia for facial nerve preservation. Otolaryngology--head and neck surgery : official journal of American Academy of Otolaryngology-Head and Neck Surgery. 2015;152(4):655-60.

130. Schmidt BL, Pogrel MA, Hakim-Faal Z. The course of the temporal branch of the facial nerve in the periorbital region. Journal of oral and maxillofacial surgery : official journal of the American Association of Oral and Maxillofacial Surgeons. 2001;59(2):178-84.

131. Domico A, Kurian S, Davis M, Fazi A, McClellan WT. Unilateral forehead paralysis following operative repair of facial trauma: a case study and review of the literature. The West Virginia medical journal. 2015;111(5):36-8.

132. Gülbitti HA, van der Lei B. Hering's law of the frontal facial branch. 2018;142(6):991e-2e.

133. Sihag R, Gupta S, Sahni D, Aggarwal A. Frontotemporal branch of the facial nerve and fascial layers in the temporal region: a cadaveric study to define a safe dissection plane. 2020;68(6):1313-20.

134. Jose A, Yadav P, Roychoudhury A, Bhutia O, Millo T, Pandey RM. Cadaveric study of topographic anatomy of temporal and marginal mandibular branches of the facial nerve in relation to temporomandibular joint surgery. Journal of oral and maxillofacial surgery : official journal of the American Association of Oral and Maxillofacial Surgeons. 2021;79(2):343.e1-.e11.

135. Lei T, Xu DC, Gao JH, Zhong SZ, Chen B, Yang DY, et al. Using the frontal branch of the superficial temporal artery as a landmark for locating the course of the temporal branch of the facial nerve during rhytidectomy: an anatomical study. Plastic and reconstructive surgery. 2005;116(2):623-9; discussion 30.

136. Trussler AP, Stephan P, Hatef D, Schaverien M, Meade R, Barton FE. The frontal branch of the facial nerve across the zygomatic arch: anatomical relevance of the high-SMAS technique. Plastic and reconstructive surgery. 2010;125(4):1221-9.

137. Barton FE, Jr. Aesthetic surgery of the face and neck. Aesthetic surgery journal. 2009;29(6):449-63; quiz 64-6.

138. Tonnard P, Verpaele A. The MACS-lift short scar rhytidectomy. Aesthetic surgery journal. 2007;27(2):188-98.

139. Samaniego E, Prada C, Rodríguez-Prieto M. [Surgical planes of the head and neck]. Actas dermo-sifiliograficas. 2011;102(3):167-74.

140. Green Sanderson K, Conti A, Colussi M, Connolly C. A simple clinical application for locating the frontotemporal branch of the facial nerve using the zygomatic arch and the tragus. Aesthetic surgery journal. 2020;40(5):Np223-np7.

141. Shin KJ, Shin HJ, Lee SH, Koh KS, Song WC. Surgical anatomy of the superficial temporal artery to prevent facial nerve injury during arterial biopsy. Clinical anatomy (New York, NY). 2018;31(4):608-13.

142. Voth H, Grunewald S, Miller B, Simon JC, Kendler M. Direct brow lift for the correction of unilateral brow ptosis due to frontal branch injury following cutaneous surgery in the frontotemporal region. Journal der Deutschen Dermatologischen Gesellschaft = Journal of the German Society of Dermatology : JDDG. 2015;13(12):1298-301.

143. Elvan Ö, Kara AB, Tezer MS, Aktekin M. The relationship of the temporal branch of the facial nerve to the fascial planes of temporal region in human fetuses. The Journal of craniofacial surgery. 2017;28(8):2151-4.

144. Spiriev T, Ebner FH, Hirt B, Shiozawa T, Gleiser C, Tatagiba M, et al. Fronto-temporal branch of facial nerve within the interfascial fat pad: is the interfascial dissection really safe? Acta neurochirurgica. 2016;158(3):527-32.

145. Ye P, Feng XL, Yang ZH, Li GP, Sun J, Wu HX, et al. The anatomy of the temporal and zygomatic branches of the facial nerve: Application to Crow's Feet Wrinkles. The Journal of craniofacial surgery. 2021;32(3):878-82.

146. Yang HJ, Gil YC, Lee HY. Anatomy of facial and trigeminal nerve branches associated with the corrugator supercilii muscle: microdissection and modified Sihler staining. Dermatologic surgery : official publication for American Society for Dermatologic Surgery [et al]. 2015;41(1):87-93.

147. Choi Y, Kim IB. Distribution of the laterally supplying facial nerve to the orbicularis oculi muscle. Aesthetic surgery journal. 2021;41(2):161-9.

148. Yang M, Gu Y, Wang D, Li J, Sun J, Lv Q, et al. Liposuction of the zygomatic arch area: a novel concept to improve the midface contour. Aesthetic plastic surgery. 2022.

149. Lee JY, Kim JN, Yoo JY, Shin KJ, Song WC, Koh KS, et al. Topographic relationships between the transverse facial artery, branches of the facial nerve, and

the parotid duct in the lateral midface in a Korean population. Annals of plastic surgery. 2014;73(3):321-4.

150. Kehrer A, Engelmann S, Ruewe M, Geis S, Taeger C, Kehrer M, et al. Anatomical study of the zygomatic and buccal branches of the facial nerve: Application to facial reanimation procedures. Clinical anatomy (New York, NY). 2019;32(4):480-8.

151. Poddar R, Bhattacharya A, Sinha I, Ghosal AK. An Anatomical study for localisation of Zygomatic branch of Facial nerve and Masseteric nerve - An aid to nerve coaptation for facial reanimation surgery: A cadaver based study in Eastern India. Indian journal of plastic surgery : official publication of the Association of Plastic Surgeons of India. 2017;50(1):74-8.

152. Biglioli F, Kutanovaite O, Rabbiosi D, Colletti G, Mohammed MAS, Saibene AM, et al. Surgical treatment of synkinesis between smiling and eyelid closure. Journal of cranio-maxillo-facial surgery : official publication of the European Association for Cranio-Maxillo-Facial Surgery. 2017;45(12):1996-2001.

153. Lam AQ, Tran Phan Chung T, Tran Viet L, Do Quang H, Tran Van D, Fox AJ. The anatomic landmark approach to extratemporal facial nerve repair in facial trauma. Cureus. 2022;14(3):e22787.

154. Doumit G, Gharb BB, Rampazzo A, McBride J, Papay F, Zins J, et al. Surgical anatomy relevant to the transpalpebral subperiosteal elevation of the midface. Aesthetic surgery journal. 2015;35(4):353-8.

155. Freed B, Coker C, Steele R, Marolt C, Motzko M, Creamer BA, et al. Communicating branches of the facial nerve: descriptions and clinical considerations. Aesthetic surgery journal. 2022;42(6):Np373-np82.

156. Wong CH, Mendelson B. Facial soft-tissue spaces and retaining ligaments of the midcheek: defining the premaxillary space. Plastic and reconstructive surgery. 2013;132(1):49-56.

157. Bendella H, Spacca B, Rink S, Stoffels HJ, Nakamura M, Scaal M, et al. Anastomotic patterns of the facial parotid plexus (PP): A human cadaver study. Annals of anatomy = Anatomischer Anzeiger : official organ of the Anatomische Gesellschaft. 2017;213:52-61.

158. Hovland N, Phuong A, Lu GN. Anatomy of the facial nerve. Operative Techniques in Otolaryngology-Head and Neck Surgery. 2021;32(4):190-6.

159. Surek CC, Kochuba AL, Said SA, Cho KH, Swanson M, Duraes E, et al. External approach to buccal fat excision in facelift: anatomy and technique. Aesthetic surgery journal. 2021;41(5):527-34.

160. Martínez Pascual P, Maranillo E, Vázquez T, Simon de Blas C, Lasso JM, Sañudo JR. Extracranial course of the facial nerve revisited. Anatomical record (Hoboken, NJ : 2007). 2019;302(4):599-608.

161. Eltohami Y, Huang S-F, Suleiman A. Origin of the buccal branch of facial nerve and anastomosis of the facial nerve branches. Journal of Clinical Case Studies. 2019;4:dx.

162. Ahmed M, Alshaikh K, Mutwakil M, Zaghloul S. Anatomical study of the facial nerve. 2015;10:267-73.

163. Thuku FM, Butt F, Guthua SW, Chindia M. An anatomic study of the facial nerve trunk and branching pattern in an African population. Craniomaxillofacial Trauma & Reconstruction Open. 2018;2(1):s-0038-1669465.

164. Tsai CH, Ting CC, Wu SY, Chiu JY, Chen H, Igawa K, et al. Clinical significance of buccal branches of the facial nerve and their relationship with the emergence of Stensen's duct: An anatomical study on adult Taiwanese cadavers. Journal of cranio-maxillo-facial surgery : official publication of the European Association for Cranio-Maxillo-Facial Surgery. 2019;47(11):1809-18.

165. Talmor G, Trang A, Ahadiat O, Paskhover B, Wysong A. Anatomic danger zones of the head and neck. Dermatologic surgery : official publication for American Society for Dermatologic Surgery [et al]. 2020;46(12):1549-59.

166. Yang H-M, Hu K, Kim H-J. Anatomical and functional consideration of the trigemino-facial nervous communication and facial expresssion muscles. Korean Journal of Physical Anthropology. 2013;26:1.

167. Sindel A, Özalp Ö, Yıldırımyan N, Oğuz N, Sindel M, Llankovan V. Evaluation of the course of the marginal mandibular branch of the facial nerve: a fresh cadaveric study. The British journal of oral & maxillofacial surgery. 2021;59(2):179-83.

168. Kikuoka Y, Kawata R, Higashino M, Terada T, Haginomori SI. Operative technique for benign submandibular gland mass without identifying the mandibular branch of the facial nerve. Auris, nasus, larynx. 2018;45(6):1221-6.

169. Thomas RJ, Whittaker J, Pollock J. Discerning a smile - The intricacies of analysis of post-neck dissection asymmetry. American journal of otolaryngology. 2022;43(1):103271.

170. Charafeddine AH, Drake R, McBride J, Zins JE. Facelift: history and anatomy. Clinics in plastic surgery. 2019;46(4):505-13.

171. Mohan R, Brown EN, Borsuk DE, Christy MR, Bojovic B, Rodriguez ED, et al. Revisiting the anatomic relationship of the marginal mandibular nerve and the posterior facial vein: a cadaveric study. Annals of plastic surgery. 2014;72(4):467-8.

172. Touré S, Vacher C, Bertrand JC. [Anatomy of the marginal mandibular branch of the facial nerve]. Revue de stomatologie et de chirurgie maxillo-faciale. 2004;105(3):149-52.

173. Yang HM, Kim HJ, Park HW, Sohn HJ, Ok HT, Moon JH, et al. Revisiting the topographic anatomy of the marginal mandibular branch of facial nerve relating to the surgical approach. Aesthetic surgery journal. 2016;36(9):977-82.

174. Batra AP, Mahajan A, Gupta K. Marginal mandibular branch of the facial nerve: An anatomical study. Indian journal of plastic surgery : official publication of the Association of Plastic Surgeons of India. 2010;43(1):60-4.

175. Gormley M, Philip J, James R, Heaton M. A rare fourth branch of the marginal mandibular nerve. Journal of Oral and Maxillofacial Surgery. 2018;76(2):460-1.

176. Touré S, Vacher C, Bertrand JC. Étude anatomique du rameau marginal de la mandibule du nerf facial. Revue de Stomatologie et de Chirurgie Maxillo-faciale. 2004;105(3):149-52.

177. Touré G, Tran de Fremicourt MK, Randriamanantena T, Vlavonou S, Priano V, Vacher C. Vascular and nerve relations of the marginal mandibular nerve of the face: anatomy and clinical relevance. Plastic and reconstructive surgery. 2019;143(3):888-99.

178. Baur DA, Kaiser AC, Leech BN, Landers MA, Altay MA, Quereshy F. The marginal mandibular nerve in relation to the inferior border of the mandible. Journal of oral

and maxillofacial surgery : official journal of the American Association of Oral and Maxillofacial Surgeons. 2014;72(11):2221-6.

179. Marolt C, Freed B, Coker C, Steele R, Johnson K, Arellanes R, et al. Key anatomical clarifications for the marginal mandibular branch of the facial nerve: clinical significance for the plastic surgeon. Aesthetic surgery journal. 2021;41(11):1223-8.

180. Mandlik V, Ruewe M, Engelmann S, Geis S, Taeger C, Kehrer M, et al. Significance of the marginal mandibular branch in relation to facial palsy reconstruction: assessment of microanatomy and macroanatomy including axonal load in 96 facial halves. Annals of plastic surgery. 2019;83(6):e43-e9.

181. Brennan PA, Mak J, Massetti K, Parry DA. Communication between the transverse cervical nerve (C2,3) and marginal mandibular branch of the facial nerve: a cadaveric and clinical study. The British journal of oral & maxillofacial surgery. 2019;57(3):232-5.

182. Rossell-Perry P. The marginal branch triangle: Anatomic reference for its location and preservation during cosmetic surgery. Journal of plastic, reconstructive & aesthetic surgery : JPRAS. 2016;69(3):387-94.

183. Kudva A, Babu K, Saha M, Puri S, Pandey L, Gunashekhar S. Marginal mandibular nerve - a wandering enigma and ways to tackle it. The Egyptian Journal of Otolaryngology. 2021;37(1):74.

184. Brennan PA, Elhamshary AS, Alam P, Anand R, Ammar M. Anastomosis between the transverse cervical nerve and marginal mandibular nerve: how often does it occur? The British journal of oral & maxillofacial surgery. 2017;55(3):293-5.

185. Werner C, D'Antoni AV, Iwanaga J, Watanabe K, Dumont AS, Tubbs RS. A comprehensive review of the great auricular nerve graft. Neurosurgical review. 2021;44(4):1987-95.

186. Pessa JE. Commentary on: cervical branch of facial nerve: an explanation for recurrent platysma bands following necklift and platysmaplasty. Aesthetic surgery journal. 2019;39(1):8-9.

187. Hwang K, Kim JY, Lim JH. Anatomy of the platysma muscle. The Journal of craniofacial surgery. 2017;28(2):539-42.

188. Sinno S, Thorne CH. Cervical branch of facial nerve: an explanation for recurrent platysma bands following necklift and platysmaplasty. Aesthetic surgery journal. 2019;39(1):1-7.

189. Malins WLE, Walker H, Guirguis J, Riaz M, Saleh DB. Defining a safe corridor of cervical branch preservation in lateral platysmaplasty surgery during facial rejuvenation surgery. Aesthetic surgery journal. 2022;42(2):Np93-np8.

190. Cakmak O, Emre IE. Surgical anatomy for extended facelift techniques. Facial plastic surgery : FPS. 2020;36(3):309-16.

191. Stuzin JM, Rohrich RJ. Facial nerve danger zones. Plastic and reconstructive surgery. 2020;145(1):99-102.

192. Righini CA, Petrossi J, Reyt E, Atallah I. An original submandibular approach technique sparing the cervical branch of the facial nerve. European Annals of Otorhinolaryngology, Head and Neck Diseases. 2014;131(2):143-6.

193. Gerard Iii NO, Tubbs RS, Iwanaga J. Duplicated transverse cervical nerve and external jugular vein. Anatomy & cell biology. 2021;54(3):404-6.

194. Khoa TD, Bac ND, Luong HV, Anh TN, Phuong NT, Nga VT, et al. Anatomical characteristics of facial nerve trunk in Vietnamese adult cadavers. Open access Macedonian journal of medical sciences. 2019;7(24):4230-8.

195. Smith OJ, Ross GL. Variations in the anatomy of the posterior auricular nerve and its potential as a landmark for identification of the facial nerve trunk: a cadaveric study. Anatomical science international. 2012;87(2):101-5.

196. Liu M, Wang SJ, Benet A, Meybodi AT, Tabani H, Ei-Sayed IH. Posterior auricular artery as a novel anatomic landmark for identification of the facial nerve: A cadaveric study. Head & neck. 2018;40(7):1461-5.

197. Kikuta S, Iwanaga J, Watanabe K, Kusukawa J, Tubbs RS. The feasibility of using the posterior auricular branch of the facial nerve as a donor for facial nerve reanimation procedures: a cadaveric study. Journal of Oral and Maxillofacial Surgery. 2019;77(7):1470.e1-.e8.

198. Colbert SD, Davies J, Aldridge T, Brennan PA. Posterior auricular nerve found anterior to the cartilage of the external auditory meatus--a previously unreported variant. The British journal of oral & maxillofacial surgery. 2013;51(5):448-9.

VITA

NAME	Sukanya Uruwan
DATE OF BIRTH	3 August 1990
PLACE OF BIRTH	Nakhonsawan
INSTITUTIONS ATTENDED	Department of Anatomy, Faculty of Medicine, Chulalongkorn University
HOME ADDRESS	Home No. 2 Village No. 3 Phanomrok, Thatako, Nakhonsawan 60160
PUBLICATION	1. Tansatit, T., Uruwan, S., & Rungsawang, C. (2021). The Crest Injection Technique for Glabellar Line Correction and the Paracentral Artery. Plastic and Reconstructive Surgery - Global Open, 9, e3982. doi:10.1097/GOX.0000000000003982 2. Rungsawang, C., Tansatit, T., Fasunloye, L., & Uruwan, S. (2021). Achieving the Most Effective Hanging Points at the Lower End of the Face for Thread Lifting: Quantitative Measurement of Tissue Resistance in Different Facial Layers. Plastic and Reconstructive Surgery - Global Open, 9, e3701. 3. Tansatit, T. , Phumyoo, T. , Jitaree, B. , Rungsawang, C. , & Uruwan, S. (2021) . Commentary on: Deployment of the Ophthalmic and Facial Angiosomes in the Upper Nose Overlaying the Nasal Bones. Aesthetic Surgery Journal. 4. Jitaree, B. , Phumyoo, T. , Uruwan, S. , Jiirasutat, N. , Pratoomthai, B. , & Tansatit, T.

(2020). Clinical Implications of the Arterial Supplies and Their Anastomotic Territories
in the Nasolabial Region for Avoiding Arterial Complications during Soft Tissue Filler
Injection. Clinical Anatomy, 34.
5. Phumyoo, T. , Jiirasutat, N. , Jitaree, B. , Rungsawang, C. , Uruwan, S. , & Tansatit, T.
(2019). Anatomical and Ultrasonography-Based Investigation to Localize the Arteries on
the Central Forehead Region During the Glabellar Augmentation Procedure. Clinical
Anatomy, 33.
6. Charoenlaka N, Nilkote R, Duangjinda M, Kongchai T, Uruwan S, Thongbaion W.
(2019). A Development of Collaborative Learning Processto Develop Sustainable Non-
Smoking Behavior in Universities. Journal of Community Development Research
(Humanities and Social Science), 12(4): 80-92
7. Watcharinrat M, Uruwan S, Choopan W. (2019). Comparisons of Achievement of
Anatomy Laboratory Learning By Cadaver and Anatomy Application on Digestive
System with First Year Nursing Students of Private University in Nakhon Pathom.
Journal of Education, 30(3):49-62
8. Jitaree B, Phumyoo T, Uruwan S, Sawatwong W, McCormick L, Tansatit T. (2018). The
Feasibility Determination of Risky Severe Complications of Arterial Vasculature

Regarding the Filler Injection Sites at the Tear Trough. Plast Reconstr Surg, 142(5):1153-1163.

9. Jitaree, B., Phumyoo, T., Uruwan, S., Sawatwong, W., Cesak, O., & Tansatit, T. (2018). Clinical Implication of the Arterial Supplies and Their Anastomotic Territories of the Nasolabial Region for Avoiding Arterial Devastation and Complications during Soft Tissue Filler injection. The FASEB Journal, 32.

10. Uruwan S, Tansatit T, Jitaree B, Phumyoo T, Rungsawang C. (2016). Anatomical Study of the Retaining Ligaments and Its Relationship to the Facial Soft Tissue of the Midface. Siriraj Medical Journal, 68(3): S42-S45.

11. Rungsawang C, Tansatit T, Phumyoo T, Jitaree B, Uruwan S. (2016). Determining safe entry sites for filler injections on the lateral canthal vertical line: anatomical study of the midface arterial perforators in soft embalmed cadavers. Asian Biomedicine, 10(6):619-625.

12. Tansatit T, Moon HJ, Rungsawang C, Jitaree B, Uruwan S, Apinuntrum P, Phetudom T. (2016). Safe Planes for Injection Rhinoplasty: A Histological Analysis of Midline Longitudinal Section of the Asian Nose. Aesthetiic Plast Surg,40(2):236-44.

AWARD RECEIVED

2012 Moral Award from Physical Therapy Council

2016 39th Annual Conference of the Anatomy Association of Thailand Award